GEOLOGICA ULTRAIECTINA

Mededelingen van het
Instituut voor Aardwetenschappen der
Rijksuniversiteit te Utrecht

No. 45

A CASE STUDY OF A MANTLED GNEISS ANTIFORM, THE HOSPITALET MASSIF, PYRENEES (ANDORRA, FRANCE)

BAS VAN DEN EECKHOUT

STELLINGEN

1. De structurele aspecten van batholiet-intrusies worden te weinig belicht.

2. Gedetailleerde structurele analyse is alleen dan zinnig indien een grote mate van continuïteit in ontsluiting is gewaarborgd.

   Williams, P.F., 1985. Multiply deformed terrains-problems of correlation. J. Struct. Geol. 7: 269-281.

3. De resultaten van zeer diepe boringen tonen in de eerste plaats aan dat de kennis van de aardkorst beperkt is.

   Kozlovsky, Ye.A., 1984. The world's deepest well. Scientific American 251 (6): 106-112.

4. De ruwweg NE-SW strekkende extensielineaties zoals die worden aangetroffen in Alpujarride eenheden rondom de boog van Gibraltar en die kennelijk samenhangen met de stapeling van deze eenheden, tonen aan dat de vorming van de boog van Gibraltar niet het gevolg is van een radiaal afglijden van deze eenheden van een Alboran topografisch hoog, zoals dat wordt gesuggereerd door Torrès-Roldan (1979).

   Torrès-Roldan, R., 1979. The tectonic subdivision of the Betic Zone (Betic Cordilleras, Southern Spain): its significance and one possible geotectonic scenario for the westernmost Alpine belt. Am. J. Sci. 279: 19-51.

   Reuber, I., Michard, A., Chalouan, A., Juteau, T. and Jermoumi, B., 1982. Structure and emplacement of the Alpine-type peridotites from Beni-Boussera, Rif, Marocco: a polyphase tectonic interpretation. Tectonophysics 82: 231-251.

   Tubia, J.M. and Cuevas, J., 1986. High temperature emplacement of the Los Reales peridotite nappe (Betic Cordillera, Spain). J. Struct. Geol. 8: 473-482.

5. Seismisch en gravitatief onderzoek kan van grote waarde zijn in het vaststellen van de driedimensionale structuur van mantled gneiss domes.

   Kadoma, K.P. and Chapin, D.A., 1984. A detailed gravity study of the Chattolanee Baltimore gneiss dome, Maryland, U.S.A. Earth Planet. Sci. Lett. 68: 286-296.

6. De bewering van Talbot (1974) als zouden asymmetrische basement lobben, zoals die worden aangetroffen in zijn gecentrifugeerde putty modellen, te vergelijken zijn met dekbladen in de Alpen is fundamenteel onjuist.

Talbot, C.J., 1974. Fold nappes as asymmetric mantled gneiss domes and ensialic orogeny. Tectonophysics 24: 259-276.

7. "Inkrimping" en "bezuiniging" lijkt vaak op het afkorten van een tafel zonder gebruikmaking van een duimstok, hetgeen uiteindelijk leidt tot de aanschaf van een nieuwe tafel.

Stellingen behorende bij het proefschrift:
"A case study of a mantled gneiss antiform, the Hospitalet massif, Pyrenees (Andorra, France). Bas van den Eeckhout, 1986.

ERRATUM

page 17 lines 9, 10 should read:

"it seems that the rising of granitic magma ... has supplied the elevating power" by means of "the lesser density of granitic magma as compared to average crystalline rock".

GEOLOGICA ULTRAIECTINA

Mededelingen van het
Instituut voor Aardwetenschappen der
Rijksuniversiteit te Utrecht

No. 45

A CASE STUDY OF A MANTLED GNEISS ANTIFORM, THE HOSPITALET MASSIF, PYRENEES (ANDORRA, FRANCE)

A CASE STUDY OF A MANTLED GNEISS ANTIFORM, THE HOSPITALET MASSIF, PYRENEES (ANDORRA, FRANCE)

EEN STUDIE VAN EEN OMHULDE GNEISANTIFORM, HET HOSPITALET MASSIEF, PYRENEEËN (ANDORRA, FRANKRIJK)

(MET EEN SAMENVATTING IN HET NEDERLANDS)

PROEFSCHRIFT

TER VERKRIJGING VAN DE GRAAD VAN DOCTOR IN DE WISKUNDE EN NATUURWETENSCHAPPEN AAN DE RIJKSUNIVERSITEIT TE UTRECHT, OP GEZAG VAN DE RECTOR MAGNIFICUS PROF. DR. J.A. VAN GINKEL, VOLGENS BESLUIT VAN HET COLLEGE VAN DEKANEN IN HET OPENBAAR TE VERDEDIGEN OP WOENSDAG 29 OKTOBER 1986 DES NAMIDDAGS TE 2.30 UUR

DOOR

BARNABAS VAN DEN EECKHOUT

GEBOREN OP 26 SEPTEMBER 1956 TE AMSTERDAM

1986
OFFSETDRUKKERIJ KANTERS B.V., ALBLASSERDAM

PROMOTOR: PROF. DR. H.J. ZWART

aan Yvonne, Tim en Marloes

aan mijn ouders

ISBN 90-71577-03-1

CONTENTS

VOORWOORD		10
SAMENVATTING		12
ABSTRACT		13
RESUME		14
RESUMEN		15
1	**AN INTRODUCTION TO MANTLED GNEISS DOMES**	17
1.1	CHARACTERISTICS OF MANTLED GNEISS DOMES	18
1.2	THE PROBLEM OF MANTLED GNEISS DOMES	19
2	**THE PYRENEAN BELT; A REVIEW**	23
2.1	PROTEROZOIC AND PALEOZOIC EVOLUTION	24
2.1.1	Proterozoic events and the basement problem in the Axial Zone	24
2.1.2	Paleozoic sedimentation	26
2.1.3	The Hercynian orogeny	27
2.2	MESOZOIC AND TERTIARY EVOLUTION	31
2.2.1	Mesozoic and pre-Pyrenean Tertiary sedimentation and tectonics	31
2.2.2	The Pyrenean orogenic phase	33
2.2.3	Post-Pyrenean Tertiary sedimentation and uplift	35
3	**THE HOSPITALET MANTLED GNEISS ANTIFORM: GNEISSES, CAMBRO-ORDOVICIAN METASEDIMENTS AND LARGE-SCALE STRUCTURE**	37
3.1	GNEISSES	38
3.2	THE GNEISS-METASEDIMENT CONTACT	41
3.3	CAMBRO-ORDOVICIAN METASEDIMENTS	43
3.3.1	Seo formation	43
3.3.2	Massana formation	46
3.4	STRUCTURE: THE RANSOL SYNCLINE	47
3.5	SUMMARY	48
	APPENDICES 1, 2	50

4	**AGE RELATIONSHIPS BETWEEN SUPRASTRUCTURE AND INFRASTRUCTURE, AND THE MODE OF GNEISS ANTIFORM FORMATION IN THE HOSPITALET MASSIF**	53
4.1	LARGE-SCALE GEOMETRY OF THE HOSPITALET MASSIF AND ADJACENT STRUCTURAL DOMAINS	54
4.2	LITHOLOGY	55
4.3	WORKING METHOD	56
4.4	SMALL-SCALE STRUCTURES IN THE HOSPITALET MASSIF (THE INFRASTRUCTURE)	56
4.4.1	South flank	57
4.4.2	North flank	68
4.4.3	The gneisses	71
4.5	SMALL-SCALE STRUCTURES IN THE MASSANA AND TOR FOLDS (THE SUPRASTRUCTURE)	71
4.6	RELATIONSHIPS BETWEEN SMALL-SCALE STRUCTURES AND LARGE-SCALE GEOMETRY	76
4.7	INFRASTRUCTURE vs. SUPRASTRUCTURE	79
4.7.1	The age of the infrastructure	79
4.7.2	Consequences of infrastructure formation for overlying rocks	79
4.8	DYNAMIC MODELS FOR GNEISS ANTIFORM FORMATION	81
4.9	TECTONIC IMPLICATIONS	85
5	**THREE DOMAINS OF LATE HERCYNIAN DEFORMATION OF THE INFRA-STRUCTURE IN THE HOSPITALET MASSIF**	89
5.1	THE MYLONITE ZONE AT THE GNEISS-METASEDIMENT CONTACT	91
5.1.1	Kinematics of the CHSZ	94
5.1.2	Microstructures in metasediments	98
5.1.3	Microstructures in gneisses	105
5.1.4	Temperature conditions of deformation	107
5.1.5	Quartz fabric analysis	108
5.1.6	Discussion and conclusions	114
5.2	THE EL SERRAT-RANSOL ZONE, A TRANSCURRENT ZONE OF REFOLDING	120
5.2.1	Small-scale structures within the ERZ	120
5.2.2	Structural interpretation of the ERZ	124
5.3	A MAJOR RECUMBENT FOLD IN THE EASTERN HINGE ZONE OF THE HOSPITALET GNEISS ANTIFORM	127

5.3.1 Small-scale structures 129
5.3.2 Discussion 133

6 **STRUCTURES AND DEFORMATION PHASES IN THE HOSPITALET AUGEN-GNEISSES** 137
6.1 SMALL-SCALE STRUCTURES 141
6.2 DEFORMATION ZONES 145
6.3 DISCUSSION 147

7 **STRUCTURAL CONSTRAINTS ON PYRENEAN TYPE METAMORPHISM IN THE HOSPITALET MASSIF** 151
7.1 GEOMETRY OF MINERAL ZONES IN THE HOSPITALET MASSIF 152
7.2 THE MINERAL ZONATION 153
7.3 DISCUSSION AND CONCLUSIONS 162
7.3.1 PT gradient during prograde metamorphism 162
7.3.2 Age of the metamorphism relative to the structural history 164
7.3.3 The retrograde path 164
7.3.4 Thermal gradients and isograd spacing 165
7.3.5 The discrepancy between estimated pressures and overburden thickness 165
7.3.6 The origin of the dome shape of the metamorphic pattern 167
7.3.7 Structural constraints on the low P/T ratio of the metamorphism 167

8 **SYNOPSIS** 173
8.1 PRE-HERCYNIAN EVOLUTION 173
8.2 HERCYNIAN EVOLUTION 173
8.3 DISCUSSION 177

REFERENCES 180

CURRICULUM VITAE 193

ENCLOSURE 1 Geological map of the western Hospitalet massif

ENCLOSURE 2 Quartz c-axis fabrics

ENCLOSURE 3 Metamorphic map of the western Hospitalet massif

VOORWOORD

In dit proefschrift wordt getracht om door middel van kleinschalige structurele analysemethoden de ontwikkeling vast te stellen van een rechtopstaande plooistructuur welke kan worden beschouwd als een omhulde gneisantiform. De problematiek omtrent omhulde gneiskoepels werd mij duidelijk in de zomer van 1981 in Groenland. Als "safety assistent" van John Grocott werd toen een gebied gekaarteerd in de Rinkian gordel (centraal west Groenland), een gebied waar gneiskoepels en -antiforms op spectaculaire wijze ontsloten zijn.
In mei 1982 kreeg ik de kans een dergelijke structuur in de Pyreneeën te onderzoeken via een betrekking bij de vakgroep Structurele en Toegepaste Geologie aan het Instituut voor Aardwetenschappen der Rijks Universiteit Utrecht. Hiertoe werd in de zomers van 1982 t/m 1985 ruim 7½ maand veldwerk verricht in het Hospitalet massief (Andorra, Frankrijk).

Aan het verloop van het onderzoek en de uiteindelijke totstandkoming van het proefschrift hebben velen bijgedragen. In de eerste plaats mijn promotor prof. dr. H.J. Zwart, die mij de kans heeft geboden het onderzoek uit te voeren, veldcontroles heeft verricht en het onderzoek naar kwartsmaaksels sterk heeft gestimuleerd. Verder stafleden en medestudenten aan het I.v.A.U., in het bijzonder Cees Mayer, Cees Passchier, Ben Jansen, Tony Senior, Amparo Garcia-Celma, Anton-Jan Bons, Raymond Franssen, Hans de Bresser, Folkert Majoor en Maarten Ploegsma voor stimulerende discussies. Professor Zwart en Cees Passchier worstelden zich door het hele proefschrift en hun opbouwende kritiek, samen met die van Amparo, Hans en Folkert heeft de tekst in zijn definitieve vorm gebracht. Amparo verzorgde de Spaanse samenvatting en samen met prof. J. Touret (V.U.) de Franse samenvatting. Martin en Jill Drury corrigeerden het Engels.

Tijdens het veldwerk, zowel in het Hospitalet massief als in het tweede-jaars veldwerkgebied in het westelijke Aston massief hebben discussies met Cees Mayer, Tony Senior en Reinoud Vissers veel bijgedragen aan het inzicht in de geologie van dit deel van de Pyreneeën. John Grocott toonde een zeer stimulerende belangstelling en de excursies met hem in het veldwerkgebied en in het Albères massief hebben veel bijgedragen tot de vorming van ideeën. Michel Westhof assisteerde twee weken in de zomer van 1983 en zonder zijn hulp was het bewerken van een aantal afgele-

gen secties nauwelijks te verwezenlijken geweest.

Het slijpkamerteam van Jan de Groot verzorgde accuraat de benodigde dunne doorsneden. Carla Mulder-Blanken (U.v.A.) loste met grote voortvarendheid marmermonsters van het Ransol-member op, die, spijtig genoeg steriel bleken. De mylonietische Devoonkalken uit de Villefranche syncline leverden wel conodonten op. Deze werden gedetermineerd door dr. v.d. Bogaard (U.v. Leiden).

Vanaf begin 1986 kwam de teken- en fotoafdeling in actie. Hans Bliek verzorgde bijsluiters 1 en 2 en de figuren. René Meye verzorgde bijsluiter 3. Isaac Santoe en Jacco van Bergenhenegouwen hielpen met correctiewerk en de negatieven en de drukproeven van de kleurenkaarten. Hans Schiet verzorgde fotografie.

De "camera-ready" versie werd verzorgd door Magda Martens, die daarvoor een aantal vrije avonden en zaterdagen heeft opgeofferd.

Hierbij bedank ik allen.

Ten slotte het belangrijkste. Yvonne, Tim en Marloes verzorgden de solide basis voor het werk van een vaak letterlijk en figuurlijk afwezige geoloog. Zonder jullie steun was dit proefschrift er niet geweest.

SAMENVATTING

Het Hospitalet massief bestaat uit een antiformale kern van monzogranietische orthogneizen en daaroverheen een tenminste 2,5 km dikke, voornamelijk siltig-zandige sedimentstapel van Cambro-Ordovicische ouderdom. Tijdens de Hercynische orogenese zijn deze gesteenten meervoudig vervormd en gemetamorfoseerd. Drie stadia kunnen worden onderscheiden in de ontwikkeling van de structuur.

Gebeurtenissen voorafgaande aan de vorming van de antiform

Noordoost-zuidwest strekkende (D1) plooien worden gevormd en vervolgens vervormd door rechtopstaande oost-west strekkende (D2) plooien en assenvlaksplijtingen, welke de suprastructuur vertegenwoordigen. Vervorming gebeurde onder laaggradig metamorfe condities, en noord-zuid verkorting heeft opgetreden, waarschijnlijk gepaard gaande met verdikking van de sedimentstapel.

Vorming van de gneis antiform

In het massief zijn de D1 en D2 structuren vervormd door vlakliggende tot zwak hellende (D3) plooien en assenvlaksplijtingen, welke de infrastructuur definieren. Tijdens deze deformatiefase werd de gneisantiform gevormd. De structuur ontstond door verticale bewegingen, samenhangend met horizontale uitrekking op de schaal van het massief. Voor en tijdens D3 begon de temperatuur te stijgen tot in hoog groenschist facies omstandigheden. Na D3 werd de infrastructuur gemetamorfoseerd onder amfiboliet facies omstandigheden in een lage druk facies serie ($65^{o}C/km$), gepaard gaande met wijdverspreide, zonaire groei van metamorfe mineralen als biotiet, andalusiet, cordieriet, stauroliet en in de hoogste graad sillimaniet. Structurele en tectono-metamorfe overwegingen suggereren dat de horizontale uitrekking grotendeels werd opgenomen door een afschuivingszone of afschuivingszones.

Gebeurtenissen welke de antiform beinvloeden

Tijdens afkoeling bij gelijkblijvende druk in hoog groenschist - laag amfiboliet facies omstandigheden, werden de gesteenten van de infrastructuur vervormd in (1) een 1 km brede zone van mylonietische vervorming op het contact van gneizen en sedimenten, (2) een 1,5 km brede zone van (D4/5) herplooiiing ten zuidwesten van de antiform, (3a) een kilometerschaal liggende plooi in de oostelijke ombuigingszone van het massief en (3b) kleinschalig liggende plooien door het gehele massief heen. Noordnoordoost-zuidzuidwest uitrekking gevolgd door westnoordwest-oostzuidoost uitrekking vond plaats en de antiformale gneiskern gedroeg zich als een star voorwerp waaromheen de sedimenten werden gedrapeerd. Dit veroorzaakte (a) schijnbaar hoge thermale gradienten en (b) (accentuering van) de antiformale vorm van het isogradenpatroon.

De drie stadia in de ontwikkeling van de Hospitalet gneis antiform worden beschouwd als vroeg (Westphaal), midden (Westphaal-Stephaan) en laat (Stephaan-vroeg Perm) Hercynische tektoniek. De genoemde structuren worden doorsneden door rechtopstaande breuken, schuifzones en plooien, welke geassocieerd zijn met laag groenschist facies mineraal-assemblages. Deze structuren zijn waarschijnlijk gevormd ten gevolge van Alpiene bewegingen.

ABSTRACT

The Hospitalet mantled gneiss antiform consists of monzo-granitic orthogneisses, which are overlain by a predominantly pelitic, at least 2.5 km thick succession of Cambro-Ordovician metasediments.
During the Hercynian orogeny the rocks were polyphase deformed and pluri-facially metamorphosed. Three stages in its tectonic evolution can be distinguished.

Pre-antiform episode

NE-SW trending (D1) folds were formed and overprinted by upright EW trending (D2) folds and foliations, defining the suprastructure around the massif. Deformation occurred at low grade conditions and NS shortening is indicated, probably accompanied by thickening of the metasedimentary pile.

Gneiss antiform formation

Within the massif the D2 structures are overprinted by flat lying to gently inclined (D3) folds and foliations, defining the infrastructure. The geometry of S3 relative to the gneiss-cover contact limits antiform formation to vertical tectonics at the scale of the massif, accommodated by horizontal extension at the same scale. Subsequently, a low P/T ratio metamorphism (65^{o}C/km) took place in the infrastructure, associated with extensive, zonal growth of biotite, andalusite, cordierite, staurolite and sillimanite in highest grade. Structural and tectono-metamorphic considerations suggest that extension was largely accommodated by an extensional shear zone or shear zones of which the infrastructure represents the upper part.

Post-antiform episode

During isobaric cooling in lower amphibolite facies conditions the infrastructure has been deformed in (1) a 1 km wide zone of mylonitic strain at the gneiss-cover contacts, (2) a 1.5 km wide zone of (D4/5) refolding SW of the gneisses, (3a) a km scale recumbent fold in the eastern hinge zone of the gneiss antiform and (3b) small-scale recumbent (D6) folds throughout the massif. The antiformal gneiss core acted as a relatively rigid body and the metasediments and mineral zones were draped around it, first in NNE-SSW stretching, afterwards in WNW-ESE stretching, causing (a) seemingly high thermal gradients and (b) the antiformal pattern of the isograds.

The three stages in the evolution of the Hospitalet mantled gneiss antiform are considered to represent early (Westphalian), middle (Westphalian-Stephanian) and late (Stephanian-early Permian) Hercynian tectonics. The structures mentioned have been cut by high angle faults, shear zones and folds, which are accompanied by low greenschist facies metamorphic conditions and which probably reflect Alpine movements.

RESUMÉ

L'antiforme gneissique de l'Hospitalet est composé d'orthogneiss de composition monzo-granitique, couverts par une série Cambro-Ordovicienne essentiellement pélitique, d'une puissance de plus de 2,5 km.

Pendant l'orogenèse Hercynienne, les roches sont polymetamorphisées et déformees de façon polyphasée. On reconnait trois stades dans leur évolution tectonique.

Épisode pré-antiformal

Des plis (D1) de direction générale NE-SO sont formés en premier lieu, puis déformés par des plis et foliations (D2) subverticaux de tendance EO. Les structures D2 caractérisent la "suprastructure" autour du massif. La déformation indique une racourcissement de direction NS, probablement accompaniée d'un épaississement des sédiments. Les conditions métamorphiques correspondent au faciès schistes verts.

Formation de l'antiforme

Au sein du massif, les plis D2 sont déformés par des structures de phase D3. Ces structures sont subhorizontales à légèrement inclinées et caracterisent "l'infrastructure". La géométrie de la relation de S3 avec le contact des gneisses et sédiments indique que la formation de l'antiforme est le produit d'une tectonique verticale, accommodée par une extension horizontale à l'échelle du massif. Ensuite l'infrastructure a été métamorphisée dans un faciès en basse pression (65°C/km), entrainant une croissance zonale de la biotite, andalousite, staurotide, cordiérite et sillimanite dans les zones de température plus élévees. Des considérations tectono-métamorphique et structurale suggerent que l'extension subhorizontale s'accompagnait par une ou quelques zones de cisaillement extensionelles dont l'infrastructure représente la partie supérieure.

Episode post-antiformal

Au cours du refroidissement isobarique l'infrastructure a été déformée en conditions de faciès amphibolite moderé produisant 1) une zone mylonitique d'épaisseur de 1 km au contact du gneiss et des metasédiments, 2) une zone de plissement D4/5 de largeur 1,5 km au SO des gneiss, 3a) un pli couché d'échelle kilométrique dans la partie Est de la charnière de l'antiforme gneissique et 3b) des plis couchés (D6) de petite échelle developés dans le massif entier. Le coeur gneissique de l'antiforme a réagi comme un corps rélativement rigide et les sédiments et les zones minérales se sont moulés autour des gneisses, en premier par une extension NNE-SSO et en second par une extension ONO-ESE. Ces déformations ont produit (a) des hauts gradients apparents et (b) une géométrie antiformale es isogrades (interprétation tectonique de "l'effet de socle").

On croit que ces trois épisodes de l'évolution de l'antiforme gneissique de l'Hospitalet reflêtent une tectonique Hercynienne précoce (Westphalien), intermédiaire (Westphalien-Stéphanien) et tardive (Stéphanien-Permien inférieur). Les structures mentionnées sont recoupées par des failles, zones de cisaillement et plis, dans des conditions métamorphiques de faciès schistes verts qui reflêtent probablement des mouvements Alpins.

RESUMEN

La antiforma gneísica de Hospitalet consiste de ortogneises monzograníticos recubiertos por una serie Cambro-Ordovícica metasedimentaria de composición predominantemente pelítica de al menos 2,5 km de espesor.

Durante la orogenia Hercínica las rocas fueron sometidas a varias fases de deformación y a metamorfismo plurifacial. En su evolución tectónica se distinguen tres estadios.

Episodio pre-antiformal

Se forman pliegues (D1) de tendencia NW-SE con sobreimposición de pliegues y foliaciones (D2) subverticales y de tendencia EW, que definen la supraestructura alrededor del macizo. La deformación, que indica acortamiento en dirección NS probablemente acompañado por engrosamiento de la serie metasedimentaria, tuvo lugar bajo condiciones metamórficas de bajo grado.

Formación de la antiforma gneísica

En el macizo mismo a las estructuras D2 se superponen pliegues y foliaciones (D3) subhorizontales a ligeramente inclinados, que definen la infraestructura. La geometría de la relación de S3 con el contacto gneis-cobertera limita la formación de la antiforma a una tectónica de tipo vertical, acomodada por extensión horizontal a la escala del macizo.

Subsecuentemente la infraestructura se vió afectada por un metamorfismo de baja pendiente P/T (65°C/km) asociado a un crecimiento zonal de desde biotita, pasando por andalucita y cordierita, hasta sillimanita. Consideraciones tectono-metamórficas sugieren que la extensión fué ampliamente acomodada por una ó varias zonas de cizalla de las cuales la infraestructura representa la parte superior.

Episodio post-antiformal

La infraestructura fué deformada durante enfriamiento isobárico en condiciones de facies anfibólica baja produciendo (1) una zona milonítica de 1 km de anchura en el contacto gneis-cobertera; (2) una zona de 1,5 km de anchura de plegamientos sobreimpuestos (fases D4/D5) al SW de los gneises; (3a) un pliegue recumbente de escale kilométrica en la parte este de la charnela de la antiforma gneísica y (3b) pliegues recumbentes (D6) de pequeña escala que afectan a todo el macizo.

El núcleo gneísico de la antiforma actuó como un cuerpo relativamente rígido y los metasedimentos y zonas minerales se distribuyeron de forma envolvente a su alrededor, primero por una extensión NNE-SSW, y después por una extensión WNW-ESE, dando lugar a (a) altos gradientes térmicos aparentes, y (b) distribución antiformal de isogradas.

Se considera que los tres estadios de la evolución de la antiforma gneísica de Hospitalet representan una tectónica Hercínica temprana (Westfaliense), media (Westfaliense-Estefaniense) y tardía (Estefaniense-Pérmico inferior). Las estructuras mencionadas fueron cortadas a gran ángulo por fallas, zonas de cizalla y pliegues, que acompañados por condiciones metamórficas de facies esquistos verdes baja probablemente reflejan movimientos alpinos.

CHAPTER 1

AN INTRODUCTION TO MANTLED GNEISS DOMES

Mantled gneiss domes are "domes having a superincumbent mantle of sedimentary strata layered parallel to the dome contacts" (Eskola 1949). Since Eskola's comprehensive review, mantled gneiss domes have been a recurring theme in geological literature. Some contributions are merely concerned with the recognition of such structures (e.g. Vail 1963). Others, such as Zwart (1963a) question whether certain mantled domes can be considered as mantled gneiss domes in the sense of Eskola. The basis for the latter type of discussion is the mode of formation which Eskola attributed to the structures: "it seems that the rising of granitic magma granitic magma as compared to average crystalline rock". "Diapiric upswelling and doming is a regular phenomenon in the intrusion of granitic magma". Although this mode of formation was speculated upon, mantled gneiss domes had been linked to diapirism, hence arousing considerable debate. A classic example of this is the interpretation of the Rum Jungle area (Australia). According to Williams (1963) the domes occurring in that area are due to fold interference. Stephansson and Johnson (1976) argue that the structural evidence favours diapirism of the core gneisses.

Two lines of study are concerned with the structures: (1) a classic field approach in which as much data as possible are extracted from the structure as to place constraints on its mode of formation and (2) a theoretical/experimental approach which focusses on the theme diapirism. This thesis follows the first line of investigation.

1.1 CHARACTERISTICS OF MANTLED GNEISS DOMES

Mantled gneiss domes predominantly occur in Precambrian areas, such as granite greenstone belts of the Pilbara block (Australia) (Hickman 1984), the Zimbabwe shield (Snowden 1984) and the Canadian shield (Schwerdtner 1984). However they also occur in more recent orogenic belts such as the Appalachians (Thompson et al. 1968, Muller and Chapin 1984), the Damaran belt (SE Africa; Sawyer 1981), the French Massif Central (Dome de l´Agout, Schuiling 1960), the Greek Cyclades (Naxos, Jansen 1973; Ios, Van der Maar 1980) and the Pyrenees.
Mantled gneiss domes are seldom solitary structures: groups or rows of domes often line up in the structural trend of the belt in which they occur (Henderson 1969, Thompson et al. 1968, Sawyer 1981).

Most domes are circular to oval in plan. Some domes are steep sided (Kröner 1984, Schwerdtner et al. 1979), while other domes are asymmetric with a steep to overturned limb and a moderately dipping limb (Eskola 1949, Naylor 1968, Hatcher 1977). Some are open with moderately outward dipping contacts (Henderson 1969, Schwerdtner 1984). Within a given belt the shape and size of the structures may vary (Thompson et al. 1968, Henderson 1969). Elongate shapes are usually parallel to the trend of the belt.
The size of the structures is in general in the order of tens of kilometers, but within the granite-greenstone belts their diameter often exceeds 50 km and occasionally 100 km (Hickman 1984).

The gneisses in the cores of the mantled gneiss domes are without exception (appreciably) older than the mantling metasediments. In some instances a sedimentary basement-cover relationship is preserved (Eskola 1949) and structures and/or metamorphic imprints of earlier orogenic episodes may be recognized in the basement (Kröner 1984, Van den Eeckhout and Grocott 1982, Stephansson and Johnson 1976).
With few exceptions (Naylor 1968) the contact between the gneisses and the metasediments is abrupt. The gneisses are in general overlain by a relatively thin (less than 1 km) succession of "shelf-type" sediments such as conglomerate, quartzite, marble and dolomite. These rocks are overlain by a monotonous sequence of metapelites and metagraywackes.
The thickness of the latter succession usually is unknown. Estimated thicknesses amount up to 5-10 km (Henderson 1969 resp. Muller and Chapin 1984).

An extreme stratigraphic thickness of 15 km is reported by Hickman (1984). This common configuration is essential in Eskola's view of the geological history of the structures:
"The mantled domes apparently represent earlier granite intrusions related to an orogenic period. The plutonic mass was later eroded and levelled, and thereafter followed a period of sedimentation. During a subsequent orogenic cycle the pluton was mobilized anew ...". "It seems that a necessary condition of the formation of mantled domes is that the area in which they occur should have been subjected to two orogenic revolutions...". However, many of the cores are not homogeneous "old" granite as indicated by Eskola. Often a complex mixture of igneous materials, metavolcanics and metasediments is described (Sawyer 1981, Van den Eeckhout and Grocott 1982).

A common feature of mantled gneiss domes is a low to intermediate P/T ratio metamorphism (Thompson et al. 1968, Grocott et al. 1986 in press). Pressure estimates in the highest metamorphic grades usually are 3-5 kbar (Sawyer 1981, Van Staal and Williams 1983), which implies that dome formation is a mid-crustal process. The gneisses are surrounded by a concentric metamorphic zonation, usually with narrow isograd spacing and increasing metamorphic grade towards them (Grocott et al. 1986 in press). Migmatisation and intrusion of new granitic material is common. According to Eskola (1949) and others such as Kröner (1984) the latter feature has been the major cause for dome formation.

Deformation in and around mantled gneiss domes is complex. Usually two or more phases of deformation can be recognized. The actual formation of the domes is often preceded by deformation, in some instances by nappe emplacement (Thompson et al. 1968, Coward 1976, Bickle et al. 1980, Kröner 1984, Duncan 1984). Later deformations may involve large-scale steep dipping shear zones (Schwerdtner et al. 1979, Hickman 1984).

1.2 THE PROBLEM OF MANTLED GNEISS DOMES

Despite their common features, the tectono-metamorphic histories of individual structures sufficiently diverge as to account for various modes of formation. However, the very fact that for one and the same structure different modes have been forwarded (e.g. Brun et al. 1981, Bowes et al.

1984) clearly illustrates the lack of consensus of how to discriminate between these modes. In general the structures are attributed either to horizontal tectonics (e.g. fold interference) or to vertical tectonics (diapirism).

In the past decades a set of diagnostic criteria has been developed in which individual criteria were forwarded, criticised and rejected, thus causing a continuous evolution of the set, which kept pace with experimental work.

In the sixties Ramberg published centrifuged layered putty models. Density contrasts between putty's caused "diapirism". The resulting shapes were and still are used as a comparative criterion for interpreting domal structures as diapirs. Criticism came from structural geologists who indicated that similar shapes could result from folding or fold interference (e.g. Ramsay 1967). In the late sixties and early seventies computed/experimental models of (buckle)folding (Dieterich 1970, Hobbs 1971) and diapirism (Dixon 1975) were published. This allowed small-scale structures such as foliations and minor folds to be compared with those following from the experiments. Hence the diagnostic criteria involved strain patterns (Stephansson and Johnson 1976, Schwerdtner et al. 1978, Platt 1980, Brun et al. 1981). In the seventies attention started to focus on kinematics of deformation. Shear zones were tackled by geometric analysis (Ramsay and Graham 1970, Ramsay 1980) and petrofabric analysis (Lister and Williams 1979, Garcia Celma 1983). The results allow the kinematics of deformation found in the natural structures to be compared with kinematics of the models (Van den Eeckhout et al. 1986).

The updated set of diagnostic criteria to discriminate modes of formation of natural domes and antiforms is listed in Fig. 1.1. It should be noted that whenever a set of features extracted from a given structure does not entirely fit these criteria, alternative modes of formation must be considered (Grocott et al. 1986).

This study is concerned with a gneiss antiform in the Pyrenees (Andorra, France). Considering the broad, non-genetic classification of mantled gneiss domes adopted here, the structure can be considered as a mantled gneiss antiform. The aim of the study is to document the small-scale deformation history of the metasediments and the gneisses and relate this history to the large-scale geometry in order to achieve structural

criteria which place constraints on its mode of formation (cf. Fig. 1.1).

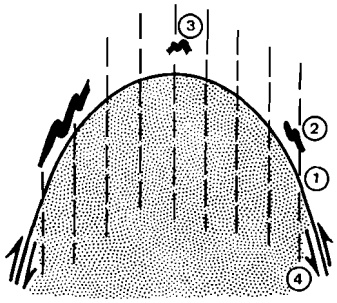

(BUCKLE)FOLD

1. foliation steeper than contact
2. minor folds and foliation-bedding relations verge towards the core
3. symmetric minor folds in the hinge zone; shortening is perpendicular to the axial plane
4. kinematics of shearing at the contact or in the core should indicate downthrow of the core; extension lineations lie in the axial plane

core material behaves relatively stiff in buckle folding

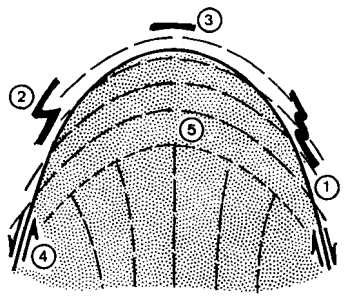

DIAPIR

1. foliation more flat lying than contact
2. minor folds and foliation-bedding relations verge away from the core
3. vertical flattening (e.g. boudinage) in the hinge zone; shortening is perpendicular to the gneiss-cover contact
4. kinematics of shearing at the contact or in the core should indicate relative rise of the core; extension lineations define radially outward patterns
5. transition zone from a steep fabric in the core to a flat lying fabric in the upper part of the structure

core material behaves relatively mobile, less stiff than overburden

Fig. 1.1 Diagnostic structural criteria (1-5) for distinguishing between a diapiric origin and a folding origin for a given antiformal structure. The minor structures should have formed simultaneously with the fold structure.
After Dixon (1975), Stephansson and Johnson (1976), Schwerdtner et al. (1978), Platt (1980), Brun et al. (1981), Van den Eeckhout et al. (1986).

CHAPTER 2

THE PYRENEAN BELT: A REVIEW

This chapter reviews the geological history of the Pyrenean mountain chain in order to provide a background for the case study of the Hospitalet mantled gneiss antiform.

The Pyrenees are subdivided in WNW-ESE trending zones. The belt is bordered by the basins of Aquitaine in France (Brunet 1984) and the Ebro in Spain (Fig. 2.1, Table 2.1). Since Mesozoic rocks are involved the zonation of the belt is caused by the Alpine orogeny.

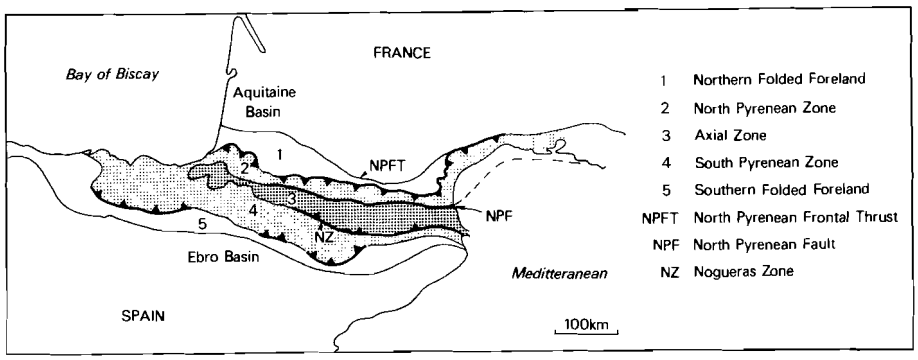

	zones and boundaries	characteristics
1.	Northern Folded Foreland	Open folds in a very thick Tertiary sequence
2.	North Pyrenean Zone	Mesozoic rocks, folded and thrusted to the north; satelite massifs (e.g. Arize massif)
	North Pyrenean fault	Fault zone with lherzolite bodies
3.	Axial Zone	Paleozoic and older (?) rocks, folded, metamorphosed and intruded during the Hercynian orogeny; Alpine shear zones
	Nogueras Zone	Complex fault zone comprising Hercynian basement rocks, post-Hercynian Paleozoic cover and Mesozoic rocks
4.	South Pyrenean Zone	Southward directed nappe transport on a decollement of Triassic evaporites underneath Tremp-Grauss basin
5.	Southern Folded Foreland	Folded Mesozoic and Tertiary sediments

Fig. 2.1 The zonation of the Pyrenean belt (after Mattauer and Henry 1974).
Table 2.1 Characteristics of the Pyrenean zones (after Mattauer en Henry 1974, Zwart 1979).

2.1 PROTEROZOIC AND PALEOZOIC EVOLUTION

2.1.1 Proterozoic events and the basement problem in the Axial Zone

The north Pyrenean massifs comprise granulite facies rocks which are attributed to a metamorphic event of late Proterozoic age (Zwart 1979). This interpretation is based on (1) radiometric age determinations by Vitrac and Allègre (1971), (2) the polymetamorphic character of the rocks and (3) differences in estimated pressures for the older, intermediate pressure type granulite facies rocks and the younger Hercynian low pressure metamorphism (Roux 1977). Another view is expressed by Vielzeuf (1984), who recognized two phases of granulite facies metamorphism. Vielzeuf attributes the older event to the Silurian and the younger event to the Hercynian orogeny. According to Matte (1986) the intermediate pressure granulite facies metamorphism is of Hercynian age. This is based on radiometric age determinations by Respaut and Lancelot (1983).

Within the Axial Zone (Fig. 2.4) the gneiss cored massifs are expected to reveal a sedimentary basement-cover relationship if it ever existed. Neither granulite facies assemblages nor clearcut erosional unconformities have been observed in these massifs and this poses a serious problem as to the nature of the gneiss-metasediment contacts and to the origin of the gneisses. This has led to two mutually exclusive views:

1. The gneisses are the original basement upon which Paleozoic sediments were deposited.
2. The gneisses are former intrusives into the sedimentary pile and no basement is observed.

The first view is expressed by Autran et al. (1966; massifs of Agly and Albères), Raguin (1977; Aston massif) and Cavet (1957) and Guitard (1970) for the Canigou-Carança massif (Fig. 2.4). Conclusions are based on the lithostratigraphic development of the basal parts of the metasedimentary sequences.

The second hypothesis is subscribed by Zwart (1968, 1979) and Soula (1982) for the massifs of Aston and Hospitalet.

Unfortunately, both hypotheses find support in radiometric age determinations by Vitrac and Allègre (1971) (Table 2.2). The main problem in interpreting these ages is the uncertainty in the age of the lower metasedimentary sequences. These unfossiliferous rocks are in general referred

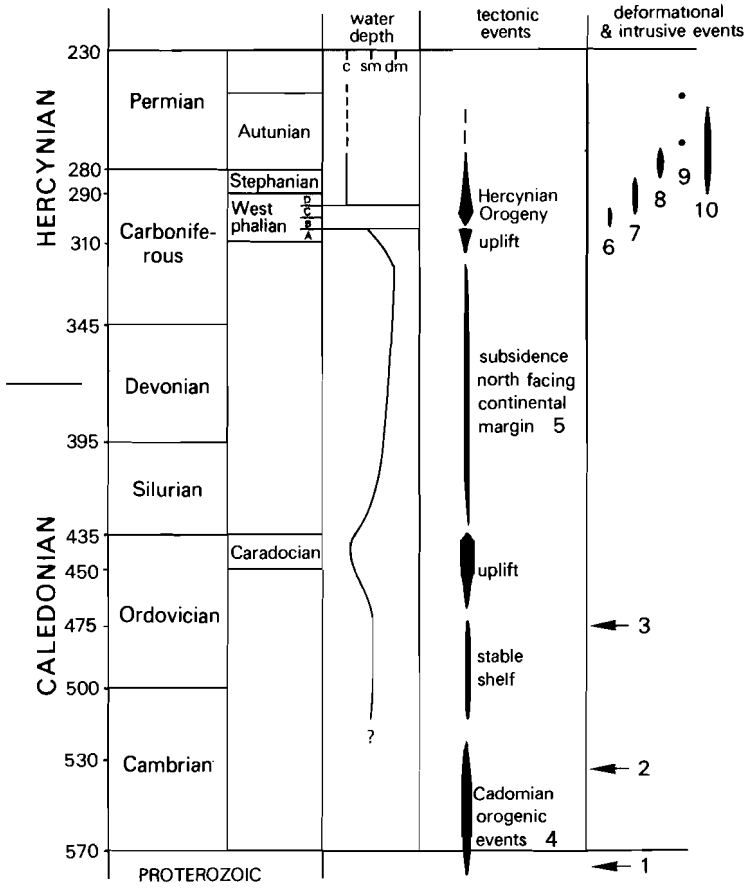

1 augengneisses Agly massif (Vitrac and Allègre 1971)

2 augengneisses Carança-Canigou (Vitrac and Allègre 1971)

3 augengneisses Aston-Hospitalet (Jäger and Zwart 1968)

4 cf. Vitrac and Allégre 1971

5 cf. Nagtegaal and de Weerd 1984

6 upright folding (Zwart 1979)

7 MGD's (? this thesis)

8 Maladeta batholith (Michard-Vitrac et al. 1980)

9 muscovite ages from a Late (Hercynian) High Strain zone in the Hospitalet massif (Jäger and Zwart 1968)

10 Late Hercynian wrench tectonics (Ziegler 1984)

Table 2.2 The Proterozoic and Paleozoic evolution of the Pyrenees. c = continental, sm = shallow marine, dm = deep marine.

to as "Cambro-Ordovician", but may be partly Proterozoic in age (Soula 1982). Jäger and Zwart (1968) determined an Ordovician age from gneisses of the Aston and Hospitalet massif (Table 2.2), which was interpreted as the age of intrusion. In the light of the age determinations by Vitrac and Allègre (1971), Zwart (1979) favoured the interpretation of Cambrian or Ordovician intrusions into the Cambro-Ordovician sediments.

2.1.2 Paleozoic sedimentation

Zwart (1979) extensively rewiews previous work on the sedimentation history of the Paleozoic. In this section the Paleozoic stratigraphic units will be shortly described. Reference can be made to the authors mentioned and Hartevelt (1970), who compiled most data on the Cambro-Ordovician, including the earlier work by Cavet (1957).
For the Devonian and Carboniferous reference can be made to Mirouse (1966), Mey (1967a, b, 1968) and Boersma (1973).

The Cambro-Ordovician shows a twofold division. The lower part consists of a monotonous sequence of siltstones and sands with some intercalations of quartzite and marble. Deposition took place in a shallow marine environment. Facies distributions, age and exact thickness are unclear. This sequence is referred to as the Seo formation by Hartevelt (1970) or in general as Cambro-Ordovician.
Better known, from a stratigraphic point of view are the overlying lithologically more varied formations. These rocks bear the oldest fossils encountered in the Pyrenees, indicative for the Caradocian epoch (Table 2.2). The stratigraphic break between the Seo formation and the overlying formations is characterized by a conglomerate (the Rabassa conglomerate). The higher formations contain conglomerates, sandstones, shales and limestones. Deposition took place in a shallow marine to continental regime. Thickness distributions of individual formations are roughly parallel to the strike of the orogen. Zwart (1979) indicates a total thickness of ca. 2 km for the Cambro-Ordovician.

The Silurian is marked by an up to 250 m thick black shale unit, that covers the Ordovician clastic sequences. The unit is widespread over the

Pyrenees. Deposition took place in a quiet marine euxinic environment.

Devonian sedimentation is marked by strong variations in thickness and facies. Carbonate deposition dominated over siliclastic influx in facies areas which trend EW, parallel to the strike of the belt. Maximum thicknesses, up to 1400 m are reached in the Northern Facies Area (Zandvliet 1960).

During the Carboniferous initially carbonate sedimentation took place in a pelagic environment, but a drastic change to coarse clastic turbiditic deposition environments, shallow marine and deltaic environments occurred towards the middle Carboniferous. This change marks the onset of the Hercynian orogeny.

2.1.3 The Hercynian orogeny

Sedimentary record. As in many other parts of the Hercynian orogen (Fig. 2.2), the pre-Hercynian sedimentary pile in the Pyrenees underwent folding in Westphalian times (Zwart 1979, 1981, Ziegler 1984). The oldest post-Hercynian sediments are of Westphalian-D age. They overlie folded and cleaved Lower Carboniferous and older rocks, but may be folded and cleaved to a minor extend themselves (Zwart 1979).

Sedimentation in Stephanian and Permian (Autunian) times is largely fluviatile to shallow marine, with much intercalated volcanoclastic and eruptive material. Sedimentation occurred in NS and EW trending grabens or half grabens, which are thought to be related to late Hercynian transcurrent movements (Soula et al. 1979, Bixel and Lucas 1983, Bixel et al. 1983, Speksnijder 1985). Ziegler (1984) discussed the role of late Hercynian wrench tectonics in the Hercynian orogen (Fig. 2.3).

Structural record. Within the Axial Zone (Fig. 2.4) the more deeply eroded parts of the Hercynian orogen are exposed. The Hercynian orogeny caused three main effects: (1) Paleozoic strata were folded in EW trending upright folds (the suprastructure), (2) domes occur on the scale of tens of kilometers that expose either metamorphic sedimentary rocks or a combination of the latter and dome shaped or sheet like gneiss bodies (the

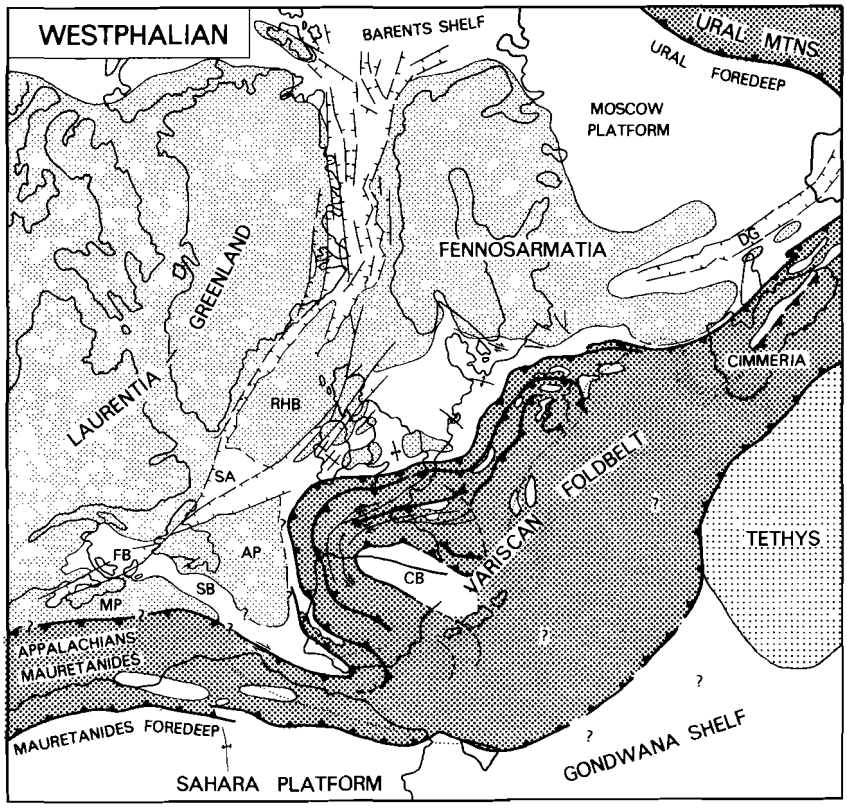

Fig. 2.2 Tentative Westphalian tectonic framework of the Arctic-North Atlantic domain; from Ziegler 1984.
AP - Avalon Platform, CB - Cantabrian Basin, DG - Dnepr-Donets Graben, FB - Fundy Basin, MP - Meguna Platform, RHB - Rockall-Halton Bank, SA - St. Anthony Basin, SB - Sidney Basin. (Published with permission of the author and the board of editors of Geologie en Mijnbouw).

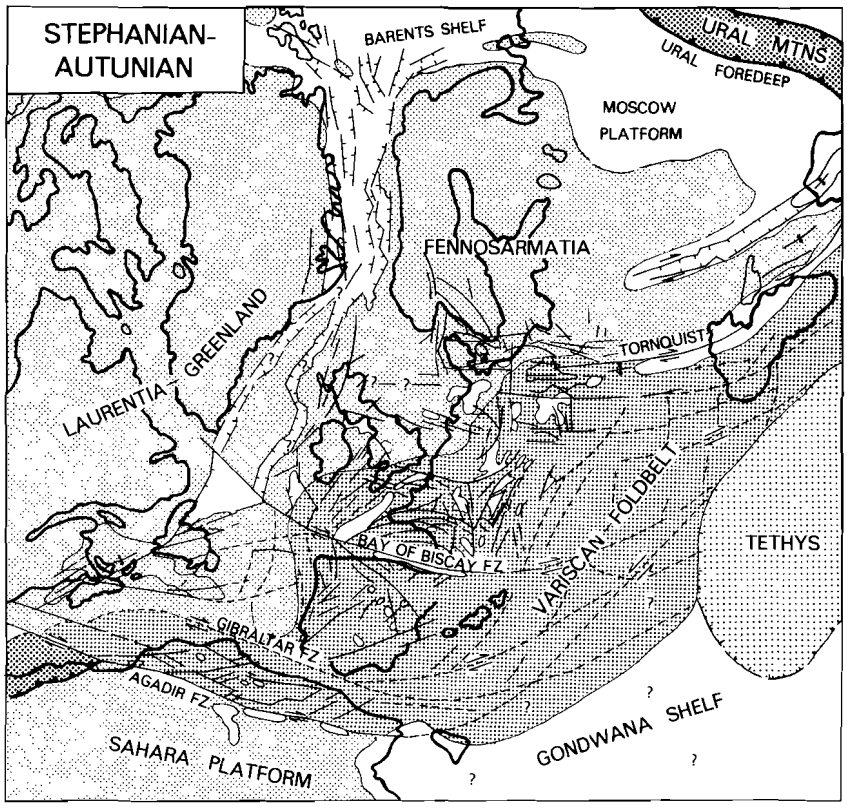

Fig. 2.3 Tentative Stephanian-Autunian tectonic framework of the Arctic-North Atlantic domain; from Ziegler 1984.
CBF - Chedabucto Fault, other abbreviations see Fig. 2.2(Published with permission of the author and the board of editors of Geologie en Mijnbouw).

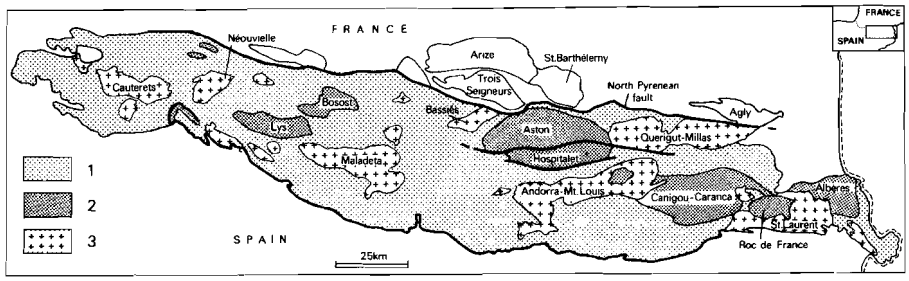

Fig. 2.4 Structural domains in the Axial Zone of the Pyrenees.

1. *Paleozoic metasediments of the suprastructure.*
2. *Paleozoic metasediments and gneisses of the infrastructure (the western massifs are metamorphic domes and the five easternmost are mantled gneiss domes).*
3. *Late Hercynian batholiths.*

infrastructure) and (3) plutonic domes/batholiths crop out over tens of kilometers, usually accompanied by a relatively narrow zone of contact metamorphism. Interference between batholiths and metamorphic c.q. gneiss domes is scanty. Most massifs are elongate parallel to the strike of the belt.

Relationships between these three structural domains are discussed by Zwart (1979) and Soula (1982). In their opinion the upright folds and cleavages developed syngenetically with the metamorphic domes and mantled gneiss domes. The domes are characterized by inclined to flat lying foliations and elevated metamorphic grade with respect to the upright fold domain.

The Pyrenean metamorphism is of the low pressure type, characterized by very steep temperature gradients: up to 150° C per kilometer (Zwart 1962, 1963b; Bosost area). Jäger and Zwart (1968) determined a Rb-Sr isochron corresponding to an age of 300 my, interpreted as the climax of Hercynian metamorphism.

The batholiths postdate the upright folds as they cut through them. The Maladeta batholith yields a lowermost Permian age (Michard-Vitrac et al. 1980). Zwart (1979), however, states that intrusion of the batholiths took place between Westphalian A and D times.

In general no proof is given that Westphalian D, Stephanian or Permian

formations contain material derived from batholiths, metamorphic domes or mantled gneiss domes within the Axial Zone. Their age has to be ascertained by radiometric methods. This has become even more necessary with the observation that the inclined and flat lying foliations are younger than the upright folds in the west part of the Aston massif (Verhoef et al. 1984), the Hospitalet massif (this thesis) and the Lys-Caillauas massif (De Bresser et al. 1986).

2.2 MESOZOIC AND TERTIARY EVOLUTION

2.2.1 Mesozoic and pre-Pyrenean Tertiary sedimentation and tectonics

Lower Triassic sedimentation occurred in the widespread Buntsandstein facies as red fluviatile and lagoonal deposits. Mid-Triassic up to and including the pre-Aptian early Cretaceous is described by Nagtegaal and De Weerd (1985) as a strongly carbonate dominated overall stable environment. The pre-Aptian Mesozoic sedimentation records the subsidence of the crust after the Hercynian orogeny.

A general change in sedimentation patterns with frequent and lateral facies changes started in Aptian times, the period of deposition of the "flysch noir" (Souquet et al. 1985). Lithologically varied sedimentation in shallow to deeper marine basins continued onwards to the end of the Cretaceous (Maastrichtian).

The changes in sedimentation patterns in Aptian times correspond well with the timing of the left lateral opening of the Bay of Biscay (Le Pichon et al. 1971, Choukroune and Mattauer 1978). According to Boillot et al. (1985) rifting may have started as early as the Upper Jurassic at the northern margin of the Iberian micro plate and continued until the end of the Aptian epoch. The main rifting event apparently took place in Aptian times and rift directions may have been controlled by the late Hercynian wrench fault pattern (Ziegler 1984).

Work on magnetic anomalies in the Atlantic and the Bay of Biscay suggests southeastward movement of Iberia followed by northwestward movement and southward subduction of the Europian plate underneath Iberia (Vielzeuf 1984, Boillot et al. 1985, Fig. 2.5, Table 2.3).

The North Pyrenean Fault zone (Figs. 2.1, 2.4) is generally considered as

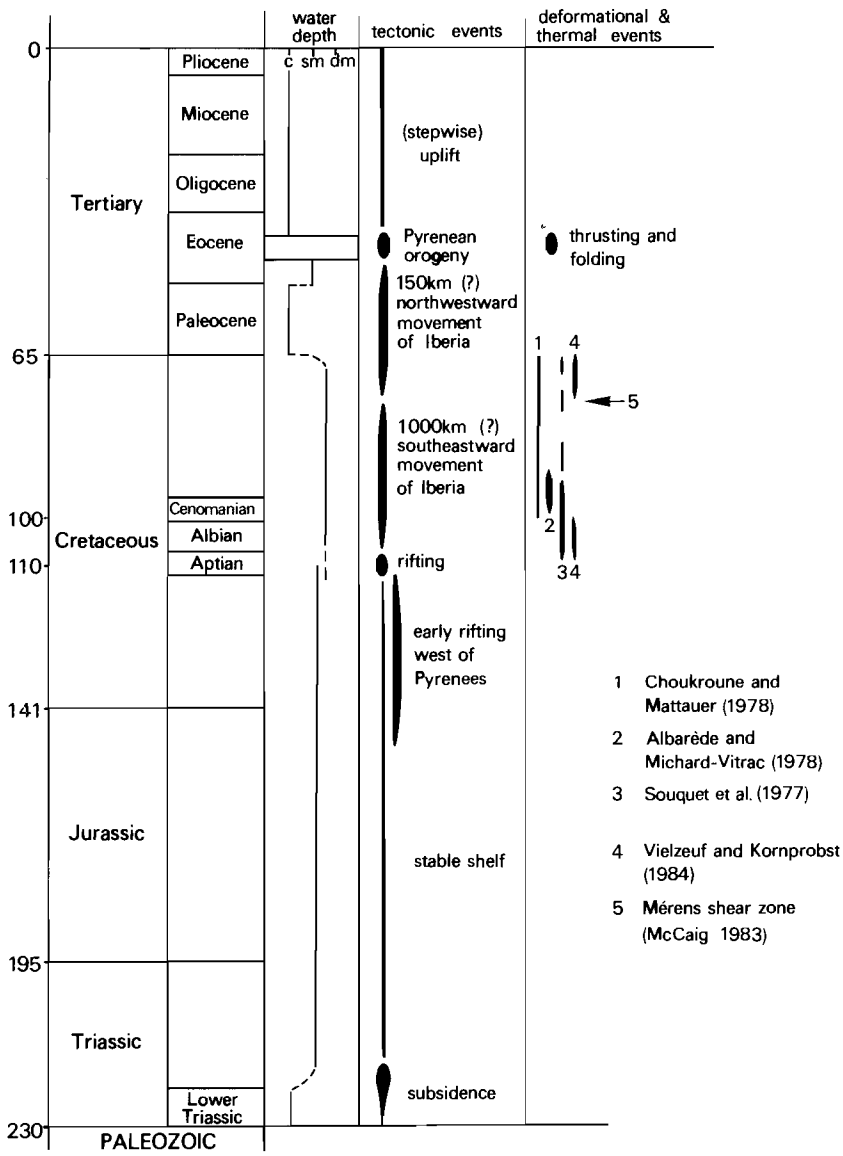

Table 2.3 The Mesozoic and Tertiary evolution of the Pyrenees. c = continental, sm = shallow marine, dm = deep marine.

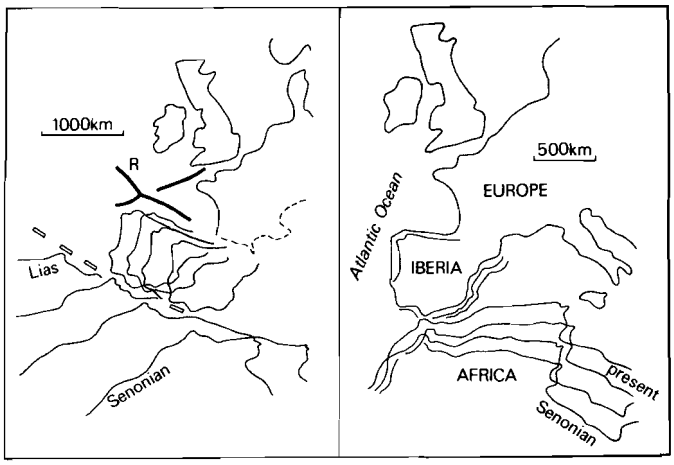

Fig. 2.5 Plate configurations of the Iberian microplate and Africa relative to stable Europe from Jurassic times to present. After Vielzeuf (1984) and Boillot et al. (1985). (R = rift).

the locus of the Cretaceous rifting and transcurrent movements in the Pyrenees. However, opinions strongly differ as to the relative and absolute timing of deformational and metamorphic events in this zone (Table 2.3).

2.2.2 The Pyrenean orogenic phase

The Pyrenean phase reflects the final stages of the northwestward movement of the Iberian plate relative to stable Europe. In this event the present day zonation of the belt was established (Fig. 2.1).

Tectonic transport has been bimodal, northward movements occurred north of the NPF and southward movements took place south of this structure (Table 2.1, Seguret 1972, Souquet et al. 1977). Recently, restored balanced cross sections have been constructed across the North Pyrenean Zone (Fischer 1984) and the South Pyrenean Zone and the Nogueras Zone (Williams 1985) and evidence for thin skinned thrust geometries is mounting in these zones (Casas and Muñoz 1985). The amount of Alpine shortening in the Axial Zone is not known, due to the absence of Mesozoic

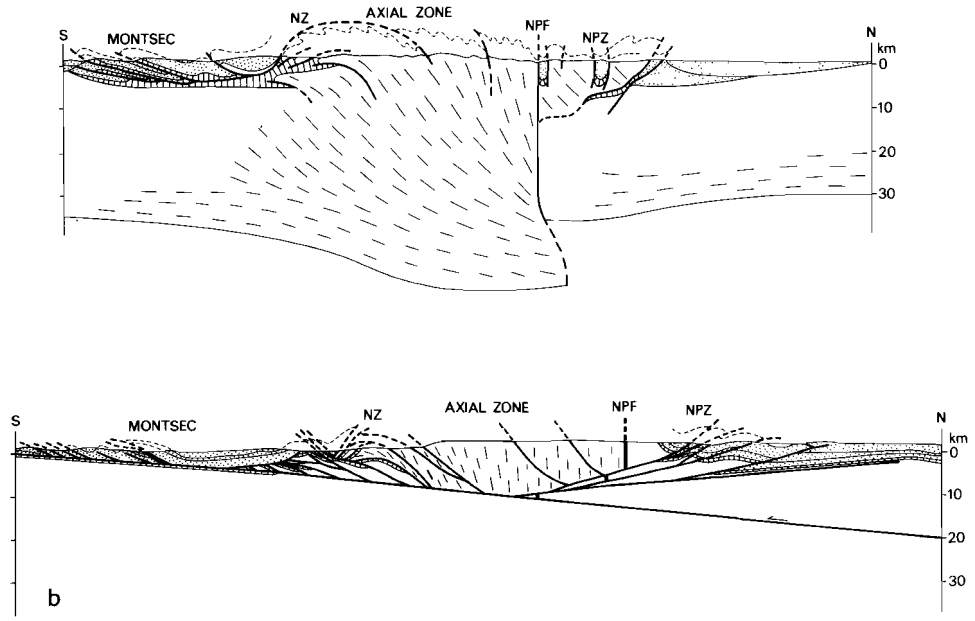

Fig. 2.6 Interpretations of the crustal structure in the Pyrenees. (a) Thick skinned (after Seguret et al. 1985) and (b) thin skinned (after Williams and Fischer 1985). The profiles run close to each other through the central Pyrenees. Scales are identical, no vertical exageration. Pre-Triassic rocks are unornamented except for the thin lines which indicate foliation attitude. Triassic rocks are striped and post-Triassic sediments are shown stippled. NZ = Nogueras Zone, NPF = North Pyrenean Fault, NPZ = North Pyrenean Zone. From Speksnijder 1986, with permission of the author.

rocks. Williams and Fischer (1985) assume an overall shortening of 30% taken up by the major Alpine shear zones within this zone.

Even more controversial is the structural evolution at depth. At present two tectonic models exist, a thin skinned and a thick skinned model (Fig. 2.6).

Deep seismics (Daignières et al. 1982) suggest that a MOHO step exists within 5-10 km from the NPF which can be traced along this structure. The Axial Zone of the Pyrenees appears to have a thicker crust (up to 35 km) than the North Pyrenean Zone (20 km). Gravity data (Malzac and Rousseau 1982) do not yield this abrupt feature. Furthermore, these data suggest that the North Pyrenean massifs are rootless fragments of Hercynian basement bounded by thrust faults (Fischer 1984).

2.2.3 Post Pyrenean sedimentation and uplift

South of the Pyrenees the erosion of the mountain chain led to deposition of clastics in alluvial fan environments. These deposits are of Late Eocene and Oligocene age and overlap the waning tectonism (Nagtegaal and De Weerd 1985). Neogene clastic sedimentation occurred in small fault bound basins (Hartevelt 1970).
The erosion and uplift of the mountain chain is characterized by discrete erosion surfaces. Hartevelt (1970) reviews opinions on these features. The "Gipfelflur" in the central Pyrenees at 2900 m altitude may date from upper Miocene peneplanisation (Pannekoek 1937).

CHAPTER 3

THE HOSPITALET MANTLED GNEISS ANTIFORM: GNEISSES, CAMBRO-ORDOVICIAN METASEDIMENTS AND LARGE-SCALE STRUCTURE

The Hospitalet massif (Fig. 3.1) consists of an antiformal gneiss core, overlain by metasedimentary rocks (Zwart 1965). The sequence of rocks passing from internally to externally in the massif consists of Cambro-Ordovician siliciclastics, Silurian black slates and Devonian carbonates (Zwart 1965, Verspyck 1965, Cavet 1957, Fig. 3.1, Encl. 1). Due to a complicated tectono-metamorphic history and absence of fossils, the origin of the contact between gneisses and metasediments and the stratigraphy of the Cambro-Ordovician metasediments are poorly understood (Chapter 2). This chapter presents data on the lithology of the gneisses, Cambro-Ordovician metasediments and their mutual contact. The data mainly follow from investigations in the eastern and western terminations of the massif.

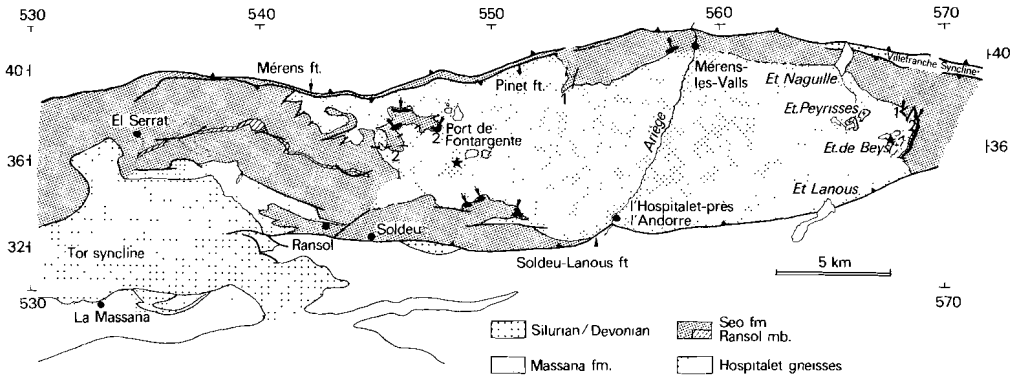

Fig. 3.1 Distribution of lithologies in and around the Hospitalet massif. The quartzite-marble succession in the Seo fm. near the gneiss-metasediment contact is marked in black and indicated by arrows; 1, 2 denote type 1 and type 2 contact rocks respectively, for explanation see text. Stars denote sample localities of SG 9262 (west, App. 1) and SG 9318 (east, App. 1).

3.1 GNEISSES

The antiformal core of the Hospitalet massif consists for ca. 80 % of a fairly homogeneous augengneiss, the Hospitalet gneiss (Zwart 1965). The thickness of the gneisses exceeds 2.5 km measured perpendicularly to the gneiss-metasediment contact. The gneisses are composed of quartz, feldspar (microcline, albite and andesine), muscovite and biotite. Locally garnet is found and sillimanite occurs in muscovite free rocks.

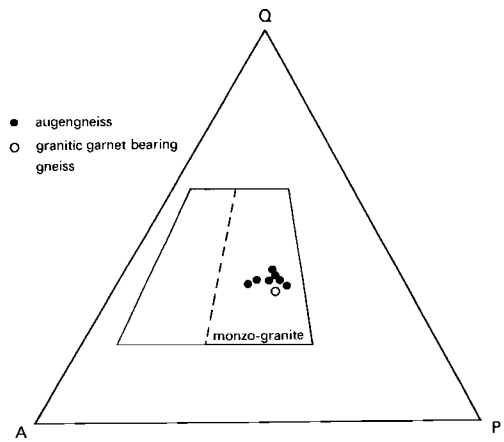

Fig. 3.2 Streckeisen diagram of 7 Hospitalet augengneisses and 1 granitic garnet bearing gneiss; calculated from Zwart (1965) and Appendix 1.

Chemically the gneisses are monzo-granitic in composition (Fig. 3.2), they are slightly aluminous with up to 2.2 weight percent of normative free corundum. They resemble an S-type granite (Chappel and White 1974), although the A/K (Al_2O_3/K_2O+Na_2O+CaO) ratio is very close to 1.1. The rocks have a medium to coarse grained matrix in which up to 5 cm large K-feldspar porphyroclasts occur (Fig. 3.3). Matrix constituents occur as individual crystals, as aggregates up to several centimeters or as elongate seams in the case of micas. Shape and orientation of these features define the foliation which curves around the augen. The K-feldspar porphyroclasts sometimes contain concentrically arranged biotite platelets parallel to cleavage traces and outlines (Fig. 3.3). Such a disposition of inclusions in large K-feldspar crystals indicates a magmatic megacryst origin (Frasl 1954, Hibbard 1965).

Fig. 3.3 Relatively low deformed Hospitalet augengneiss. Note the concentrically arranged biotite platelets parallel to the outlines of the K-feldspars above the lense cap.

Other features which indicate derivation of the gneisses from an originally magmatic body are (1) the homogeneity of the rock mass (Zwart 1965) and (2) the (rare) occurrence of thick coarse grained feldspar rich bands, which are interpreted as a magmatic layering. Dark coloured fine grained biotite rich rocks are found in trails of up to 1 m long lenses parallel to the foliation. These rocks are interpreted as basic xenoliths or relics of a basic layering, as exemplified by a 50 cm thick layer which shows a decrease in biotite content and consequently grades into a fine grained leucocratic gneiss towards its present top.

The Hospitalet gneisses have been intruded by bodies and dykes of granite, pegmatite and aplite (App. 2) and late veins of quartz and tourmaline. A sequence of intrusive events, deduced from contact relationships, is summarized in Fig. 3.4. All rock types have been deformed, with relatively narrow dykes folded or boudinaged and larger bodies developing a shape fabric of the constitutive minerals.

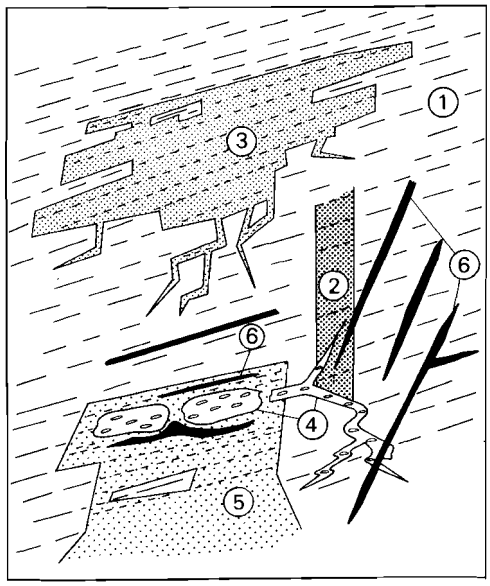

Fig. 3.4 Sequence of intrusive events in the Hospitalet gneisses.
(1) Hospitalet gneiss, (2) granitic garnet bearing gneiss, (3) granitic quartz feldspar gneiss, (4) biotite aplites, (5) granitic two mica gneiss, (6) aplites and pegmatites.
The upper part of the figure is a sketch profile of the cliff SE of Et. d'En Beys (Fig. 3.1; 568-36). The top of the sheet (3) lies ca. 200 m below the gneiss-cover contact. The lower part of the figure refers to the situation around and to the north of Et. de Peyrisses (Fig. 3.1).
Scale impression: sheet (3) is ca. 200 m thick. Vein thickness (4, 6) and blocks of Hospitalet gneiss in (3) and (5) exaggerated.

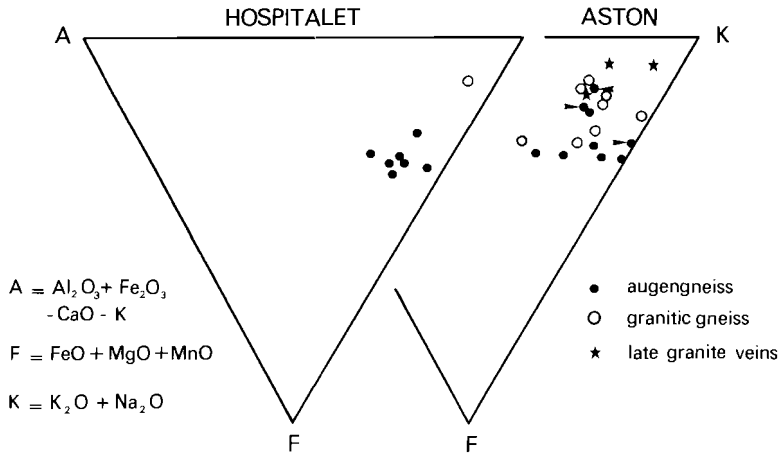

Fig. 3.5 AKF diagram of various rocktypes in the massifs of Hospitalet and Aston, calculated from Zwart (1965) and Appendix 1. The arrows denote samples taken near or from within the Ax-les-Thermes granite (Zwart 1965). The extreme compositions of these rocks probably indicate (partial) re-equilibration of the augengneiss with this younger intrusive material. Note the relatively large variation in A/K ratio in the Aston massif.

Comparison with the Aston massif shows that the augengneisses in the Hospitalet massif are texturally and chemically similar to those in the Aston massif (Zwart 1965, Verspyck 1965, Fig. 3.5). Furthermore, biotite aplite veins (Fig. 3.4, App. 2), granitic garnet bearing gneisses (Fig. 3.4, App. 2) and mappable granite intrusions occur in both massifs. This suggests that both massifs went through a similar geological history of intrusive events.
The intrusives may have formed in the late stages of the plutonic event in which the protolith of the augengneisses formed. However, part of the intrusives may have formed dictinctly later in the geological history of the massifs and were derived from the augengneisses or from underlying rocks. This possibility hampers a straightforward correlation between various rocktypes as suggested by Jäger and Zwart (1968). This weakens their argument that intrusion of the protolith of the gneisses took place in Ordovician times.

3.2 THE GNEISS-METASEDIMENT CONTACT

Contact relationships and associated lithologies

The contact between the orthogneisses and the overlying metasediments is sharp. No discordant relationships, such as offshoots of gneissose material into the metasediments have been observed.

The gneisses near the contact differ from the bulk of the gneisses; they can be separated in two groups (Fig. 3.1): (1) platy fine grained micaceous gneisses with quartz and feldspar augen up to 1 cm and (2) gneisses in which the augen gradually disappear towards the contact. The upper 20 m of these gneisses are fine to medium grained leucocratic rocks with some small K-feldspar augen and little biotite. These rocks may show parting parallel to the gneiss-metasediment contact and oblique to the gneissossity. A good example is west of the Port de Fontargente (Fig. 3.1), where the upper part of these rocks shows a repetition of thinly bedded gneissose material and biotite schist and in this manner grades into the overlying biotite schists. This succession is folded with the foliation in the gneisses and schists as axial plane structures.

The lowermost part of the metasedimentary envelope of the Hospitalet

gneisses often contains lenses of fine grained leucocratic quartz feldspar rock up to 1 m long. Sheets of gneiss up to 10 m thick intercalated in the metasediments have been observed in two locations in the eastern part of the massif.

About 10 to 40 m above the contact a discontinuous up to 40 m thick sequence of marbles and quartzite is found. Both pure calcite marbles and vesuvianite-garnet-diopside marbles occur. The quartzites are carbonate rich and usually pale coloured. The largest outcrop is found in the eastern part of the massif (Fig. 3.1).

Interpretation: the nature of the gneiss-metasediment contact is usually considered to be primary in origin, either intrusive or erosive. The absence of clearcut erosional unconformities led Zwart (1965, 1979) to suppose an intrusive nature of the contact, associated with emplacement of a batholith in Ordovician times. Indications for an intrusive nature of the contact, however, are also lacking: (1) no clearcut intrusive contacts have been observed and (2) no indications have been found for a shallow contact metamorphism which predates the formation of the Hercynian foliation in the massif.
Such phenomena may have been wiped out by later deformation and metamorphism but one expects regions where they have been preserved.
Indications for one or the other origin would be expected to be found in the lowermost metasediments and the uppermost part of the gneisses. However, these rocks may be interpreted in several ways. For example, the fine grained and bedded upper part of the gneisses may be interpreted as (1) a chilled margin and the interleaving of schists and gneisses on top of this as offshoots of the granite, now deformed and rotated into parallelism with the contact, or, alternatively, (2) as arkose sedimentation gradually changing in a sedimentary environment dominated by psammites and pelites, now converted to biotite schists. Cavet (1957) described micro granite-rhyolite and minor andesite intercalations of "volcano-sedimentary origin" in the lowermost metasedimentary sequences on top of the Canigou-Carança massif, another possible interpretation of the observed features.
The nature of the contact is tectonic at present and, although no indications for large-scale movement across the contact are found, the rocks near it suffered from all the deformation episodes in the massif. The fine grain size of the first group of rocks at the contact is, in this respect,

interpreted as deformation induced grain size reduction.

At the scale of the massif a striking aspect of the lowermost metasediments is the occurrence of the discontinuous marble-quartzite sequence near the contact. No comparable lithological sequence has been found in the Cambro-Ordovician succession and it seems most likely therefore that only one level is present which follows the contact throughout the massif. This configuration suggests an original erosive nature of the contact as it seems improbable that intrusion of magma would be parallel to bedding on this scale. The situation is similar to the massif of Canigou-Carança (Cavet 1957, Guitard 1970).

3.3 CAMBRO-ORDOVICIAN METASEDIMENTS

In the Pyrenees the Cambro-Ordovician mainly is a succession of siliciclastics (Cavet 1957, Hartevelt 1970, Fig. 3.7). In the Hospitalet massif two formations have been distinguished, the Seo formation and the overlying Massana formation (Encl. 1, Figs. 3.1, 3.6, 3.7). Both formations are cut by dykes of quartz-(feldspar)-porphyry, aplite and diabase (App. 2). Furthermore, they contain conspicuous horizons of brown weathered white phyllites and quartzites, and concretions of calc-silicate rock.

3.3.1 Seo formation

The Seo formation (Hartevelt 1970) mainly consists of an unfossiliferous, at least 2 km thick monotonous alternation of laminated to thinly bedded psammites and pelites. In the lower part some thin marble intercalations occur. Deposition took place in a shallow marine environment (Hartevelt 1970). At chlorite-muscovite grade the rocks vary in colour from pale grey to dark grey and black. At higher metamorphic grades grey phyllites and brown schists occur. Some variation in composition, colour and pelite/psammite ratio is present (Fig. 3.6), but recognition of this aspect is guided by the presence of three marker beds, the Ransol formation of Zwart (1965). This formation has been ranked as a member in the Seo formation by Hartevelt (1970). Since it proves impossible to distin-

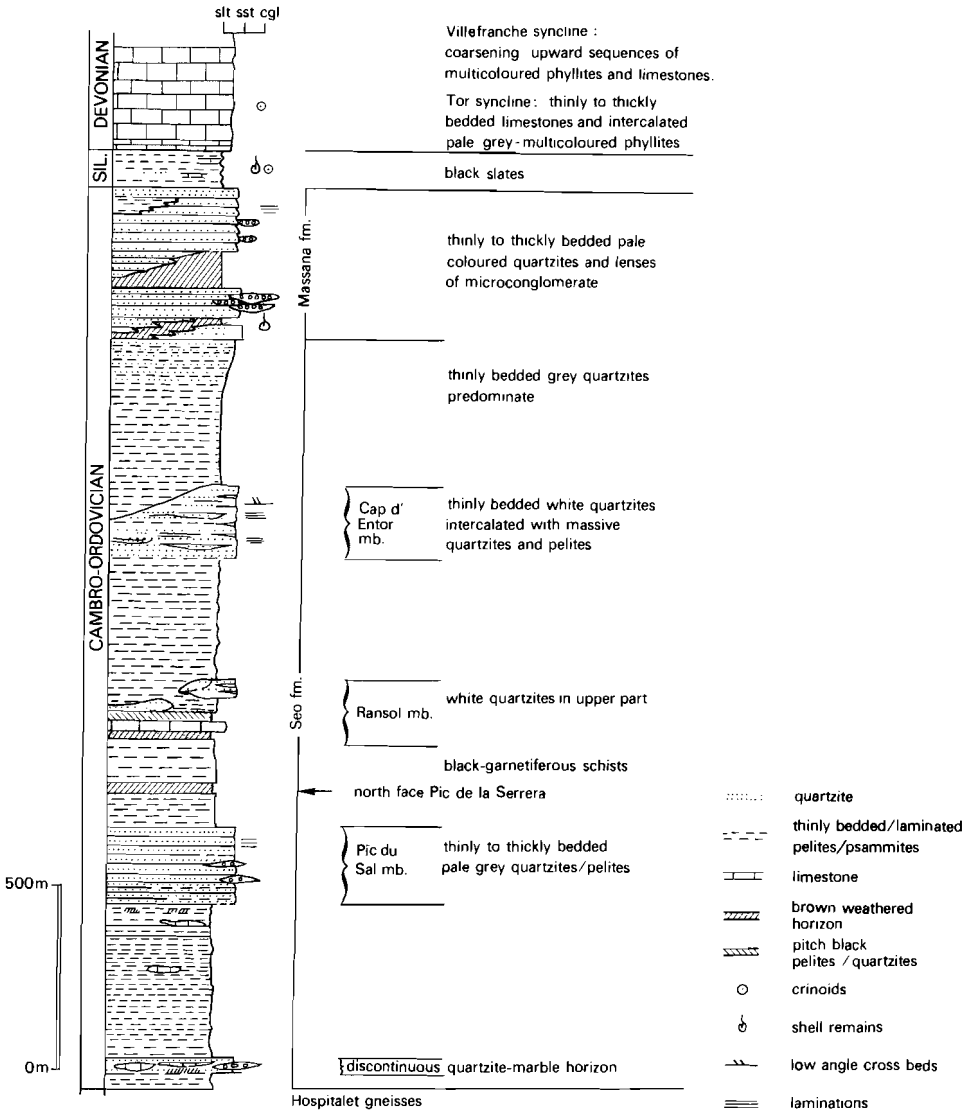

Fig. 3.6 Lithological column of the metasediments in the Hospitalet massif, restored for non-homogeneous deformation. The Devonian carbonates of the Villefranche syncline contain the M. Devonian conodont species Icriodus sp.. The succession is similar to the lowest carbonate sequence of the "serie de la Fajolle" of Raymond and Weyant (1982).
slt = siltstone, sst = sandstone, cgl = conglomerate

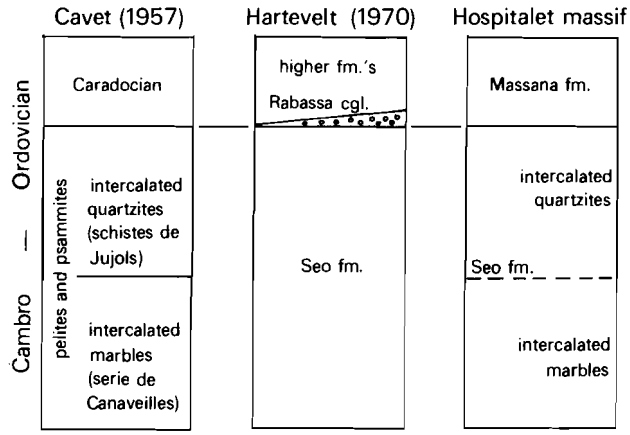

Fig. 3.7 Correlation of the Cambro-Ordovician stratigraphy in the Pyrenees. According to Soula (1982) the lowest part of the succession may be Proterozoic in age.

guish underlying from overlying rocks whenever these marker beds are absent the three marker beds are considered as individual members in this study (Fig. 3.6, Encl. 1).

The marble horizon of the Ransol member consists of pale grey to white calcite marbles, containing quartz, talc and tremolite at higher metamorphic grades. Its lower part is characterized by an alternation of thinly bedded marbles and psammites, which at higher strain gives way to a strongly folded marble with rounded fragments of this more competent material. The thickness of the layer is usually less than 40 m, but it is up to 100 m thick and intercalated with brown weathered horizons in the west part of the region (Encl. 1), a feature possibly explained by folding. Thickly bedded white quartzites mark the upper 20 m of the member in the east part of the map area, whereas towards the west a 50 m thick level of thinly bedded pale coloured quartzites is found at some distance above the black lithologies.

Correlation: The three members in the Seo formation have been recognized further west (Lleret-Bayau series of Zandvliet (1960), Zwart 1965). However, most studies of the Seo formation reveal one quartzite level only

(Hartevelt 1970), which may be correlated with the highest quartzite member in the Hospitalet massif.
The Seo formation is far thicker than previously thought. The general absence of the other marker beds west and southwest of the massif can therefore be explained as due to insufficient depth of erosion rather than due to stratigraphic reasons (cf. Hartevelt 1970). Furthermore, thinning of the formation towards the north, as indicated by Hartevelt (1970) is improbable.
The stratigraphy of the metasediments in the western Aston massif (Verhoef et al. 1984) is still obscure. In this region the Merens shear zone (Fig. 3.1) has an offset probably less than 1 km. Hence lithologies on both sides of this structure must be similar. The Etang Blaou series (McCaig 1983) in the Aston massif is remarkably similar to the Ransol member. Regarding the uniqueness of this marker in the Hospitalet massif it is tentatively suggested that the Etang Blaou series is its high metamorphic equivalent.

The Seo formation in the western Hospitalet massif is similar to successions in the eastern Pyrenees (Cavet 1957, Fig. 3.7) in that the lower part contains limestones and the upper part is devoid of such rocks (Figs. 3.6, 3.7). This implies a larger uniformity of the deposition area of the Seo formation than previously thought.

3.3.2 Massana formation

The Massana formation (town of la Massana;532/28; Fig. 3.1) is defined as the clastic upper part of the Cambro-Ordovician. It overlies the Seo formation with a gradational contact and is abruptly overlain by the black slates of the Silurian. A division can be made in a lower part, which comprises mappable conglomerate lenses and brown weathered horizons, and an upper part which is a quartzite-pelite alternation. The lower boundary is taken at the first occurrence of pale coloured quartzites, that may coincide with the occurrence of a brown weathered horizon (Fig. 3.6, Encl. 1). Lense shaped bodies of conglomerate, up to 200 m long occur circa 100 m above the base of the formation. The conglomerates consist of up to 50 cm thick beds of usually monomict quartz conglomerate with a pebble size not exceeding 1.5 cm. Graded beds and EW directed channels

occur.
The quartzites of the formation comprise laminations, fining upward beds and rhytmic bedding.

South of the Tor syncline (Fig. 3.1) the quartzites of the Massana formation are overlain by dark grey carbonaceous slates (Estana formation of Hartevelt 1970), which in turn are overlain by quartzites (Bar quartzite of Hartevelt 1970). These formations have not been found north of the Tor structure.

Correlation: The Massana formation is probably best correlated with the Ordovician Cavá formation of Hartevelt (1970), which implies a similar age for the Massana formation. Hartevelt (1970) indicates a general wedging out of the Cavá formation to the north. In the Hospitalet massif a thickness of ca. 400 m is reached and northwest of the Aston massif a similar succession is found over 1 km thick. Correlation implies strong thickness variations of the Cavá formation across the Axial Zone.
The conglomerates in the Massana formation occur at a stratigraphic level similar to the Rabassa conglomerate (Figs. 3.6, 3.7). Correlation between the two is doubtful because of the differences in lithology, absence of continuity of beds and the presence of micro quartz conglomerates at other stratigraphic levels in the Massana formation.

3.4 STRUCTURE: THE RANSOL SYNCLINE

The interpretation of the lithological succession ascribed to the Cambro-Ordovician is intimately related to the interpretation of the polyphase deformation history of these rocks. In the west part of the Hospitalet massif Zwart (1963a, 1965) inferred the presence of a large scale synclinal structure, the Ransol syncline (Fig. 3.8). The present author doubts the existence of this structure since the distribution of lithologies over the area (Encl. 1, Fig. 3.8) shows no mirror image repetition of strata as would be expected across the axial trace of a fold. Furthermore, no changes in cleavage bedding relationships of any of the deformation phases in these rocks (Chapter 4) have been found to support the existence of the structure. Finally, the conglomerate layer in the "overturned south limb" of the structure youngs to the south, which ex-

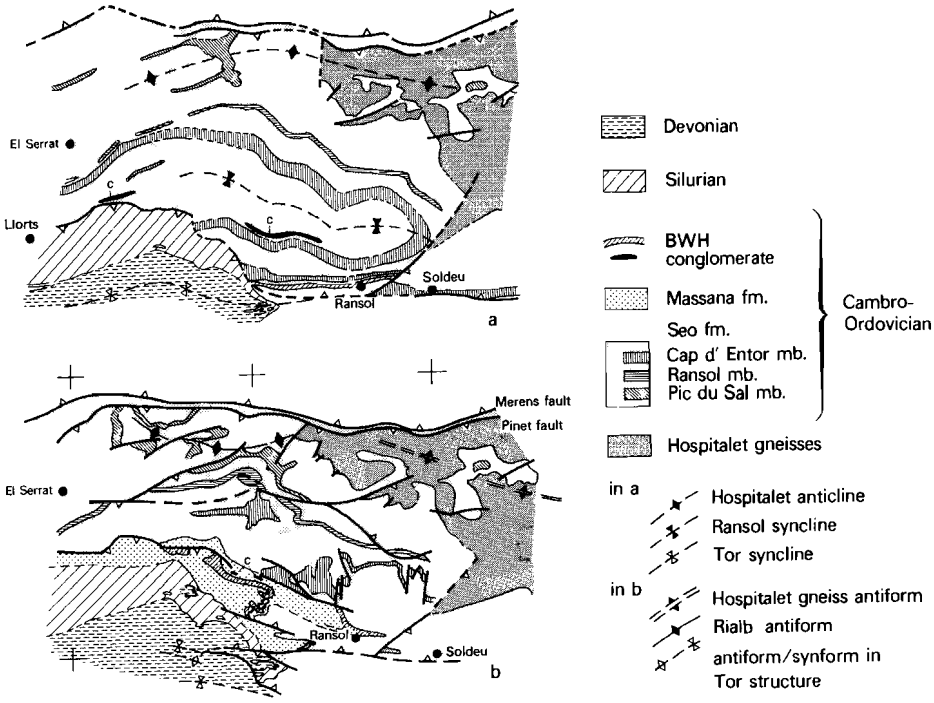

Fig. 3.8 Interpretation of the distribution of lithologies SW of the Hospitalet gneisses, (a) according to Zwart (1965), (b) present interpretation.

cludes the structure from being a syncline.
Remapping and structural analysis show that the lithological succession in the Cambro-Ordovician in fact represents one single stratigraphic pile, which is at least 2.5 km thick when corrected for non-homogeneous deformations.

3.5 SUMMARY

The disposition of rocktypes in the Hospitalet massif suggests a geological history in which the protolith of the augengneisses probably served as a basement to Paleozoic sedimentation. The age of this protolith, at that time a relatively undeformed megacryst granite, is considered

to be lower Cambrian. This conforms with the age determinations by Vitrac and Allègre (1971) of other massifs. The sedimentation pattern of the lower sequences deposited upon the unroofed megacryst granite, appears to be quite uniform from the Hospitalet massif towards the eastern Pyrenees, although in the latter area relatively more marble intercalations occur. Thereafter, a shift in sedimentation occurred whereby carbonate sedimentation ceased.

During the Hercynian orogeny the granite and its ca. 5 km thick sedimentary cover were involved in the formation of an anticlinal structure.

This geological history is typical for mantled gneiss dome terrains: older (basement) granite or gneiss is incorporated in domal or antiformal structures which are mantled by an originally discordantly deposited sedimentary cover (Eskola 1949, Henderson 1969, Thompson et al. 1968, Stephansson and Johnson 1976, Kröner 1984). Zwart (1963a) noted that the shape of the gneiss cored massifs in the Pyrenees deviates from the typical mantled gneiss dome shapes as described by Eskola (1949). However, since the term refers to a broad group of domal and/or antiformal structures, the Hospitalet massif can be classified as a mantled gneiss antiform.

APPENDIX 1

	SG 9262	SG 9318
SiO_2	71.18	72.62
TiO_2	0.47	0.02
Al_2O_3	14.14	13.42
Fe_2O_3	0.88	0.33
FeO	2.28	0.95
MnO	0.03	0.02
MgO	0.81	0.07
CaO	1.61	0.79
Na_2O	3.10	3.72
K_2O	4.22	4.66
P_2O_5	0.22	0.04
H_2O	1.25	0.68
	100.19	97.32

Whole rock chemistries of 1 Hospitalet gneiss and 1 granitic garnet bearing gneiss analysed by the service laboratory of the Institute of Earth Sciences, State University of Utrecht.

APPENDIX 2

Intrusives in the Hospitalet gneiss (numbers refer to Fig. 3.4).

(2) Granitic garnet bearing gneiss (SE of the Etang d'En Beys (Fig. 3.1) in a 50 m wide nearly vertical EW trending dyke). The rocks are leucocratic, medium grained, equigranular and consist predominantly of quartz and feldspar and contain minor amounts of biotite and small red garnets. Chemically and texturally these rocks resemble the granitic gneisses and flaser gneisses from the Aston massif (Fig. 3.5). These latter gneisses include the garnet bearing "gneiss de Peyregrand" (Destombes and Raguin 1960). A sedimentary origin of these rocks as proposed by Raguin (1977) is, therefore, highly improbable considering the intrusive contact relationships in the Hospitalet massif.

(3) White granitic quartz feldspar gneiss, devoid of garnet and biotite occur as dykes low in the cliff SE of the Etang d'En Beys and form a body halfway the cliff. Similar rocks are found in the west part of the massif. Contacts with the Hospitalet gneisses are sharp and straight.

(4) Rather widespread are leucocratic biotite aplites, which occur as dykes and intrusive bodies upto more than 100 m across. Distinctive are biotite aggregates upto several centimeters long and elongate in the foliation. Small offshoots are locally devoid of biotite. Texturally these rocks resemble some of the "discordant veins" in the Aston massif (Zwart 1965, fig.28).

(5) Granitic two mica gneiss, composed of medium grained equigranular quartz, feldspar, white mica and biotite occur in mappable bodies around and to the north of the Etangs de Peyrisses. Near the sharp contacts with

the Hospitalet gneisses locally a rim zone is found where concentration of biotite causes a faint mineral fabric, accentuated by the parallel alignment of numerous thin and ocassionally thick and massive pegmatites. Some angular blocks of augen gneiss were found in these granitic gneisses, with the foliation continuous across the contact.

(6) Straight veins of pale grey pegmatite and aplite up to 50 cm thick occur mostly in the east part of the massif. These veins contain K-feldspar, quartz and some tourmaline. Zoned veins are composed of aplite and pegmatite.

Quartz-tourmaline veins occur as infillings of tension and shear joints and display a central quartz rich zone locally. Quartz veins occur throughout the massif, often parallel to the foliation. Both types of veins have been deformed in the later stages of the Hercynian deformation.

Intrusives in the metasediments

The rocks contain the foliation of the surrounding metasediments and have been metamorphosed accordingly.

(1) Quartz-feldspar-porphyries (quartz-diorite porphyries, cf. Zwart 1979) are parallel to bedding and occur in up to 5 m thick layers. The rocks are characterized by bluish quartz phenocrysts and plagioclase phenocrysts. The latter are largely converted to white micas. The fine grained groundmass consists of quartz, feldspar, biotite (or chlorite depending on metamorphic grade), white mica and accessory apatite, zircon and epidote.

(2) Aplite dykes are usually found in the Silurian slates in which their yellowish white colour strongly contrasts with the black colour of the slates. Thickness is usually less than 2 m. Lateral continuity may exceed several hundreds of meters.

(3) Diabase occurs in three isolated outcrops which line up in the general trend of bedding and the foliation which is axial planar to the Tor syncline. The rocks display a relic subophitic texture of plagioclase and pale green amphibole. Biotite, chlorite and albite formed during metamorphism.

CHAPTER 4

AGE RELATIONSHIPS BETWEEN SUPRASTRUCTURE AND INFRASTRUCTURE, AND THE MODE OF GNEISS ANTIFORM FORMATION IN THE HOSPITALET MASSIF

The Axial Zone comprises two main structural domains which have been formed during the Hercynian orogeny, the infrastructure and the suprastructure (Zwart 1963a, 1979, Fig. 4.1). Zwart (1963a) introduced these terms (after Wegman 1935) to differentiate between domains with gently inclined to flat lying foliations and relatively elevated metamorphic grade (infrastructure) and domains with upright EW trending folds, steep foliations and low grade of metamorphism (suprastructure). Both domains comprise Paleozoic metasediments which range from Cambrian to Carboniferous in age. The infrastructure is exposed in several massifs (Fig. 4.1). The five easternmost massifs comprise bodies of augengneiss. Both infrastructure and suprastructure have been intruded by Late-Hercynian batholiths (Fig. 4.1).

A classic problem in the Pyrenees concerns the relation between the infrastructure and the suprastructure. According to Zwart (1963a, 1979), Soula (1982) and Soula et al. (1986) the foliations in the infrastructure and the suprastructure are of the same relative age. According to Matte (1969) the flat lying structures precede the steep structures. Recently, Verhoef et al. (1984) recognized that flat lying structures overprint the steep structures in the western Aston massif (Fig. 4.1). Hence the infrastructure is younger than the suprastructure in that area.

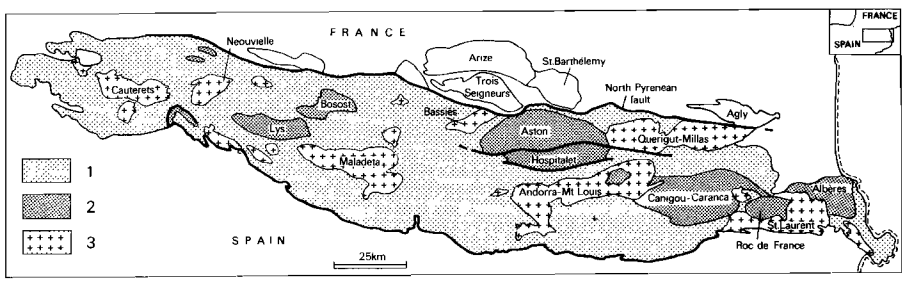

Fig. 4.1 The Hercynian structural domains within the Axial Zone. 1. suprastructure, 2. infrastructure, 3. late Hercynian batholiths.

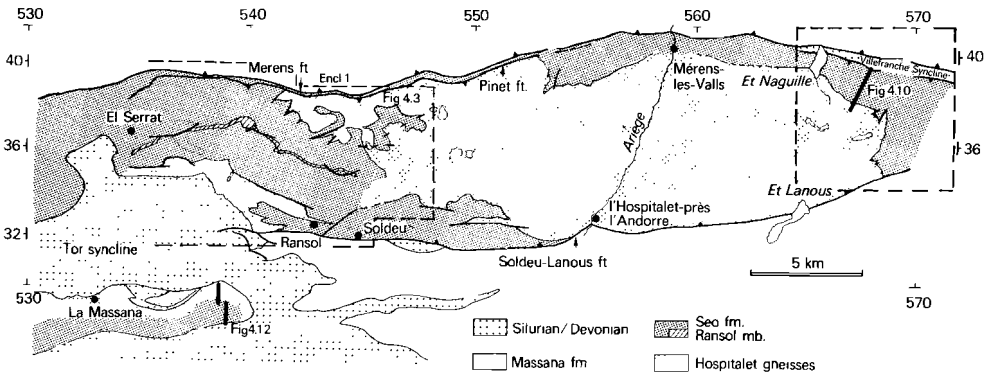

Fig. 4.2 Distribution of lithologies in and around the Hospitalet mantled gneiss antiform. Insets show key-areas and -sections.

Another problem concerns the relation between structures in gneisses, metasediments and the large-scale geometry of the massifs. According to Zwart (1963a) structures such as the Hospitalet gneiss antiform (Figs. 4.1, 4.2) developed prior to the foliation as so-called pre-main phase folds. According to Soula (1982) and Soula et al. (1986) the large-scale geometry of the massifs developed simultaneously with the foliation. They noted a general concordant relationship between foliation and gneiss-cover contacts.

This chapter is concerned with the problems outlined above in the Hospitalet massif (Figs. 4.1, 4.2).

4.1 LARGE-SCALE GEOMETRY OF THE HOSPITALET MASSIF AND ADJACENT STRUCTURAL DOMAINS

The overall geometry of the Hospitalet massif is the least complicated of the five Pyrenean gneiss cored massifs: an elongate doubly plunging gneiss antiform flanked and overlain by outward dipping strata (Fig. 4.2). This configuration is obliquely cut by the Merens and the Soldeu-Lanous shear zones, which define the northern and southern boundaries of the massif respectively. Both shear zones have a consistent north side up sense of shear with a slight dextral component (McCaig 1983,

Encl. 1). The zones are considered to be mainly due to Alpine movements. Minor shear zones splay of the main zones. These zones are associated with folds and cut Hercynian structures. Retrogressive chlorite-grade metamorphism occurs in the highest deformed parts.
North of the Hospitalet massif lies the Aston massif, which is characterized by a sheet of predominantly augengneisses, up to 4 km thick. The gneisses are overlain and underlain by metasedimentary rocks of varying metamorphic grade (Zwart 1965, Verspyck 1965, Laprê 1965, Verhoef et al. 1984).

To the south, between the Hospitalet massif and the batholith of Mt-Louis/Andorra, a zone of low grade metamorphic slates and carbonates is found, folded in EW trending upright folds, with a steep axial plane foliation. This zone is part of the suprastructural domain of the Axial Zone. Southwest of the Hospitalet massif two major folds, the Massana anticline and the Tor syncline occur within this domain. Small-scale structures within these major folds are treated after the description of the small-scale structures in the Hospitalet massif.

4.2 LITHOLOGY

The gneisses which occupy the antiformal core of the Hospitalet massif are mainly coarse grained augengneisses of monzo-granitic composition (Chapter 3). They are at least 2.5 km thick measured perpendicularly to the gneiss-metasediment interface. The metasediments which overly the gneisses comprise three stratigraphic units in normal position, (1) Cambro-Ordovician siliciclastics, (2) Silurian black slates and (3) Devonian carbonates (Chapter 3). The Cambro-Ordovician comprises (a) an at least 2 km thick succession of laminated to thinly bedded pelites and psammites (Seo fm.) with two quartzite dominated members and a marble member in intermediate position, which is overlain by (b) a ca. 400 m thick succession of mainly quartzites (Massana fm., Chapter 3). These sediments have been metamorphosed in a low P/T metamorphic event (Chapter 7) to phyllites and schists which contain porphyroblasts of andalusite, staurolite and cordierite. Metamorphic grade increases towards the gneisses and several mineral zones have been mapped.

The zonation is oblique to the gneiss-cover contact and crosscuts

the antiform: the isograds are more flat lying than the outward dipping gneiss-cover contact.

4.3 WORKING METHOD

The approach adopted to study the mantling sediments and the gneisses of the Hospitalet massif consists of tracing foliations and recording overprinting relationships along continuously exposed sections ("crawling along section structural analysis") combined with convential lithological mapping. Two areas were selected that cover both plunging noses and north and south flank of the structure (Fig. 4.2). The areas were selected assuming cylindricity of the structure which allows projection of one area to the other.

Two schemes for the small-scale deformation history in the Pyrenees have been published (Zwart 1979, Soula 1982). To my opinion the deformation histories put forward do not sufficiently take into account the criticism reworded by Williams (1985), who states that deformation intensity may strongly vary from place to place and correlations on style may prove treacherous. This is especially true in areas comprising different structural domains and metamorphic grades as the Pyrenees. Correlations based on intensity of foliation development (e.g. "main phase") are doubted on the same grounds. These difficulties can be overcome if exposure is continuous; therefore the technique of "crawling along section", although laborious, yields the most reliable results.

4.4 SMALL-SCALE STRUCTURES IN THE HOSPITALET MASSIF (THE INFRASTRUCTURE)

The sequence of deformation phases and their areal distribution in the metasedimentary envelope of the Hospitalet gneisses is based on the sections indicated in Figs. 4.3 and 4.10. Results differ largely from those presented by previous authors (Oele 1966, Zwart 1965, 1979, Soula 1982) and a description of the structures and their overprinting relationships will be presented. Here we are mainly concerned with the deformations which are related to the infrastructure-suprastructure relationship

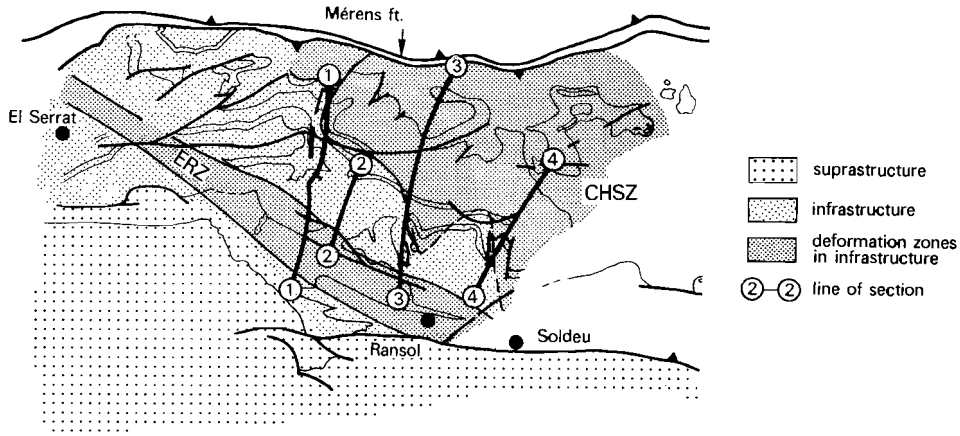

Fig. 4.3 Deformation zones in the metasediments and the gneisses in the western Hospitalet massif. CHSZ: zone of mylonitic strain at the gneiss-metasediment contact. ERZ: zone of refolding SW of the gneisses. Lithological contours from Fig. 4.1 and Encl. 1. Sections refer to Fig. 4.4.

and the formation of the large-scale geometry. In the next chapter younger deformation phases are described.

Throughout these chapters the terms cleavage vergence and fold vergence are used in the sense of Bell (1981) and Weijermars (1982). The terminology of foliation morphology is after Borradaile et al. (1982).

The next sections deal with the small-scale structures in the south flank and north flank of the Hospitalet gneiss antiform. In each of these areas or sections a deformation scheme has been set up. These schemes only apply to the region under consideration and are not directly linked to the deformation schemes in the other areas. A correlation between the schemes is discussed afterwards. "Deformation phase" is used synonymously to "set of deformation structures".

4.4.1 South flank

Detailed structural work has been carried out in the well exposed west slopes of four valleys (Figs. 4.3, 4.4, Encl. 1). A correlation between the sections was made on the similarity of overprinting relationships and the occurrence of several 200-300 m scale folds (Encl. 1). The upper quartzite member in the Seo fm. (Cap d'Entor mb.) was the key

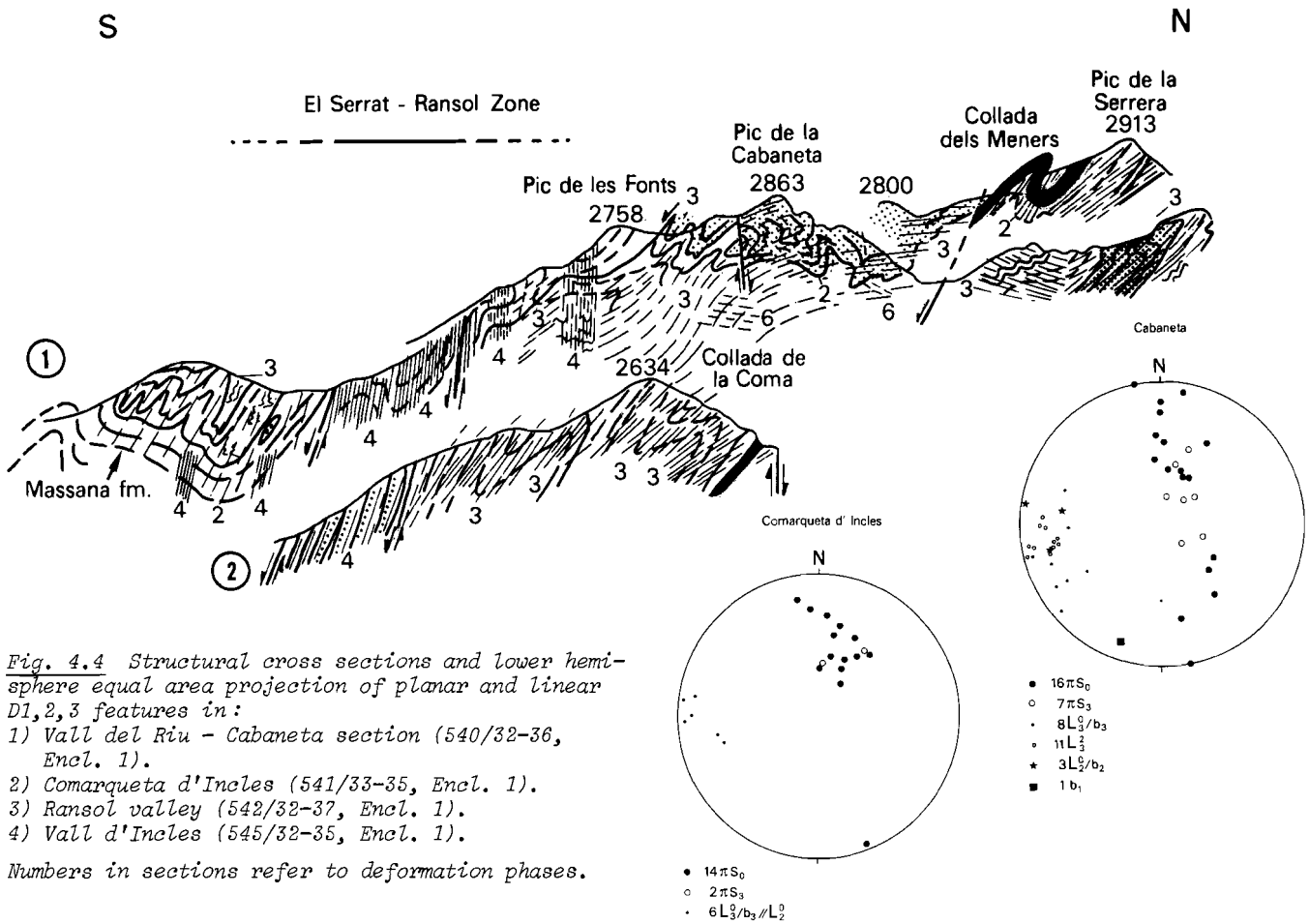

Fig. 4.4 Structural cross sections and lower hemisphere equal area projection of planar and linear D1,2,3 features in:
1) Vall del Riu - Cabaneta section (540/32-36, Encl. 1).
2) Comarqueta d'Incles (541/33-35, Encl. 1).
3) Ransol valley (542/32-37, Encl. 1).
4) Vall d'Incles (545/32-35, Encl. 1).

Numbers in sections refer to deformation phases.

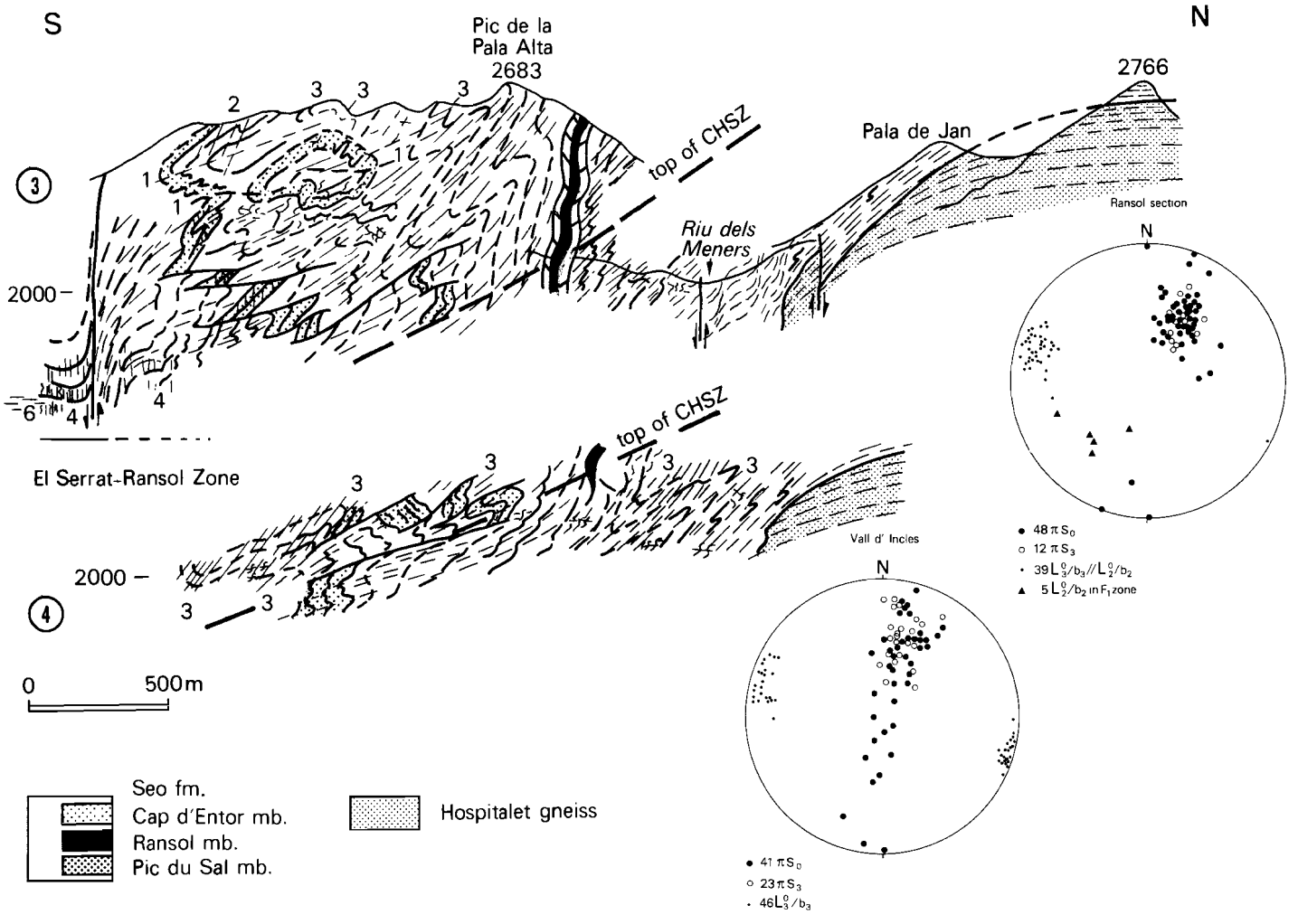
S
N
Pic de la
Pala Alta
2683
2766
Pala de Jan
top of CHSZ
Riu dels
Meners
Ransol section
2000 –
El Serrat-Ransol Zone
top of CHSZ
Vall d' Incles
2000 –
0
500m
Seo fm.
Cap d'Entor mb.
Ransol mb.
Pic du Sal mb.
Hospitalet gneiss
N
• 48 π S0
○ 12 π S3
· 39 L03/b3//L02/b2
▲ 5 L02/b2 in F1 zone
N
• 41 π S0
○ 23 π S3
· 46 L03/b3

horizon in the unraveling of the deformation history. Several deformation phases have been recognized. The oldest deformation structures, all grouped as D1, are preserved only locally. The second and third phases of deformation produced structures which occur throughout the structural sections. Locally these structures are refolded by flat lying open folds. The relationships between bedding, D2 and D3 structures are overprinted and locally obscured in two zones, (1) a 1 km wide zone of mylonitic schists and gneisses at the gneiss-cover contact (section 5.1), and (2) a 1.5 km wide zone of refolding SW of the gneisses, the El Serrat-Ransol zone (ERZ, Fig. 4.3, section 5.2).

D1 structures

This deformation phase comprises all deformation structures which predate D2. D2 serves as a reference deformation phase since these structures are traceable throughout the area.
Some mesoscopic and one macroscopic D1 fold pair occur (Figs. 4.5, 4.6a). D1 folds are tight, their axial planes dip moderately to the NW and fold axes plunge SW. Vergence, where verifiable is SE. No cleavage to the D1 folds has been observed, but its existence is indicated by (a) a lineation which is refolded by D2 folds and (b) the local appearance of S2 as a crenulation cleavage in thin section.
No evidence has been found for a bedding parallel foliation or isoclinal fold phase predating D2.

D2 structures
(upright folds)

D2 structures are mainly preserved in quartzite/psammite layers. D2 folds are found on all scales (Figs. 4.4 - 4.6). The folds are open to isoclinal. Axial planes that are least affected by later deformation are south dipping to upright. The overall vergence is to the north. South vergent D2 folds are in general tighter than north vergent folds, which occur in normally positioned strata, indicating a higher strain in the overturned limbs.

An S2 foliation is only locally preserved in metapelites but is common in quartzose rocks as a centimeter spaced stylolytic cleavage

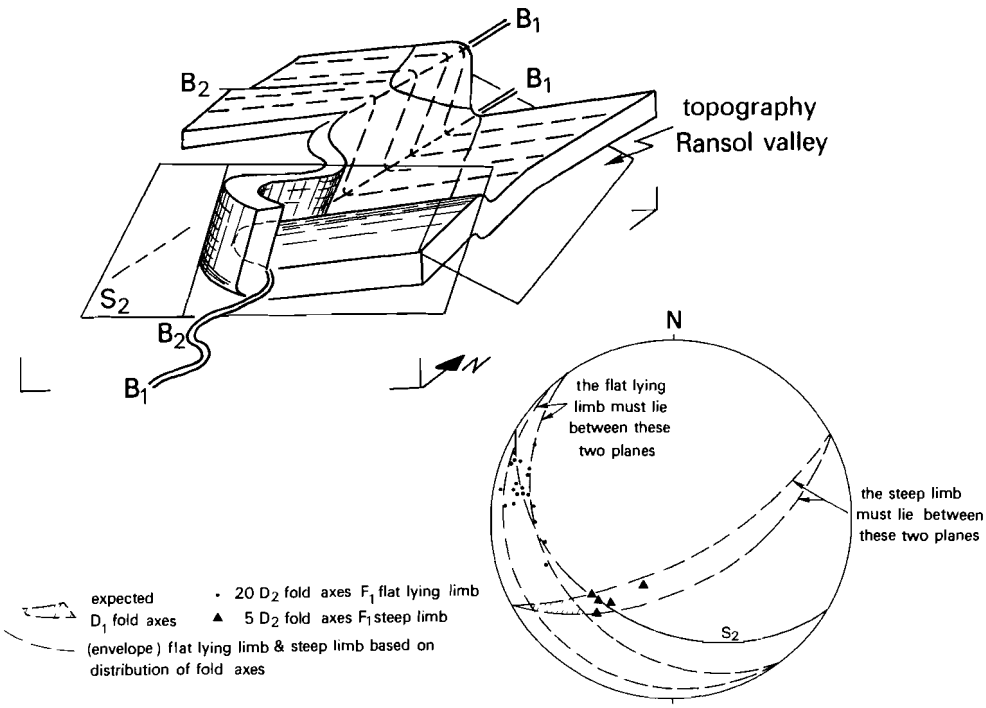

Fig. 4.5 Illustration of the D1 fold pair in the Coma de Ransol section. The block diagram shows "schlingenbau" in the steep limb of the D1 structure caused by the overprint of an inclined S2 and D2 folds. A D2 anticline in the flat lying D1 limb corresponds to a west closing D2 fold in the steep D1 limb and vice versa. The eye shaped outcrop pattern of white quartzites is due to curvature of the D1 fold axes.

The stereogram shows the approximate orientations of the D1 limbs.

(Fig. 4.6a) often most pervasive in inner arcs of buckle folds.

D2 fold axes and cleavage bedding intersections slightly plunge west in the western sections and curve towards WNW-ESE trending towards the east (Fig. 4.4).

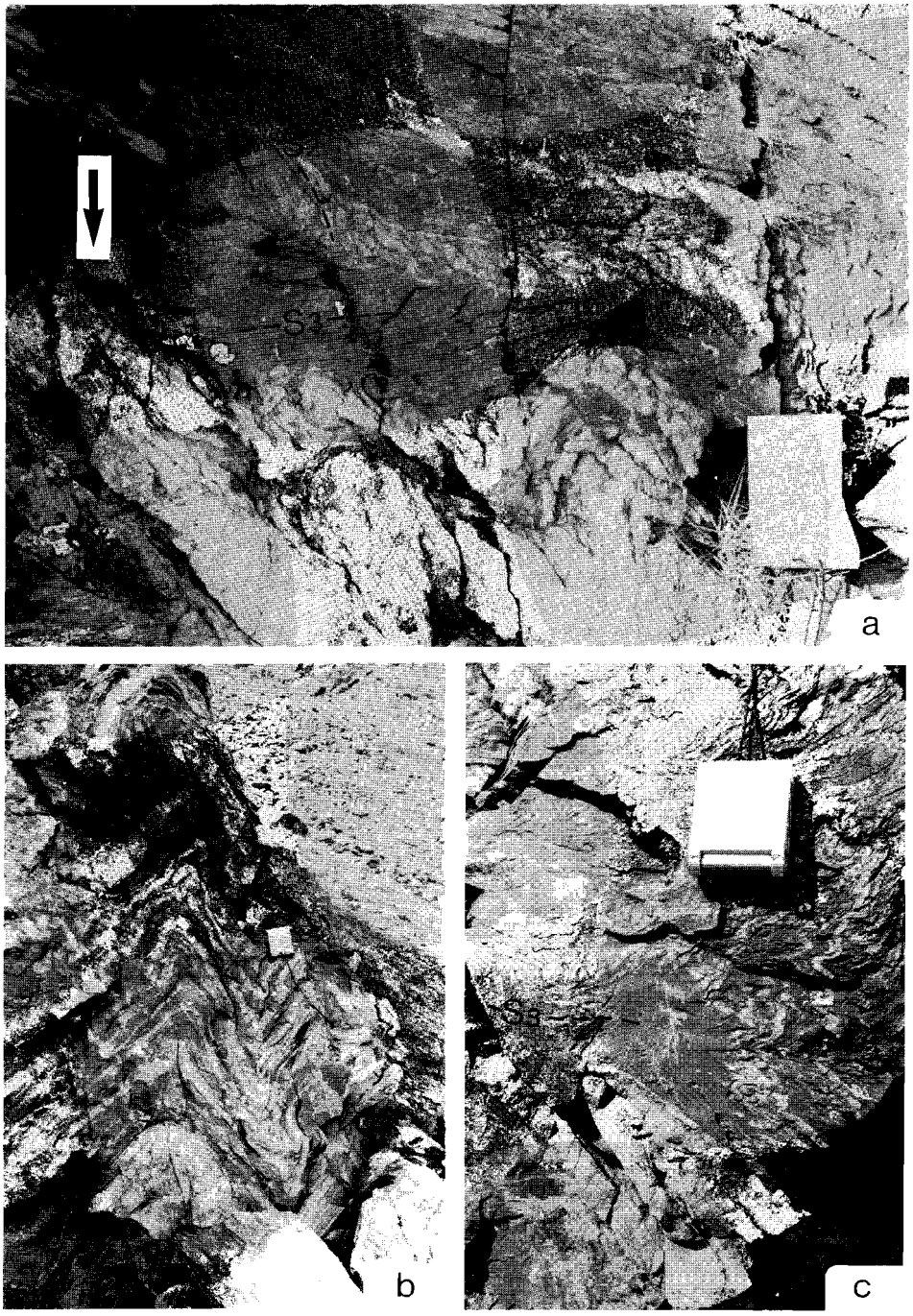
a
b
c

d

Fig. 4.6

a. D1 fold in quartzite layer, refolded by upright D2 folds. Note the presence of a spaced S2 foliation in the quartzites. Within the interbedded metapelites S3 is the main foliation.

b. Upright D2 fold in quartzite-pelite alternation. Note the open D3 folds in the D2 axial trace and the flanks in the upper part of the D2 fold.

c. Tight south vergent D2 fold in quartzite. The pelites above the D2 fold show a well developed S3 foliation and D3 folds in thin quartzites.

d. Detail of the D2 fold shown in b. Note horizontal S3.

e. Thin section of S2/S3 relationship, scale bar indicates 1 mm.

a, b, c, d north is to the right. compass is 10 cm wide. Cabaneta section.

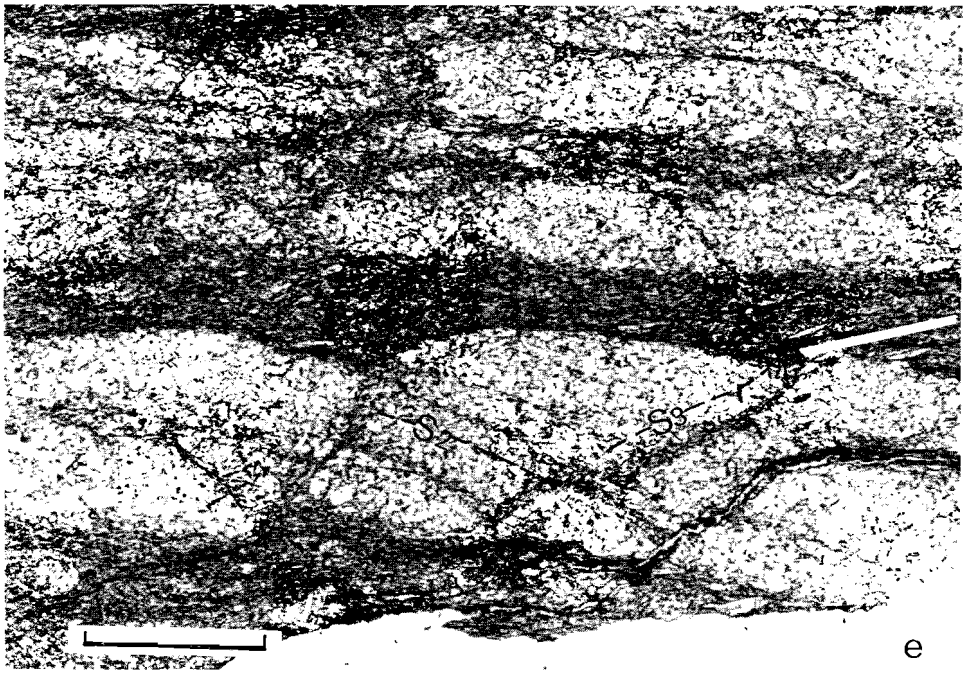

e

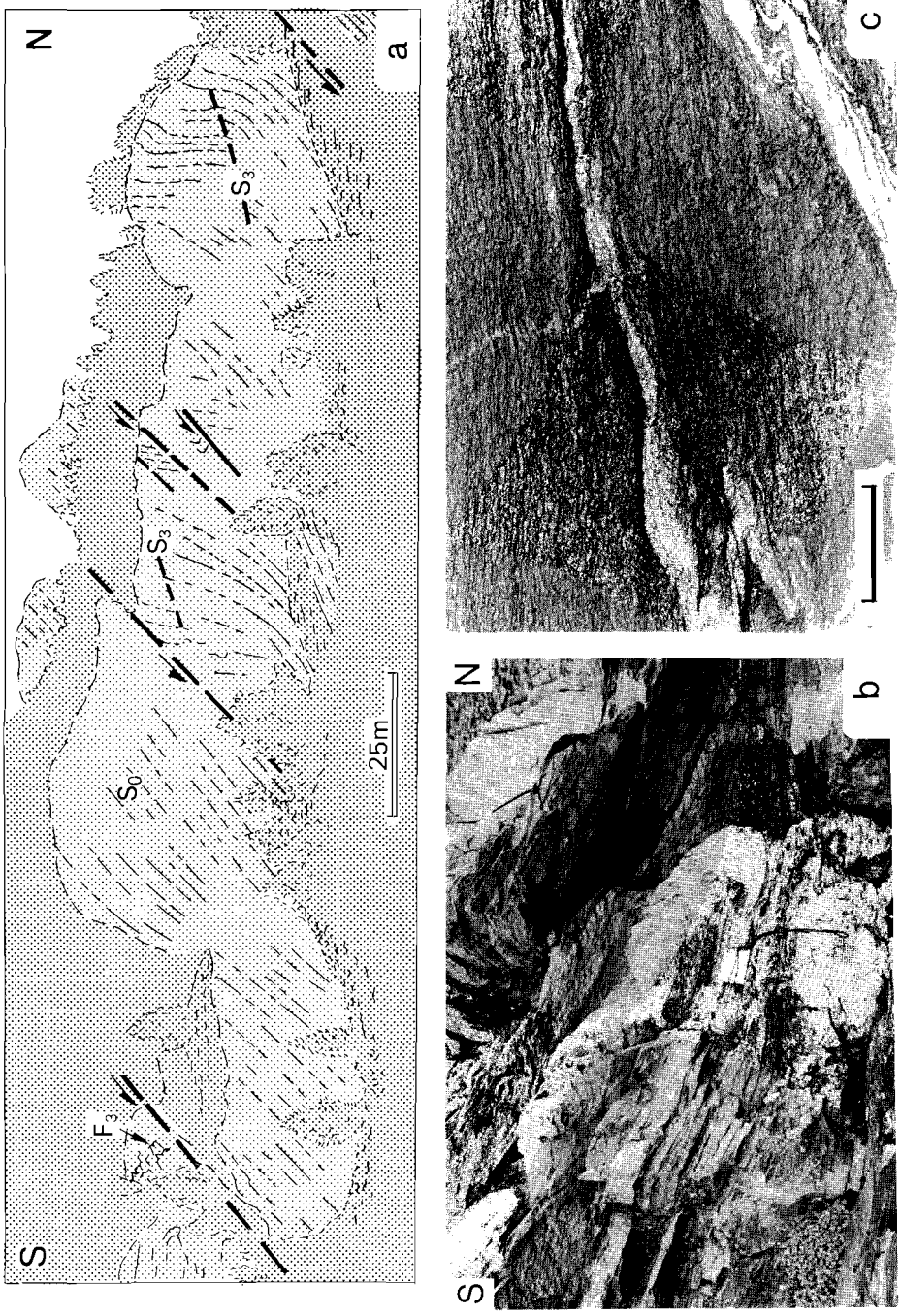
N
S
a
F_3
S_0
S_3
S_3
25m
N
S
b
c

D3 structures
(inclined structures)

D3 structures comprise folds and an axial plane cleavage. Many examples of D2 folds have been found which are transsected by S3 or refolded by D3 folds (Fig. 4.6).
D3 folds have gently inclined to flat lying axial planes (Figs. 4.6, 4.7). Minor folds and cleavage/bedding relationships change vergence at 200-300 m scale (Fig. 4.4, Encl. 1). These larger folds appear disrupted within or below the hinge zones in the quartzites (Encl. 1, Figs. 4.4, 4.7a). The overall vergence of D3 folds and S3/bedding relationships is south. S2/S3 relationships are often symmetrical. S3/bedding intersections and fold axes are in general parallel to the D2 linear structures (Fig. 4.4).

The morphology of S3 varies with metamorphic grade (Fig. 4.8). In low grade metapelitic rocks S3 is the most prominent foliation, developed as a finely spaced differentiated crenulation cleavage. With increasing metamorphic grade S3 becomes the schistosity, marked by a biotite preferred orientation. In this region the S3 foliation often is the most pervasive planar structure and marked as such on the map (Encl. 1).

The relationship between S3 and the gneiss-metasediment interface can be studied in the Vall d'Incles and Coma de Ransol sections (Fig. 4.4). Here the S3 foliation can be traced towards the contact. An angle between S3 and the interface is preserved (Fig. 4.9a), although S3 is deformed in the mylonite zone at the gneiss-cover contact. The S3 foliation dips more gently to the south than the interface and can continuously be traced from the metasediments through the contact into the gneisses (Fig. 4.9b). South vergent folding of the contact has been observed in outcrops outside the structural sections.

◄ *Fig. 4.7*

a. Outcrop of Cap d'Entor quartzites in the Ransol valley. Repetition of the succession is caused by D3 normal faults.
b. Isoclinal D3 fold in Cabaneta section. Note the thinned lower limb.
c. Tight D3 folds at micro-scale. Note the differentiated aspect of the S3 crenulation foliation, which has been crenulated by D4. Ransol valley; scale bar indicates ½ cm.

Fig. 4.8 Variation of S3 morphology with metamorphic grade in a) the upper biotite zone, b) the straurolite zone and c) the staurolite-out zone. Scale bar indicates 200 micron.

Fig. 4.9 ►

a. Field aspect of the angle between the S3 foliation and the gneiss-metasediment contact (Pala de Jan, for location see Fig. 4.4).

b. Hand specimen containing the gneiss-metasediment contact; note the continuity of the S3 foliation and the foliation in the gneisses across the contact (Incles valley); scale bar indicates 2 cm.

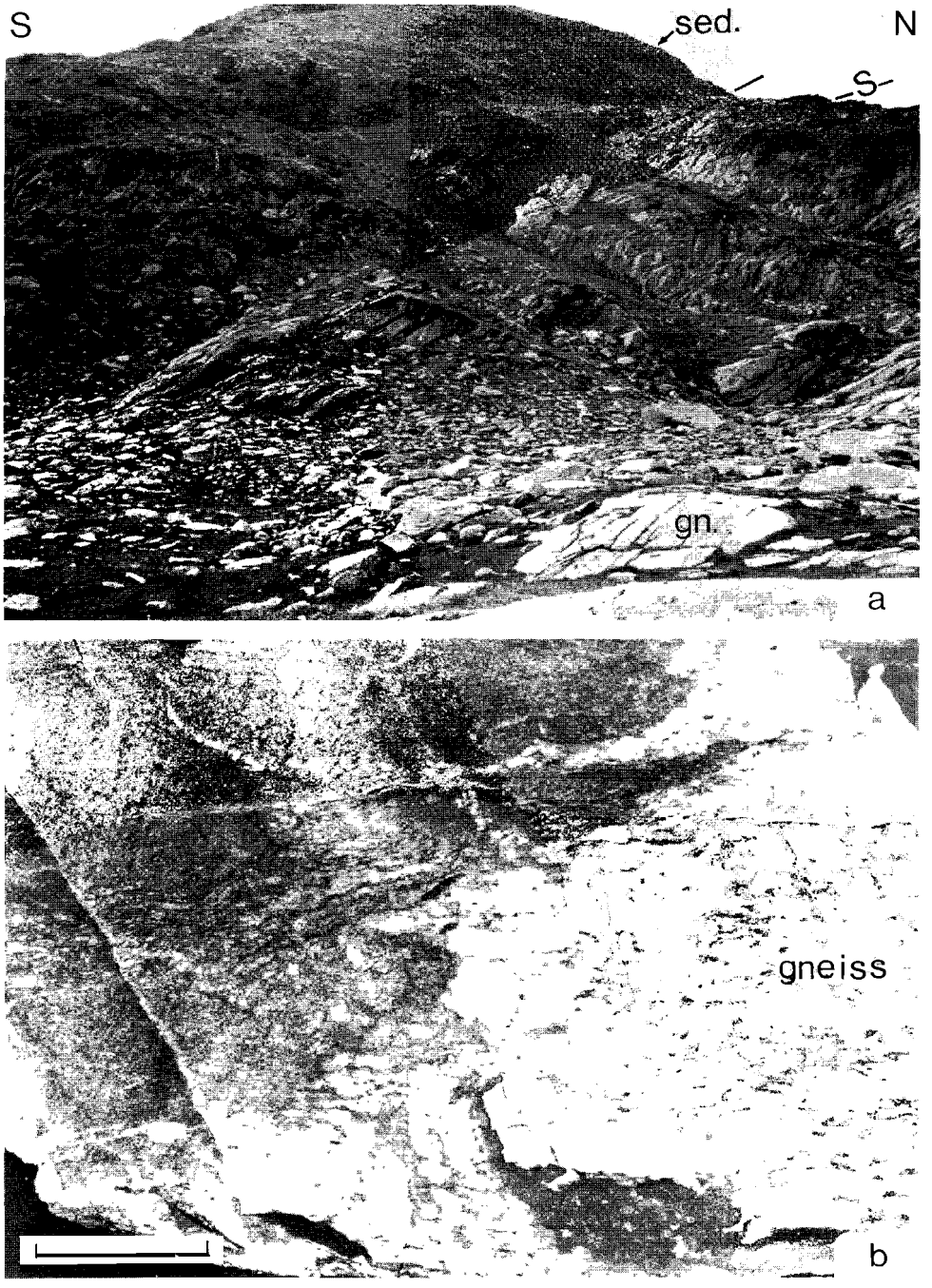
S
sed.
N
S
gn.
a
gneiss
b

Summary

The structural history of the metasediments of the south flank of the Hospitalet gneiss antiform is dominated by two phases of deformation, D2 and D3. The most characteristic overprinting relationship in pelite-psammite alternations is a north vergent S2-bedding relationship in the psammites and a south vergent S3-bedding relationship in the intercalated pelite beds. D2 produced north vergent upright structures. D3 produced gently inclined south vergent structures that become increasingly important towards the gneisses. S3 is the most prominent foliation in the metasediments and it is traceable through the gneiss-metasediment contact into the gneisses.
D1 folds occur only locally but they systematically show moderately NW dipping axial planes, SW plunging foldaxes and SE vergence.
The relationships between D1, D2 and D3 structures are obscured in two zones of later deformation, the E1 Serrat-Ransol zone and a mylonite zone at the gneiss-cover contact.

4.4.2 North flank

A form surface map of the metasediments on the north flank of the Hospitalet gneiss antiform is shown in Fig. 4.10. The map shows a change in the general attitude of the most pronounced foliation, steep N dipping in the north to steep to moderately NE dipping towards the gneisses in the south. This is due to two phases of deformation (D1 and D2) which produced folds and axial plane cleavages. Younger effects comprise locally developed crenulations and zones of high strain, the widest of which occurs at the gneiss-metasediment contact (Chapter 5).

D1 structures
(upright structures)

Upright tight folds, associated with a steeply oriented axial plane cleavage are found in the north part of the section in steep quartzose and conglomeratic beds. Folds and cleavage/bedding relationships are south vergent. The structures face upwards. Fold axes and cleavage/bedding

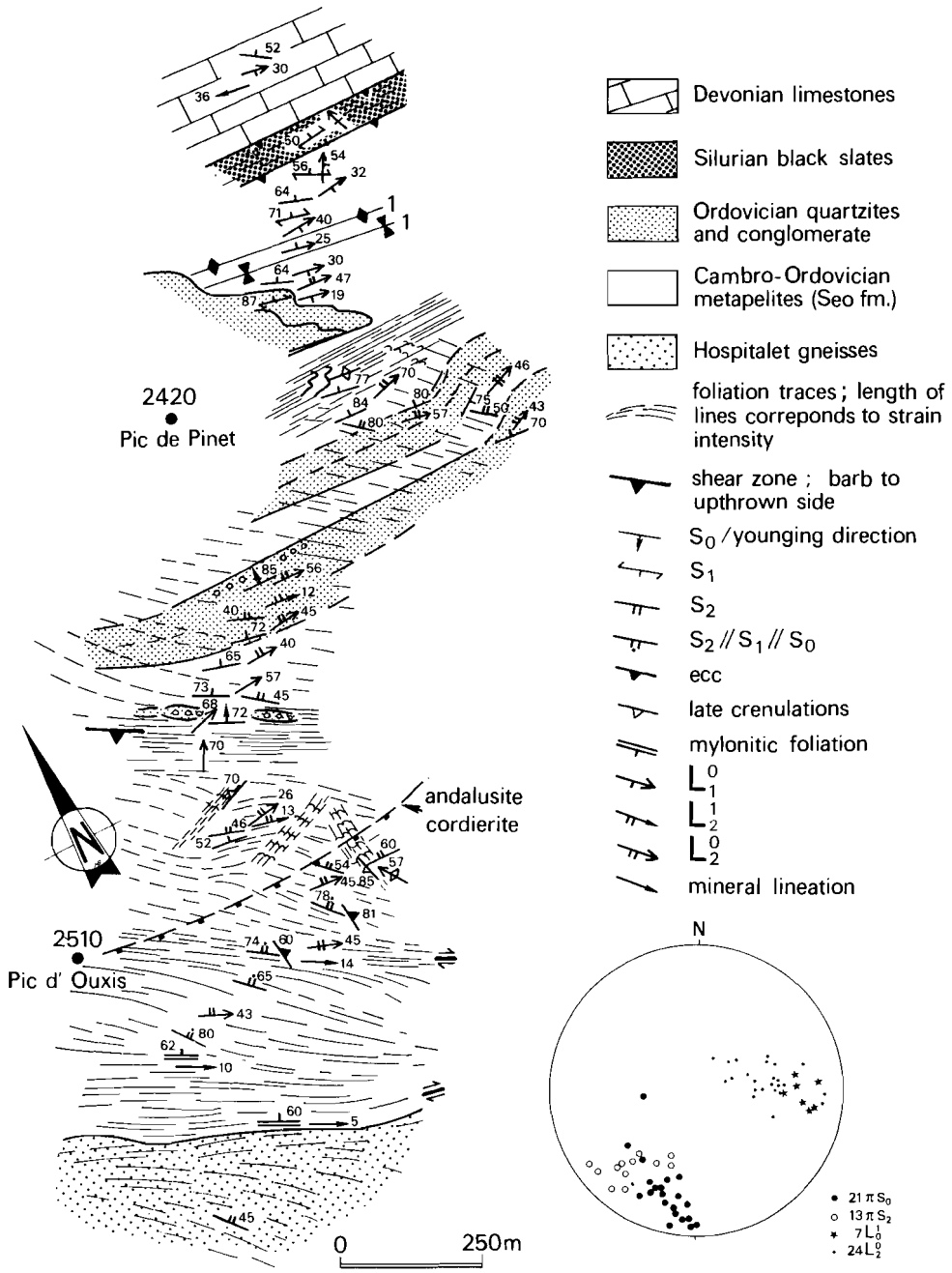

Fig. 4.10 Structural map and orientation data across the north flank of the Hospitalet mantled gneiss antiform (for location see Fig. 4.2). Senses of shear in the post-D2 high strain zones have been deduced from curvature of D2 lineations.

intersections plunge shallow to the east (Fig. 4.10).

D2 structures
(inclined structures)

This deformation phase is characterized by few folds and a cleavage (S2), which are locally developed in the north part of the section where they overprint the upright D1 folds and cleavages. D2 folds are open to tight and vary in style between various lithologies.
S2 is the most prominent foliation in the metapelitic sequence adjacent to the gneisses where it is a finely spaced differentiated crenulation cleavage. Biotite plates are found parallel to S2 near the gneisses.
D2 fold axes and cleavage/bedding intersections moderately plunge E-ENE.
In post D2 high strain zones lineations curve towards the attitude of the mineral lineations in these zones. The original relationship between S2 and the gneiss-metasediment contact in Fig. 4.10 is obscured by such a high strain zone. Mylonitic schists and gneisses are exposed and no angle between the foliation and the contact is observed. Outside this high strain zone both the foliation in the gneisses (in the south) and in the schists (in the north) dip more shallow to the north than the contact. Several hundreds of meters lower in the topography isolated outcrops indicate an angle between the foliation and the interface with a north vergent relationship. Apparently, the foliation in the gneisses is continuous with the S2 foliation in the schists. Here the mylonite zone is more weakly developed than in the map shown in Fig. 4.10.

Summary

The structures in the metasediments on the north flank of the Hospitalet gneiss antiform are characterized by upright south vergent D1 folds and cleavages away from the gneisses, which are overprinted by north vergent moderately inclined D2 structures. Towards the gneisses S2 becomes the most prominent foliation in the metasediments. It is continuous with the foliation in the gneisses. The geometry is cut by several high strain zones.

4.4.3 The gneisses

In the gneisses fewer structures occur than in the metasediments as folds are generally absent. A single gneissic layering has been observed in the areas investigated. This foliation is defined by (1) shape fabrics of quartz, feldspar and biotite aggregates, and (2) a grain shape preferred orientation of micas and K-feldspar augen. This fabric is deformed in shear zones where it is overprinted by secondary fabrics (Chapter 6). The foliation marks the antiformal shape of the massif. An angle between the foliation in the gneisses and the gneiss-metasediment contact has already been documented. The foliation is more flat lying than the outward dipping gneiss-cover contacts. Hence, relationships are symmetrical: north vergent north of the gneisses and south vergent south of the gneisses. On top of the gneisses south vergent relationships occur. Hence, the gneiss antiform is not upright but slightly overturned to the north (Fig. 4.13).

The elongate aspect of the mineral shape fabrics defines a linear fabric. This lineation trends EW. Another lineation, a faint finely spaced quartz-mica grain shape preferred orientation, can also be found. The latter lineation consistently trends WNW-ESE at a ca. 30^{o} angle to the main lineation and can be shown to be a stretching lineation (Chapter 5).

4.5 SMALL-SCALE STRUCTURES IN THE MASSANA AND TOR FOLDS (THE SUPRASTRUCTURE)

The Massana and Tor structures (Fig. 4.2) are major upright folds which are assigned to the suprastructural domain around the Hospitalet massif (Zwart 1979). In this section small-scale structures within these folds are described and a correlation is proposed between this typical suprastructure domain and the infrastructure domain described above.
Mapping and structural analysis of the Massana and Tor structures reveals parasitic folds with various wavelengths and amplitudes (Encl. 1). A cleavage which is axial planar to the parasitic folds is developed everywhere and is the most prominent structure locally. The cleavage differs in each rocktype (Fig. 4.11). In the low grade metapelitic rocks a continuous (slaty) cleavage is found. In hinge zones of buckle folds a crenulation of a continuous mica fabric is visible. Quartzites show a variety in spaced

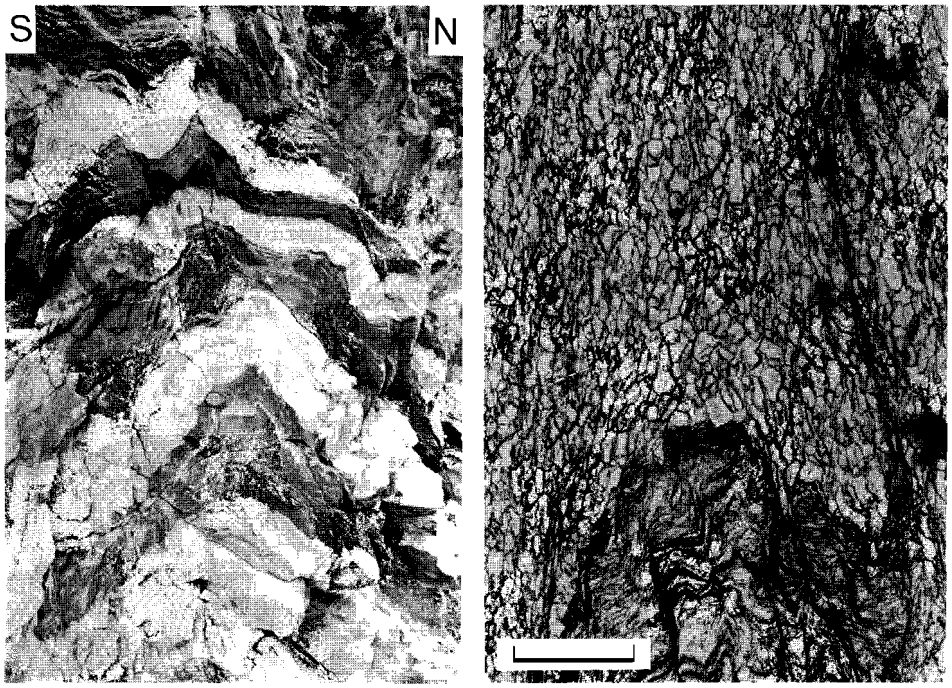

Fig. 4.11

a. D2 fold in the Massana antiform; locality d in the section of Fig. 4.12; lense cap for scale.
b. Calcite grain shape fabric in Devonian limestone. Note crenulated mica fabric in pelitic layer. North of Pont de Mereig (Fig. 4.12 section).

cleavages. In the Devonian carbonate rocks a calcite grain shape fabric is found.

Fold axes and cleavage-bedding intersections gently plunge west in the Tor syncline. Detailed structural work in road sections south of Canillo (Fig. 4.2), across the north and central part of the Massana structure revealed the following characteristics. Cleavage-bedding intersections and fold axes show strong variation in plunge, especially in the central part of the structure, whereas another, more faint lineation has a consistent steep orientation (Fig. 4.12). In most outcrops the origin of the latter lineation is unclear.

Quartz fabric analysis of a deformed quartz vein (Fig. 4.12) suggests stretching parallel to the gently plunging fold axes. In the micro-conglomerates north of the Tor syncline, long axes of pebbles are parallel to gently plunging fold axes. A slightly constrictional strain ellipsoid

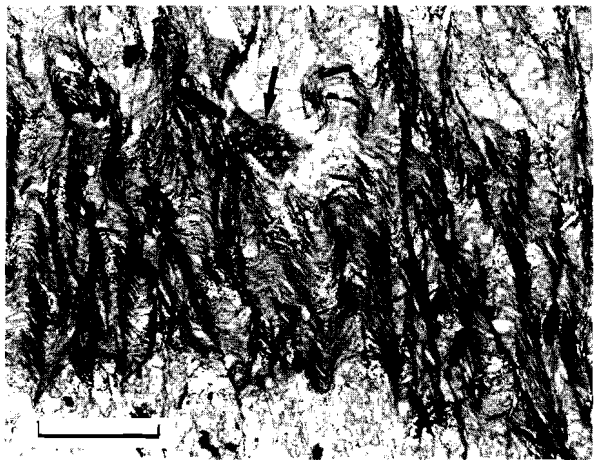

Fig. 4.11c Continuous mica fabric, crenulated in hinge of D2 buckle fold. Note pre-D2 pyrite grains and zoisite porphyroblast. Same locality as 4.11a; scale bar indicates 200 micron in b, c.

(k=1.7) follows from these conglomerates (centre-to-centre method of Fry 1979, Hanna and Fry 1979: Rxz=2, Rxy=1.5, Ryz=1.3). These observations indicate that the steep lineation is at a large angle to the stretching direction. Therefore the steep lineation is interpreted as an intersection with an older planar fabric. In fact, an angle between two foliations with such a steep intersection has been observed in the central part of the structure.

The observations are hard to explain with one phase of deformation only and pre-existing (D1) folds and cleavages have to be accounted for. A reconstructed D1 fold (Fig. 4.12) has a gently NE plunging fold axis and a steeply NW dipping axial plane. In the north flank of the Massana antiform (Fig. 4.12) the ratio of steep and gently plunging cleavage-bedding intersections indicates that D1 folds have a gently NW dipping long limb and a steep short limb. They consequently verge SE. The geometry and orientation resembles the oldest structures in the Hospitalet massif.

Hartevelt (1970) deduced the existence of D1 folds (Hartevelt's pre-cleavage folds) in the Massana antiform more to the west. He argued (p. 213) that the Massana antiform itself is such a pre-cleavage fold. The data presented here suggest that the Tor and Massana structures represent D2 folds.

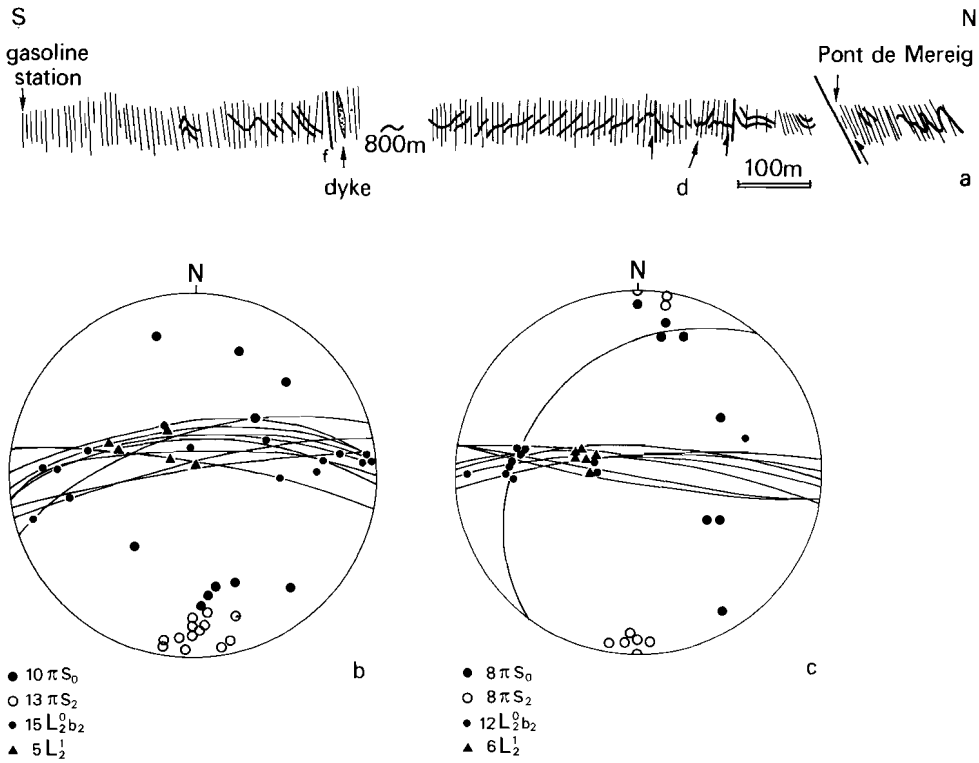

Fig. 4.12

a. Structural profile across the north flank and the central part of the Massana antiform (for location see Fig. 4.2).

b,c. Equal area projection of planar and linear features of the central part (b) and the north flank (c) of the Massana antiform. In b. note the large spread in attitude of the cleavage-bedding intersection lineations. In c. the variation in lineation attitudes allows deduction of a pre-cleavage bedding orientation (310/36). The variation in cleavage attitude is considered to be primary.

d. Quartz c-axis plot of a deformed quartz vein from location d in Fig. 4.12a.

e. Block diagram of a S2 cleavage/bedding relationship south of the dyke in Fig. 4.12a. The stereogram shows the reconstruction of the D1 fold axis. The S1 cleavage is not indicated, but lies close to bedding plane 3 as it must pass through b_1 and the L_2 lineations from 4.12b and c.

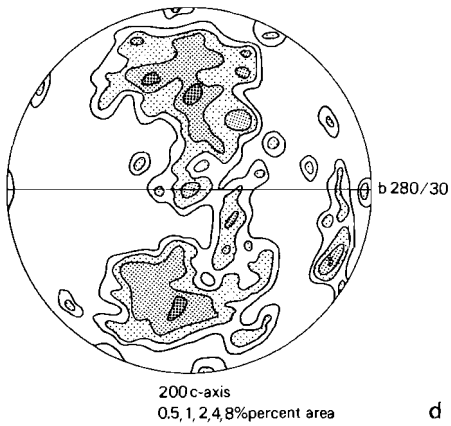

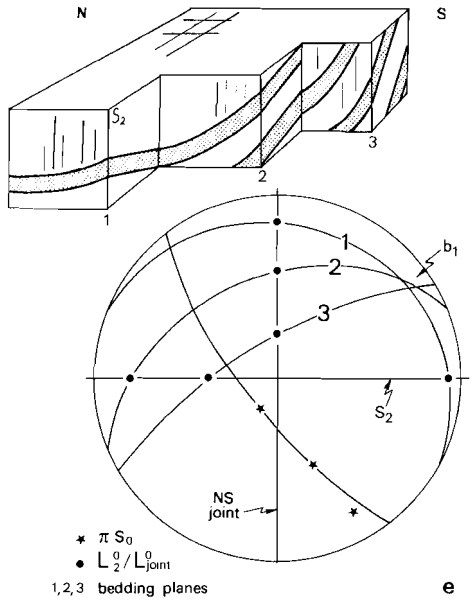

Fig. 4.12d,e

Relation with the Hospitalet massif

Structural sections 1, 2 and 3 in the Hospitalet massif (Fig. 4.4) show strong refolding of the D2 and D3 structures in their southern parts in the E1 Serrat-Ransol Zone (Fig. 4.3). South of this zone upright north vergent folds occur. It seems most probable that these folds represent the same fold generation as the D2 folds from the key sections north of the E1 Serrat-Ransol Zone. These upright folds can be traced towards the Tor synform and the Massana antiform. Local overprint of the upright folds by a flat lying S3 (?) is found north of the Tor structure but is absent further south.

Summary

The Massana and Tor structures are upright EW trending D2 folds. The associated foliation and minor folds overprint older (D1) folds which trend NE-SW, verge SE and are accompanied by a cleavage. The advocated relation between the structural history of the Massana and Tor structures and the Hospitalet massif is such that the D1 and D2 phases in both domains are equivalent.

4.6 RELATIONSHIPS BETWEEN SMALL-SCALE STRUCTURES AND LARGE-SCALE GEOMETRY

The geometries and small-scale deformation histories of the suprastructure and the north and the south flank of the Hospitalet gneiss antiform can be summarized as follows (Fig. 4.13):
Upright folds and steeply dipping cleavages distant from the gneisses become progressively overprinted by a moderately inclined to flat lying foliation and associated folds towards the central gneiss body. The inclined foliation is traceable up to and locally through the contact into the gneisses.
This geometry is symmetric on both flanks of the gneiss antiform and has the axial plane of the gneiss antiform as a mirror plane.
A correlation between the north flank and the south flank of the antiform is made based upon the fact that in the gneisses one foliation has been observed only, which suggests that this foliation is due to the same phase of deformation everywhere and hence serves as a reference plane (Fig. 4.13).
The regions where a specific deformation phase is present or can be considered as "main phase" are indicated in Fig. 4.14.

The geometry sketched in Figs. 4.13 and 4.14 allows discussion of (1) the infrastructure-suprastructure configuration and (2) the mode of gneiss antiform formation in the Hospitalet massif.

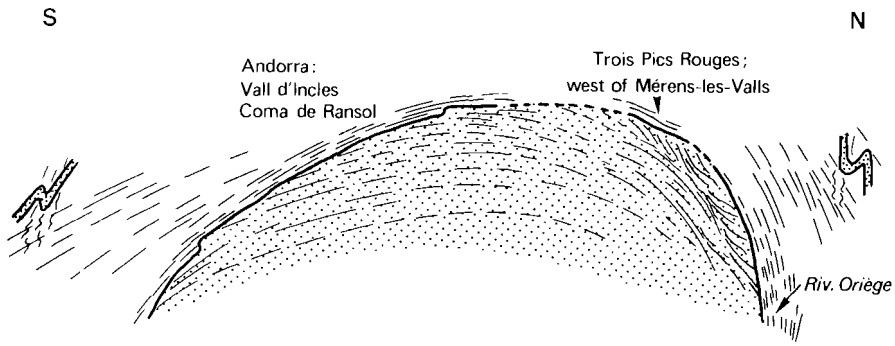

Fig. 4.13a Composite section across the Hospitalet mantled gneiss antiform; width ca. 10 km. Upright older structures away from the gneiss antiform correspond to D2 and D1 structures respectively south and north of the antiform (cf. Figs. 4.4 and 4.10). No vertical exaggeration.

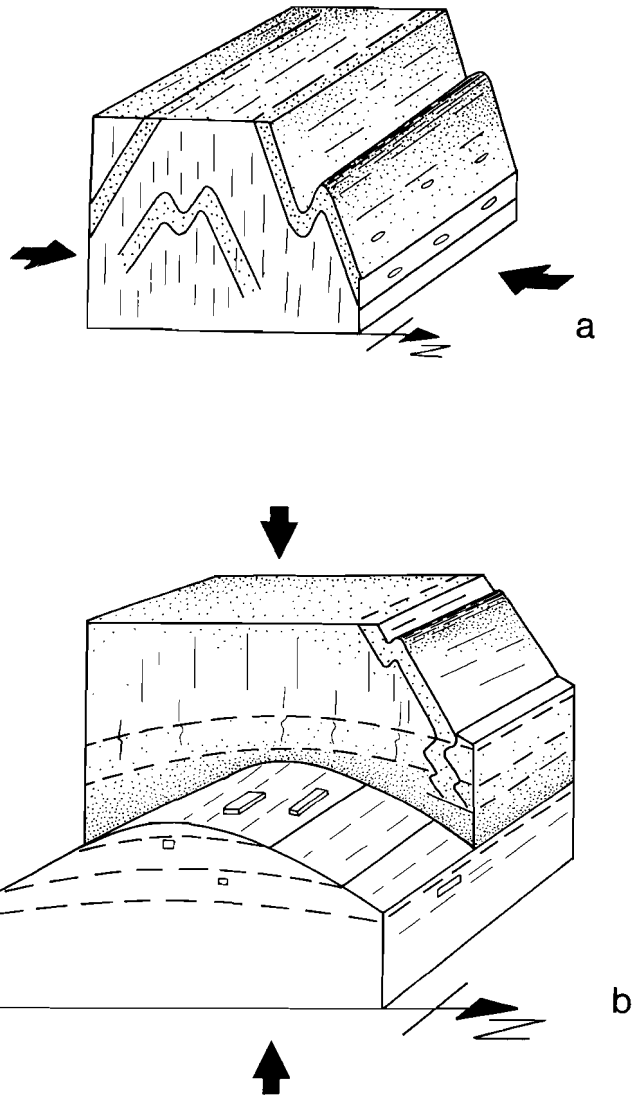

Fig. 4.13b

a. Formation of suprastructure by upright D2 folding and foliation development.
b. Formation of infrastructure by flat lying D3 folding and foliation development during formation of the Hospitalet gneiss antiform.

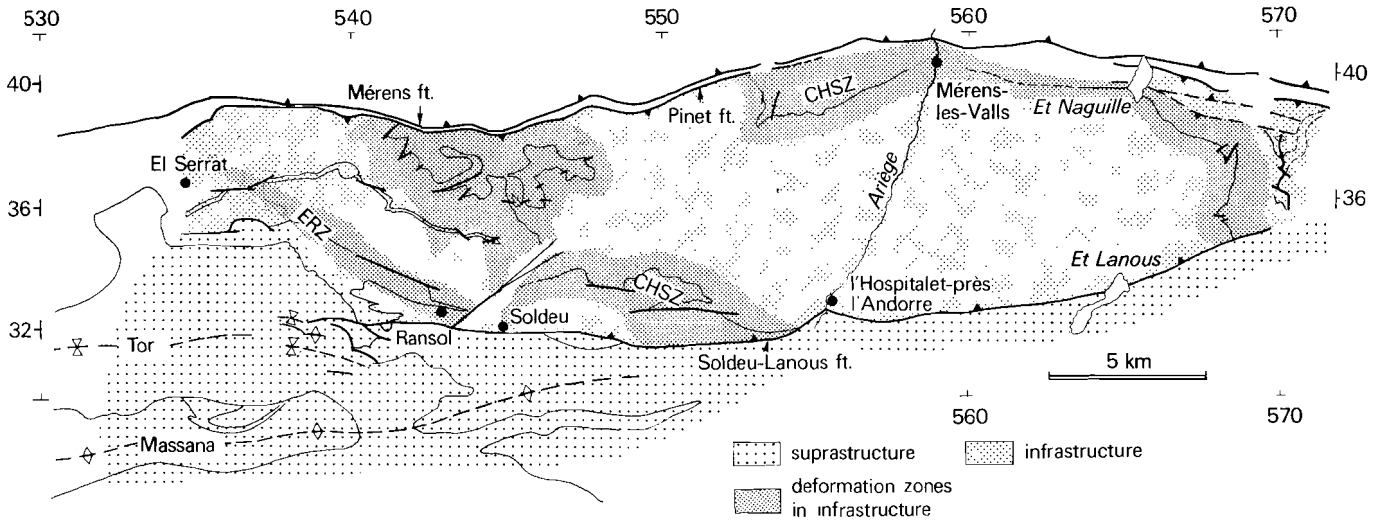

Fig. 4.14 Distribution of deformation phases in the Hospitalet massif and the Massana and Tor structures. The regions where the foliation of a certain deformation phase is most prominent in metapelitic rocks are denoted:

Suprastructure: D2 structures.
Infrastructure: D3 structures.
ERZ: D4, D5 refolding of D3 and older structures.
CHSZ: mylonitic deformation of D3 structures at the gneiss-metasediment contact.

4.7 INFRASTRUCTURE vs. SUPRASTRUCTURE

The observed overprint of the D3 structures in the region which is classically attributed to the infrastructure on structures which can be correlated with those classically defining the suprastructure, indicates that the infrastructure is younger than the suprastructure in the Hospitalet massif (Fig. 4.13b).
It is suggested that the terms infrastructure and suprastructure, which have been introduced by Zwart (1963a) to distinguish regions with different foliation attitudes, may still be of use in the Hospitalet massif as to denote the regions where the older steep structures dominate (the suprastructure) versus regions where the younger gently inclined to flat lying structures are most prominent (the infrastructure).
The relative age relationship between the infrastructure and the suprastructure in the Hospitalet massif is similar to that in the western Aston massif (Verhoef et al. 1984).

4.7.1 The age of the infrastructure

The recognition of the relative age difference between the infrastructure and the suprastructure, raises the question of the true age of the infrastructure. According to Zwart (1979) the suprastructure formed in Westphalian times, but before the Westphalian D, as the oldest post-Hercynian deposits are Westphalian D in age. However no proof is given that Westphalian D or even younger (Stephanian-Permian) deposits contain clasts derived from the infrastructure. Consequently, the infrastructure could have formed in late Westphalian times or later, in Stephanian or even in Permian times. An upper limit to its age is provided by the intrusive batholiths. The Maladeta batholith yields a lowermost Permian age (Michard-Vitrac et al. 1980).

4.7.2 Consequences of infrastructure formation for overlying rocks

The gently inclined to flat lying foliation in the infrastructure implies a steeply inclined to vertical shortening direction. A rough

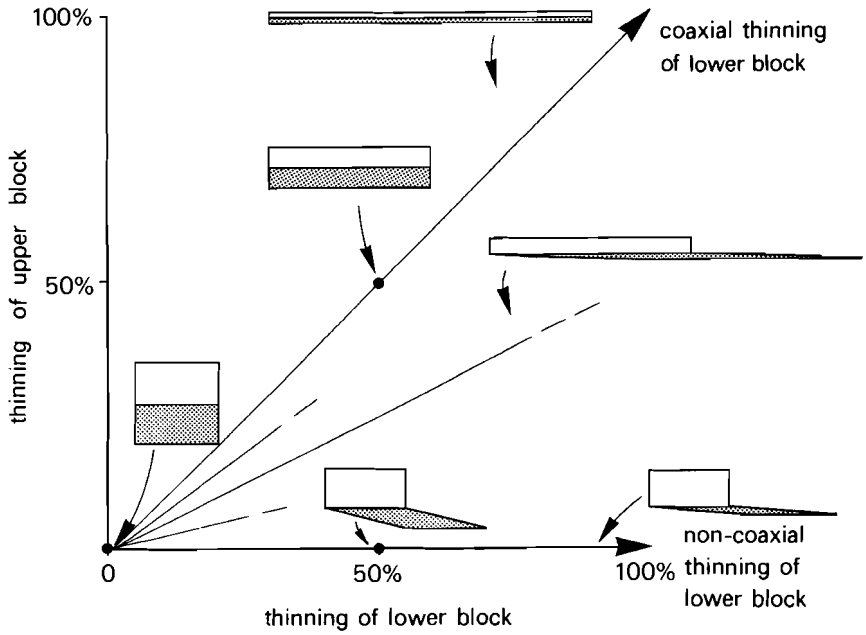

Fig. 4.15 Coaxial vs. non-coaxial thinning of the lower part of a two-layer block and consequences for the overlying part.

estimate of 50 % shortening is indicated by the tight D3 folds. Since no large-scale repetitions formed during this phase, thinning of the infrastructure perpendicularly to the foliation is implied. Since the infrastructure formed at 7-10 km depth (Chapter 7) and considering the size of the massif, ca. 10 x 35 km, this must have consequences for the 7 km of rocks above the infrastructure. In constant volume deformation the thinning of the infrastructure must be compensated by a certain amount of thinning of the suprastructure (Fig. 4.15).

These rocks did not undergo flattening by folding and cleavage formation. Faulting is implied.

An impression of the intensity of faulting in the overlying rocks may be gained from the following example. The 50% thinning of the lower block requires 50 % thinning of the upper block in coaxial flow (Fig. 4.15), and thus cause extension of the upper block with a factor of 2. If we consider this extension being accommodated by steep faults, say parallel to the S2

foliation, with say 70° dip and ca. 100 m of normal offset, than 28 of such faults have to occur over 2 km (formerly 1 km) of width of the upper block. Such an amount of faults has not been recognized and neither is the presence known of normal faults with larger offset. From this it may be concluded that deformation in the infrastructure has had a large non-coaxial component, which leaves the upper block relatively undisturbed (Fig. 4.15).

In the south of the Axial Zone evidence is found for Westphalian D, Stephanian and Permian sedimentation in NS and EW trending grabens (Bixel and Luxas 1983, Speksnijder 1985). According to Speksnijder (1985) graben formation was initiated in a tensile regime.
Since the age of the infrastructure is no longer constrained and regarding the geometrical necessity of at least some extension of the suprastructure (Fig. 4.15), it may be that that initial (Westphalian D?) tensile regime proposed by Speksnijder (1985, 1986) reflects formation of the infrastructure at depth.

4.8 DYNAMIC MODELS FOR GNEISS ANTIFORM FORMATION

The foliation in the infrastructure (S3) is more flat lying than the outward dipping gneiss-metasediment contact (Fig. 4.13). This geometry limits foliation development to be either contemporaneous with, or younger than the formation of the antiform in the contact.
The latter possibility implies overprint of the foliation on an existing gneiss antiform, which, regarding its orientation, could have been formed during the formation of the suprastructure (D2).
However, the S3 foliation is developed in the gneisses and in the metasediments adjacent to the gneisses. It diminishes away from the antiform. Therefore, the antiform and the foliation are considered to have developed simultaneously.
Such a relationship allows comparison of the geometry with models of fold formation, such as buckle folding due to lateral shortening and formation of a diapiric antiform.

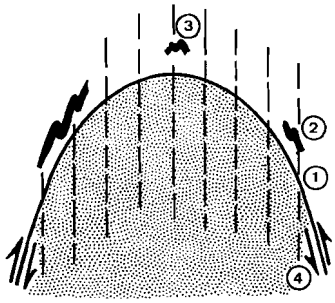

(BUCKLE)FOLD

1. foliation steeper than contact
2. minor folds and foliation-bedding relations verge towards the core
3. symmetric minor folds in the hinge zone; shortening is perpendicular to the axial plane
4. kinematics of shearing at the contact or in the core should indicate downthrow of the core; extension lineations lie in the axial plane

core material behaves relatively stiff in buckle folding

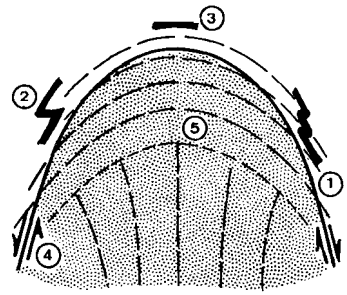

DIAPIR

1. foliation more flat lying than contact
2. minor folds and foliation-bedding relations verge away from the core
3. vertical flattening (e.g. boudinage) in the hinge zone; shortening is perpendicular to the gneiss-cover contact
4. kinematics of shearing at the contact or in the core should indicate relative rise of the core; extension lineations define radially outward patterns
5. transition zone from a steep fabric in the core to a flat lying fabric in the upper part of the structure

core material behaves relatively mobile, less stiff than overburden

Fig. 4.16 Diagnostic structural criteria (1-5) for distinguishing between a diapiric origin and a folding origin for a given antiformal structure. The minor structures should have formed simultaneously with the fold structure. After Dixon (1975), Stephansson and Johnson (1976), Schwerdtner et al. (1978), Platt (1980), Brun et al. (1981), Van den Eeckhout et al. (1986).

Folding

Several models of folding due to lateral shortening have been published (Dieterich 1970, Hobbs 1971, Lisle 1985). None of these models yields a fold-foliation configuration as found in the Hospitalet antiform (compare Figs. 4.13, 4.16). It can be concluded that the structure did not form by folding as a result of lateral NS shortening during the development of the S3 foliation.

Diapirism

An alternative mode of formation of a gneiss antiform, by means of a diapiric density inversion (buoyant diapir, Schwerdtner 1981), has been experimentally investigated by Dixon (1975), who determined strain trajectories in four centrifuged putty models. The foliation-contact relationships which follow from Dixon's data fit the observed features of the Hospitalet antiform (compare Figs. 4.13, 4.16). Therefore the antiform may have risen as a low amplitude (buoyant) diapir into the metasediments.

However, evidence for diapiric uprise of the antiform is not conclusive. Inspection of Fig. 4.16 shows that only three of the criteria to recognize a diapir are fulfilled (criteria 1, 2, 3).
Critical arguments in the interpretation of a given structure as a diapir are (1) the kinematics of the event which caused the development of the structure (here: D3) and (2) the rheological behaviour of the gneisses and metasediments (Fig. 4.16). These items are evaluated below.

(a) Kinematics of D3. In the mylonite zone at the gneiss-cover contact the S3 foliation is strongly deformed. Therefore, the kinematic axes of this younger deformation cannot be taken as the kinematic axes of D3 (Chapter 5). D3 kinematic indicators, such as quartz lattice preferred orientations are destroyed by the younger event and this poses a problem as to the kinematic framework of D3, in particular to the D3 elongation direction. The most conspicuous structure that might represent the D3 elongation direction is the EW trending lineation in the gneisses. Alternatively, the structure might represent an intersection of the gneiss foliation with an older, completely destroyed (D2) foliation.
Care has to be taken in ascribing a kinematic significance to a given linear structure since relative movements parallel to it are implied. Therefore, the present author favours the interpretation that the structure represents an intersection lineation. In the metasediments S2 is a pervasive mica preferred orientation which can be traced (in thin section) up to the gneisses. Since the gneisses existed prior to the Hercynian orogeny (Chapter 3) they must have undergone D2 deformation. Hence, they might have possessed an S2 foliation.

(b) Rheological behaviour of the gneisses. In diapirism the gneisses are expected to behave more mobile than the metasediments (Fig. 4.16). Since the rheology of the rocks is unknown the gneisses may have behaved

relatively less mobile.

In conclusion, the kinematic framework of D3 and the rheological behaviour of the involved rock types are insufficiently known to place constraints on the origin of the antiform. Hence, alternative modes of formation must be considered.

Push-up

In case the gneisses acted relatively stiff, the geometries in the Hospitalet gneiss antiform may be explained as pushing up of the gneisses by underlying (buoyant) material.

Sheath folding

Henderson (1981, 1984) reports large-scale sheath folds from the Foxe fold belt (Canada). Brun and Van den Driessche (1985) suggest sheath fold development at this scale in the formation of mantled gneiss domes and gneiss-cored nappes. In the Hospitalet massif no small-scale sheath folds occur and this argues against the presence of such folds at a larger scale.

Mega-boudinage of the gneisses

Referring to the "core complexes" of the western United States Davis (1981) suggested megaboudinage of a basement layer as a possible cause for its uplift in elongate domal structures. The overall extension was accommodated by partitioning of megaboudin crustal units marked by shoulders and necks of ductile shearing. In boudinage deformation is most intense near the boudinage necks. The overall development of S3 and the geometry sketched in Fig. 4.13 argues against such a mode of formation.

Mega-boudinage of the metasediments

In the two-layer model of Davis (1981) the lower part has been necked. Alternatively, one may consider a situation in which the lower part behaved relatively mobile and the metasedimentary overburden being boudinaged in an extensional regime. This will cause vertical uprise of

the lower part into the boudinage neck, actually resembling a buoyant diapir.

4.9 TECTONIC IMPLICATIONS

Of the various modes of gneiss antiform formation mentioned above some may apply to the Hospitalet massif, (1) a diapiric density inversion, (2) a relative push-up and (3) necking of the overburden in extension causing the gneisses to rise in the boudinage neck.
Either mode of formation implies vertical tectonics at the scale of the massif.
However, at a larger scale than the massif fundamental differences exist between the underlying processes that cause the structure. A buoyant diapir or a push-up is a local feature which may originate in a crustal segment with fixed boundaries. In extension at the same scale these boundaries move away from each other. Structural criteria such as depicted in Fig. 4.16 apply to a given structure and not to the tectonics that caused it (Van den Eeckhout et al. 1986).
Therefore, additional information is required. This may be supplied by regional investigations or, alternatively at a local scale by the metamorphic event which is linked to the formation of the structure. Of particular interest is the attitude of the isograds relative to the antiformal structure.
Theoretical models consider a density contrast to induce (buoyant) diapirism. Two models have been elaborated in the literature based on

(1) a density contrast between two different types of rock ("heavy" metasediments vs. "light" gneisses) (Ramberg 1967, 1981) and
(2) a thermally induced density contrast (Talbot 1971, 1974, 1979, Den Tex 1975).

In the latter model conductive heating of the base of a given volume of rock of initially homogeneous density causes a density contrast, which subsequently leads to buoyant diapirism of the basal parts of that particular volume of rock: thermal convection occurs.
In this model diapirism thus takes place in a thermally layered material. Hence, the diapir ought to deflect (bring up) the established isograd pattern. In the Hospitalet massif the heat front rose during and after

formation of the gneiss antiform since (1) the porphyroblastesis (and mineral zonation) postdates the S3 foliation (Chapters 5, 7), and (2) the isograds are flat lying and crosscut the antiformal structure (Chapter 7). The latter geometry is similar to that of the Canigou-Carança massif (Guitard 1970). Consequently, the thermal convection model does not apply to both massifs.

In the example of thermal convection quoted by Talbot (1979), the isograd pattern had been deflected and the basal parts of the involved layer had been partly molten (migmatites). This would have dramatically increased the density contrast between the top and the base of this layer (cf. Talbot 1979). Therefore, thermal convection can be expected to be a more rapid process than a non-thermal density inversion at low metamorphic grade. The fact that thermal convection appparently did not occur thus circumstantially argues against buoyant diapirism prior to the medium grade metamorphism.

Pushing up of the gneiss antiform by underlying buoyant material raises the problem of the nature of this material. The most obvious candidate would be a batholith of some kind. However, in those massifs where we are able to study the rocks underneath the gneisses (Aston massif and Canigou-Carança massif, Fig. 4.1) increasingly higher grade para- and orthogneisses and migmatites are observed. Therefore it is probable that the Hospitalet massif will be underlain by similar rocks. Migmatitic upwelling of these rocks (Talbot 1979) may have had a pushing-up effect on the Hospitalet gneisses. However, in this concept the timing of melting relative to the deformation is of importance. From the western Aston massif, where migmatites are present, it is known that the peak of metamorphism occurred relatively late in the structural history (Verhoef et al. 1984), similar to the situation in the Hospitalet massif. Hence, migmatisation may actually have postdated the formation of the domes and cannot a priori be taken as a cause for dome formation.

Crustal stretching during D3 and the formation of the Hospitalet gneiss antiform is considered to be a plausible tectonic scenario, since (a) it is consistent with structural evidence in the Hospitalet massif and (b) it is consistent with the observed relationship between deformation and metamorphism in the massif (Chapter 7).

The lack of knowledge concerning the extension direction in the Hospitalet massif and all other infrastructural massifs prevents a more precise

solution to be offered.

However, deformation must have been largely non-coaxial to produce an infrastructure underneath a relatively undisturbed suprastructure. The presence of an extensional shear zone or zones is implied.

CHAPTER 5

THREE DOMAINS OF LATE HERCYNIAN DEFORMATION OF THE INFRASTRUCTURE IN THE HOSPITALET MASSIF

The most prominent foliation in the infrastructure of the Hospitalet massif is a third phase structure (S3) (Chapter 4). This foliation has been deformed in three structural domains, (1) a mylonite zone at the gneiss-cover contact, (2) a zone of refolding SW of the gneisses, the El Serrat-Ransol Zone and (3) a large-scale recumbent fold in the hinge zone of the gneiss antiform (Fig. 5.1).

These domains have no clearcut mutual relationship and differ in (micro) structural aspects. Therefore, the (micro)structural characteristics and the structural significance of these domains are separately described and discussed.

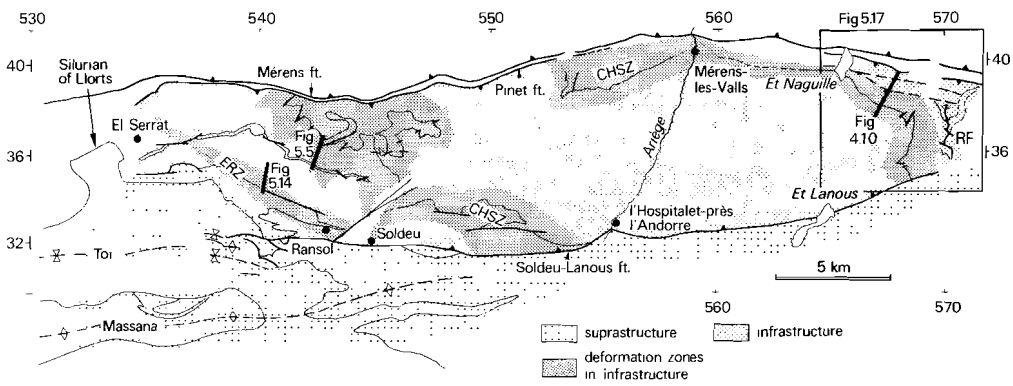

Fig. 5.1 *The three domains of infrastructure reworking in the Hospitalet massif.*

CHSZ - mylonite zone at the gneiss-cover - section 5.1
ERZ - zone of refolding SW of the gneisses - section 5.2
RF - recumbent fold in the eastern hinge zone of the gneiss antiform. - section 5.3

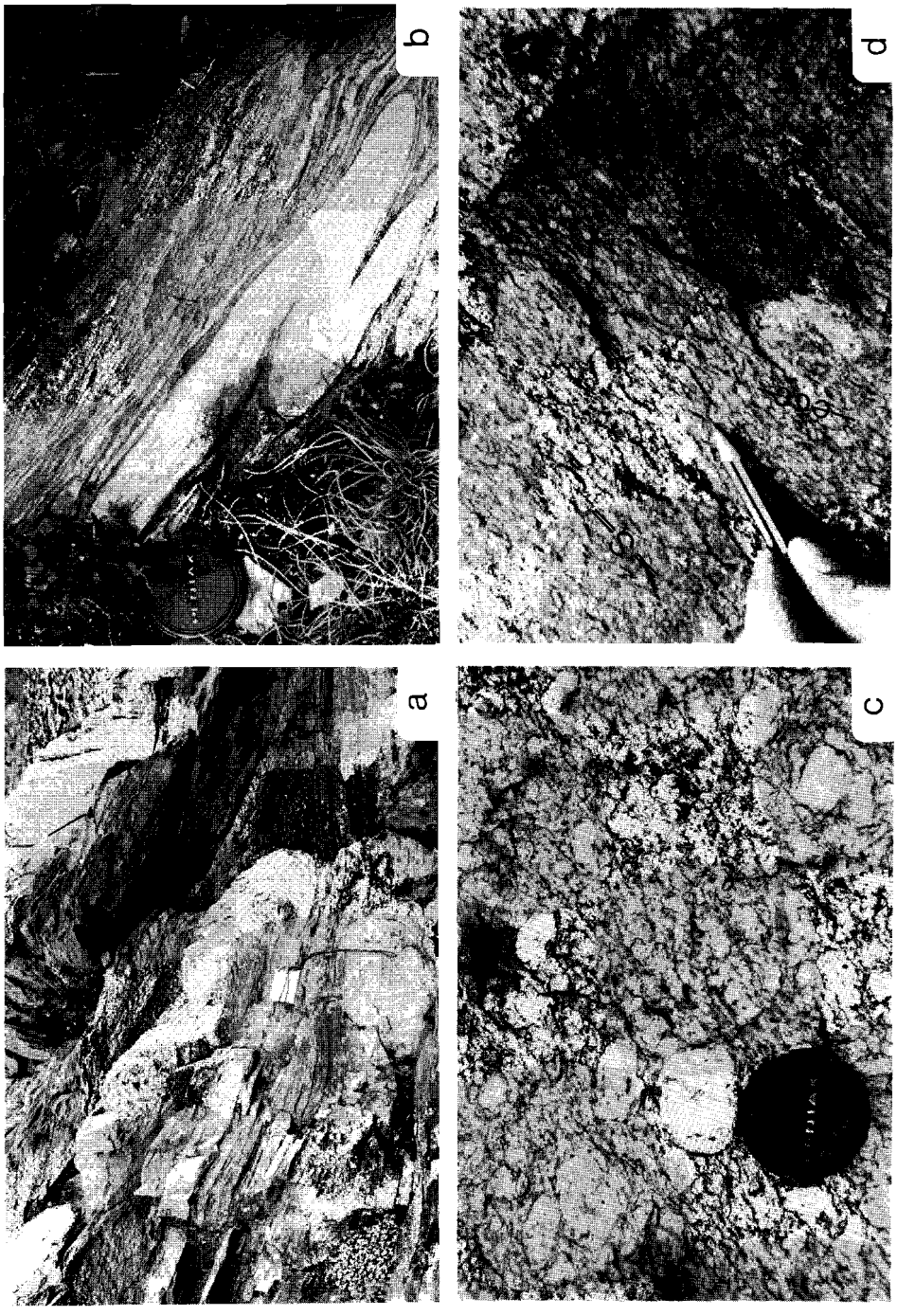
b
d
a
c

5.1 THE MYLONITE ZONE AT THE GNEISS-METASEDIMENT CONTACT

In the infrastructure, field evidence exists for deformation which took place after the main episode of porphyroblast growth in the metasediments. This deformation is restricted to a zone at the gneiss-metasediment contact. A strain increase exists towards that contact. The occurrence of the same features southwest, north and northeast of the gneisses suggests the existence of a single zone of contact high strain, the CHSZ for short. Evidence amounts to the following:

(1) As one approaches the gneisses, the phyllites and schists show a decrease in the angle between bedding and S3 foliation. Furthermore, pre existing (D3) folds show a decrease in interlimb angle towards the gneisses, as shown by Soula (1982) (Fig. 5.2a, b).

(2) Somewhat closer to the contact, extensional crenulations occur which are locally associated with small-scale normal offsets of compositional bands. Towards the contact the wavelength of the extensional crenulations decreases and a spaced, discrete extensional crenulation cleavage (ecc) is found. The spacing is locally less than 1 cm.

(3) Within a 250 m wide zone at the gneiss-metasediment contact and associated with the most intense development of ecc, quartz lenses are rod shaped and show a lineation defined by a preferred orientation of elongate quartz grains and biotite plates (quartz-biotite lineation). This lineation is most pronounced in the quartz segregation lenses, but it can also be observed in the gneisses and to a lesser extent in the schists (Fig. 5.6b).

(4) Away from the gneisses the S3 foliation abuts against porphyroblasts and continuity of Si-Se fabrics across the phase boundaries indicates overgrowth of the porphyroblasts on this foliation. Towards the gneisses this same S3 foliation is wrapped around porphyroblasts (Fig. 5.3), rotated Si-Se configurations are observed and boudinage of porphyroblasts occurs. Boudinage usually is parallel to the quartz-biotite lineation indicating that the latter is a stretching lineation.

◄ *Fig. 5.2*

a. Isoclinal D3 fold away from (above) the CHSZ.
b. Flattened D3 buckle fold within the CHSZ. Note the presence of extensional crenulations.
c. Low deformed Hospitalet gneiss from underneath the CHSZ.
d. Platy Hospitalet gneiss with ecc development within the CHSZ.

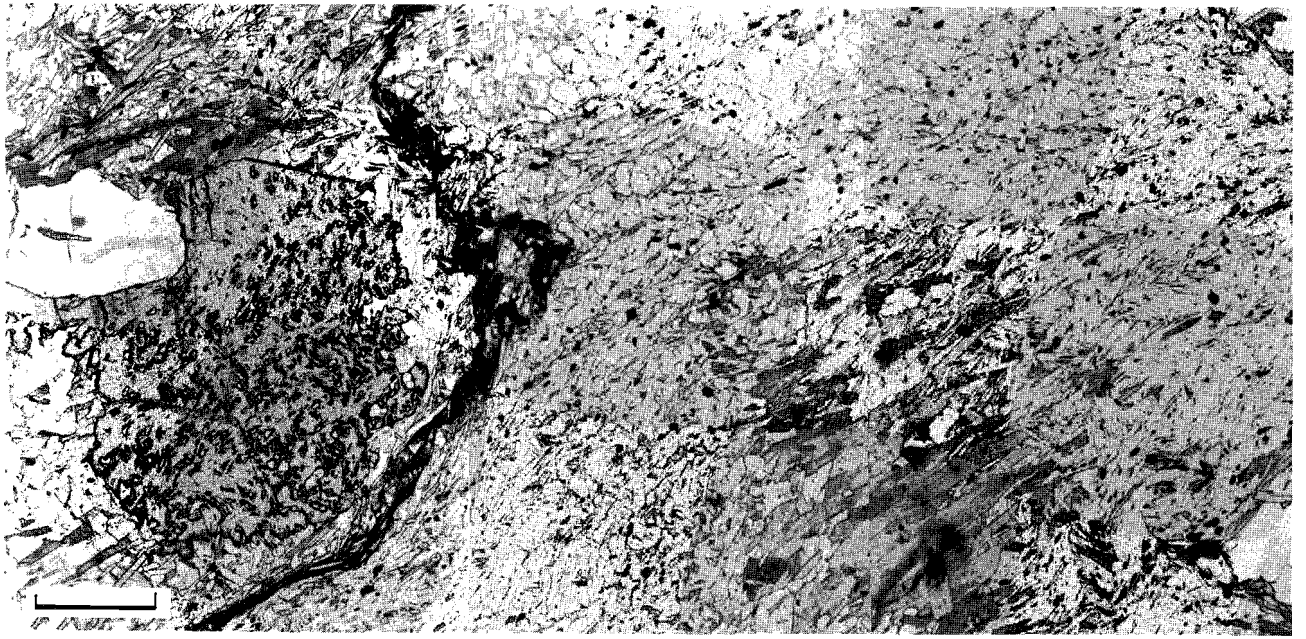

Fig. 5.3

a. General aspect of a schist from the staurolite zone. S3 is a crenulation cleavage of a S2 mica fabric. Biotite shows (001) traces parallel to S3. A staurolite porphyroblast has overgrown S3 as indicated by the helecitic crenulations. The axial plane of the crenulation is continuous with S3, and flanks are continuous with the micas, which define S2 above and below the staurolite. Scale bar indicates 300 micron.

b. (Opposite page). General aspect of a schist from the upper staurolite zone, which has been deformed in the CHS2. Note the wavy aspect of S3 and curvature of S3 around a staurolite porphyroblast. The staurolite includes differentiated crenulations. The flanks of these crenulations and the axial traces of the crenulations curve outside the porphyroblast towards S3 indicating rotation of the staurolite after it had overgrown the D3 crenulations. Scale bar indicates 0.5 mm.

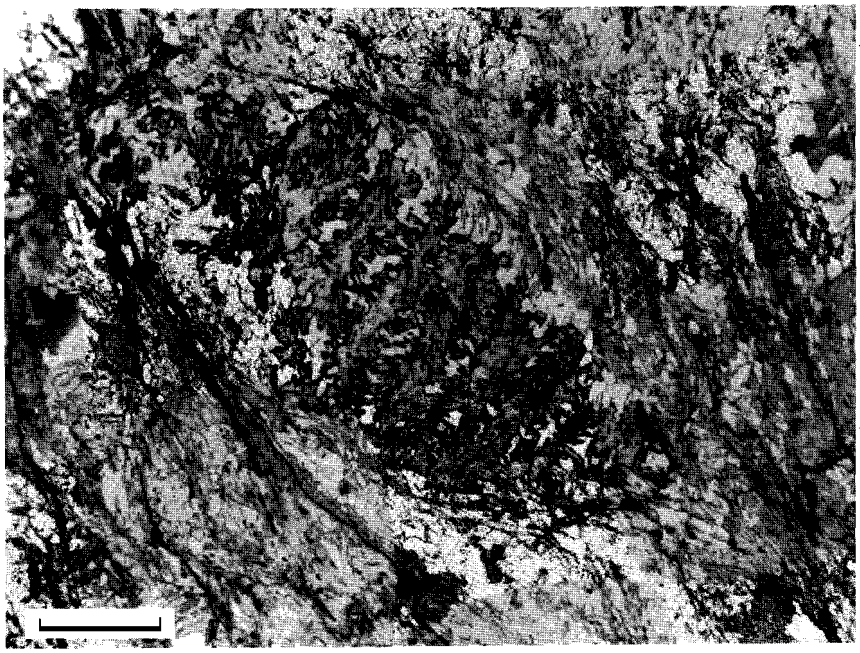

Fig. 5.3b

(5) The foliation in the Hospitalet augengneisses becomes increasingly platy approaching the gneiss-metasediment contact (Fig. 5.2a, d). The gneisses locally grade into augen-bearing mylonites. Extensional crenulations and ecc are widespread (Chapter 6).

(6) At the scale of the massif the isograds are oblique to the gneiss-cover contact. The CHSZ follows this contact and is oblique to the isograds.

Refolding effects

Away from the CHSZ the S3 foliation in the metasediments locally has been refolded by flat lying open (D6) folds and crenulations (Fig. 4.4, Chapter 4). These are locally associated with a mm spaced discrete crenulation cleavage and are often found near quartz segregation lenses (< 50 cm). Crenulation lineations are widespread and parallel to the mineral lineations in the CHSZ (Fig. 5.5). Parallel to the crenulation lineations andalusites have been boudinaged. Within the CHSZ no overprint of D6 structures on the highly strained schists has been demonstrated.

D6 structures are south vergent SW of the gneisses and north vergent

Fig. 5.4 D6 fold in staurolite-andalusite schist. Note curvature of S6 around staurolites.

north of the gneisses. Above the CHSZ in the hinge zone of the Hospitalet gneiss antiform there occurs a major SSE closing recumbent fold (section 5.3), which probably is of similar age as the D6 structures.

5.1.1 Kinematics of the CHSZ

Several fabric elements provide a clue to the orientation of the kinematic axes of the deformation in the CHSZ. These are (1) mineral lineations, (2) ecc, (3) boudinage, (4) rotated and boudinaged porphyroblasts and (5) the variation in attitude of pre existing structures outside the zone towards it (Fig. 5.5, Encl.2, Table 5.1). These features indicate uniform WNW-ESE directed elongation in the CHSZ throughout the massif.

However, SW of the gneisses a more complex situation occurs. In this region two elongation directions are observed, (1) NNE-SSW directed elongation is indicated away from the gneisses, whereas (2) near the gneisses WNW-ESE directed elongation is observed. In the latter domain also NNE-SSW stretching features can be found (Fig. 5.6), but to a lesser extent. Within the gneisses both orientations can be found.

The geometries of the kinematic indicators SW of the gneisses (Fig. 5.6a)

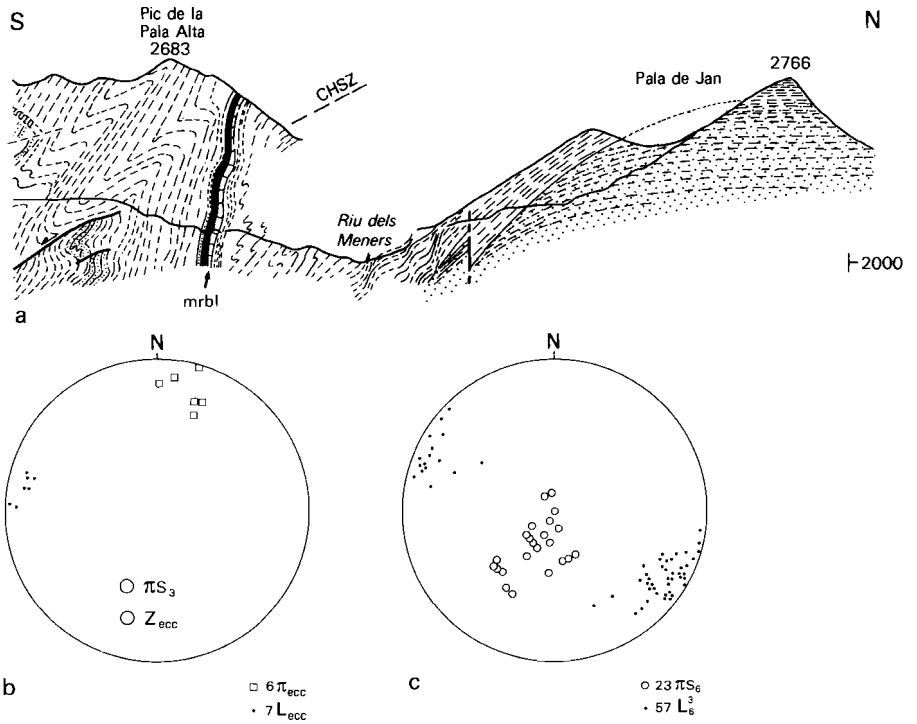

Fig. 5.5

a. Structural section across the CHSZ southwest of the Hospitalet gneisses. Note the increase in tightness of D3 folds towards the gneisses and the presence of steep high strain zones near the gneisses. Gneisses are stippled, bedding is indicated in the metasediments.

b. Lower hemisphere equal area projections of ecc from the section shown in 5.5a. Zecc denotes the shortening direction deduced from the ecc orientations.

c. Lower hemisphere equal area projection of D6 structures.

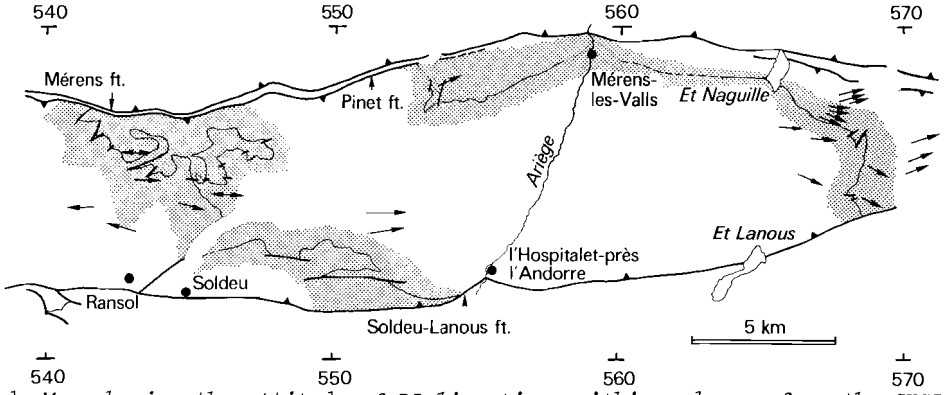

d. Map showing the attitude of D3 lineations within and away from the CHSZ. CHSZ is ornamented.

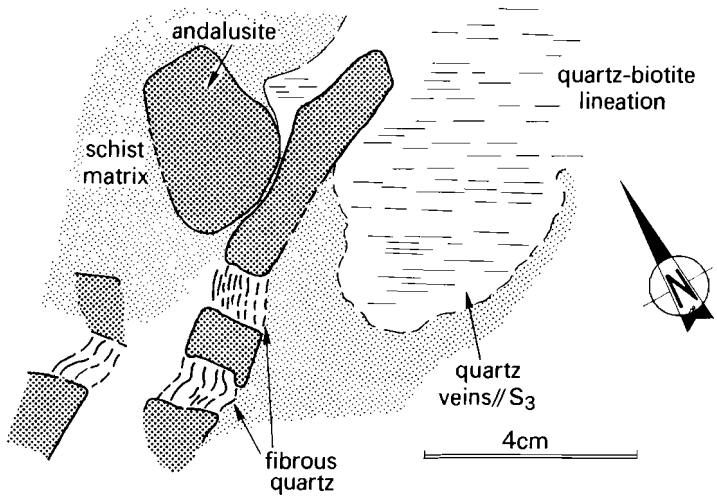

Fig. 5.6a NNE-SSW extended andalusite porphyroblast embedded in a schist matrix and quartz vein. On the quartz vein a quartz-biotite lineation is visible suggesting WNW-ESE extension, perpendicular to the extension direction indicated by the andalusite. Sample SG 14344 looking on the schistosity.

	dip of S3	plunge of L3	plunge of quartz-biotite lineation and direction of boudinage	plunge of L_3^{ecc}
north flank (west of Mérens-les-Valls)	subhorizontal-gently NNE	N060E	subhorizontal WNW-ESE	NNE
northeastern part	moderately-steep NNE	NE	subhorizontal to gently ESE	steep NNE
hinge zone in the eastern plunging nose	gently NE-SE	N065E	gently ESE	NNE-SSW
southwestern part (Andorra)	subhorizontal-moderately SW	EW to WNW-ESE	WNW-ESE some NNE-SSW	N240E many EW

Table 5.1 Orientation of planar and linear structures in the CHSZ in various parts of the massif. The plunge of L_{3ecc}^{3} is in general parallel to the rotation axis of those porphyroclasts, which have rotation axes near the foliation. Elongate porphyroclasts often have rotation axes at a high angle to the foliation. These porphyroclasts rotate towards WNW-ESE.

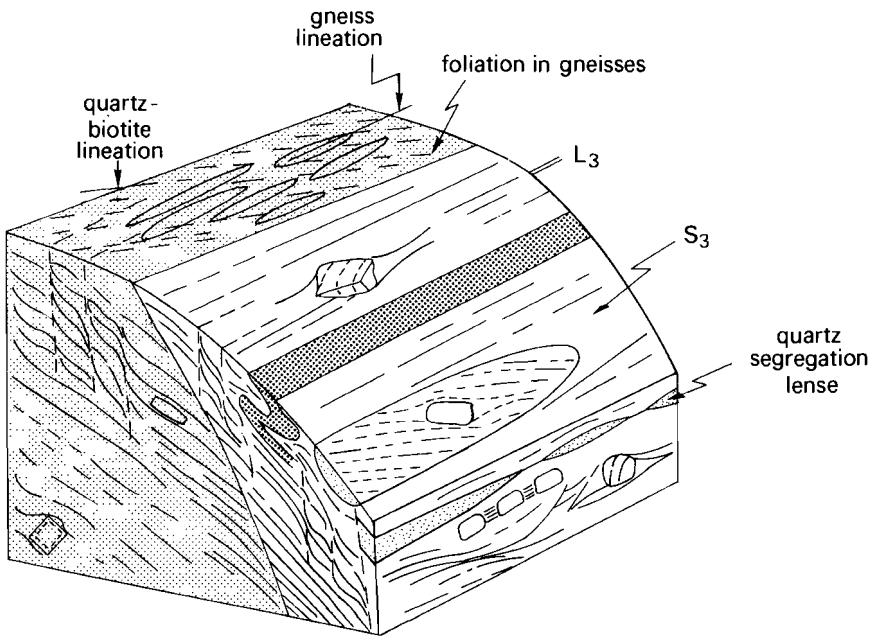

Fig. 5.6b Composite block diagram representing structures near the gneiss metasediment contact, as observed SW of the gneisses. Note the steep ecc.

suggest either (1) an overprint situation of two deformation phases within the CHSZ, or (2) a flattening strain regime in the rocks near the gneisses. The latter possibility seems improbable regarding the well defined quartz-biotite lineation and the absence of elongation directions intermediate between WNW-ESE and NNE-SSW. Furthermore, long dimensions of quartz rods are parallel to the D3 lineation. Locally, these rods represent isoclinal folds, but foliation parallel quartz lenses show a pinch and swell structure parallel to L3 indicating NS stretching. The quartz grain shape lineation on these rods is oblique to their long dimensions and directed WNW-ESE (Fig. 5.6b). This geometry seems to indicate that the quartz rods have been overprinted by the quartz-biotite lineation.
It is concluded therefore, that an overprint situation exists of two orthogonally oriented elongation directions SW of the gneisses, of which the WNW-ESE direction reflects the younger event.

The next sections provide a detailed description of the microstructures in the metasediments and the gneisses, since these provide insight

in temperature conditions during deformation, and the mode in which grain size reduction of various minerals was achieved.

5.1.2 Microstructures in metasediments

The S3 foliation in the schists is a differentiated crenulation foliation, outlined by a preferred orientation of colourless micas and at higher grades by biotite. Within the CHSZ, especially in relatively high strained rocks, the foliation is phacoidal and symmetric and asymmetric foliation boudinage and ecc are observed (Fig. 5.7).

Foliation boudinage is not often found in the field, but is observed at micro scale. Especially where colourless micas (50 micron) define the foliation the typical pinch and swell shapes are found. Within the swells the colourless micas define an oriented decussate fabric. Kinking is quite common, as well as brittle behaviour near the pinch regions. These are often relatively rich in biotite.

Extensional crenulation cleavage (ecc) may be restricted to mica rich bands between quartz rich compositional bands or foliation parallel quartz veins. Commonly it extends and crosscuts and offsets compositional bands. Microlithons show curvature of the foliation, consistent with the description of ecc by Platt and Vissers (1980). Compositional bands become thinner and curve into the ecc traces in the same fashion as the S3 foliation.

Fig. 5.7 ►

a. Phacoidal S3 foliation in biotite schist. S3 is disrupted by a single NE-SW trending ecc set (staurolite-out zone).
b. Detail of an ecc band. Note inward curvature and recrystallization of biotites, which define EW trending S3 away from the ecc band. Within the ecc trace very fine grained andalusite-quartz symplectites are present (staurolite-out zone).
c. Pinch-and-swell structure in colourless micas, which define S3. Note enrichment of biotite in the pinches (arrow) (staurolite zone).
d. Colourless mica "fish" (m), which contains remnants of staurolite (arrows) evidencing that decomposition of staurolite took place prior to mylonitization (staurolite-out zone).

Scale bars indicate 200 micron, except in a: 500 micron.

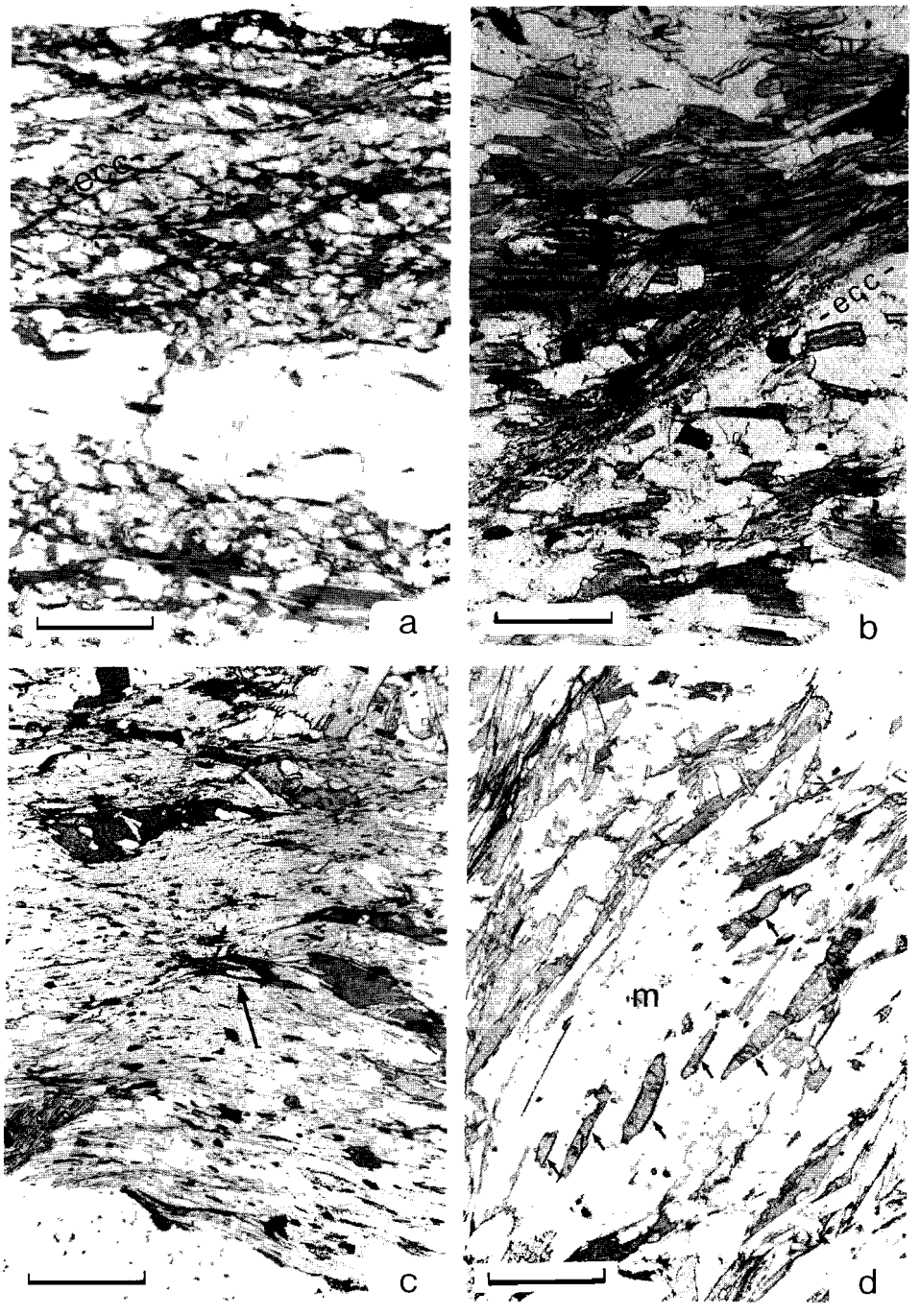
ecc
a
ecc
b
c
m
d

Angles between ecc and S3 traces range from 25-35 degrees. Usually one set predominates. Conjugate sets give rise to the typical "button" shapes. Ecc traces range in width from a few micron to up to 50 micron. Biotite, colourless micas and Mg-rich chlorites up to 10 micron, but occasionally up to 50 micron occur with (001) parallel to the trace boundary. Inward curved micas and quartz wedges, either optically strain free or showing undulatory extinction, subgrains and new grains help to define the ecc.

Stylolitic residual seams at high angles to the foliation occur locally near porphyroblasts.

Deformation structures in minerals

Ecc and foliation boudinage are often associated with pre-existing porphyroblasts such as biotite, andalusite, cordierite, staurolite and colourless micas.

Mica. Biotite porphyroblasts and muscovite pseudomorphs after staurolite with (001) parallel to S3 show barrel shapes, indicating necking (Fig. 5.7d). Kinks occur in micas positioned with (001) at high angles to the foliation (Fig. 5.8b). In biotite, kinking, boudinage, slip on (001), neoformation and indications for solution transfer processes are all observed (Fig. 5.8). Rotational and rotated inclusion patterns indicate prekinematic, but also synkinematic growth of these porphyroblasts with respect to the deformation event that affected the S3 foliation.

Staurolite occurs in crystals up to 1 centimeter in diameter. They display rotated Si-Se configurations (Fig. 5.3b), local overgrowth by andalusite-quartz (AQ) symplectites and no optical signs for lattice deformation.

Fig. 5.8 ►

a,b. Biotite porphyroblasts with central dusty parts, clear rims and pressure fringes. Lamellae of Mg-chlorite and colourless mica occur within the blasts. The pressure fringes are also composed of biotite and colourless mica and Mg-chlorite. Note kinking.

c. Biotite porphyroblasts with rotational inclusion patterns and well developed opaque rich regions at their interfaces suggesting diffusive mass transfer.

d. Biotite porphyroblasts with dusty cores and clear rim zones. Note kink folds of the inclusion pattern in the left part of the central porphyroblast, possibly indicating slip along (001).

a-d scale bar indicating 150 micron.

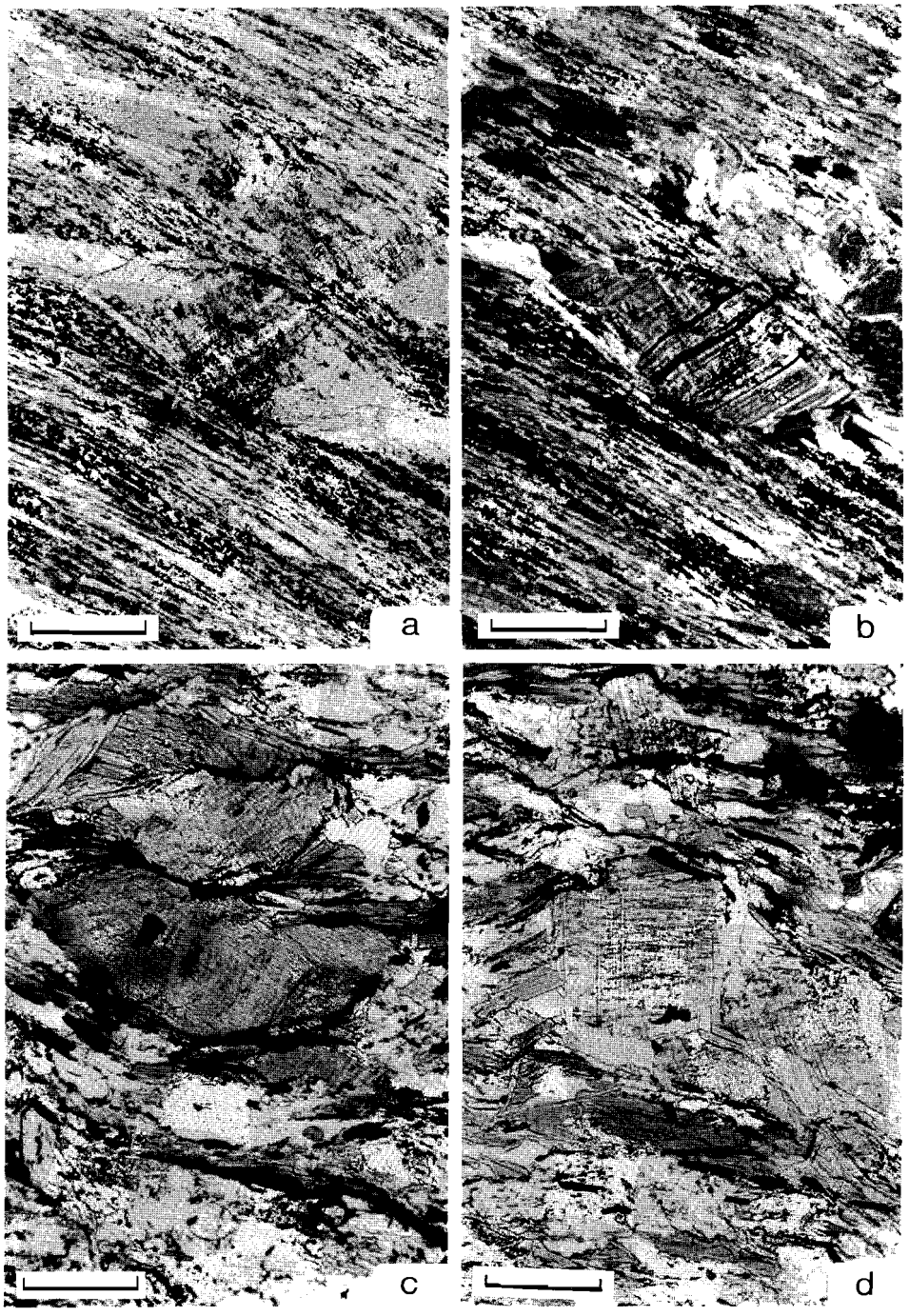
a
b
c
d

Cordierite (Fig. 5.9), up to several centimeters in diameter shows rotated Si-Se patterns, large subgrains, local boudinage and truncation by colourless mica bands at low angles to the foliation. At high angles to the foliation a conjugate, veinlike system is locally found, indicating fracture of the porphyroblasts. These "veins" contain AQ symplectites, colourless micas, biotite and Mg-rich chlorite in varying amounts and ratios. Some more intensely retrogressed and flattened cordierites show a "pseudo-ophitic" texture defined by micas (biotite, Mg-rich chlorite and colourless mica) with interstitial remnants of cordierite.

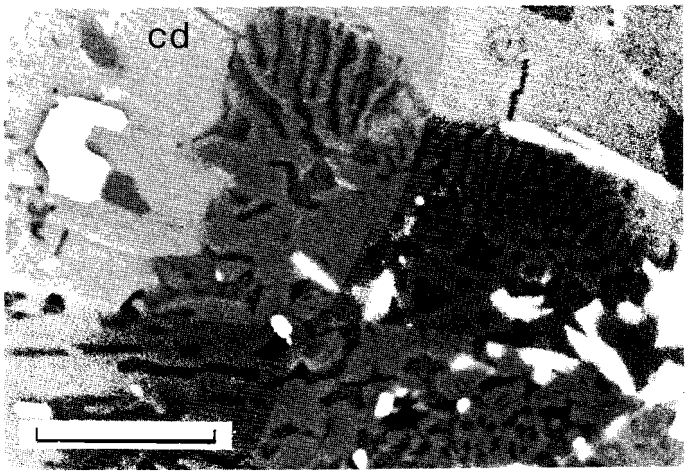

Fig. 5.9a SEM backscatter image of andalusite-quartz symplectite, which has grown into cordierite (cd.). Scale bar indicates 200 micron.

Andalusite porphyroblasts have been boudinaged, show rotated Si-Se configurations and locally lattice deformation (Fig. 5.9). Indentation of andalusite porphyroblasts into each other may indicate solution transfer processes. In between pulled apart fragments of andalusite colourless mica, Mg-rich chlorite, biotite and quartz in varying amounts and ratios are observed. Locally the colourless micas have been overgrown by AQ symplectites or by andalusite.

Quartz in the schist matrix in general shows little sign of internal strain. Pinning of grain boundaries and grain size depence on mica distribution is common. Within porphyroblasts and strain shadows relatively large quartz grains occur which include micas. These quartz grains have long shape axes parallel to the S3 foliation. In quartz veins and impure quartzites well developed core-mantle structures, ribbon quartz and single

Fig. 5.9b,c Microstructures in andalusite (a). Boudinage of andalusite occurs accompanied by wrapping of S3 around the andalusite crystals (in 5.9c). Note the presence of domainal extinction in 5.9b, indicating subgrain (and new grain?) development. Note cracks in andalusites. Boudinage necks contain Mg-rich chlorite (chl. in 5.9b) and/or colourless micas and quartz.

Scale bar in b 250 micron.
Scale bar in c 1 cm.

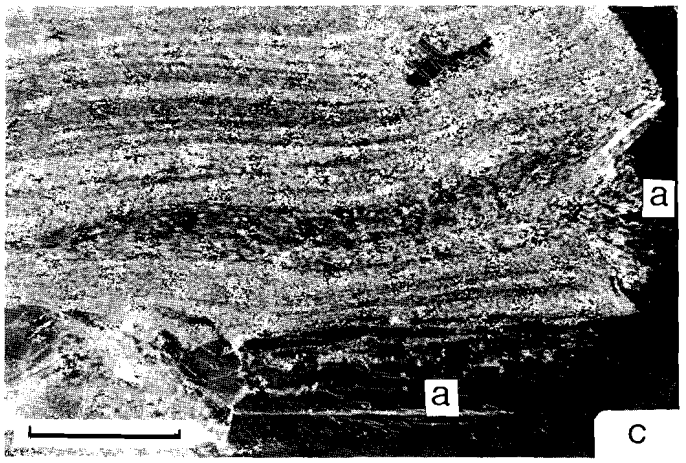

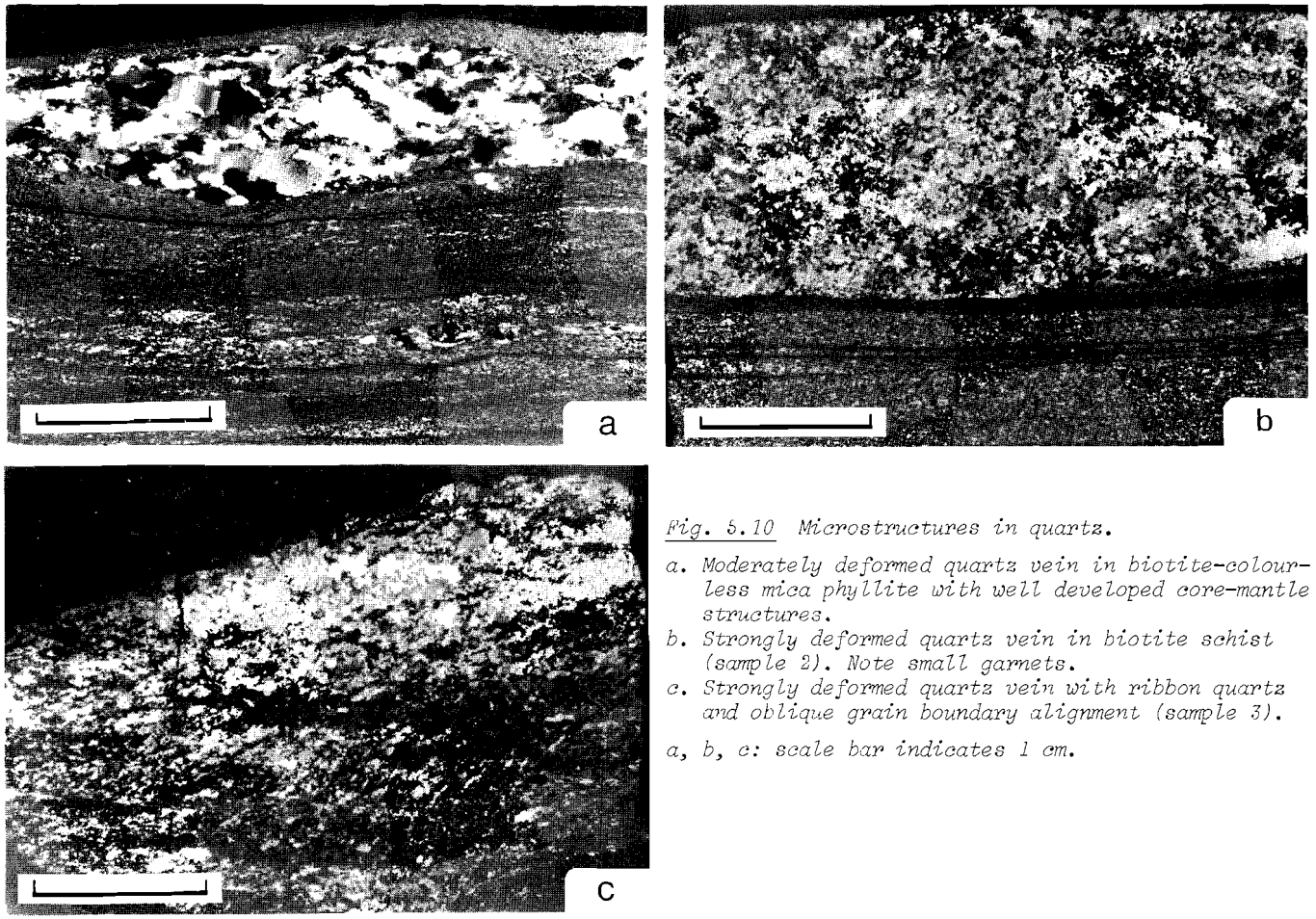

Fig. 5.10 *Microstructures in quartz.*

a. Moderately deformed quartz vein in biotite-colourless mica phyllite with well developed core-mantle structures.

b. Strongly deformed quartz vein in biotite schist (sample 2). Note small garnets.

c. Strongly deformed quartz vein with ribbon quartz and oblique grain boundary alignment (sample 3).

a, b, c: scale bar indicates 1 cm.

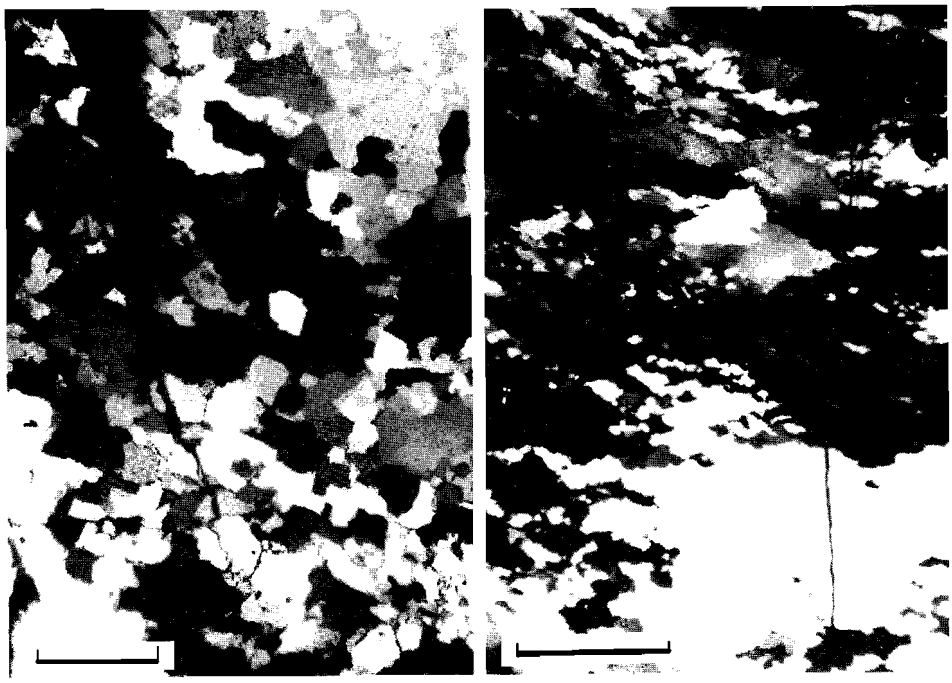

Fig. 5.10

d. Conjugate, nearly orthogonal grain boundary alignment (sample 8).
e. Conjugate grain boundary alignment with a dominant (NW-SE) direction (sample 3).

d: scale bar indicates 200 micron; e: scale bar indicates 500 micron.

and conjugate grain boundary alignments indicate plastic strain (Fig. 5.10). Several of these rocks have been subjected to quartz c-axis analysis (see below).

Feldspar is a common constituent of biotite schists. No optical evidence for intracrystalline deformation has been observed.

5.1.3 Microstructures in gneisses

Microscopically, the foliation is defined by a preferred orientation of micas, shape fabrics of quartz and biotite aggregates and a preferred orientation of feldspar augen with their strain shadows (Fig. 5.11). Ecc traces are up to 200 micron wide and often centimeters apart. Mineralogically they mainly consist of colourless micas besides biotite, quartz

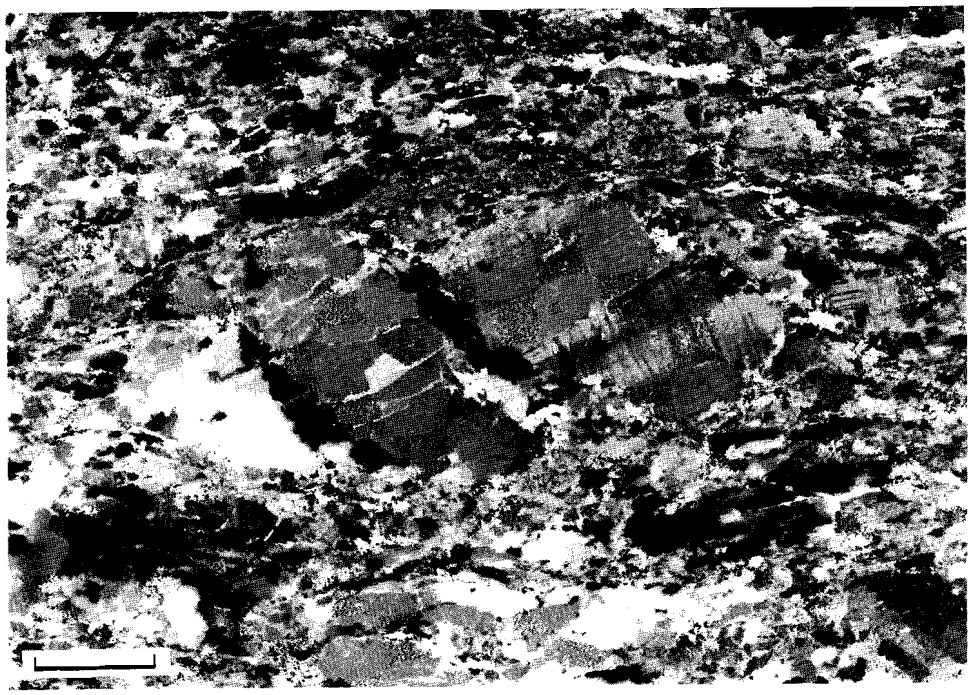

Fig. 5.11 Microstructures of gneiss in the CHSZ. Broken and pulled apart K-feldspar porphyroclast. Within the boudinage necks quartz occurs (in extinction).
Scale bar indicates 1 mm.

and stylolitic residual seams.
Some bands occur which offset the foliation near relatively rigid inclusions (here feldspars). They have the same characteristics as ecc traces, except that the angle between the bands and the foliation is larger and seams are less smooth than ecc traces.

Deformation structures in minerals

Quartz occurs as (1) old grains up to several millimeters with well developed core-mantle structures, (2) trails of 40-50 micron large new grains with foam texture and preferential extinction, indicating domainal fabrics (Garcia Celma 1982), and (3) relatively undeformed, 300-500 micron large grains between fragments of boudinaged feldspars (Fig. 5.11).

Feldspar megacrysts are wrapped by trails of quartz and mica which display intracrystalline features coherent with the curvature of the trails. Intracrystalline deformation of feldspar is indicated by undulatory extinction. The occurrence of strain shadows, boudinage and relative rotation of feldspar fragments suggests rigid behaviour of the feldspar relative to the matrix during deformation. At grain boundaries myrmekites and albite (< 100 micron) grains occur (Fig. 5.11). Common is the occurrence of colourless mica films, up to 100 micron wide at porphyroclast-matrix contacts.

Micas define an oriented decussate fabric in foliation traces. Bending, kinking and recrystallization at kink band boundaries is common. Biotite may show exsolution of small ilmenite grains.

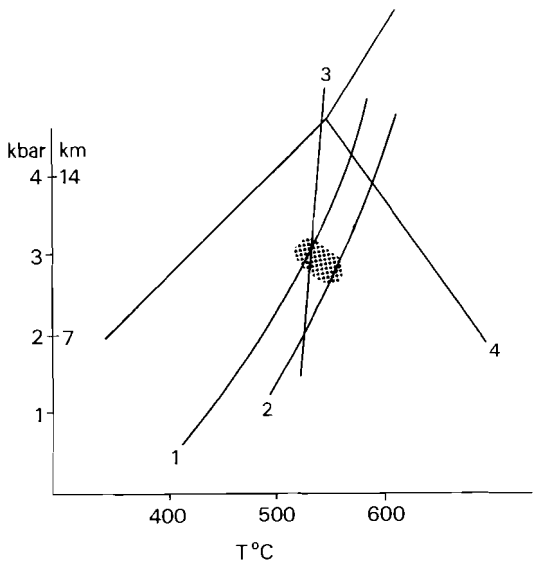

Fig. 5.12 PT conditions of deformation recorded in the CHSZ, based on the breakdown of cordierite. PH_2O = Ptot.

1. *andalusite + Mg-chlorite + Q → Mg-cordierite + biotite (Seifert and Schreyer 1970).*
2. *muscovite + Mg-chlorite + Q → Mg-cordierite + biotite + Vap. (Seifert 1970).*
3. *FeMg-chlorite + muscovite → FeMg-staurolite + biotite + Q + Vap. (Hoschek 1969).*
4. *Aluminosilicates (Greenwood 1976).*

5.1.4 Temperature conditions of deformation

Metamorphic conditions of the deformation in the CHSZ can be inferred from the retrogradation of cordierite producing (1) colourless micas and Mg-rich chlorite and (2) andalusite and Mg-rich chlorite (Fig. 5.12). Staurolite in the staurolite zone largely remained stable during deformation, but local overgrowth by andalusite-quartz symplectites may indicate somewhat lower temperatures (Fig. 5.12). This indicates temperatures ran-

ging from 500-550°C at ca. 3 kbar.

Colourless micas and Mg-rich chlorite occur in relatively strongly retrogressed and flattened cordierites whereas AQ symplectites occur in less retrogressed cordierites. Therefore the latter reaction is considered to be younger. Hence, a temperature decrease occurred during deformation.

5.1.5 Quartz fabric analysis

Studies of lattice preferred orientations of quartz in naturally deformed rocks show a tendency for c-axes to be oriented at a high angle to a mineral lineation which is shown to be the direction of elongation. This feature becomes increasingly pronounced at higher strains eventually resulting in narrow girdles or clusters of c-axes in stereographic projection (Sylvester and Christie 1968, Eisbacher 1970, Burg et al. 1981, Garcia Celma 1983).

Computer simulations using the Taylor-Bishop-Hill analysis (Lister et al. 1978, Lister and Paterson 1979, Lister and Hobbs 1980) show that "model quartzites" (hypothetical monomineralic quartz rocks with an initially random distribution of c-axes) undergo reorientation of c-axes when dislocation glide occurs during deformation. In a plane strain situation these simulations result in concentrations of c-axes at a high angle to the axis of extension and in largely c-axis free areas surrounding this axis. Furthermore, they predict a variety of distinct c-axes patterns for various types of deformation (plane, flattening and constrictional strain) and activity of different slip systems.

The studies of naturally deformed rocks and the computer simulations provide a test whether mineral lineations (in quartzose rocks) have a kinematic significance. To investigate whether the kinematics of the mylonite zone at the gneiss-metasediment contact as deduced from field evidence are corroborated by quartz c-axes preferred orientations, thirteen samples from the zone and two mylonitized migmatites from underneath the Aston gneisses were selected. Emphasis was laid upon the southwestern part of the massif regarding the inferred overprint of WNW-ESE and NS extension (8 samples). From the northern part of the massif 3 samples were selected and 2 samples come from the north eastern hinge zone of the structure.

C-axis fabrics have been measured with the automatic U-stage equipment of the structural and applied geology department of the State University of Utrecht. In each sample 200 or more c-axis measurements have been made in runs of 70-100 grains per domain and/or per group of grains (old-new grains) in order to check (1) homogeneity of the sampled domain relative to the thin section and (2) differences in fabric between groups of grains. The results are depicted in Encl. 2 and Table 5.2.

According to Lister and Hobbs (1980) and Brunel (1980) quartz fabrics mainly reflect the closing stages of the deformation. Therefore the fabrics reported here probably formed in the lower part of the above established temperature range, say at 500-525° C.

The following general observations have been made (Encl. 2, Table 5.2):

(1) All c-axis fabrics show a distinct c-axes free area surrounding the quartz-biotite lineation (2,3,4,6,7,8,9,11,14) or relatively few c-axes in that region (1,5,10,12,13,15), confirming extension in this direction.

(2) Three domains of fabric types and/or orientations can be distinguished:

zone a- This "zone" is furthest away from the gneisses and represented by diagram 1. Plane strain with a NNE stretching direction is indicated. Comparison of old grain and new grain orientations (Fig. 5.13a) shows that both old and new grains c-axis fabric patterns show a girdle perpendicular to the lineation and the foliation and a maximum at a high angle to the girdle and near the lineation. The diagrams differ in that the new grain girdle is more continuous and the maximum near the lineation is less important than in the old grain c-axis pattern. Since the microstructure of the sample points to rotation recrystallization, the maximum near the lineation and the differences between both c-axis patterns could be due to host control (Hobbs 1968).

zone b- This zone is represented by diagrams 2, 5 and 13b. A cleft girdle distribution (2) or pseudo cleft girdle distribution is found with maxima (small circles ?) perpendicular to the main girdle occur (5, 13b). Similar fabrics occur in the Taylor-Bishop-Hill analysis. Model quartzite B (Lister and Hobbs 1980, p. 362) yields fabrics of type 5 and 13b at relatively high constrictive strains, of a type intermediate between k=1 and k= ∞. The fabric of diagram 2 may be found in the constrictive deformation of model quartzite A (Lister and Hobbs 1980, p. 361). New grain c-axis orien-

sample	rock type	non-quartz content	microstructure: quartz grain size	microstructure: grain boundary alignment in veins	microstructure: foliation	c-axis fabric	inferred (late) strain increment
1. (SG9264)	quartzite	<20% colourless mica, feldspar apatite, zircon	old ∿100μm new 20-30μm	-	seams of non-quartz	old: single girdle new: single girdle type I	plane non-coaxial
2. (SG12658)	quartz vein in schist	<10% feldspar, biotite, apatite	old >½mm new 100-200μm	conjugate	phacoidal quartz lenses at 200-300 μm scale in schist	old: cleft girdle new: clusters	constriction coaxial
3. (SG12653)	quartz vein in schist	<5% biotite	old ∿2mm new 30-70μm	single	ribbon quartz mica seams	new: incomplete crossed girdle domainal	plane non-coaxial
4. (SG15500)	quartz vein in gneiss	<2% feldspar	old 1-2mm new(1) 0.2-0.5mm new(2) 10-20μm	conjugate	domainal grain size distribution	new(1): single girdle	plane undef.
5. (SG15525)	quartzite	<30% feldspar (biotite, Mg-rich chlorite)	50-100μm	-	shape preferred orienta-	pseudo cleft girdle	constriction coaxial
6. (SG15523)	quartz vein in schist	<2%	old ∿2mm new 50-150μm	conjugate	old-new grain ribbons, domainal	incomplete crossed girdles	plane coaxial
7. (SG15520)	quartz vein in schist	<20% biotite	50-200μm	single	grain shape preferred orientation single ecc	ill defined single girdle	plane non-coaxial
8. (SG9249)	quartz vein in gneiss	<5% feldspar, colourless mica	old ∿1mm new 50-100μm	weak conjugate	domainal grain size distribution, single ecc in gneiss	pseudo single girdle, type I	plane non-coaxial

9. (SG15503)	quartzite	<30% biotite	25-250μm	-	phacoidal conjugate ecc	type II girdles	plane coaxial
10. (SG15505)	quartzite	<40% feldspar, zoisite	30-100μm	-	compositional banding, single ecc	type II girdles	plane non-coaxial
11. (SG15506)	quartz-mica mylonite, K-feldspar augen	<2% in quartz-ribbons	new 50μm	-	quartz ribbons domainal grain shape P.O., compositional banding	girdle	plane undef.
12. (SG14324)	mylonitic Hospitalet gneiss	<5% in quartz-ribbons	new 25-75μm	-	quartz ribbons mica bands single ecc	type II girdles	plane non-coaxial
13. (SG14326)	quartz vein in biotite phyllite	<20% biotite	old >300μm new 30-50μm	conjugate	phacoidal conjugate ecc	parallel section type II (?) clusters	constriction(?) coaxial
14. (SG14334)	quartz rich compositional band in Aston migmatite	<35% biotite, sillimanite	ribbons >0.5 mm long	-	quartz ribbons compositional banding	pseudo crossed girdle	plane non-coaxial
15. (SG14335)	id.	<25%	old 0.5mm new 50-200μm	conjugate	phacoidal	type II girdles	plane coaxial

Table 5.2

tations in this sample (Fig. 5.13b) differ strongly from those of old grains.

zone c- This zone is closest to the gneiss-metasediment contact. It is represented by the majority of the fabrics (3,4,6,7,8,9,10,11,12), from which the inferred strain is plane and stretching occurred in WNW-ESE direction. Incomplete type I single girdles (8) (Lister and Williams 1979), and crossed girdles (3, 6) mainly occur in the south western part of the massif. Type II fabrics (Lister and Williams 1979) occur in the north flank and the hinge zone (9,10,12).

(3) Some peculiar fabrics occur:

Diagram 12 is a type II diagram resembling the diagrams presented by Behr from the Saxony granulite terrain (reviewed by Lister and Dornsiepen 1982). It shows an opening angle of the III maxima (Fig. 5.13c) which is larger than would be expected in deformation in greenschist up to mid amphibolite facies (cf. Lister and Dornsiepen 1982). Its marked asymmetry would correspond to a dextral sense of shear taking the single ecc set as a sense of shear indicator (Simpson and Schmid 1983). The III maxima appear to have an orthogonal relationship with the ecc.

Diagrams 4 and 11 show a distribution of c-axes with a symmetric disposal relative to the foliation but not to the normal to the foliation. The samples were cut exactly parallel to the mineral lineation and come from near the contact, i.e. the strongest deformed zone. No adequate solution can be offered for this feature.

(4) A consistent orthogonal relationship exists between the traces of ecc in stereographic projection and the disposition of maxima of c-axes in diagrams 7,8,9,12,13a,14,15. Such a geometry has been noted by others (Casas 1982, García Celma 1983, Law et al. 1984).

C-axis patterns and microstructures

Grain boundary alignment of quartz (Simpson and Schmid 1983, Burg 1986) is common in quartz veins: single, conjugate, and conjugate alignment with a dominant direction occurs (Fig. 5.10).

Conjugate distribution of ecc traces and/or quartz grain boundary alignment and/or a phacoidal microstructure apparently goes with a symmetric distribution of quartz c-axes (the foliation being mirror plane) in diagrams 2 (new grains), 4,6,9,13 and 15, whereas asymmetry of such fea-

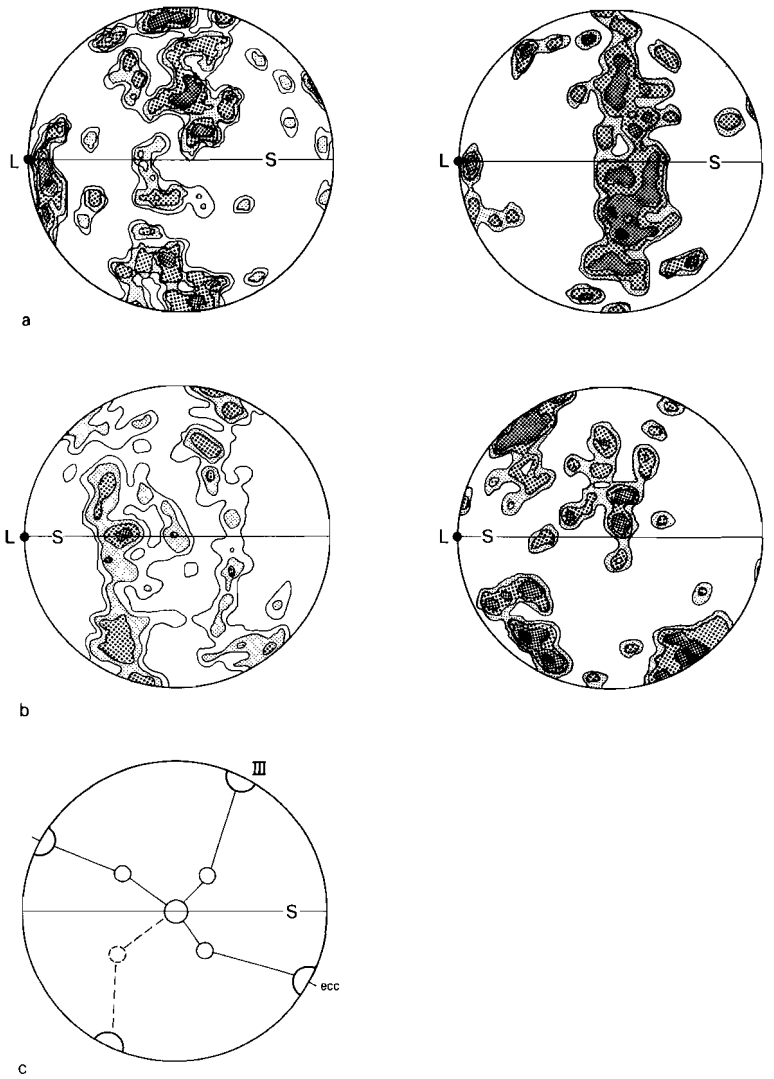

Fig. 5.13

a. Old grain c-axis plot (left) and new grain c-axis plot (right) of sample 1. For discussion see text.
b. Old grain c-axis plot (left) and new grain c-axis plot (right) of sample 2.
c. Fabric skeleton of sample 12. For discussion see text.

tures goes with asymmetry of the quartz c-axis fabric (3,7,8,10,12). Samples 11 and 14 display a very weak single ecc, their overall microstructure being rather symmetrical.

5.1.6 Discussion and conclusions

Field evidence and microstructures support the existence of a lower amphibolite facies mylonite zone at the contact of gneisses and metasediments in the Hospitalet mantled gneiss antiform. Temperatures during deformation exceeded Rb-Sr closing temperatures for micas, and therefore the 250-270 Ma muscovite ages obtained by Jäger and Zwart (1968) from gneisses near the gneiss-metasediment contact indicate that the mylonite zone formed in late Hercynian times.

The field observations indicate WNW-ESE directed stretching throughout this zone, slightly oblique to the EW trending gneiss antiform. Locally, particularly in the southwestern part of the massif indications exist for an older NNE-SSW stretching event within this zone. Quartz c-axis fabrics confirm this interpretation: in rocks near the gneiss-cover contact, such as depicted in Fig. 5.6, NNE-SSW stretching is indicated by elongated andalusites and other features, whereas the quartz c-axis fabric indicates WNW-ESE stretching (Encl. 2). Since the c-axis fabric reflects the final stages of deformation (Lister and Hobbs 1980) the WNW-ESE stretching represents the younger event.

Shear sense in the mylonite zone

Zones of relatively high ductile strain are usually found at sites where intracrustal movement is inferred or has taken place (Bouchez and Pecher 1981 (Himalayas), Burg et al. 1981 (Hercynian transcurrent zone in Southern Spain), Behrmann and Platt 1982, Konert and Van den Eeckhout 1983 (Betic Zone, southern Spain)). Therefore it is interesting to investigate the kinematic properties of the CHSZ in this respect. The flow pattern in zones of movement can be determined by means of sense of shear indicators (reviewed by Simpson and Schmid 1983), which include relative rotation of porphyroclasts, orientation of ecc and asymmetry of quartz c-axis fabrics and quartz (sub)grain preferred orientations.

The early NNE-SSW event

The high strain zones southwest of the gneisses (Fig. 5.5) indicate relative uplift of the gneisses. The same sense of movement can be inferred from the orientation of the ecc/shear bands relative to the S3 foliation, and the asymmetry of quartz c-axis fabric 1b conforms to this sense of shear.
The orientation of the finite shortening direction as can be deduced from the orientation of the ecc planes (Fig. 5.5). It is at a high angle to the pre-existing S3 foliation, consistent with the strong flattening of this structure around porphyroclasts.

The WNW-ESE event

The senses of shear deduced from various indicators during the WNW-ESE event are shown in Table 5.3. Non-coaxial eastward flow of the metasediments relative to the underlying gneisses apparently has occurred in the eastern hinge zone of the gneiss antiform. This is supported by moderately to steeply outward dipping zones of increased ductile strain within the gneisses in this region. These zones suggest uplift of the central part of the gneisses relative to the margins (Chapter 6). In the northern part of

	ecc	rotation of porphyroblasts	curvature of L3 lineations	quartz c-axis fabrics
north flank (west of Mérens-les-valls)	conjugate set ↔	-	-	9 ↔ 10 ← 11 -
northeastern part	conjugate with a dominant set ↔	-	→	-
hinge zone in the eastern plunging nose	single set →	-	←	12 →
southwestern part (Andorra)	conjugate set ↔	N-NW	←	3 → 4, 6 ↔ 7, 8 ←

WNW-ESE → denotes movement of the metasediments relative to the underlying gneisses

Table 5.3 Shear senses in the CHSZ at various localities in the Hospitalet massief.

the massif strain is largely coaxial. In the northeastern part a situation is found intermediate between the north flank and the hinge zone: ecc is largely conjugate, but one set prevails. Southwest of the gneisses no clearcut sense of movement can be deduced.

To conclude, during the WNW-ESE event the rocks in the CHSZ again underwent shortening at a high angle to the pre-existing foliation. No clear cut sense of movement can be deduced from various shear indicators at the scale of the massif. Largely coaxial strain at this scale is implied.

The rheology of metasediments and gneisses

In a rockpile which consists of two major rock units, such as the metasediments and the gneisses the rheological behaviour of both rock types is of interest in order to understand the distribution of deformation structures.

The strain increase in the CHSZ towards the gneiss-cover contact suggests that the contact acted as a mechanical boundary. From the microstructures it can be inferred that the gneisses and metasediments differ fundamentally in the deformational behaviour of quartz. Overall plastic strain occurred in the quartz of the gneisses, whereas grain boundary diffusion processes predominate in the quartz of the schists. Assuming that differences in deformation of quartz reflect differences in bulk deformation, higher stresses could have been present in the gneisses relative to the schists at constant strain rate. This would correspond to a mechanical situation in which the gneisses behaved as a relatively rigid body.

A dynamic model for the late Hercynian deformation in the Hospitalet massif

It has been shown that the gneiss antiform is linked to the formation of the S3 foliation in the massif (Chapter 4). Hence, its formation predates the CHSZ.

According to Soula (1982) the structures in the CHSZ reflect "the ultimate result" (p. 326) of the deformation phase that formed the most prominent foliation in the massif (his D2; D3 in the present concept). The overprint of two deformational events, which both resulted in mylonitic structures,

argues against Soula's interpretation. Furthermore, the S3 foliation developed prior to the peak of metamorphism, whereas the CHSZ formed during retrogression. The interkinematic porphyroblastesis also hampers a direct correlation between the kinematic axes of D3 and those of the early NNE-SSW stretching in the CHSZ.

Dynamic models for the late Hercynian deformation within the Axial Zone have to account for the two stages of activity of the mylonite zone at the contact of gneisses and metasediments in the Hospitalet massif, and, furthermore, for other late structures in the massif. The latter structures comprise the El Serrat-Ransol zone (section 5.2), the kilometer scale fold in the eastern hinge zone of the gneiss antiform (section 5.3), and the small-scale D6 recumbent folds. On the basis of (a) similar metamorphic conditions and (b) the orientation of the kinematic axes, in particular the elongation direction, it is suggested that the WNW-ESE event in the mylonite zone at the gneiss-metasediment contact, the ERZ and the recumbent folds are part of one deformational episode in the massif. Overprint of D6 structures on S4 and S5 in the ERZ (section 5.2) indicates that these features did not form simultaneously though. The older NNE-SSW directed stretching event in the CHSZ is considered to represent a seperate deformational episode.

Data concerning the NNE-SSW stretching event are scarce, which prevents inferences to be made on the dynamics of the event.

During the WNW-ESE stretching event the finite shortening direction is consistently oriented at a high angle to the previously existing foliation and hence to the gneiss-cover contact. This contact is antiformal in shape and the orientation of the finite shortening direction thus systematically varies across the massif. A similar distribution of finite shortening directions can be seen in one of the experiments by Ghosh and Ramberg (1976) around a rigid inclusion. On basis of (a) the rheological inferences made above and (b) the variation in orientation of finite shortening directions it may be concluded that the Hospitalet gneiss antiform acted as a relatively rigid body during formation of the CHSZ. The metasediments were draped around this body with the formation of D6 recumbent folds away from the gneisses and the mylonite zone at the gneiss-cover contact.

Implications for late Hercynian tectonics in the Axial Zone of the Pyrenees

In this section attention is drawn to structures in metamorphic rocks in other massifs in the Axial Zone of the Pyrenees.
In the western Lys-Caillauas massif (Fig. 4.1) De Bresser et al. (1986) report a deformation phase (their D3) which is broadly contemporaneous with metamorphism. In the late stages of this phase rotation of porphyroblasts occurred with NNE-SSW directed rotation axes. Rotation is dextral looking north. They describe a WNW-ESE directed mineral lineation which in their opinion formed simultaneous with the rotation of the porphyroblasts. Stretching in WNW-ESE direction with a subvertical shortening axis is implied.
From the deeper exposed parts of the Bosost area Zwart (1962, 1979) describes rotation of porpyroblasts similar in sense and direction of rotation to the Lys-Caillauas area. Zwart (1962) inferred simple shear, the pre-existing foliation acting as slip plane. He calculated an eastward top-over-base shear with $\gamma = 4-5$, indicating 4-5 km displacement for every kilometer of thickness of the zone.
In the western Aston massif Verspyck (1965) describes NW-SE elongated quartz-sillimanite nodules. Quartz c-axis fabrics (Encl. 2) and NE-SW trending foliation boudins at the contact of gneisses and migmatites east of Etang de Gnioure imply stretching in NW-SE direction.
In the Canigou-Carança massif, situated east of the Hospitalet massif (Fig. 4.1), Guitard (1970) reports flattening of the foliation around porphyroblasts, but no orientations of kinematic axes of this flattening event are known.
Finally, observations in the metamorphics of the Albères massif again indicate flattening of the foliation around porphyroblasts and NW-SE oriented mineral lineations. These observations suggest that WNW-ESE to NW-SE oriented stretching with a steep shortening axis of porphyroblast bearing rocks is a feature which all mentioned massifs have in common. This probably indicates that the features formed as a response to a deformation of regional extent. The relative importance of this event is yet poorly understood. Is it, as suggested by Zwart (1962) for the Bosost area, a bulk non-coaxial deformation ? Or, as indicated in the Hospitalet massif, a bulk coaxial deformation? Obviously, more data on senses of

shear during the event from all massifs are needed to answer this question. However, it has to be borne in mind that local flow partitioning (Means et al. 1980, Lister and Williams 1983) can happen in situations in which a bulk deformation affects previously anisotropic rocks and/or materials with different rheological properties. Around rigid bodies a non-coaxial bulk flow can be locally decomposed in flow in the same sense and flow in opposite sense, with intermediate areas governed by coaxial deformation (Garcia-Celma 1983). Therefore local contradictions in flow senses can fit a general flow picture, but utmost care has to be taken when trying to extend inferences valid for a local situation to a bulk picture. Hence, conclusions about flow in the CHSZ only apply to the Hospitalet massif and a larger scale model should take them into account, but they cannot be used as indicators of the flow regime at a larger scale.

The late Hercynian tectonic regime has to account for (1) flattening with a subvertical shortening axis, (2) uniform stretching of the massifs and (3) the presence of steep shear zones such as the (dextral) ERZ (section 5.2). Based on these features a tectonic working hypothesis may be formulated. It is suggested that the Pyrenean belt was (part of) an extensional or transtensional deformation zone in late Hercynian times. The hypothesis is in agreement with the model proposed by Speksnijder (1985, 1986): sedimentation simultaneously acting with deformation in Stephanian-early Permian EW trending grabens suggest graben formation in a transcurrent tectonic setting. Soula et al. (1979) ascribe post-Variscan basins to transcurrent tectonics and Bixel et al. (1983) suggest that late Hercynian plutonism occurred in a transcurrent regime.

5.2 THE EL SERRAT-RANSOL ZONE, A TRANSCURRENT ZONE OF REFOLDING

The El Serrat-Ransol Zone (ERZ, Fig. 5.1) is up to 1.5 km wide and defined as the area where D4 structures are present. Within aproximately the same area a fifth foliation is locally developed. Zwart (1965) and Verspyck (1965) report refolding (their D4) of the most prominent foliation north of El Serrat, a region taken as part of the ERZ in this thesis. Their D4 structures may partly coincide with the structures described here.
Most characteristic of the ERZ is the large spread of cleavage/cleavage and cleavage/bedding intersection attitudes. On the map (Fig. 5.1) the ERZ is hardly influenced by topographical effects and therefore its attitude is steep. It is at a high angle to the shallowly SW-dipping mineral zonation in the massif (Chapter 7) and affects rocks of the biotite zone, the andalusite-cordierite (AC) zone and the staurolite zone. Towards the WNW the ERZ probably is cut off by the younger Mérens shear zone. Towards the ESE, in the vicinity of Soldeu, it probably merges into the mylonite zone at the gneiss-cover contact.

5.2.1 Small-scale structures within the ERZ

Bedding is recognizable in most outcrops and D2 and D3 structures can usually be observed, depending on the intensity of D4 structures.

D4 structures

D4 structures comprise folds, cleavages and lineations.
In quartzites D4 folds are often disharmonic, open to tight buckle folds with upright axial planes. In outcrop and at the scale of the map the folds are locally disrupted in the flanks (Fig. 5.15a). The attitude of D4 fold axes in bedding strongly varies, depending on pre-D4 bedding attitudes. The axial plane foliation (S4) is steeply inclined and strikes EW (Fig. 5.14). Intersections of S4 on S3 gently plunge west, those on S2 plunge steep.
S4 morphology varies with rocktype and strain intensity as indicated by variation in tightness of D4 folds. In the biotite zone semipelitic rocks

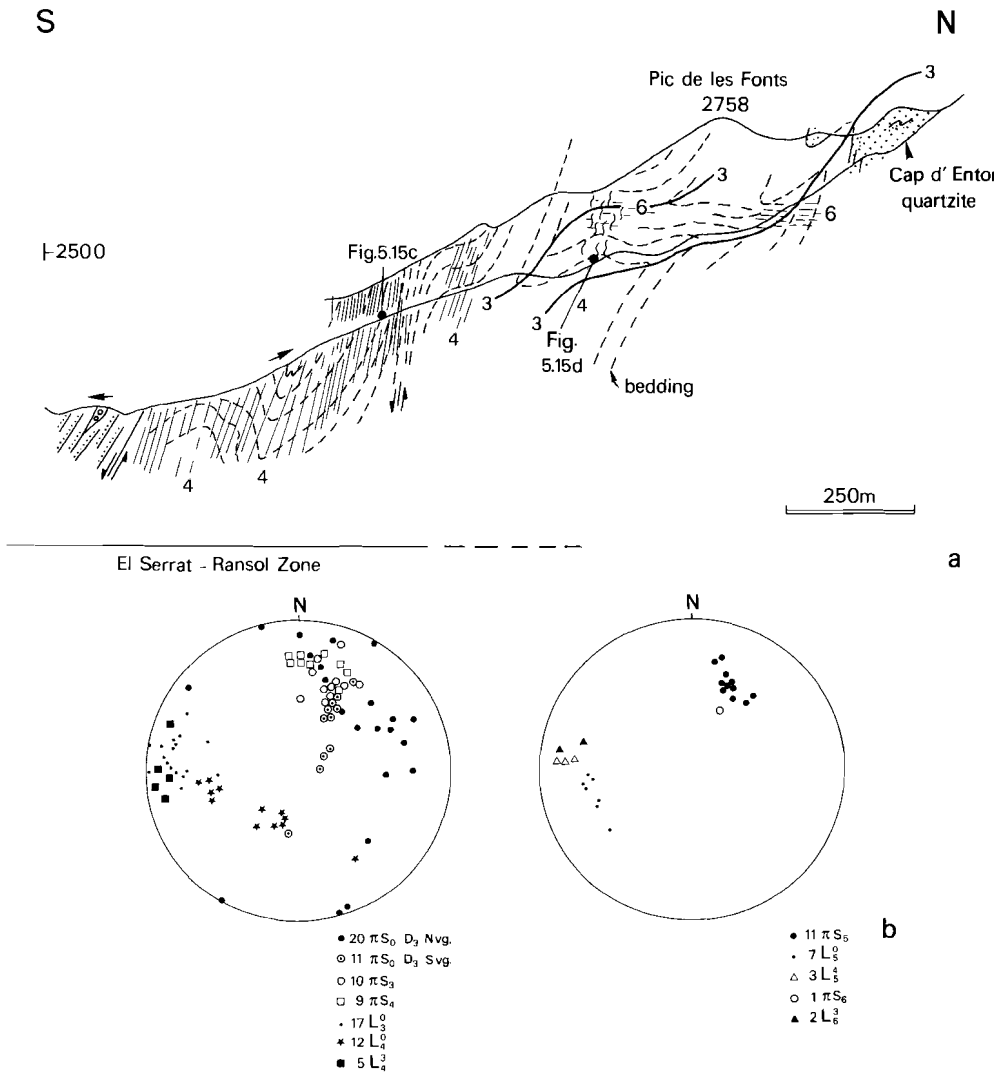

Fig. 5.14

a. Structural cross section through the ERZ in the Vall del Riu (for location see Fig. 5.1). The S4 foliation is indicated, other foliations except S6 are omitted. To the north, D4 structures become crenulated by D6 structures and diminish afterwards. D5 structures are not indicated. Arrows in the south part denote younging direction.

b. Lower hemisphere equal area projections of D3, D4 and D5 planar and linear structures of the section shown in a. Note the spread in L4 lineations and the variation in bedding attitudes with changing D3 vergence.

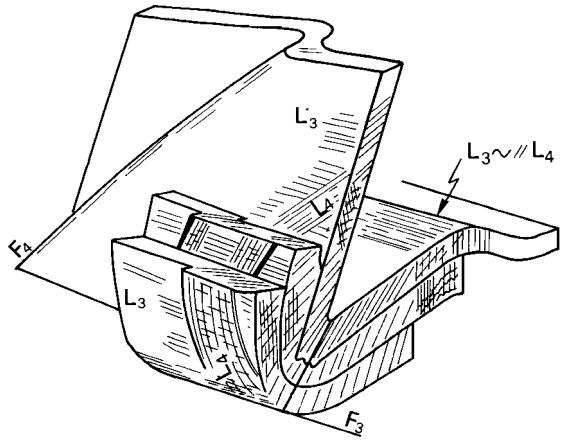

Fig. 14c Block diagram showing S4/F3 overprint relationship. Note the large spread in L4 lineations across the D3 fold.

display a mm spaced differentiated crenulation cleavage and pelites show a continuous cleavage. In metapelites in the AC and staurolite zone S4 is a up to 5 mm spaced, locally differentiated crenulation foliation. In quartzites S4 is lacking.

In the AC and staurolite zones S4 curves around porphyroblasts of andalusite, cordierite and staurolite, but S4 is commonly included in late andalusite porphyroblasts with ragged outlines in the staurolite zone north of El Serrat (Fig. 5.16).

Microscopically S4 is characterized by deformation-recrystallization textures of micas and textures indicative for solution transfer of quartz in all metamorphic zones. Neoformation of biotite porphyroblasts with

Fig. 5.15

a. D4 fold pair in upper Seo fm. The structures refold bedding and the S3 foliation. Hairpin in the road leading into the Ransol valley.
b. D4 synform cut by D5 differentiation bands. Note concordancy of S5 and bedding in the southern limb. Same locality as a.
c. Overprint of NS trending S4 on bedding (trends NW-SE) and D2 differentiated foliation (trends NE-SW). Vall del Riu. For locality see Fig. 5.14a.
d. Open D6 refolding with subhorizontal EW trending axial plane of S4 foliation (trends NS), which still can be seen to crenulate the S3 foliation. Vall del Riu. For locality see Fig. 5.14a. In the same region D6 can be observed to crenulate the S5 foliation. (Not shown in photographs).

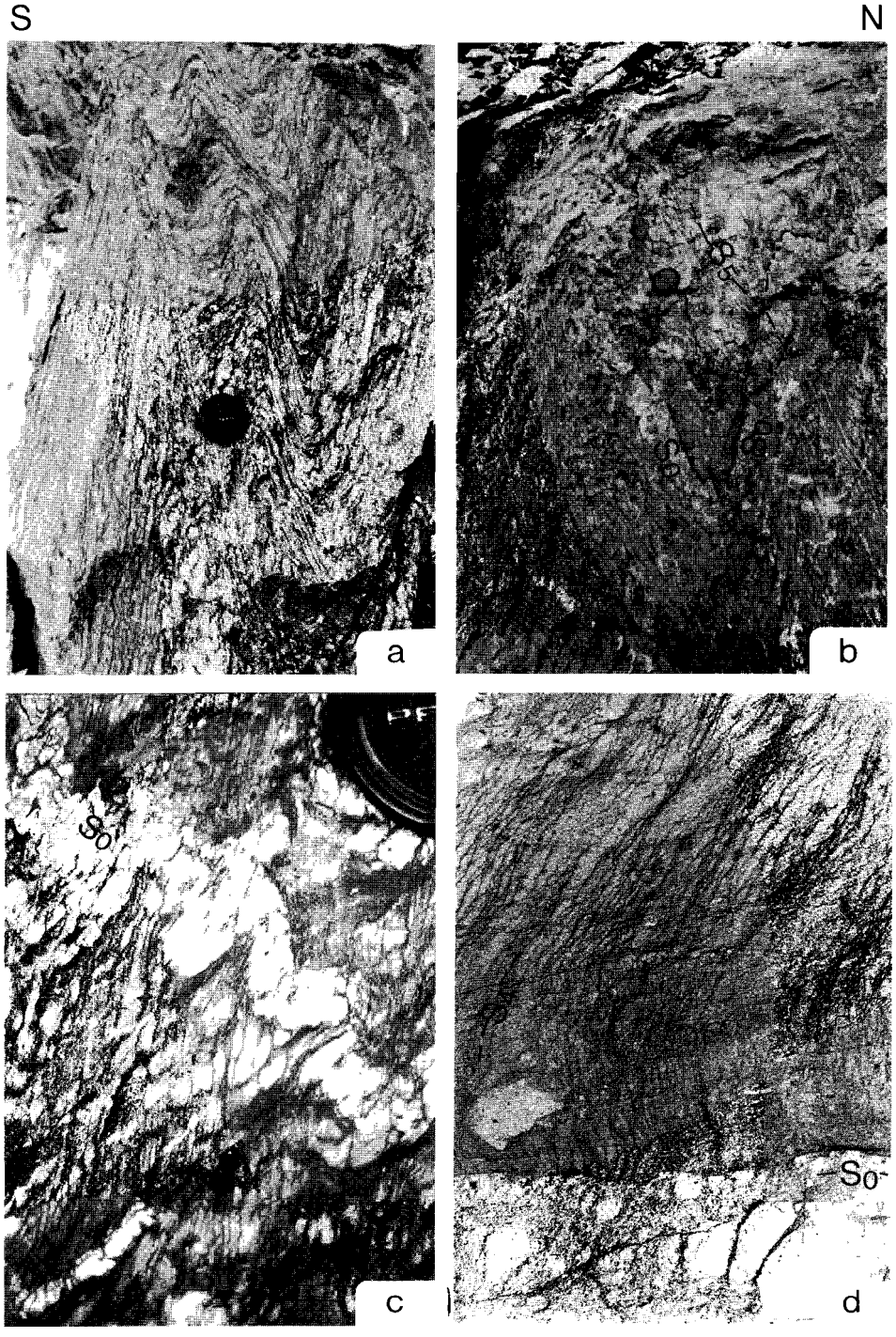
S
N
a
b
c
d
So
So

(001) traces parallel to the S4 crenulation traces is restricted to the AC and staurolite zones, whereas neoformation of andalusite is restricted to the staurolite zone. Cordierite shows retrogression to andalusite/Mg-rich chlorite aggregates in fold hinges in the staurolite zone. This suggests similar metamorphic conditions as in the mylonite zone at the gneiss-cover contact (section 5.1, Fig. 5.12).

D5 structures

The S4 foliation and D4 folds are locally overprinted by D5 structures, which are defined by rather peculiar differentiation bands (Fig. 5.15b). The bands are pale coloured, ca. 0.5 cm wide, remarkably straight and traceable across several meters. They occur individually or in packets up to 20 cm thick. The bands mainly consist of quartz, but locally appreciable amounts of albite are found within them. Adjacent pelitic lithologies show a decrease in quartz content.

D6 structures

Away from the ERZ the metasediments of the infrastructure have been locally refolded in recumbent open folds and crenulations (Chapter 4, section 5.1). Overprint of these structures on S4 and S5 in the ERZ (Figs. 5.15d, 5.16) suggests that the recumbent folds are sixth phase structures, younger than the ERZ.

5.2.2 Structural interpretation of the ERZ

The increase in strain, as recorded by (a) tightness of D4 folds and (b) the amount of D4 structures, from the rims towards the central part of the zone, suggests that the ERZ acted as a zone of differential movement,

Fig. 5.16 Interference of D4 and D6 structures (D5 is absent in this handspecimen). S4 is included in late andalusite porphyroblasts. From the road cut which leads from the Riu de Rialb into the Sorteny valley, north of El Serrat. ►

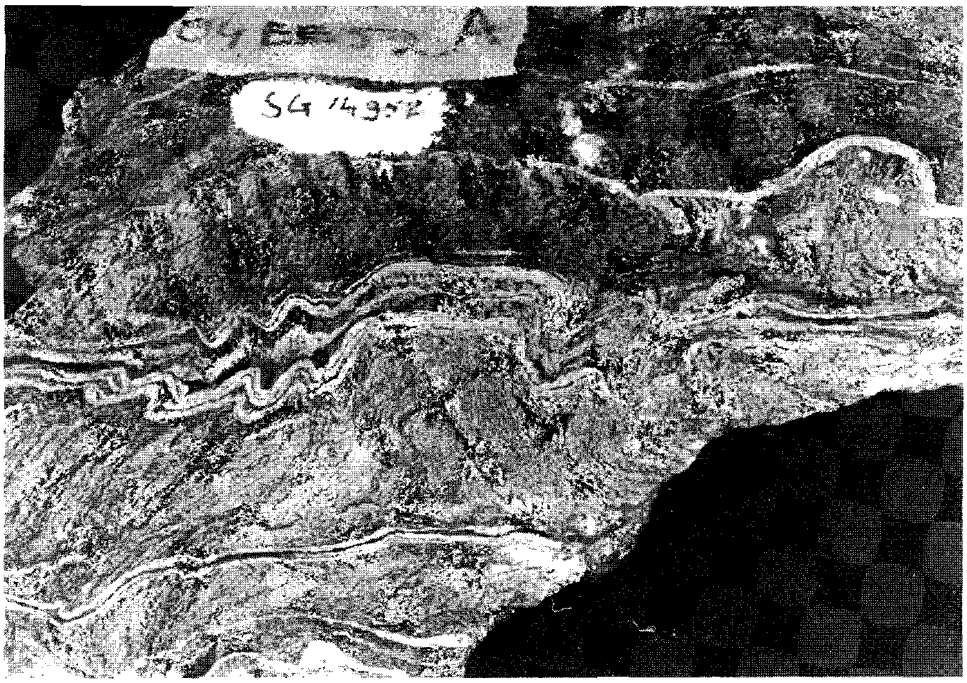
SG 1495

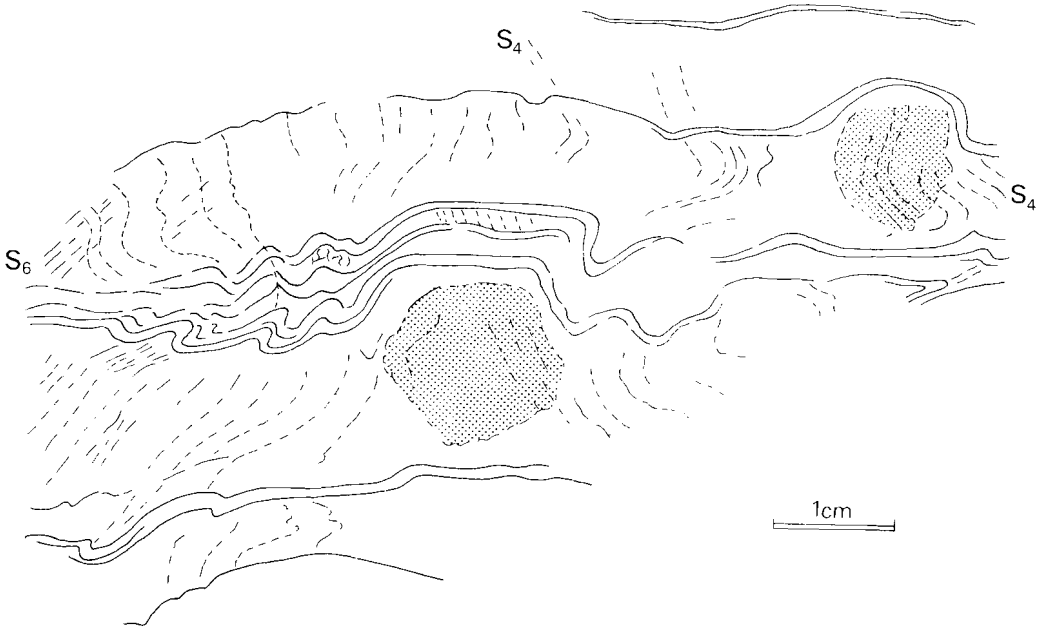
S4
S4
S6
1cm

i.e. a shear zone. The offset of lithological markers within the highest strained zone adds to this interpretation.
The obliquity of the S4 foliation with respect to the boundaries of the ERZ (Fig. 5.14b, Encl. 1) probably reflects the angular relationship between finite strain fabrics and shear zone boundaries often found in nature (Ramsay 1980), in this case indicative for a dextral sense of shear.
The isograd pattern had been established before the ERZ was active and as no marked offset of the gently SW dipping isograds occurs, the movement direction within the zone must lie near its intersection with the isograds, which is nearly horizontal.
To get a rough impression of the amount of offset across the zone one may, for the sake of argument, assume simple shear across it. For the 30^{o} angle between S4 foliation and the zone boundaries, this yields a shear strain of 1.16 (Ramsay 1967, fig. 3-22). This corresponds to a maximum offset of 1750 m, which is not a very high value, but consistent with the slightly disturbed aspect of the lithological markers. Such a shear strain corresponds to 40% shortening across the zone (Ramsay 1967, fig. 3-21), consistent with the presence of the newly formed S4 foliation within it.

On basis of (1) the similar metamorphic conditions, and (2) the similar orientation of the elongation direction, it is suggested that the ERZ and the WNW-ESE stretching event in the mylonite zone at the gneiss-metasediment contact are part of one deformational episode in the massif. The age of the mylonite zone at the gneiss-cover contact is considered to be late Hercynian (section 5.1). The ERZ therefore is also of late Hercynian age.

Recognition of zones such as the ERZ is largely aided by porphyroblast/foliation relationships. Absence of porphyroblast as in the suprastructural domain of the Axial Zone of the Pyrenees, would cause overprint of one slaty cleavage by another, as can be inferred from the structural relationships in the lower biotite zone metapelites in the ERZ. In these domains recognition of ERZ type zones will be considerably more difficult than in the infrastructural domain.

5.3 A MAJOR RECUMBENT FOLD IN THE EASTERN HINGE ZONE OF THE HOSPITALET GNEISS ANTIFORM

In the east part of the Hospitalet massif (Figs. 5.1, 5.17) Cambro-Ordovician metasediments overlie the SE plunging nose of the gneiss antiform and flank the gneisses to the north. To the north these metasediments are tectonically overlain by sheared Silurian black slates, mylonitic Devonian carbonates and mylonitic Cambro-Ordovician siliclastics. This zone is separated from the mylonitic metamorphics of the Aston massif by the Mérens fault. Tectonic contacts are steep to north dipping.

Within the Cambro-Ordovician metasediments a large-scale recumbent fold has been mapped (Figs. 5.17, 5.18), outlined by a lithological succession dominated by thinly bedded, pale coloured quartzites. The lower (western) limb of this structure dips moderately to steep N-NE and youngs northward. Hence, the structure is a syncline. Its lower limb is cut by two shear zones which merge westward. Both shear zones terminate eastward in open upright folds in the north part of the upper limb. This limb is cut off by the Pinet fault to the north.

The recumbent fold is a third phase structure according to the local deformation scheme set up in the section shown in Fig. 5.18. It refolds north vergent D2 folds and a somewhat obscure D1 fabric.

The fold overlies the gneisses via a zone of highly strained andalusite-cordierite-biotite phyllites, the CHSZ (section 5.1). The transition from the fold to the CHSZ is largely obscured by scree. A gradual tightening of D3 folds towards deeper structural levels, i.e. the CHSZ, is indicated in the southern part of the section in Fig. 5.18. A similar transition can be observed along the ridge north of Etang Bleu in the south part of the map (Fig. 5.17). WNW-ESE directed flow in the CHSZ is indicated by elongated andalusite and cordierite porphyroblasts and rodded quartz lenses (section 5.1). The metasediments were translated in ESE direction relative to the gneisses (section 5.1).

The fold and the CHSZ are cut by several steep faults, in the vicinity of which the foliations are crudely crenulated by fourth phase structures.

The next section provides a description of the involved deformation structures based on observations in the section of Fig. 5.18b.

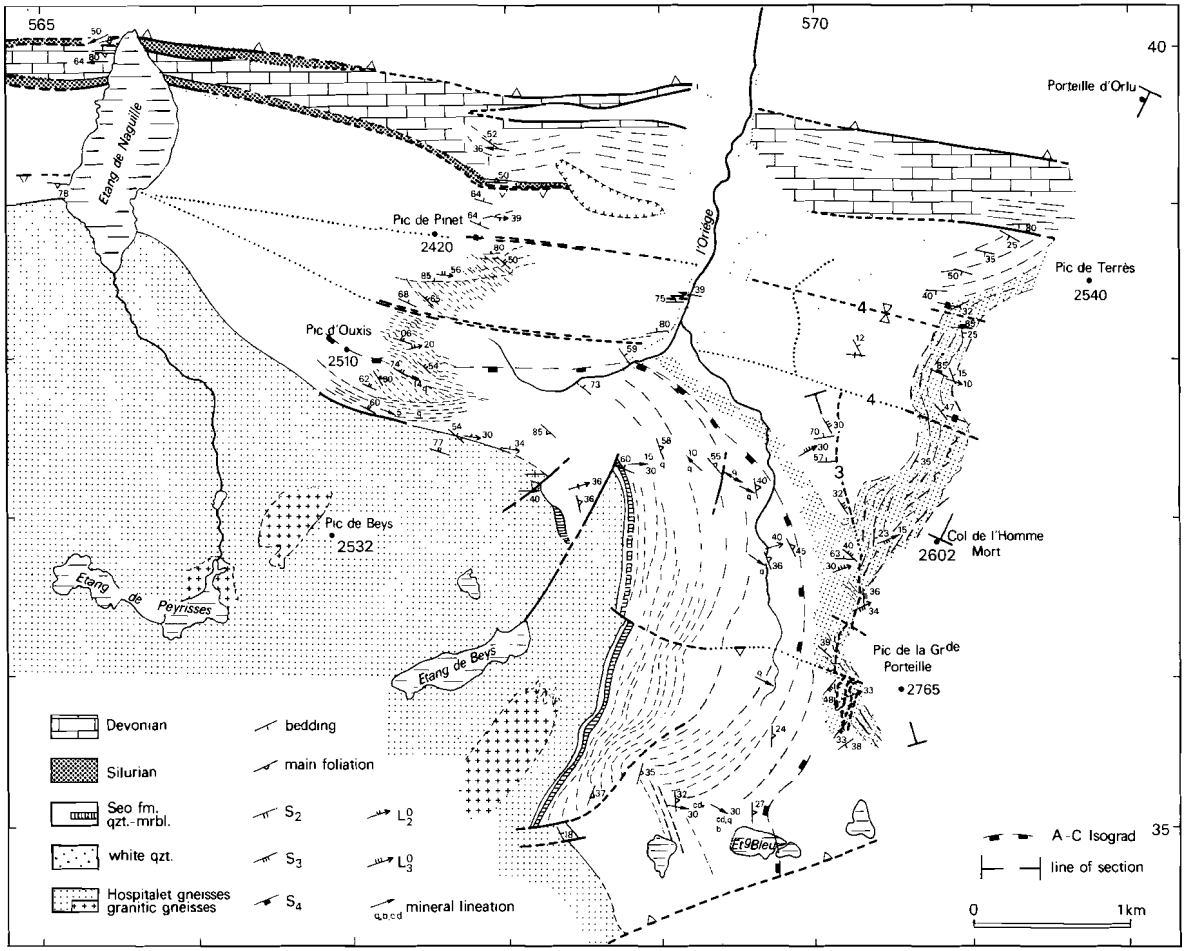

Fig. 5.17 *Geological map of the eastern Hospitalet massif.*

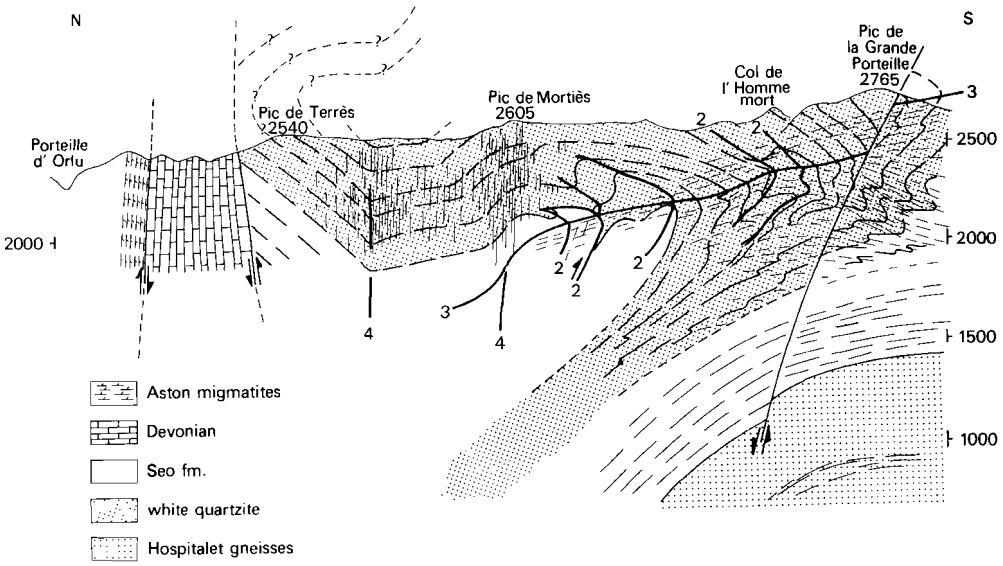

Fig. 5.18a Section showing the recumbent fold above the Hospitalet gneiss antiform. Numbers refer to deformation phases. The cleavage indicated in the north part of the flat lying limb is S4.

5.3.1 Small-scale structures

D1 structures

Some quartzite beds contain a discrete spaced cleavage which is oblique to bedding and the D2 structures. These structures have been attributed to D1.

D2 structures

D2 folds and an S2 axial plane cleavage can be traced throughout the section of Fig. 5.18b. Minor folds and cleavage/bedding relationships change vergence indicating the existence of 200-400 m scale north vergent folds. Fold axes and cleavage/bedding intersections gently plunge ENE (Fig. 5.18b).

The style of the D2 folds is illustrated in Figs. 5.18-5.20:

(a) Limbs with south vergent minor folds show open to tight upright folds. The angle between cleavage and bedding is ca. 30^{o} (Fig. 5.19a).

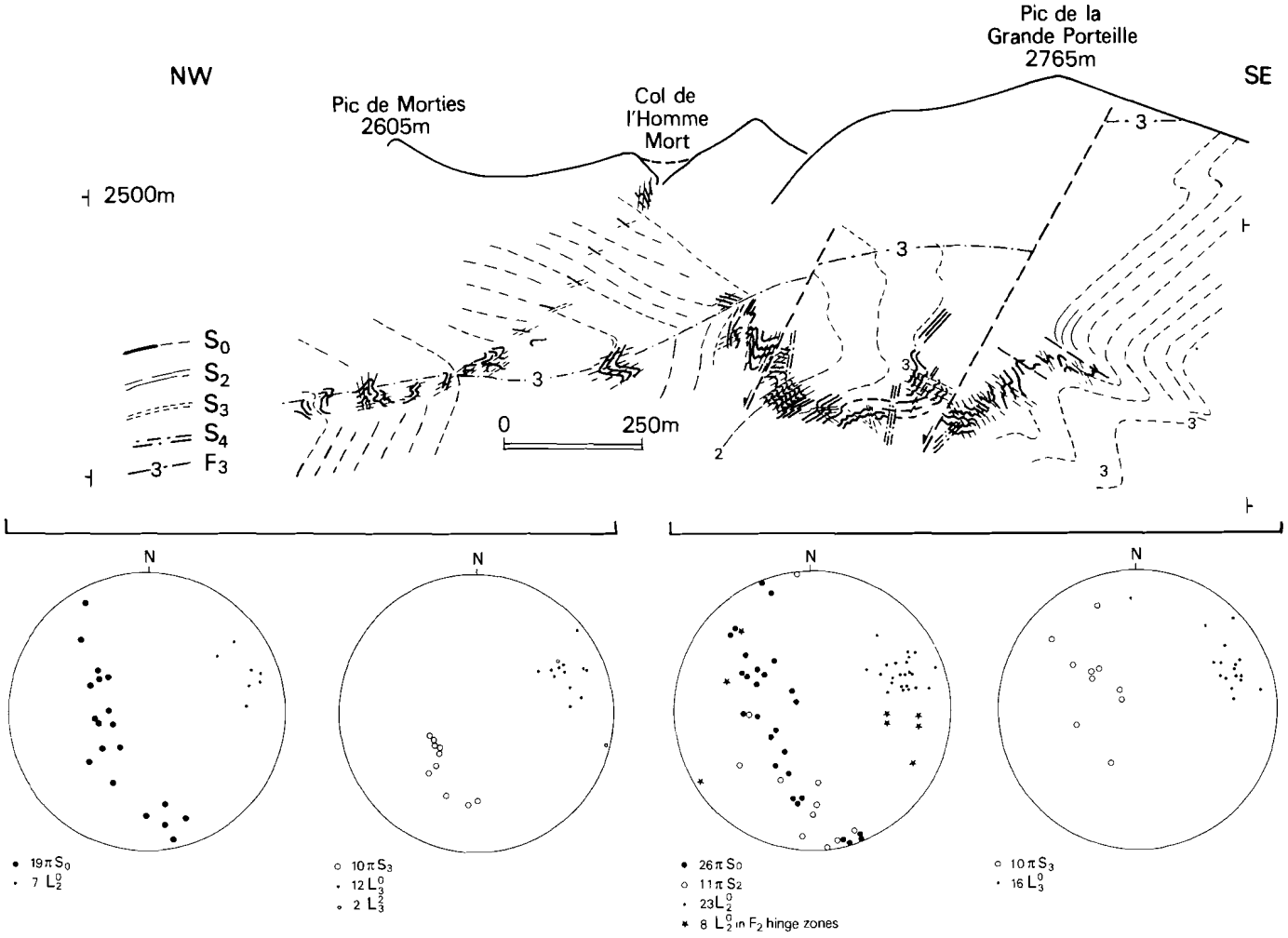
NW
SE
Pic de Morties
2605m
Col de
l'Homme
Mort
Pic de la
Grande Porteille
2765m
2500m
S_0
S_2
S_3
S_4
F_3
0
250m
N
19π S0
7 L2 0
10π S3
12 L3 0
2 L3 2
26π S0
11π S2
23L2 0
8 L2 in F2 hinge zones
10π S3
16 L3 0

(b) Hinge zones are disrupted by transposition zones (Fig. 5.19b) where fold axes and intersection lineations deviate from the general ENE plunge direction towards E and ESE. The curved aspect of the D2 axes and overprint by D3 folding causes mushroom shaped fold patterns (Fig. 5.20a).

(c) Limbs with north vergent minor folds show platy bedding and tight to isoclinal folds (Fig. 5.19c). The angle between cleavage and bedding is 5-10°. Foliation, bedding and quartz veins are boudinaged locally.

The axial plane cleavage (S2) is a less than 1 mm spaced differentiated crenulation cleavage in the low grade metapelitic rocks and a discrete centimeter spaced cleavage in quartzose beds.

D3 structures

D3 structures comprise folds and an axial plane cleavage which locally are the most prominent structures. Elsewhere D3 structures can hardly be found. D3-D2 overprint relationships are found in many outcrops and an illustrative example is shown in Fig. 5.20b. Fold axes and cleavage/bedding intersections are parallel to the D2 linear structures (Fig. 5.18b). D3 folds are open to tight with gently inclined axial planes. Locally they are faulted along their axial planes. Offset amounts to several meters. Thick quartz veins may accompany this feature. D3 folds occur at all scales and the cliff of the Pic de la Grande Porteille (Fig. 5.18) is dominated by the major SSE closing recumbent D3 syncline. The D3 foliation is a 2-4 mm spaced crenulation cleavage in metapelites and a spaced discrete cleavage in quartzose rocks in the zones of D3 folding.

D4 structures

D4 structures comprise shear zones, faults and folds which deform the D3 recumbent syncline. These structures are accompanied by small-scale minor folds, often with kinklike or chevron type geometries. Locally, as in the folds in the upper limb of the D3 recumbent structure, a crudely spaced anastomosing discrete cleavage occurs (Fig. 5.18a).

◄*Fig. 5.18b Structural cross section and lower hemisphere equal area projections of structures through the recumbent fold, corresponding to the southern part of Fig. 5.18a. Observations are more heavily indicated, numbers refer to deformation phases.*

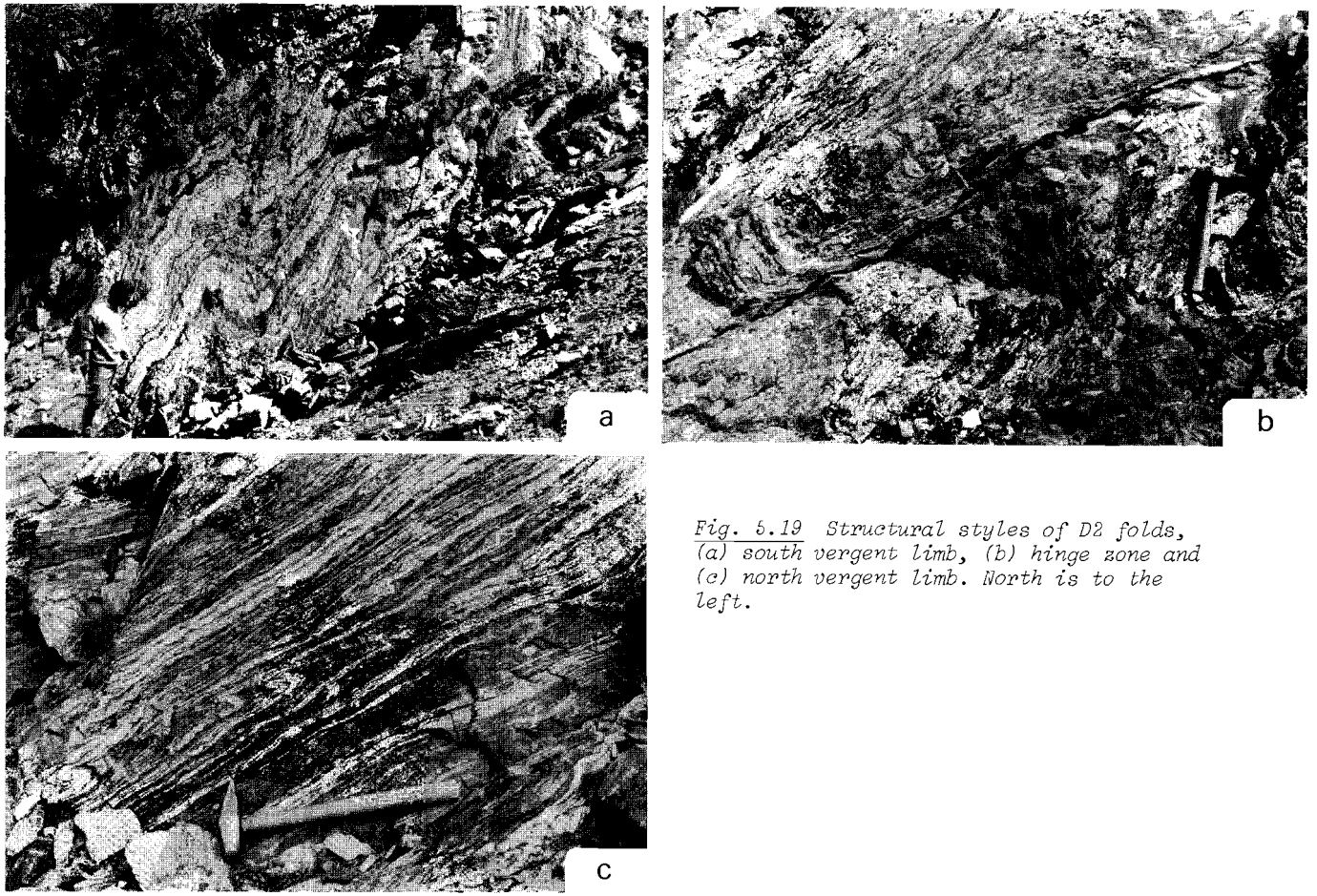

Fig. 5.19 Structural styles of D2 folds, (a) south vergent limb, (b) hinge zone and (c) north vergent limb. North is to the left.

Fig. 5.20 D3 overprint on (a) a F2 hinge zone, and (b) a south vergent F2 fold. In (a) the mushroom shaped interference pattern is due to overprint of F3 on a D2 hinge zone with curved fold axes. North is to the left.

5.3.2 Discussion

The increase in tightness of the D3 folds towards the CHSZ suggests that after the recumbent fold formed, its lower limb was thinned in this mylonite zone. Considering (1) the gradual transition from the D3 structure towards the CHSZ, and (2) the lack of interkinematic porphyroblas-

tesis between D3 and the strain recorded in the CHSZ (such as observed southwest of the gneisses, section 5.1), the mylonitic strain in the CHSZ may represent ongoing D3 deformation.
In this interpretation, the ESE directed subhorizontal flow of the metasediments relative to the gneisses in the CHSZ can be taken as the kinematic framework of D3.

The older D2 structures indicate relative flow in a similar direction, since D2 fold axes in the highest deformed domains curve towards ESE.
The D2 structures in the hinge zone of the Hospitalet gneiss antiform probably are equivalent to the D2 structures north of the gneisses, in the lower limb of the D3 recumbent fold. In this lower limb D3 minor structures are virtually absent. The D2 phase probably represents the formation of the infrastructure in the eastern Hospitalet massif (Chapter 4) and reflects the third phase of deformation at a regional scale. The D3 structures in the hinge zone of the gneiss antiform and the CHSZ represent Late Hercynian reworking of the infrastructure (section 5.1). Size and attitude of the D3 recumbent fold are comparable with, though mirror image of the north closing body of black Silurian slates near Llorts in the west part of the Hospitalet massif (Fig. 5.1, Verspyck 1965).
The fourth phase structures are parallel to and therefore probably related to the tectonic boundary between the Hospitalet massif and the Aston massif. These structures are of Alpine age.

CHAPTER 6

STRUCTURES AND DEFORMATION PHASES IN THE HOSPITALET AUGENGNEISSES

The structural history of gneisses is usually more difficult to unravel than in metasedimentary rocks. Homogeneous gneisses apparently have a "shorter memory" than layered sedimentary sequences. This is due to differences in composition and grain size, and the absence of buckling instabilities and porphyroblast matrix relationships.
The presence of metasediments in contact with gneisses and the possibility of tracing deformation structures from the metasediments into the gneisses offers a chance to separate deformation episodes in the gneisses with the aid of the scheme in the metasediments. In this respect the deformation scheme in the metasedimentary envelope of the Hospitalet gneisses can be used as a reference frame for various structures in the Hospitalet massif.

In the augengneisses of the Hospitalet massif two areas have been mapped in detail by means of form surface mapping. These areas are the Etang d´En Beys region and the Etang du Sisca region (Fig. 6.1). In both regions three discernable fabrics occur: (1) the gneiss foliation, (2) extensional crenulation cleavage and (3) a steep foliation at a high angle to the gneiss foliation.

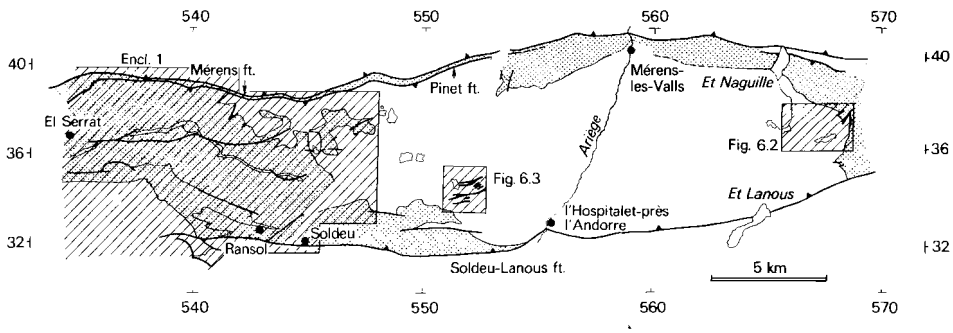

Fig. 6.1 The Hospitalet massif. The insets show the regions that have been mapped in detail in the Hospitalet augengneisses. Cambro-Ordovician metasediments are stippled, the gneisses are left unornamented.

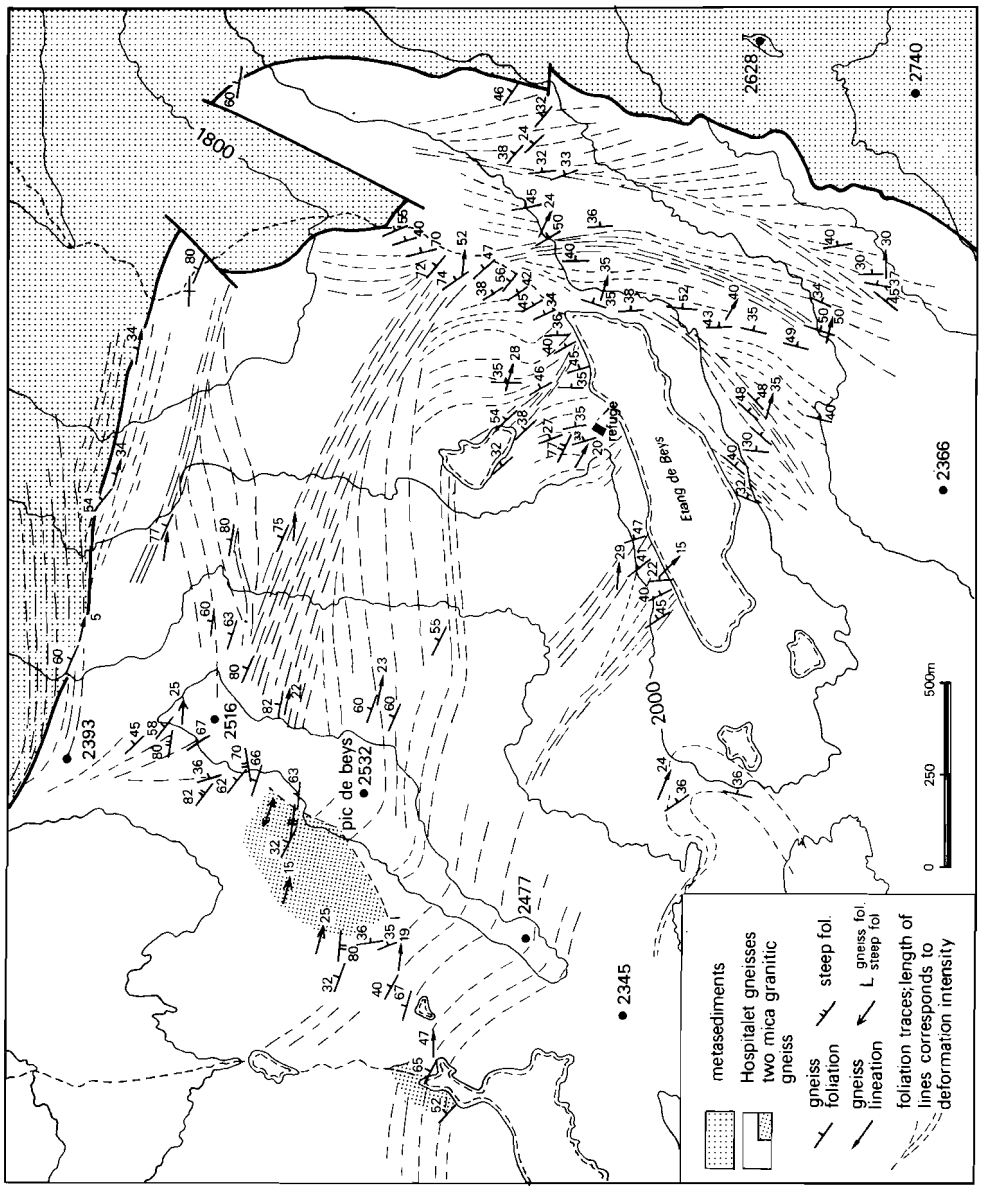

Fig. 6.2 Etang d'En Beys region: form surface map and lower hemisphere equal area projection of linear and planar structures in the gneisses. High strain intensity gneisses have not been indicated.

Note:

1. *The difference in attitude of of the low vs. moderate strain intensity gneisses in areas f and g.*
2. *Ecc defines a conjugate set in the north flank of the gneiss antiform*

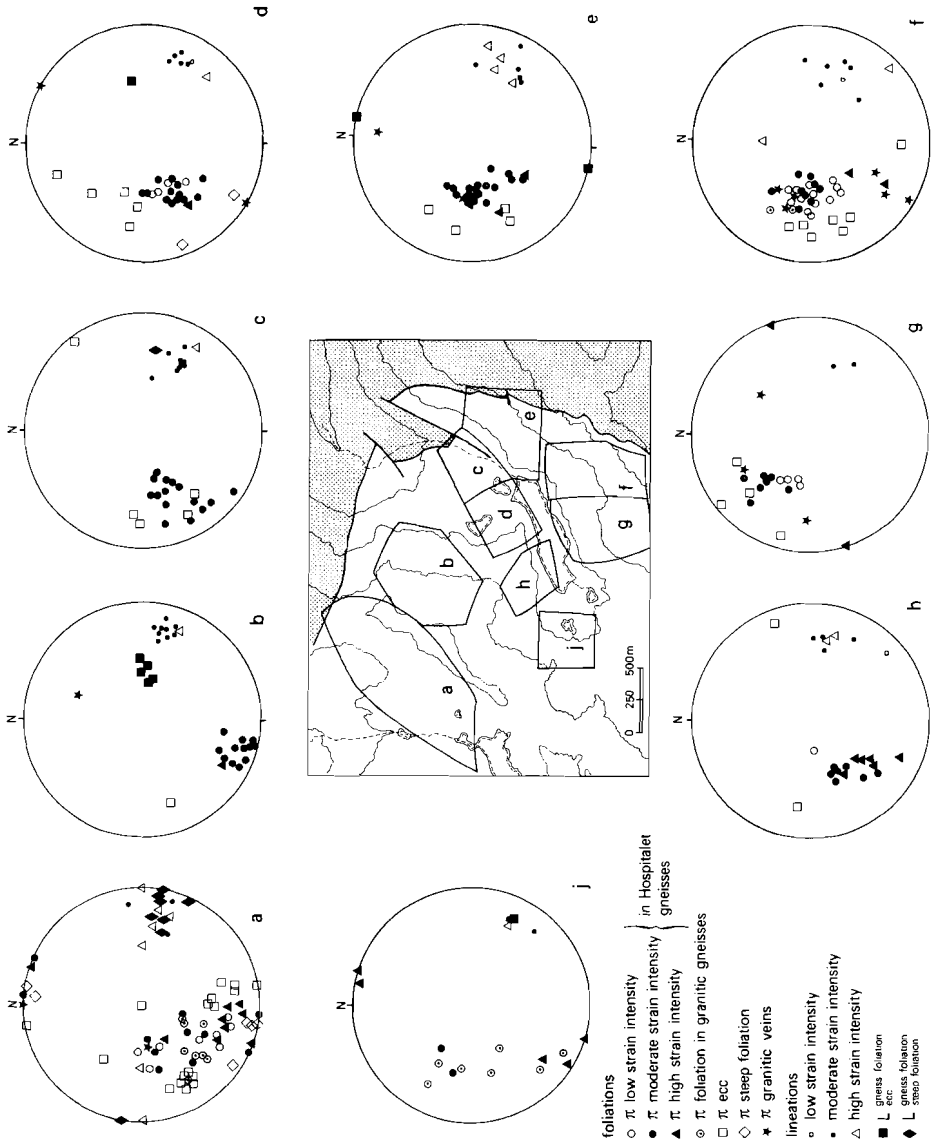

(regions a, b, plot a) with a more pervasively developed NE dipping set. In the nose of the antiform (areas and plots c-f) ecc predominantly is a single set, which dips more steeply E-SE than the gneiss foliation

3. *The steep foliation occurs in the area north of Et. de Peyrisses (plot a) and diminishes towards the east (plot d).*
4. *The difference in attitude of S2 and the conjugate sets of ecc in the north flank of the antiform (plot a).*

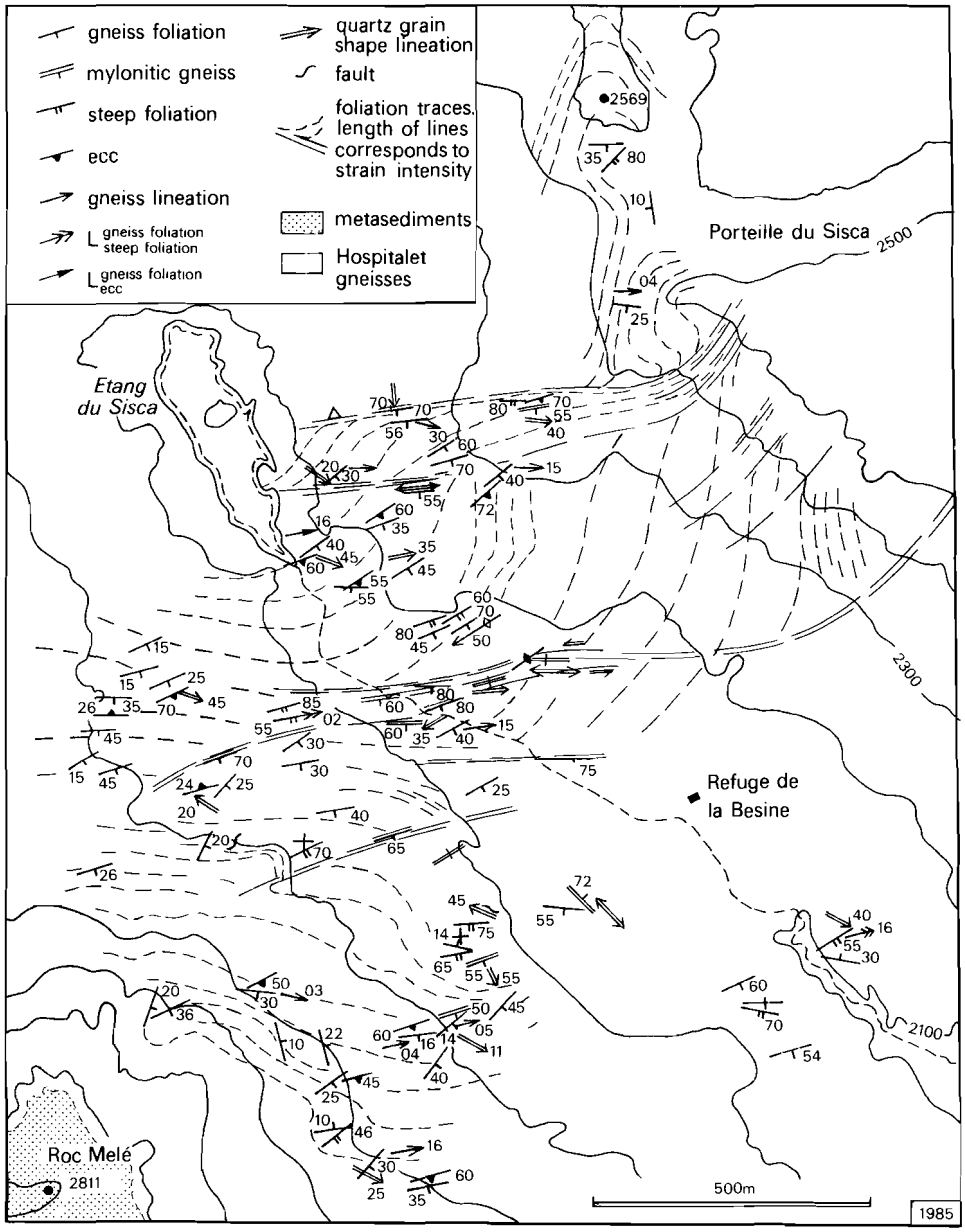

Fig. 6.3 Sisca region: form surface map and lower hemisphere equal area projection of planar and linear structures in the gneisses. Note the difference in attitude of the gneiss foliation in "ecc dominated" gneisses and that in pencil gneisses (containing the steep foliation) in stereogram a.

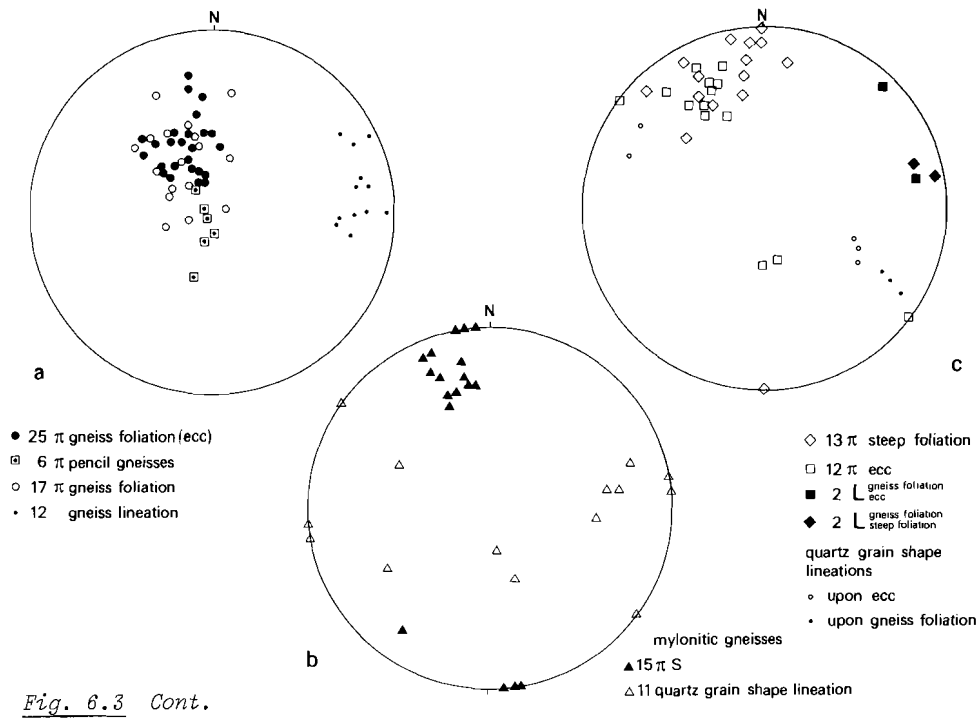

Fig. 6.3 Cont.

6.1 SMALL-SCALE STRUCTURES

The gneiss foliation

The foliation in the augengneisses is defined by shape fabrics of quartz, feldspar and biotite aggregates, and a preferred orientation of micas, mica seams and K-feldspar augen. At a large scale the foliation defines the antiformal shape of the massif. It is at an angle to the gneiss-metasediment contact (Chapter 4). At the scale of the map (Figs. 6.2, 6.3) a considerable variation in the attitude of the foliation exists due to the occurrence of deformation zones within the augengneisses. Within these zones the gneisses have been deformed into moderate strain intensity gneisses and high strain intensity gneisses (mylonites). The various deformation intensities have been characterized as follows:

(1) Low strain intensity (e.g. Fig. 5.2c). The rocks display an irregular foliation which is wrapped around rectangular K-feldspar

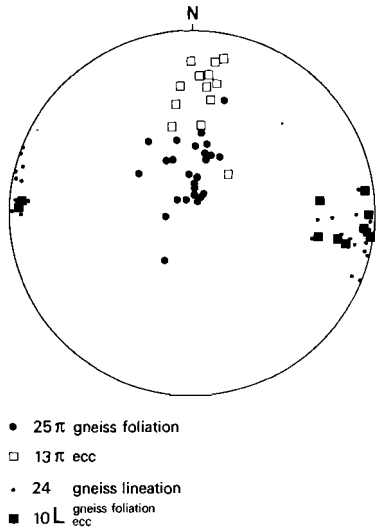

Fig. 6.4 Lower hemisphere equal area projection of foliations and lineations from the gneisses in the western Hospitalet massif.

porphyroclasts. The porphyroclasts show little sign of deformation.

(2) Moderate strain intensity (e.g. Figs. 5.2d, 6.6). The gneisses show a platy foliation and elongated K-feldspar porphyroclasts, which show microstructures indicative for brittle and plastic strain (section 5.1, Fig. 5.11).

(3) High strain intensity (Figs. 6.6, 6.7). Platy rocks with a closely spaced foliation, few relics of K-feldspar augen and boudinage and folding of veins.

Two types have been distinguished, (1) type a mylonitic gneisses (Fig. 6.6.) and (2) type b mylonitic gneisses (Fig. 6.7). Both types differ from each other in internal structure (see below).

Lineations

The long dimensions of the shape fabrics which define the foliation, define the gneiss lineation. The gneiss lineation plunges ca. 20° towards N100E in the Beys region (Fig. 6.2), ca. 20° towards N080E in the Sisca region (Fig. 6.3) and is nearly horizontally directed N095E in the western termination of the gneisses on the map (Fig. 6.4).

On the gneiss foliation two other lineations can be observed.

(1) In moderately deformed gneisses a faint quartz-(biotite) grain shape fabric is observed. This lineation is invariably oriented WNW-ESE

and quartz c-axis fabrics (Chapter 5) indicate that it is a stretching lineation.

(2) In moderately and highly deformed gneisses an open crenulation or a discrete intersection lineation of extensional crenulation cleavage is observed.

Extensional crenulation cleavage (ecc)

Ecc occurs as discrete, centimeter spaced secondary structures across which displacement of markers, such as thin granitic veins can be demonstrated.
Conjugate sets of ecc are found but the amount of conjugate versus single sets varies. This is particularly well demonstrated in the Beys region (Fig. 6.2). In the Sisca region (Fig. 6.3) ecc is only locally developed, predominantly as a single set. The intersection of conjugate sets appears to lie within the gneiss foliation.
Parting parallel to ecc occurs locally. On the ecc planes a quartz-mica lineation plunging ESE is observed, which is similarly oriented as the second quartz-biotite lineation on the foliation.

According to Platt and Vissers (1980) ecc can be considered as a conjugate pair of shear zones. The elongation direction during formation of ecc is perpendicular to the intersection of both sets and lies in their acute angle. The elongation direction deduced in the Sisca and Beys region invariably indicates WNW-ESE stretching. In the southwest of the gneisses NNE-SSW stretching is indicated in this manner in moderately deformed gneisses, whereas highly deformed gneisses suggest WNW-ESE stretching. The latter elongation direction conforms to the mineral lineations on the gneiss foliation and the ecc planes. The other elongation direction is probably related to the earlier NS stretching in the mylonite zone at the gneiss-cover contact (Chapter 5).

Steep foliation

This structure occurs as an up to 3 cm spaced, discrete, locally anastomosing foliation. It is usually more widely spaced than the gneiss foliation. The steep foliation is predominantly characterized by mica seams. The intersection of this foliation with the gneiss foliation gives

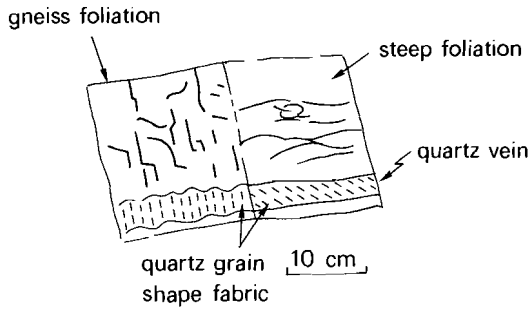

Fig. 6.5 Block diagram of pencil gneiss. The intersection of the gneiss foliation and the steep foliation gives rise to a strong lineation on both foliations. In other gneisses than the augengneisses the front (left part) of the diagram, which is perpendicular to the lineation shows a granitic texture.
Drawn from field sketch.

rise to "pencil gneisses" (Figs. 6.5, 6.7). In the Sisca region mapping of the pencil gneisses suggests a close association with type b mylonite zones (see below). The lineation in the pencil gneisses is parallel to the elongation direction indicated by boudinaged tourmalines. Parting via the steep foliation is uncommon, but when observed a faint quartz grain shape lineation plunging ESE (Fig. 6.5) can be observed on it. This lineation resembles the quartz-biotite lineation on the gneiss foliation and the lineation on ecc cleavage planes. Therefore it is thought to represent a stretching direction.

Quartz veins (up to 15 cm thick) and pegmatites (up to 50 cm thick) are folded in the areas where the steep foliation is present. The folds contain the structure as axial plane foliation. The steep foliation is less common than ecc in both areas. Overprint of ecc on the steep fabric outside high strain zones has been found only once. Relationships between both structures, such as shown in Fig. 6.7, suggest that they formed in the same deformation event.

The morphology of the steep foliation is similar to the "C-surfaces" of Berthé et al. (1979). C-planes are believed to be small-scale shear zones which lie close to the bulk flow plane (Jegouzo 1980, Lister and Snoke 1984, Platt 1984). Alternatively the structure may resemble a foliation which lies close to the XY plane of the local strain ellipsoid. A more detailed study is required to reveal the true nature of this structure.

6.2 DEFORMATION ZONES

Moderate strain intensity gneisses

Mapping of (1) the relative degree of deformation intensity and (2) the attitude of the foliation, revealed the existence of 100-300 m scale bands of moderate strain intensity gneisses in the Beys region (Fig. 6.2).

A general observation is that moderate strain intensity becomes increasingly important towards the gneiss-metasediment contact. Ecc shows a closer spacing in the moderate strain intensity zones than in the low strain intensity gneisses.

Movement on the moderate strain bands is indicated by the general curvature of the gneiss foliation and locally by curvature of granitic dykes into the zones. A dip slip displacement component is indicated, suggesting relative uplift of the central parts of the gneisses relative to its margins in the Beys region. The true direction of shear is hard to establish since the most prominent lineation, i.e. the gneiss lineation has been inherited from the low strain intensity gneisses and consequently has no direct bearing on the kinematics of the moderate strain zones.

Type a mylonite gneisses

Type a mylonite bands occur in the Beys region only. They are up to 50 cm wide and consist of a fine to medium-grained schistose matrix of quartz, feldspar and biotite. Some small K-feldspar augen occur (Fig. 6.6). The bands have a slightly different, usually steeper attitude than the surrounding gneiss foliation (Fig. 6.2): the pole to the bands lies usually within 30^{o} of the mean pole to the foliation. Curvature of the gneiss foliation into the zones, the orientation of the stretching lineation and displacement of granite veins suggests a general oblique slip displacement on the zones and uplift of the central part of the gneisses. The amount of offset is, where verifiable less than a few meters. The sense of shear on the zones tends to be consistent with the sense of shear as deduced from ecc/foliation relationships. In the north flank of the MGA, where ecc is conjugate (Fig. 6.2, plots a,b) the NE dipping ecc set prevails in the gneisses, whereas the north dipping ecc set prevails in the mylonite bands.

Fig. 6.6 Type a mylonite band in moderate strain intensity gneisses.

Type b mylonitic gneisses

Bands of type b mylonitic gneiss are found in the Sisca region (Fig. 6.3). Type a mylonite bands as described above are absent in this region. The type b mylonitic gneisses appear to be a complex interplay between the gneiss foliation, the steep foliation and ecc. Fig. 6.7 shows a cross section from relatively undisturbed gneiss towards a mylonitic gneiss band. The foliation in the mylonitic gneisses consists of (1) the gneiss foliation which becomes progressively reoriented and transposed into (2) the steep fabric. In Fig. 6.7c a transition from pencil gneisses through ecc dominated gneisses to mylonitic gneisses is shown. The intersection of the steep foliation and the gneiss foliation is also found in the mylonitic gneisses. A strong lineation is the result. However, this lineation has no direct relation to the kinematics of the zone. The movement direction can be deduced from quartz grain shape lineations on deformed quartz veins. Some zones display downdip oriented mineral lineations and a dip slip sense of shear. Other bands show shallowly plunging mineral

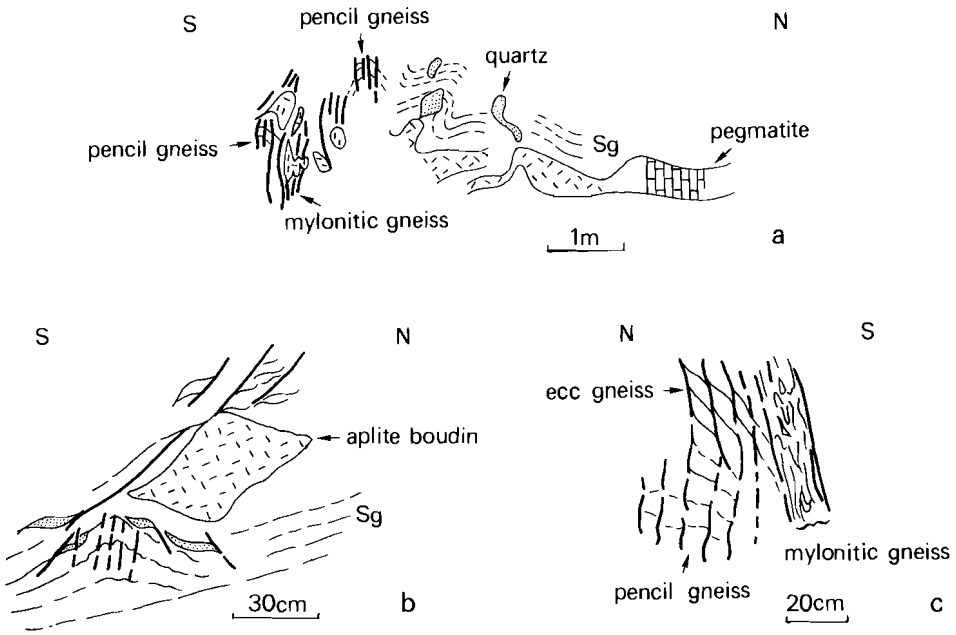

Fig. 6.7 Field sketches of type b mylonitic gneiss bands from the Sisca region illustrating the interplay between gneiss foliation, steep foliation and ecc.

lineations, indicating strike slip movement. Within the mylonitic gneiss bands crudely spaced ecc is found, with a different attitude than ecc outside the zones. The ecc/foliation relationship suggest essentially sinistral movement in the latter zones.

6.3 DISCUSSION

The advocated correlation between small-scale structures and deformation zones in the metasediments and gneisses is shown in Table 6.1. Several points from this table are of interest.

(1) From the field data no discrimination can be made whether the moderate strain zones (event 5) represent (a) progressive deformation of the low strain intensity gneisses (event 3), or (b) two distinct phases of deformation, the kinematics of which are mutually independant. The inter-

event	structures in metasediments	structures in gneisses
7 NS shortening	folds, faults and shear zones (Enl. 1)	shear zones
6 WNW-ESE stretching (sub) vertical shortening	El Serrat-Ransol zone (D4/5, section 5.2)	steep foliation, folds, ecc, type b mylonitic gneisses
	CHSZ; mineral lineation oblique to L3, ecc, boudinage (section 5.1)	mineral lineation oblique to gneiss lineation, ecc, boudinage, type a mylonitic gneisses
5 NNE-SSW stretching	CHSZ: ecc (mineral lineations), quartz rods, boudinage (section 5.1)	moderate strain bands, ecc, amplification gneiss lineation
4 metamorphic climax	porphyroblastesis (Chapters 5, 7)	static recrystallization
3 formation of infrastructure	D3 structures (Chapter 4)	foliation, lineation
2 formation of suprastructure	D2 structures (Chapter 4)	foliation, now completely destroyed
1 NW-SE shortening	D1 structures (Chapter 4)	?

Table 6.1 Correlation of events in gneisses and metasediments. CHSZ - Contact High Strain Zone.

kinematic porphyroblastesis (event 4) observed in the metasediments points to the latter possibility.

(2) The moderate strain zones at the gneiss-metasediment contact and at deeper structural levels in the gneisses must have formed during NNE-SSW stretching (event 5) since ecc formed in this event affects moderately strained gneisses in the southwest part of the massif.

(3) The kinematic interpretations of (a) the steep foliation/ecc/mylonitic gneiss association and (b) the relationship between (i) moderate strain zones and low deformation intensity gneisses and (ii) the relatively narrow mylonite zones and the foliation in the moderate strain zones is shown in Fig. 6.8. Different attitudes of flow planes relative to the older foliation give rise to different structures in shear zones.

(4) The foliation in the low strain intensity gneisses is the oldest structure observed in these rocks. However, in the metasediments the same foliation is due to a third phase of deformation (event 3), which represent the formation of the infrastructure. D3 in the metasediments is predated by a deformation phase (D2) which is associated with a pervasive foliation. This S2 foliation can be traced in thin section as a crenulated fabric in the infrastructure. The gneisses existed prior to the Hercynian orogeny (Chapter 3) and must have been affected by D2. The S2 foliation

Fig. 6.8 Interpretation of various structures in terms of shear zones.

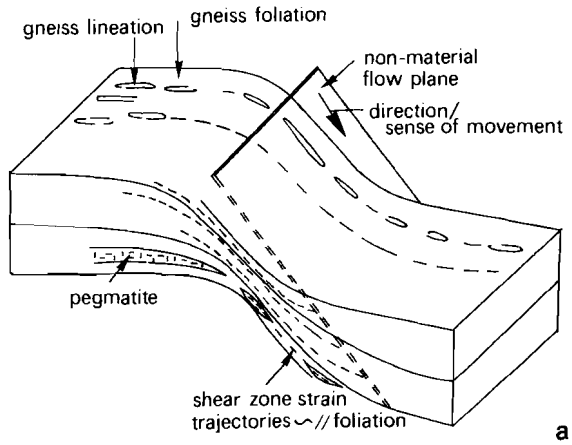

a. Type a mylonitic gneiss bands; the flow plane and the pre-existing foliation are at an angle less than 30° and the movement direction is situated at a high angle to the flow plane/foliation intersection.

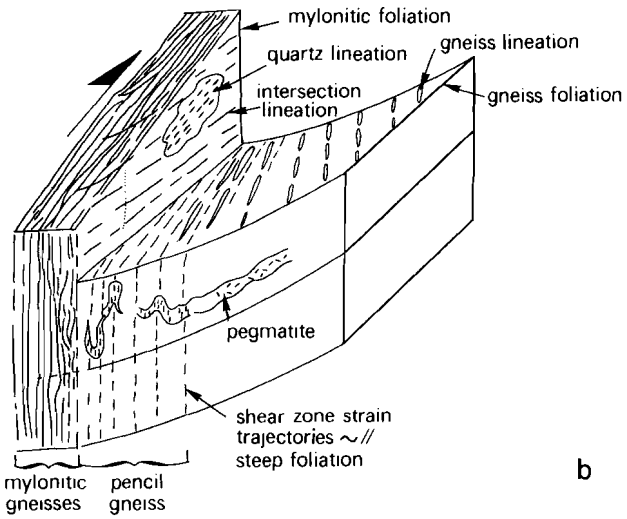

b. Type b mylonitic gneiss bands; transcurrent shear regime affecting the older foliation in such a manner that movement direction and intersection of flow plane and older foliation are at a low angle, and foliation and flow plane are at a high angle.

steeply strikes EW an intersections of S3 and S2 trend EW. This trend is parallel to the gneiss lineation and therefore it is thought that the gneiss lineation represents an intersection lineation of the flat lying gneiss foliation with an older more steeply oriented S2 foliation, now completely destroyed.

CHAPTER 7

STRUCTURAL CONSTRAINTS ON PYRENEAN TYPE METAMORPHISM IN THE HOSPITALET MASSIF

The Hercynian metamorphic event in the Pyrenees is of the low P/T type (Zwart 1963), and is also known as Hercyno-type metamorphism (Zwart 1967, 1969). The metamorphic rocks are exposed in various massifs in the Axial Zone (Fig. 7.1). Despite the amount of (micro)structural work carried out in these massifs (Oele 1966, Laprê 1965, Zwart 1979, Soula 1982, Verhoef et al. 1984, Soula et al. 1986), various problems still occur, concerning (1) the discrepancy between estimated pressures during metamorphism and the estimated overburden thickness (Zwart 1979), (2) the dome shape of the metamorphic massifs (Fonteilles and Guitard 1964, Soula 1982, Williams and Fischer 1984), and (3) the actual cause for the low P/T metamorphism (Wickham and Oxburgh 1986).

A study has been made of relationships between metamorphic minerals and small-scale structures in the Hospitalet massif. Furthermore, the mineral zonation in the western and eastern part of the massif has been mapped. The small-scale structures have been related to the large-scale geometry of the massif (Chapters 4,5). Since the massif has a regional significance, the regional significance of the small-scale structures has been established in this manner. This allows the regional problems outlined above to be discussed with respect to the Hospitalet massif.

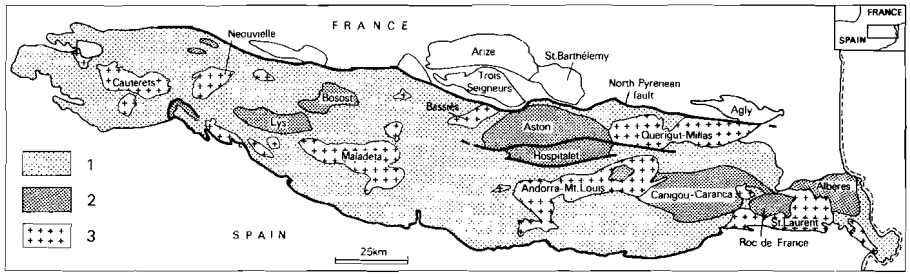

Fig. 7.1 *The Axial Zone of the Pyrenees.*

1. Very low grade and low grade metamorphic rocks of the suprastructure.
2. Low and medium grade metamorphic rocks of the infrastructure.
3. Late Hercynian batholiths.

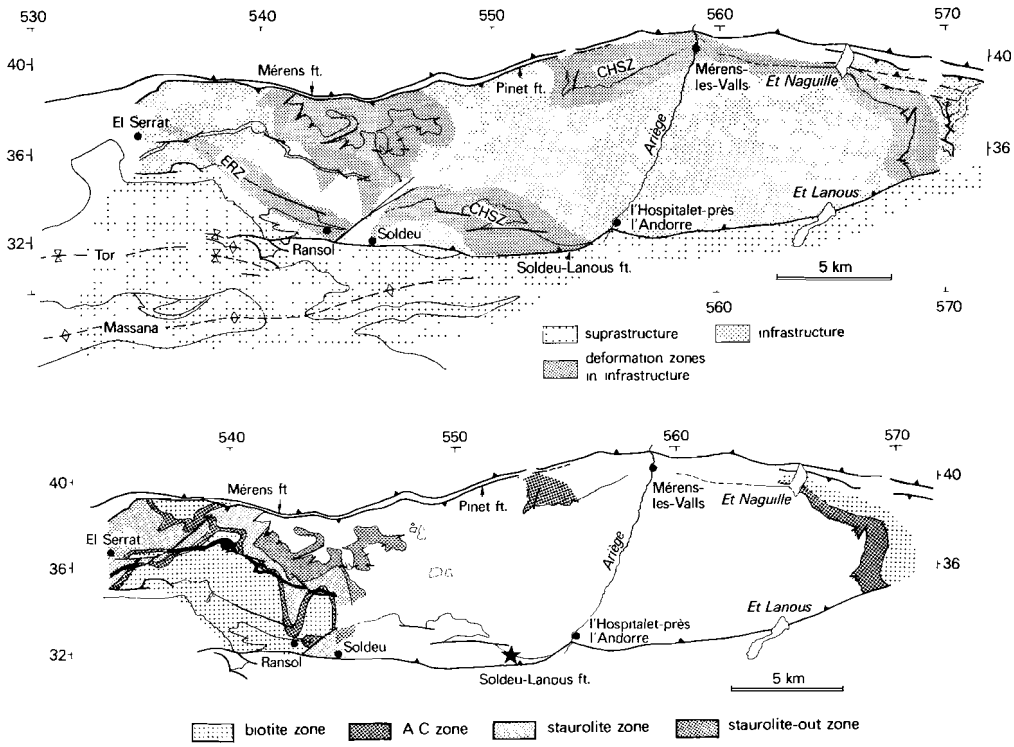

Fig. 7.2

a. Deformation zones in the Hospitalet massif.
b. Mineral zones in the Hospitalet massif.
The star denotes the occurrence of sillimanite-K-feldspar rock (Zwart 1965).

7.1. GEOMETRY OF THE MINERAL ZONES IN THE HOSPITALET MASSIF

Five mineral zones have been mapped within the Cambro-Ordovician metapelites SW of the gneisses (Encl.3), which are, from lower to higher grade and towards the gneisses, (1) the chlorite zone, (2) the biotite zone, (3) the andalusite-cordierite (AC) zone, (4) the staurolite zone and (5) the staurolite-out zone. Higher grade rocks, comprising sillimanite and K-feldspar, have been reported by Zwart (1965) west of l'Hospitalet-près-l'Andorre (Fig. 7.2). Sillimanite zone rocks occur in most other metamorphic massifs.

From Encl. 3 and Fig. 7.2 several features emerge:

(1) The chlorite zone is restricted to the suprastructure. All higher grade zones are confined to the infrastructure. The Silurian black slates in the suprastructure are andalusite bearing north of the Tor syncline.

(2) The boundaries between the mineral zones are oblique to bedding. The attitude of the boundaries between the biotite zone, the AC zone and the staurolite zone dip ca 225/15 in the region SW of the gneisses. The attitude of bedding is ca 225/45 in this area. This angle between bedding and mineral zones remains constant to the west, towards the region of El Serrat. Zwart (1965) assumed the presence of a thermal high in this region without a direct connection to the isograd pattern near the Hospitalet gneisses. However, the pattern on the maps is due to topographical effects. Therefore the geometry does not support an independant thermal high in the El Serrat region.

(3) The boundaries between mineral zones are oblique to the gneiss-cover contact. At the western termination of the gneisses on the map, the boundary between the staurolite zone and the staurolite-out zone is oblique to the gneiss-metasediment contact, similar to the geometry of bedding and isograds further south in this region as described above. This geometry is in accordance with the occurrence of higher grade rocks at the contact towards the east.

(4) The boundaries between mineral zones are oblique to the large-scale antiformal structure. At the scale of the massif a crosscutting attitude of the mineral zones with respect to the gneiss-cover interface is indicated by (a) the presence of the above mentioned occurrence of K-feldspar/sillimanite rocks, and (b) the absence of higher grade rocks than those belonging to the AC zone in the eastern plunging nose of the gneisses and on top of the gneisses, west of Merens-les-Valls.
This large-scale crosscutting attitude of the mineral zones relative to the gneissic core is similar to the situation in the Canigou-Carança massif (Guitard 1970).

7.2. THE MINERAL ZONATION

The next sections are concerned with the five mineral zones. The account is based on observations in the metapelitic Cambro-Ordovician

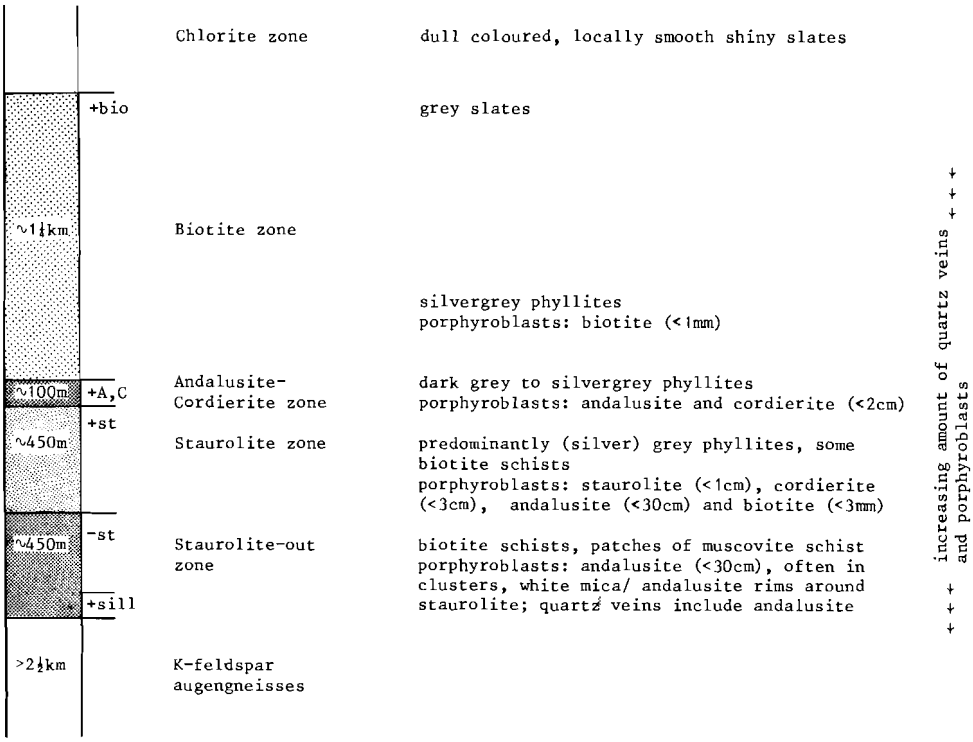

Table 7.1 Column showing thickness of mineral zones in the southwestern Hospitalet massif (Encl. 3), and general aspect of rock types; ornamentation refers to Fig. 7.2.

sediments of the SW part of the massif only, unless stated otherwise. A metamorphic columnar section is presented in Table 7.1. Table 7.2 shows (1) the distribution of minerals over the zones and (2) the deduced growth episodes of these minerals relative to foliations. The chemical composition of various minerals has been confirmed by Electron Microprobe analyses (EMP), X-Ray Diffraction (XRD), or with an Energy Dispersive X-ray Spectrometre (EDS) fitted to a Scanning Electron Microscope (SEM).

Chlorite zone

The slates of the Massana anticline (Fig. 7.2) contain chlorite and colourless mica, some as individual grains, others as chlorite/mica aggregates ("chlorite stacks"). Chlorites and micas define the foliation in the slates (S2). Elongate quartz grains and pyrite grains or aggregates add to the definition of the S2 foliation. Zoisite (XRD, SEM) occurs as porphyroblasts (< 150 micron). Si-Se configurations indicate pre- as well as

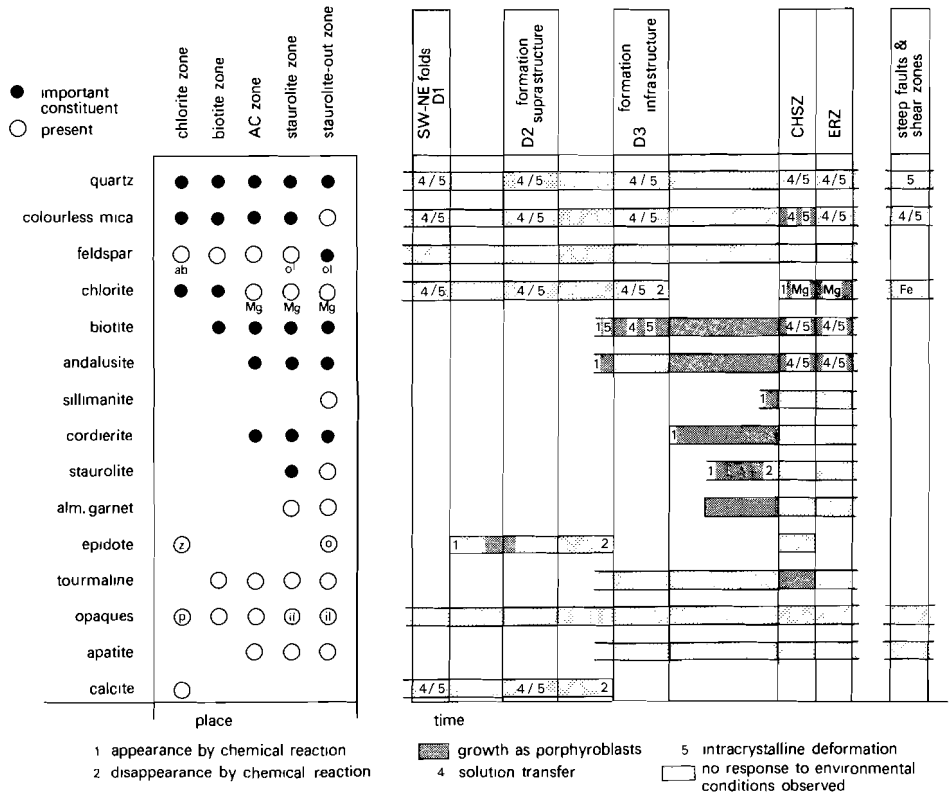

Table 7.2 (left) Distribution of minerals of mineral zones and (right) tectono-metamorphic scheme.
Abbreviations: AC zone - andalusite-cordierite zone, ab - albite, ol - oligoclase; Fe, Mg denote Fe, Mg-rich chlorite, z - zoisite, o - orthite, p - pyrite, il - ilmenite.

synkinematic growth with respect to D2 microfolding. Growth occurred at the expense of white mica and chlorite. Quartz/calcite veins are present. They have been deformed during D2.

Biotite zone

The lower temperature boundary of the biotite zone is poorly defined. Biotite is absent in the quartz porphyry within the Devonian carbonates of the Tor syncline and thus the biotite-in boundary lies in the lowermost Devonian carbonates or somewhere in the andalusite bearing Silurian black

slates. Biotite first occurs in psammites and quartz veinlets conform Mather's (1970) findings. Towards the AC zone biotite also occurs in pelitic lithologies. It is ubiquitous in the last 100 m before the AC zone, often as small porphyroblasts with (001) parallel to S3.

Chlorite persists to the higher temperature ranges in the chlorite stacks. Calcite and zoisite porphyroblasts are absent.

Microstructures in the slates and phyllites show S2 which is outlined by colourless mica and chlorite in the lower temperature range and by colourless mica only in the higher temperature range. S3 is marked by biotite porphyroblasts with (001) parallel to axial traces of crenulations. Later deformations, except for the youngest shear zones, are marked by continuous deformation and recrystallization of micas. Some biotite porpyroblasts show Si-Se geometries indicative for pre-D3 microfold growth.

Andalusite-Cordierite (AC) zone

In the field, the AC zone is marked by spotted phyllites. Round spots have been interpreted as cordierite, rectangular spots as andalusite. Biotite is ubiquitous. S3 abuts against the porphyroblasts but is wrapped around them in the CHSZ and ERZ. Quartz veins are locally rich in biotite. The metapelites are often enriched in biotite and andalusite at the contact with the quartz veins.

Microscopically, colourless micas outline S2 and S3. The latter foliation is further a biotite preferred orientation. S3 can be traced inside andalusites, indicative of post D3 growth (Fig. 7.3a). Some Si configurations suggest that andalusite may have started to grow before the onset of D3 microfolding. Later deformations postdate andalusite growth indicated by refolding and flattening of S3 around the porphyroblasts (Chapter 5).

Mg-rich chlorites (EMP) occur as porphyroblasts parallel to traces of later folds. They are interpreted as retrogressive features during these later deformations.

Reactions indicated by the presence of porphyroblasts at sites formerly occupied by micas and chlorite in the AC zone comprise in-situ growth of andalusite at the expense of colourless mica, and of cordierite at the expense of colourless mica, biotite and chlorite. The absence of

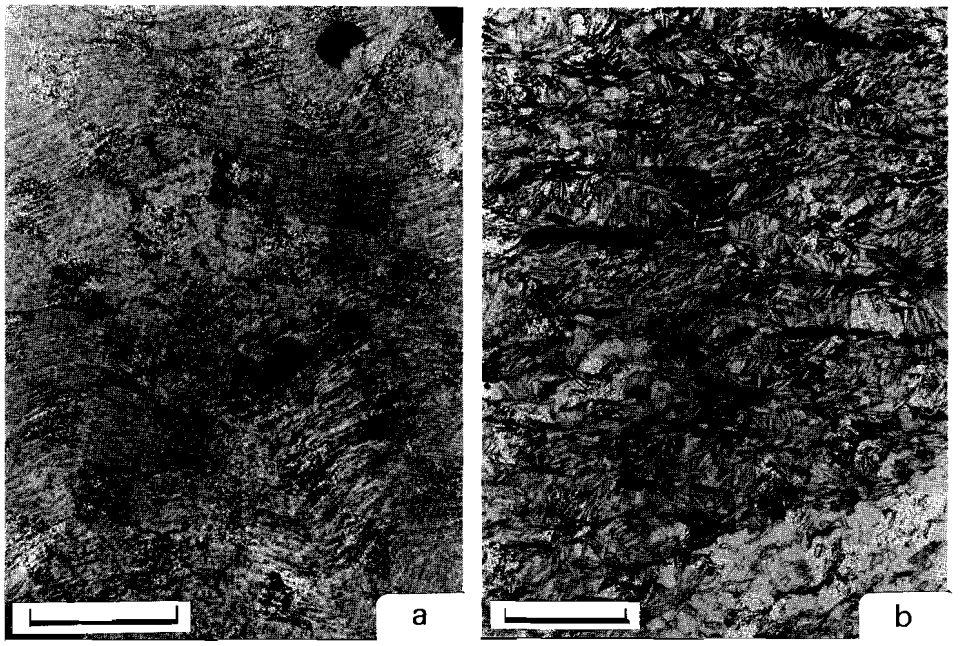

Fig. 7.3

a. Andalusite porphyroblast in AC zone, which has overgrown S3 crenulation foliation. S3 has been slightly flattened around the andalusite by D6 deformation. Scale bar indicates 1 cm.

b. Appearance of biotite phyllite from the upper biotite zone in thin section. EW trending S3 is a crenulation of older (S2) mica fabric. Note neo-formation of biotite with (001) parallel to S3. This microstructure is taken as indicative for synkinematic growth of biotite with respect to S3 foliation development. Scale bar indicates 200 micron.

primary chlorite suggests the bulk reaction:

col. mica + chl + bio(a) + qtz = and + cd + bio(b) + fluid.

Staurolite zone

The staurolite zone shows a heterogeneous distribution of staurolite. Andalusite is observed to overgrow complete metapelitic bands and cordierite occurs throughout the zone but its amount increases towards the staurolite-out zone. Quartz veins and lenses contain biotite and andalusite. At their contact, the phyllites show enrichment in biotite and andalusite and occasionally staurolite. Similar to the AC zone, S3 abuts against the porphyroblasts and is wrapped around them in the CHSZ and the ERZ. In the field, S3 can locally be traced into the porphyroblasts, indicating that they grew after formation of S3.

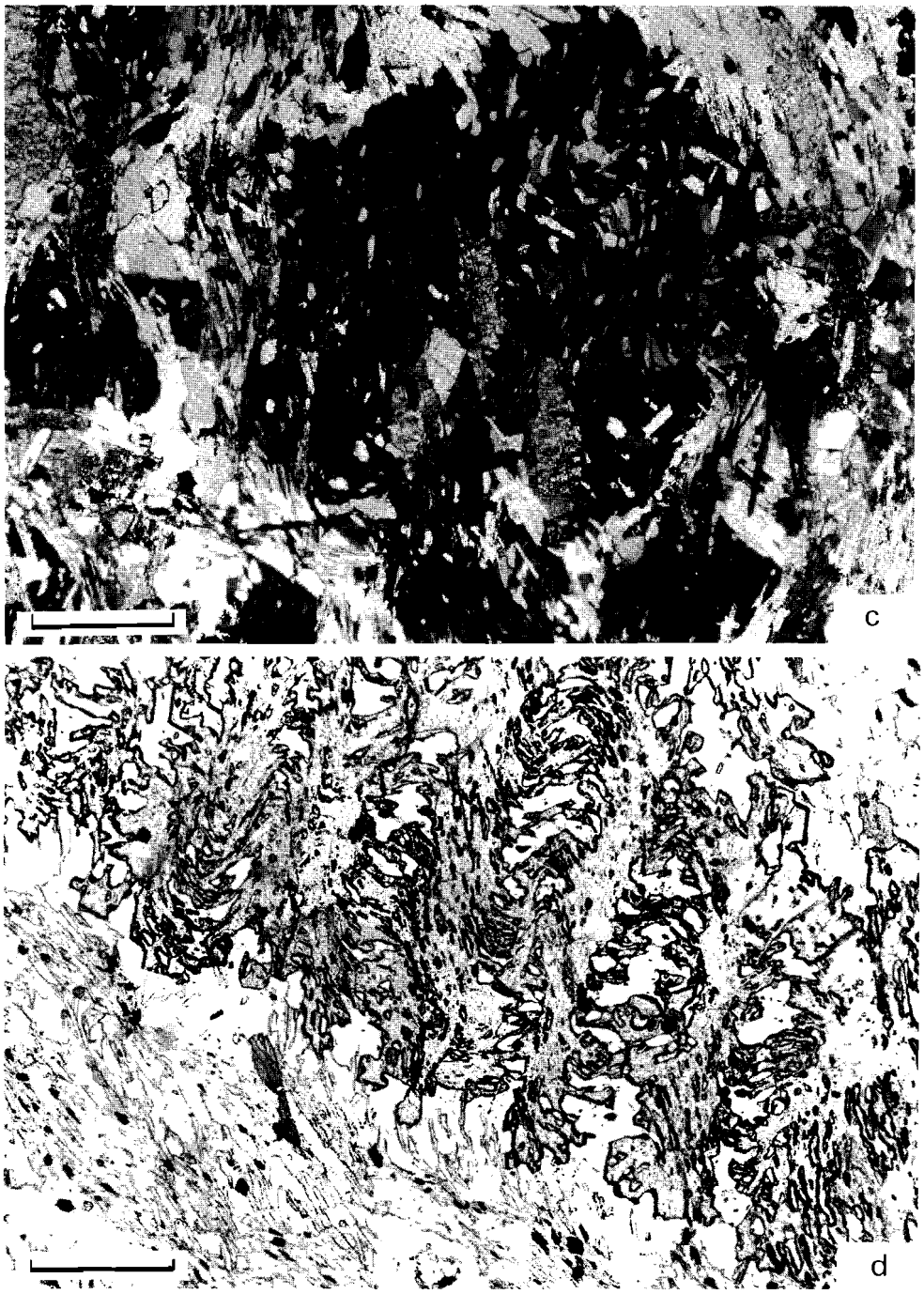

Fig. 7.3 Inclusion patterns indicating growth of c) cordierite, d) staurolite (→ staurolite zone). Scale bars indicate 200 micron.

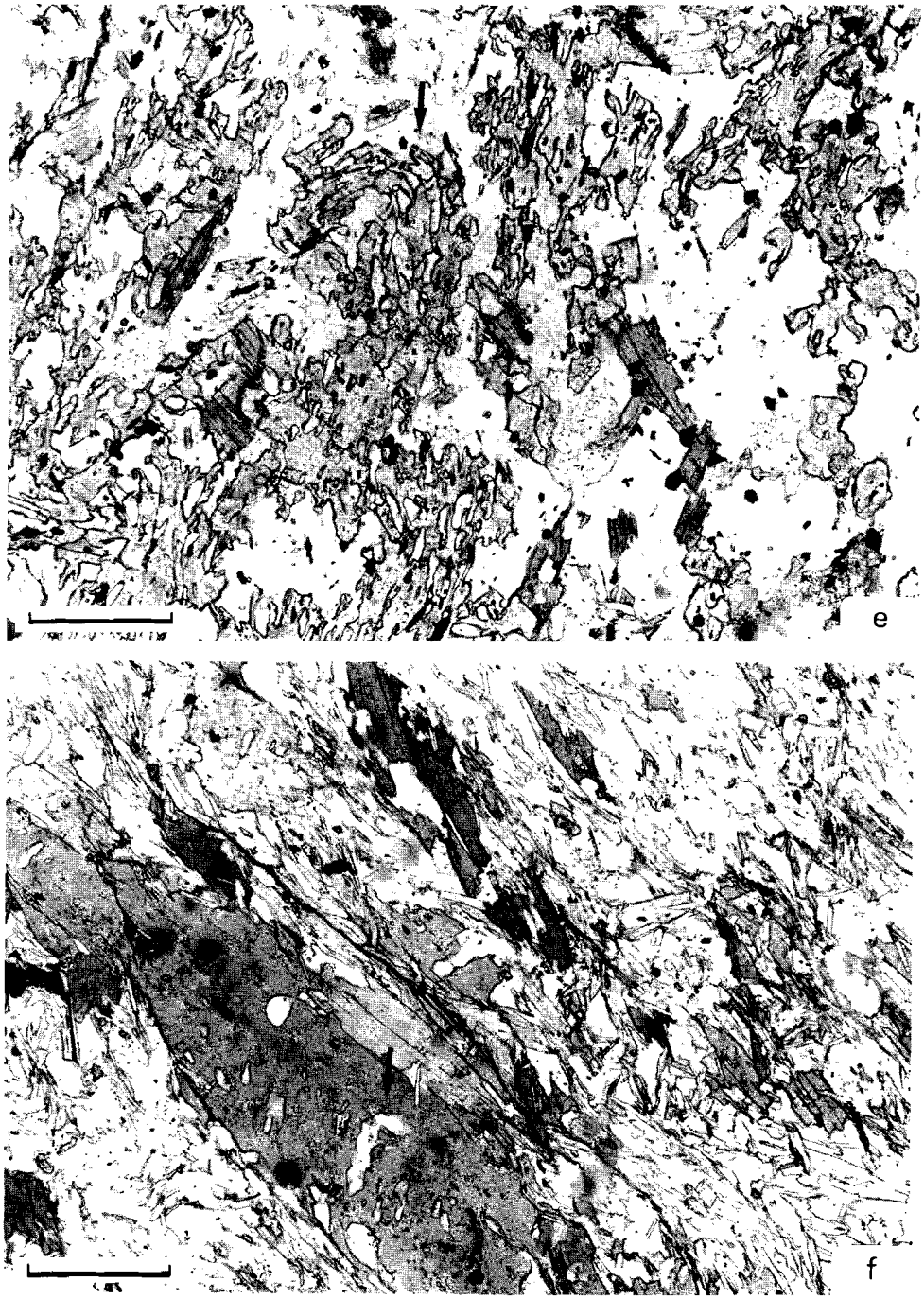

lite, e) andalusite and f) biotite over the S3 crenulation foliation (upper

In thin section, colourless micas outline S2, which is crenulated to form S3. The porphyroblasts contain an internal fabric, which outlines a crenulated fabric. This internal foliation can be traced towards S3 (Fig. 7.3). Microstructures of these rocks in the CHSZ and ERZ have been treated in Chapter 5. Most thin sections contain staurolite or cordierite. When found in one thin section together they are usually not in contact. Locally (e.g. fig. 9, Verspyck 1965), cordierite encloses staurolite but no indications for resorption of staurolite are found. Locally, e.g. north of El Serrat, tiny almandine-rich garnets (EMP) occur.

The microstructures and field observations show andalusite, cordierite, staurolite and biotite porphyroblasts at sites formerly occupied by colourless micas and biotite suggesting the bulk reaction:
col. mica + bio(a) = and + cd + st + bio(b).

Staurolite-out zone

In the staurolite-out zone staurolite is decomposed to a minor or major extent, manifested by the occurrence of rims of colourless mica and, closer to the gneisses, also andalusite rims. The zone largely coincides with the CHSZ (Fig. 7.2).

Colourless mica is absent as a matrix former and the patches and streaks of colourless micas are interpreted as retrogression products. However, around staurolite relics, colourless micas occur in a decussate fabric. The S3 foliation is outlined by the parallel arrangement of biotite grains and the elongate aspect of quartz and oligoclase grains. This fabric has been strongly deformed by post-porphyroblastesis deformations in the CHSZ (Chapter 5). Si-Se configurations are often absent in this zone. Internal fabrics of staurolite reflect an earlier crenulated fabric, S3, which has been obliterated outside the porpyroblasts. Included in staurolite are quartz, oligoclase and apatite (SEM). The following observations suggest in situ reaction of staurolite, andalusite and cordierite.

(a) Embayed remnants of staurolite in andalusite and randomly dispersed biotite flakes in these andalusites (Fig. 7.3) indicate:
st + qtz + fsp = and + bio

Fig. 7.3 Staurolite resorbing reactions as evidenced by embayed remnants of staurolite in g) andalusite (and), reaction 5, Fig. 7.4, h) muscovite (m; EMP), i) cordierite (cd), reaction 6, Fig. 7.4. Scale bars indicate 100 micron, except in h, 200 micron. ►

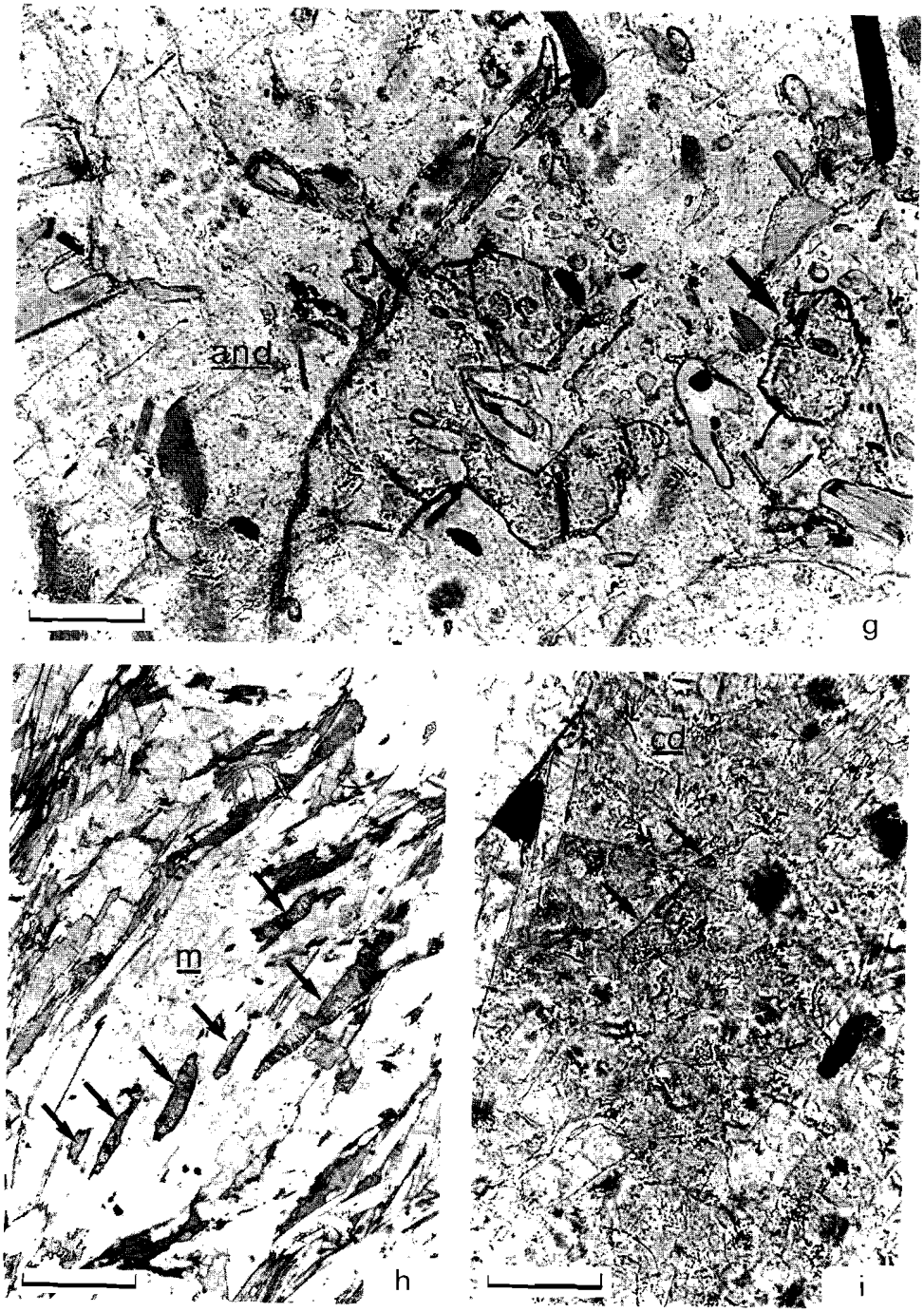
and
g
m
h
cd
i

(b) Embayed remnants of staurolite in colourless mica (Fig. 7.3), intergrown with biotite, suggests:

st + qtz + fsp = col. mica + bio

These two reactions are the main staurolite resorbing processes. However, the persistence of staurolites with quartz rims suggests that pre-existing colourless micas were involved. Hence the reactions reflect the stability of staurolite in the presence of colourless mica:

st + col. mica + (qtz + fsp) = and/col. mica + bio

The absence of the pre-existing colourless micas in the matrix is largely attributed to the decomposition of staurolite. K-feldspar is lacking in this zone and the reaction, muscovite and quartz producing K-feldspar and andalusite did not occur.

The rims of colourless mica around staurolite are interpreted in the same sense as the andalusite rims, that is, as a prograde reaction, which conforms with the interpretation of Zwart (1979) and De Bresser and Majoor (1984, internal report). Persistence of these rims into the highest grades reached is explained as being caused by the absence of quartz in contact with these micas.

(c) Rocks closest to the gneisses contain fibrolitic sillimanite which has overgrown biotite. Here embayed remnants of staurolite in cordierite (Fig. 7.3) indicate:

st + qtz (+ fsp) = cd

Some rocks close to the gneisses contain garnet, locally included in andalusite. It is not known whether this is due to decomposition of staurolite or if garnet originated at lower grades.

7.3 DISCUSSION AND CONCLUSIONS

7.3.1 PT gradient during prograde metamorphism

Fig. 7.4 shows the PT gradient of the metasediments exposed SW of the Hospitalet gneisses, corresponding to P=2.8 kbar at 650^{o} C at highest grades. The curve passes below the cordierite-in (3), staurolite-in (4) intersection since cordierite occurs prior to staurolite. It crosses the staurolite field (between 4 and 5), into the staurolite-out zone, marked by decomposition of staurolite (+ colourless mica) towards andalusite and

colourless micas (across 5). Afterwards, it crosses curve 6 producing cordierite and finally sillimanite is formed.

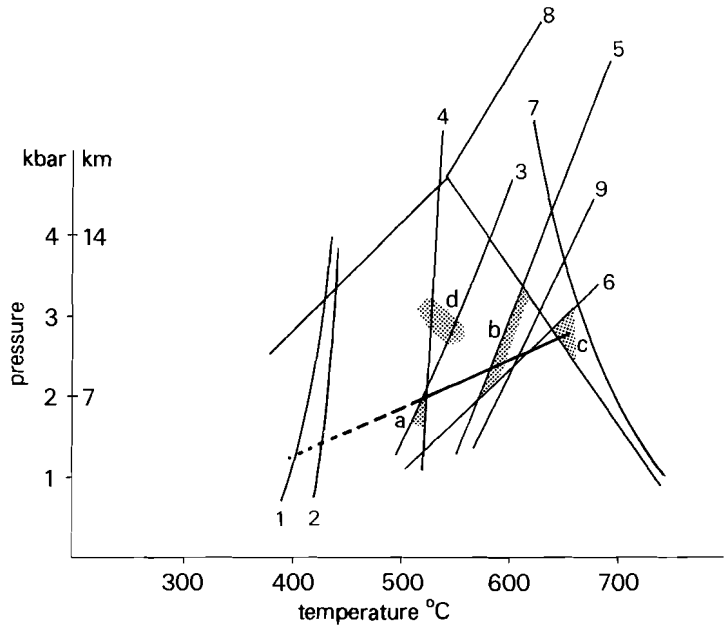

Fig. 7.4 PT gradient of metasediments from a: AC zone, b: lowermost staurolite-out zone and c: uppermost staurolite-out zone. Field d indicates the retrograde breakdown of cordierite in the staurolite-out zone and upper staurolite zone (Chapter 5).
P_{max} = 2.8 kbar at T_{max} of 650°C. When use is made of the Holdaway (1971) aluminosilicate triple point P_{max} would be ca. 2.5 kbar at T_{max} = 620°C.

1. *Pyrophyllite → andalusite + 3 quartz + H_2O (Kerrick 1968).*
2. *Stilpnomelane + phengite → biotite + chlorite + quartz + H_2O (Nitsch 1970).*
3. *Chlorite + muscovite + quartz → biotite + cordierite + vapour (Seifert 1970).*
4. *FeMg-chlorite + muscovite → FeMg-staurolite + biotite + quartz + vapour (Hoschek 1969).*
5. *FeMg-staurolite + muscovite + quartz → andalusite/sillimanite + biotite + vapour (Hoschek 1969).*
6. *Fe-staurolite + quartz → Fe-cordierite + andalusite/sillimanite + H_2O (Richardson 1968).*
7. *Minimum melt curve (Luth et al. 1964).*
8. *Aluminosilicates (Greenwood 1976).*
9. *Muscovite + quartz → K-feldspar + andalusite/sillimanite (Evans 1965).*

7.3.2 Age of the metamorphism relative to the structural history

Field observations and microstructures reveal that most porphyroblasts have overgrown the foliation in the infrastructure (S3) (Table 7.2). No variation in internal fabrics is found within porphyroblasts or between different porphyroblasts. Furthermore, no variation is found in the morphology of the internal fabric between various zones. This indicates that the porphyroblasts overgrew a crenulation foliation which did not change its morphology while the porphyroblasts were growing and the temperature was rising. In other words, the porphyroblasts statically overgrew S3.

An intimate relationship between D3 and the metamorphism is favoured (Fig. 7.5) since (1) biotite growth occurred pre- as well as synkinematic with respect to D3 microfolding, (2) andalusites may have started to grow before D3 microfolding and (3) the metamorphic zonation coincides with the infrastructure.

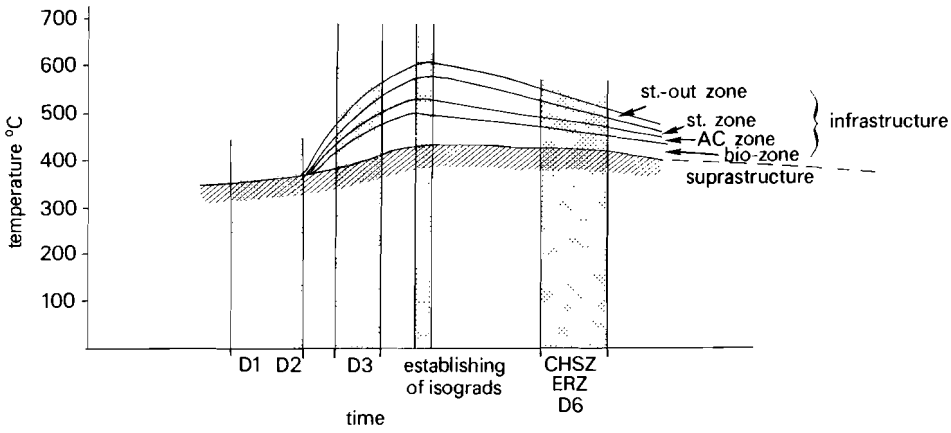

Fig. 7.5 Schematic temperature time paths of rocks within a given mineral zone.

7.3.3 The retrograde path

The rocks of the upper staurolite zone and the staurolite-out zone have been severely deformed in the mylonite zone at the gneiss-metasediment contact. PT conditions during this event have been estimated at 550-500° C at ca. 3 kbar (Figs. 7.4, 7.5, Chapter 5). Pressures appear to be similar to those during the prograde event, implying isobaric cooling.

7.3.4 Thermal gradients and isograd spacing

The thermal gradient which follows from peak temperatures and pressures is ca. 65° C per km. However, this figure represents an averaged value and gradients may have been higher or lesser throughout the pile. Gradients deduced from isograd spacing are certainly deceptive in the Hospitalet massif if no account is taken of the post-porphyroblastesis deformation. For example, the thickness of the staurolite-out zone according to the prograde path would be ca. 1750m whereas the present thickness does not exceed 500 m. The first estimate corresponds to 42° C per km whereas the second falsely suggests 150° C per km.
The biotite zone southwest of the gneisses is situated outside the domain of mylonitic, post-porphyroblastesis deformation. A temperature difference of ca. 90°C would have existed between the top and base of the zone (cf. Fig. 7.4). The thickness of the zone is ca. 1.25 km (Table 7.1) which corresponds to a thermal gradient of 72°C/km. This value is close to the average value of 65°C/km, which may therefore be an appropriate value of the thermal gradient in the infrastructure prior to the post-porphyroblastesis deformations.

7.3.5 The discrepancy between estimated pressures and overburden thickness

Zwart (1962) described the mineral zonation in the Bosost area (Fig. 7.1). Hess (1969) derived a Schreinemakers net for the lower pressure series of metamorphism and fitted the mineral zonation from the Bosost area into this diagram. However, the position of this net in PT space based on experimentally derived reaction curves (Hess 1969, Myashiro 1973, Winkler 1976) suggests higher lithostatic pressures than the thickness of the stratigraphical column in the Pyrenees can account for (Zwart 1979).

The stratigraphy of the Paleozoic in the Axial Zone of the Pyrenees consists of ca 4.5-5 km sediments (Fig. 7.6), corresponding to ca. 1.4 kbar pressure. This figure is far too small to explain the up to 4 kbar pressure estimates of the regional metamorphism and a factor 2 too small to explain the pressure estimated for the Hospitalet massif.
The recognition that the metamorphism is younger than the foliation in the

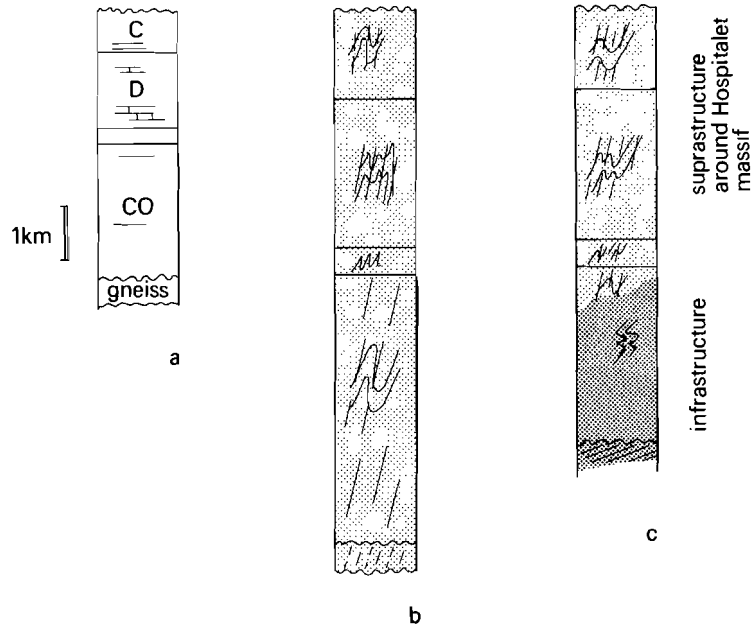

Fig. 7.6 The variation in thickness of the Paleozoic metasediments through time.

a. Pre-Hercynian stratigraphy (stratigraphic thickness from Chapter 3 and Zwart 1979); CO - Cambro-Ordovician; D - Devonian; C - Carboniferous
b. Thickness of the pile after formation of the suprastructure; thickening factor 2. The thickness of the Carboniferous in a. probably represents a minimum. Addition of Carboniferous sediments will decrease the necessary amount of D2 thickening.
c. Thickness of the pile after formation of the infrastructure (schematic).

infrastructure in the Hospitalet massif, which in turn has been shown to be younger than the suprastructure around the massif, may provide an elegant explanation for this discrepancy, provided that the upright folds and foliation in the suprastructure caused thickening of the succession. The stratigraphic pile above the infrastructure-suprastructure boundary (Fig. 7.6) accounts for ca. 2.5 km of rocks, whereas the pressure estimate requires ca. 4.5 km of rock to have been present. Thickening during the formation of the suprastructure by a factor of 2 may explain the discrepancy. Consequently, the rocks presently occupying the infrastructure must have thickened twice as well, but were thinned afterwards during the development of the infrastructure and the CHSZ (Fig. 7.6).

7.3.6 The origin of the dome shape of the metamorphic pattern

Two of the gneiss cored massifs, the Canigou-Carança (Guitard 1970) and the Hospitalet massif, show a mineral zonation which is more flat lying than the gneiss-metasediment contact and consequently crosscutting the gneissic cores of these massifs. This geometry implies that the dome shape of these massifs is primary and not due to later (Alpine) folding over ramps in shear zones as suggested by Williams and Fischer (1984). However, a general (slight) outward dip of the isograds, away from the gneisses, exists.

To explain the geometry of mineral zones relative to the large-scale domal shape of the Canigou-Carança massif, Fonteilles and Guitard (1964) introduced the basement effect ("effet du socle"). This model explains the close association of regional metamorphism and gneiss bodies as due to "the influence of the pre-Hercynian basement on the thermal structure of the Paleozoic envelope during metamorphism" (Guitard 1970, p. 285, transl. by the author).

It has been shown in Chapter 5 that during post-porphyroblastesis mylonitisation of the rocks at the gneiss-metasediment interface the metasediments have been draped around the gneiss core. Hence, the deflection of the isograds can be elegantly explained. It is postulated that the isograds originated in a more flat lying attitude than presently observed and that their gentle dome shape is due to post-metamorphic flattening of the metasediments around the gneiss core (Fig. 7.7). This mechanism provides a rock mechanic alternative for the "effet du socle" as proposed by Fonteilles and Guitard (1964), the "socle" instead being a relatively rigid gneiss antiform in a deformation phase which postdates the formation of the isograds.

7.3.7 Structural constraints on the low P/T ratio of the metamorphism

To explain the low P/T ratio of the metamorphism "something hot" must have been emplaced below the gneiss antiform. "It" can not have been the antiform itself since it is crosscut by the isograd pattern, which indicates that the heat front rose after its formation. The following explanatory models can be thought of: a local feature, such as an under-

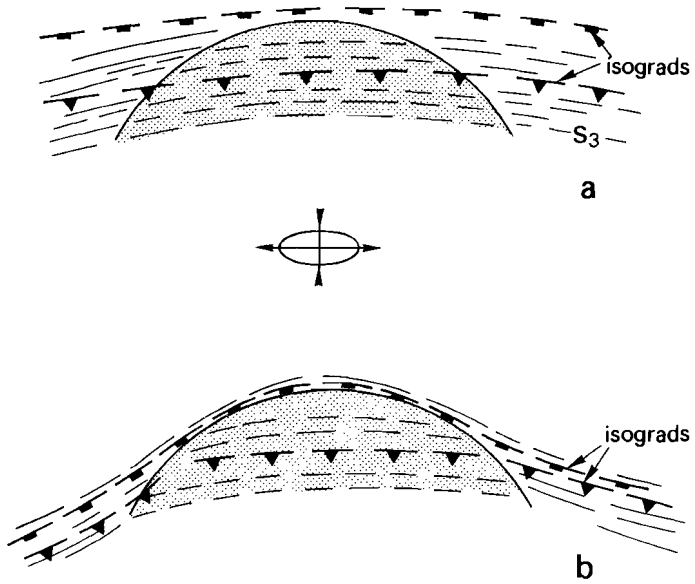

Fig. 7.7 Draping of the metasediments (unornamented) around the antiformal gneiss core (ornamented) caused by regional extension (Chapter 5). a. Before draping, b. after draping. The draping causes (1) telescoping of the isograds giving rise to false thermal gradients and (2) flexure of the isograds, which give rise to a false thermal dome/antiform.

lying batholith, or focussed passage of hot fluids of deep seated origin (Schuiling and Kreulen 1979), or a regional feature, such as a batholith (or mantle diapir, cf. Den Tex 1975) of regional extent or an extensional shear zone which placed relatively cold suprastructure onto hot (possibly granulite facies) lower crustal material.

Even in the deepest levels of the infrastructure, such as that exposed in the massifs of Canigou-Carança and Aston, no evidence exists of the presence of batholiths. Instead, increasingly higher metamorphic, strongly deformed ortho- and paragneisses are exposed. On this regional basis the existence of a deformation phase associated with the metamorphism is more plausible than the emplacement of a "batholith".

Based on work on the thermal dome of Naxos (Greece), Schuiling and Kreulen (1979) suggested that passage of mantle derived CO_2-rich fluids could cause the large variation of geothermal gradients over small horizontal distances, which is characteristic for thermal domes. However, deuterium/hydrogen studies on rocks from the Trois Seigneurs massif (Wickham

and Oxburgh 1985) suggest that the metamorphic rocks were flushed by circulating seawater during or before the metamorphic maximum. Therefore, it is considered improbable that mantle derived fluids have played an important role in the formation of the Pyrenean thermal domes.

The Hospitalet antiform formed due to vertical tectonics at the scale of the Hospitalet massif, which implies horizontal stretching at this scale (Chapter 4).

In the past decade a theoretical basis has been made for low P/T ratio metamorphism (crustal stretching; McKenzie 1978). Instantaneous crustal stretching causes isostatic uplift of the mantle. An initial increase in heat flow is followed by cooling and subsidence of the crust in a fashion which explains subsidence histories of various sedimentary basins. Other types of subsidence histories led Sclater et al. (1980) to propose modifications of the McKenzie model. These models apply to subsiding basins and little is known about the tectonics of the underlying crust. Low P/T ratio belts obviously are the best candidates to look for effects of a stretching event. Wickham and Oxburgh (1985) indeed suggested crustal stretching as the main cause for the metamorphism in the Pyrenees.

In the remainder of this section stretching (of local or regional extent) will be elaborated further. The infrastructure deformation diminishes upwards. This upper boundary may correspond to the brittle (suprastructure)-ductile (infrastructure) transition in a homogeneous stretching event (Fig. 7.8a). Alternatively, the diminishing deformation may indicate that stretching deformation is largely absent in the suprastructure domain. The latter situation applies to a discontinuity (fault or shear zone) accommodating the extensional deformation (Fig. 7.8b). Such a structure would cut out, or greatly thin, a portion of the crust. PT paths resulting from these situations are depicted in Figs. 7.8c,d,e. In Fig. 7.8c an initial pressure decrease is followed by isobaric cooling. The same situation applies to path y in Figs. 7.8d and 7.8e. Path x in Figs. 7.8d and 7.8e merely shows isobaric heating, but the rocks have not been affected by deformation. These situations are unlike the prograde metamorphic path in the Hospitalet massif.

Path z in Fig. 7.8e is considered to be appropriate, since

(1) it accounts for the observed (D3) deformation, and

(2) it accounts for the porphyroblastesis-deformation relationship.

From this it can be concluded that the infrastructure and the metamorphism

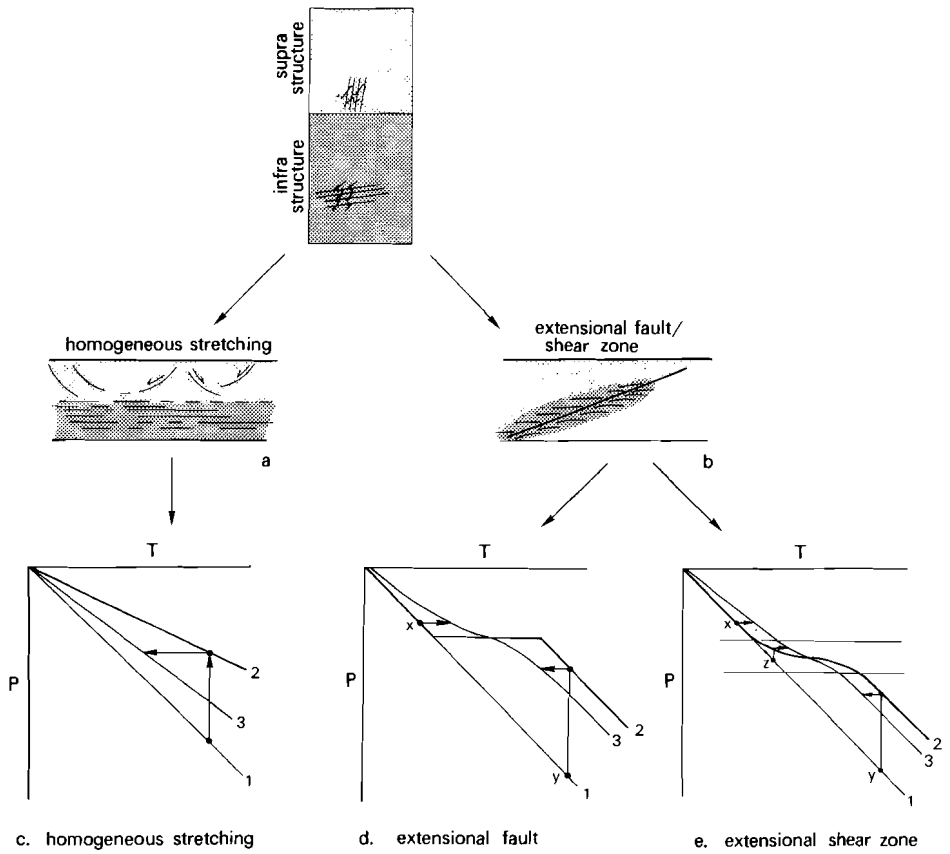

Fig. 7.8 PT paths resulting from different modes of extension of a crustal segment (for discussion see text).

1. *Initial geotherm*
2. *Geotherm directly after extension.*
3. *One relaxed geotherm.*

For the sake of clarity these diagrams do not take into account subsidence of the crust, accumulation of sediments on top of it, and a corresponding pressure increase during cooling, as indicated by McKenzie (1978).

occurred as a consequence of the activity of an extensional shear zone. The infrastructure exposed in the Hospitalet massif reflects the upper part of this zone.

Structural arguments presented in Chapter 4 also suggest that the infrastructure in the Hospitalet massif formed in an extensional shear zone or shear zones. Therefore, it can be concluded that the stretching which occurred in the area which is now occupied by the Hospitalet massif during the formation of the infrastructure was accommodated by an extensional shear zone or shear zones.

This kinematic picture may possibly apply to a larger scale than the massif in a crustal stretching event (Fig. 7.9).

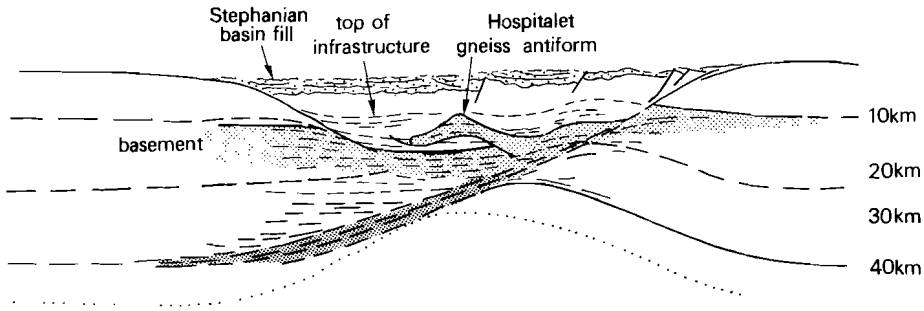

Fig. 7.9 Cartoon showing a section through the Hercynian crust when extending the extensional shear zone model for the Hospitalet gneiss antiform to a larger scale.

CHAPTER 8

SYNOPSIS

In the final chapter of this thesis the conclusions from the foregoing chapters are combined to an evolutionary model for the Hospitalet gneiss antiform. Several problems are outlined to provoke further studies of the structural domains within the Pyrenees as to gain a better insight in the dynamics of gneiss dome formation and the Hercynian orogeny in this belt.

8.1 PRE-HERCYNIAN EVOLUTION

The orthogneisses in the Hospitalet massif are considered to represent a basement to Cambro-Ordovician sedimentation. Sedimentation during the larger part of the Cambro-Ordovician took place in a uniform, possibly slowly subsiding shelf environment. Upper Ordovician (Caradocian) uplift is recorded by the relatively varied upper part of the Cambro-Ordovician stratigraphic pile. At that time EW striking fault-controlled facies belts were initiated (Hartevelt 1970). Afterwards, Silurian black shale deposition occurred, followed by Devonian carbonate dominated sedimentation and lower Carboniferous deep pelagic environments.

8.2 HERCYNIAN EVOLUTION

Pre-antiform episode

In and around the Hospitalet massif the Hercynian orogeny caused the formation of NE-SW trending (D1) folds. This phase is probably equivalent to the pre-main phase folds of Zwart (1979). Speksnijder (1986 p. 95-97) presents a review of these structures in the Pyrenees.
Subsequently these folds were refolded by EW trending upright (D2) folds, defining the suprastructure. This phase is probably equivalent to the overall development of the suprastructure in the Pyrenees ("main phase" of

Zwart 1979).

Regarding the 2-3 kbar pressure of the (younger) metamorphism and the less than 5 km thickness of the stratigraphic pile, these phases must have caused thickening of the metasediments with a factor of ca. 2. How this thickening was achieved is obscure since the kinematics of the deformation phases are unknown. It is possible that the sheets of gneiss in the Canigou-Carança massif (Guitard 1970) and the Aston massif were emplaced in this event. Considering the homogeneity of the Cambro-Ordovician sediments, deformation may have been homogeneously accommodated, which invites to a detailed analysis of structures and strain in the suprastructure domain. Raymond and Weyant (1982) describe two superposed Devonian nappes in the Eastern Pyrenees. Provided that the structures formed in this stage of the deformation history the Devonian carbonates may have accommodated the NS shortening by fold and nappe formation. The Silurian black shales possibly acted as a decollement between the Cambro-Ordovician and the Devonian (Fig. 8.1).

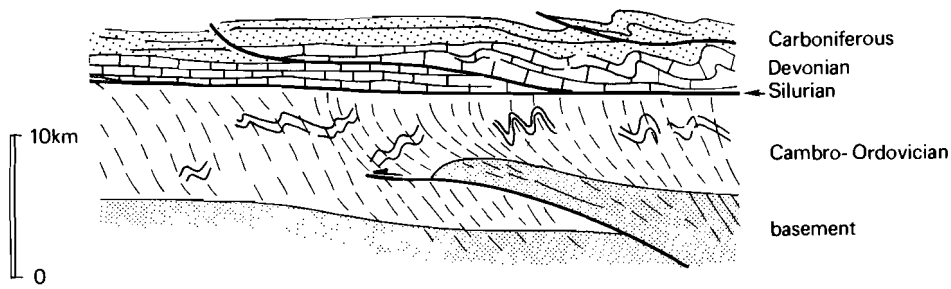

Fig. 8.1 Hypothetical section through the upper crust after D2 deformation had ceased.

Antiform formation

In the Hospitalet massif the upright EW trending D2 folds became overprinted by gently inclined to flat lying D3 foliations and folds, defining the infrastructure. Regarding the geometric relationships between the suprastructure (NS shortening) and the infrastructure (vertical shortening) in the massif, a fundamental change in tectonic regime must have

taken place.

The S3 foliation is more flat lying than the outward dipping gneiss-cover contact north and south of the gneiss antiform, which indicates that the formation of the antiform is due to vertical tectonics at the scale of the massif. The overlying suprastructure remained relatively undisturbed which implies that D3 reflects the activity of an extensional shear zone or shear zones, the bulk kinematic picture of which remains unclear. Subsequently the infrastructure (S3) foliation and the gneiss antiform were overprinted by a low P/T ratio (65^{o}C/km) metamorphism, causing extensive porphyroblast growth. Temperatures started to increase before and during D3. The post-kinematic formation of the mineral zones with respect to D3, and their more flat lying attitude than the outward dipping gneiss-cover contact and bedding, indicates that the heat front rose after D3 structures and the gneiss antiform had been formed. Such a time relationship between deformation and metamorphism can be adequately explained in terms of the activity of an extensional shear zone, the locus of which is situated below the massif and the upper part of which is represented by the infrastructure within the massif.

On basis of (1) the structural criteria and (2) the relationship between deformation and metamorphism it is suggested that during D3 extension has taken place of the region which is presently occupied by the Hospitalet massif. Extension must have been accommodated by an extensional shear zone or shear zones. This extension phase may have been of regional extent (Fig. 8.2).

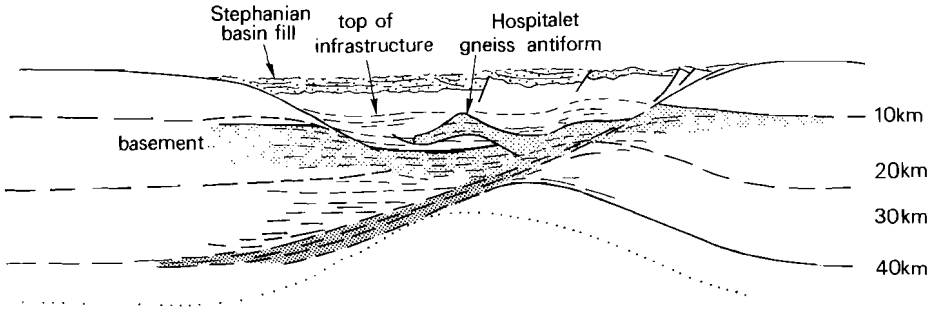

Fig. 8.2 Hypothetical section through the crust after D3 deformation had ceased. In this cartoon the conclusions drawn with respect to the Hospitalet massif have been extended to a crustal scale.

Post-antiform episode

During retrogression in lower amphibolite facies conditions the D3 structures and the isograd pattern were deformed in a mylonite zone at the gneiss-cover contact. The data support two episodes of deformation in this mylonite zone. First NNE-SSW stretching occurred, afterwards WNW-ESE stretching took place. The metasediments and the isograd pattern were draped around the relatively rigid gneiss antiform in this event which caused (1) the present day outward dipping attitude of the isograds and hence the antiformal metamorphic pattern and (2) the thinning of the mineral zones: the isograd spacing was reduced giving the false impression of very steep (150°C/km) thermal gradients.

The kinematics of the younger WNW-ESE stretching event are clear in the Hospitalet massif and suggest largely coaxial strain at the scale of the massif. Similarly oriented elongation structures in porphyroblast bearing rocks occur in various other massifs in the Axial Zone, but the bulk kinematic picture (coaxial vs. non-coaxial) in the Axial Zone is uncertain. The lower amphibolite facies mylonite zone in the Hospitalet massif shows a variety of (micro)structures and quartz c-axis fabrics. Detailed analysis of these features may provide insight in this problem. In the WNW-ESE stretching event a steep dextral transcurrent zone of refolding developed SW of the massif. Above the gneisses (large-scale) recumbent folding took place. The features suggest vertical thinning of the infrastructure combined with transcurrent movement. A regional extensional or transtensional setting is advocated (compare Speksnijder 1986, fig.III.14.h).

The event fits the late Hercynian "desintegration of the Hercynian belt" of Ziegler (1984). However, Ziegler's working hypothesis only accounts for (1) formation of the Hercynian fold belt in Westphalian times and (2) late Hercynian desintegration of this belt. With respect to the Hospitalet mantled gneiss antiform an extensional regime should be fitted in between.

	deformation events in the Hospitalet massif	regional events	
Stephanian-Early Permian	- recumbent folding (D6) WNW-ESE stretching in the mylonite zone at the gneiss-cover contact; transcurrent (dextral) movement in the El Serrat-Ransol zone (D4/5)	- late Hercynian transcurrent movements; sedimentation in NS and EW trending grabens, volcanism and emplacement of batholiths	trans/extension
	- NS stretching in the mylonite zone at the gneiss-cover contact		
▼	- metamorphic climax in infrastructure at 2-3 kbar, 600-650°C		↑
Late Westphalian	- infrastructure formation: D3 gently inclined to flat lying structures delvelop above/as top of extensional shear zone(s), upper greenschist facies conditions	- formation of mantled gneiss domes and antiforms; uplift and erosion of suprastructure	extension
▼	- suprastructure formation: D2 steep EW striking folds and foliations; thickening of metasediments, greenschist facies (and lower) metamorphic conditions	- formation of fold-and-thrust(?) belt, interleaving of basement (gneiss) sheets in metasediments (?)	↑
Early Westphalian	- NE-SW trending, SE vergent D1 folds	- sedimentation shifts from deep pelagic to coarse clastic shallow marine	NS shortening

Table 8.1 Correlation table of local and regional events. Arrows indicate the "snap shots" shown in Fig. 8.1 (lower arrow) and Fig. 8.2 (upper arrow).

8.3 DISCUSSION

The evolution of the Hospitalet mantled gneiss antiform has many aspects in common with other mantled gneiss domes (Chapter 1). However, contrary to other mantled dome type structures, such as those in the Yilgarn block (Australia) where the structures can be attributed to folding (Platt 1980, Myers and Watkins 1985), the Hospitalet mantled gneiss antiform can be attributed to vertical tectonics.

In the Pyrenees the timing of events is far better constrained than in Proterozoic or Archean mantled gneiss domes. Apparently the succession of events is quiet rapid since the entire evolution lasted no longer than ca. 30-40 Ma, which leaves probably less than 20 Ma for antiform formation. This rapid evolution suggests that the formation of this type of mantled gneiss domes may be a process related to plate motions. Regarding the position of the Pyrenees in the Hercynian orogen it is suggested, there-

fore, that such structures may form in continental back-arc basins. In this respect it is interesting to inspect other continental orogenic arcs. An example possibly resembling the Hercynian oroclinal bend in Iberia and France, may be provided by the Alpine Pannonian basin within the Carpathian arc (Sclater et al. 1980, Royden et al. 1982). In particular, Royden et al. (1982) indicate relative eastward movement of the continental crust underneath the Pannonian basin, followed by EW extension of this crust. This situation may possibly resemble the enigmatic shortening-followed-by-extension as described in this thesis for the Hospitalet massif in the Hercynian Pyrenees.

REFERENCES

Albarède, F. and Michard-Vitrac, A., 1978. Age and significance of the north Pyrenean metamorphism. Earth. Planet. Sci. Lett. 40: 327-332.

Autran, A., Fonteilles, M. and Guitard, G., 1966. Discordance du Paléozoique inférieur métamorphique sur un socle gneissique antéhercynien dans le massif des Albères (Pyrénées orièntales). C.R. Ac. Sci. 263: 317-320.

Behrmann, J.H. and Platt, J.P., 1982. Sense of nappe emplacement from quartz c-axis fabrics; an example from the Betic Cordilleras (Spain). Earth and Planet. Sci. Lett. 59(1): 208-216.

Bell, A.M., 1981. Vergence: an evaluation. J. Struct. Geol. 3: 197-202.

Berthé, D., Choukroune, P. and Jegouzo, P., 1979. Orthogneiss, mylonite and non-coaxial deformation of granites: the example of the South Armorican shear zone. J. Struct. Geol. 1: 31-42.

Bickle, M.J., Bettenay, L.F., Boulter, C.A., Groves, D.I. and Morant, P., 1980. Horizontal tectonic interaction of an Archean gneiss belt and greenstones, Pilbara block, western Australia. Geology 8: 525-529.

Bixel, F., Kornprobst, J. and Vincent, P., 1983. Le massif du Pic du Midi d'Ossau: un "cauldron" calco-alcalin stéphano-permien dans la Zone Axiale des Pyrénées. Revue de Géol. Dyn. et de Géogr. Phys. 24(4): 315-328.

Bixel, F., and Lucas, C., 1983. Magmatisme, tectonique et sédimentation dans les fosses stéphano-permiens des Pyrénées occidentales. Revue de Géol. Dyn. et de Géogr. Phys. 24(4): 329-342.

Boersma, K.Th., 1973. Devonian and Carboniferous conodont biostratigraphy, Central Spanish Pyrenees. Leidse Geol. Meded. 49: 303-377.

Boillot, G., Temime, D., Malod, J.A., Capde Vila, R., Cousin, M. Dupeuble, P.A., Gonzalez-Lodeiro, F., Lamboy, M. Lepvrier, C., Martinez-Catalan, J.R., Mascle, G., Muller, C., Pastouret, L., Taugourdeau-Lantz, J. and Vanney, J.R., 1985. Exploration by submersible of the NW Iberian margin. Bull. Soc. géol. Fr. (8)I: 89-102.

Borradaile, G.J., Bayly, M.B. and Powell, C.McA., 1982. Atlas of deformational and metamorphic rock fabrics. Springer-Verlag.

Bouchez, J-L. and Pecher, A., 1981. The Himalayan main central thrust pile and its quartz-rich tectonites in central Nepal. Tectonophysics 78: 23-50.

Bowes, D.R., Halden, N.M., Koistinen, T.J., Park, A.F., 1984. Structural features of basement and cover rocks in the eastern Svecokarelides, Finland. In: Precambrian Tectonics Illustrated, eds.: A. Kröner and R. Greiling: 147-171.

Bresser de, J.H.P., Majoor, F.J.M. and Ploegsma, M., 1986. New insights in the structural and metamorphic history of the western Lys-Gaillauas massif (Central Pyrenees, France). Geol. Mijnbouw 65(2).

Brun, J.P., Gapais, D. and Le Theoff, B., 1981. The mantled gneiss domes of Kuopio (Finland): interfering diapirs. Tectonophysics 74: 283-304.

Brun, J.P. and Driessche van den J., 1985. Diapiric gneiss domes in collision belts. MMM International Conference on Tectonic and Structural Processes: 20.

Brunel, M., 1980. Quartz fabrics in shear-zone mylonites: evidence for a major imprint due to late strain increments. Tectonophysics 64: T33-T44.

Brunet, M-F., 1984. Subsidence history of the Aquitane basin determined from subsidence curves. Geol. Mag. 121(5): 421-428.

Burg, J.P., 1986. Quartz shape fabric variations and c-axis fabrics in a ribbon mylonite: arguments for an oscillating foliation. J. Struct. Geol. 8(2): 123-133.

Burg, J.P., Iglesias, M., Laurent, Ph., Matte, Ph., Ribeiro, A., 1981. Variscan intracontinental deformation: the Coimbra-Cordoba shear zone (SW Iberian Peninsula). Tectonophysics 78: 161-177.

Casas, J.M., 1982. Pseudo-two-girdles c-axis fabric patterns in a quartz-feldspar mylonite (Costabona granodiorite, Canigó massif). Acta Geol. Hisp. 17: 151-157.

Casas, J.M. and Muñoz, J.A., 1985. Sequences of mesostructures related to the development of Alpine thrusts in the Eastern Pyrenees. MMM International Conference on Tectonic and Structural Processes, Utrecht, p. 22.

Cavet, P., 1957. Le paléozoique de la Zone Axiale des Pyrénées orièntales françaises entre le Rousillon et l'Andorre. Bull. Serv. Carte Géol. Fr. 55/254: 303-518.

Chappell, B.W. and White, A.J.R., 1974. Two contrasting granite types. Pacific. Geol. 8: 173-174.

Choukroune, P. and Mattauer, M., 1978. Tectonique des plaques et Pyrénees: súr le fonctionnement de la faille transformante nord-pyrénéenne; comparaison avec les modèles actuels. Bull. Soc. géol. Fr. XX(5): 689-700.

Coward, M.P., 1976. Archean deformation pattern in southern Africa. Phil. Trans. R. Soc. Lond., Ser. A 283: 313-331.

Daignières, M., Gallart, J., Banda, E. and Hirn, A., 1982. Implications of the seismic structure for the orogenic evolution of the Pyrenean range. Earth. Planet. Sci. Lett. 57: 88-100.

Davis, G.H., 1981. Metamorphic core complexes - expressions of regional ductile stretching and rotational, listric (?) faulting. Geol. Soc. Am. Abstr. with programs 13, p. 51.

Destombes, J.P. and Raguin, E., 1955. Etude de la partie occidentale du Massif de l'Aston. Bull. Soc. géol. Fr. (6) 5: 101-113.

Dieterich, J.H., 1970. Computer experiments on mechanisms of finite amplitude folds. Can. J. Earth Sci. 7: 786-813.

Dixon, J.M., 1975. Finite strain and progressive deformation in models of diapiric structures. Tectonophysics 28: 89-124.

Duncan, I.J., 1984. Structural evolution of the Thor-Odin gneiss dome. Tectonophysics 101: 87-130.

Eeckhout van den B. and Grocott, J., 1982. Investigations on the Precambrian rocks of Svartenhuk Halvø, central west Greenland. Rapp. Grønlands Geol. Unders. 110: 22-26.

Eeckhout van den B., Grocott, J. and Vissers, R.L.M., 1986. On the role of diapirism in the segregation, ascent and final emplacement of granitoid magmas - Discussion. Tectonophysics 127: 161-169.

Eisbacher, G.H., 1970. Deformation mechanics of mylonite rocks and fractured granites in Cobequid Mountains, Nova Scotia, Canada. Geol. Soc. Am. Bull. 81: 2009-2020.

Eskola, P., 1949. The problem of mantled gneiss domes. Quart. J. Geol. Lond. 104: 461-476.

Evans, B.W., 1965. Application of a reaction-rate method of the breakdown equilibria of muscovite and muscovite plus quartz. Am. J. Sci. 263: 647-667.

Fischer, M.W., 1984. Thrust tectonics in the North Pyrenees. J. Struct. Geol. 6(6): 721-726.

Fonteilles, M. and Guitard, G., 1964. L'effet de socle dans le métamorphisme hercynien de l'enveloppe paléozoique des gneiss des Pyrénées. C. R. Ac. Sc. t 258: 4299-4302.

Frasl, G., 1954. Anzeigen schmelzflüssigen und hochtemperierten Wachstums an den grossen Kalifeldspaten einer Porphyrgranite, Porphyrgranitgneisse und Augen-gneisse Österreiches: Austria. Geol. Bundesanstalt, Jahrb., Bd. 97:71-132.

Fry, N., 1979. Random point distributions and strain measurements in rock. Tectonophysics 57:

Garcia Celma,A., 1982. Domainal and fabric heterogeneities in the Cap de Creus quartz mylonites. J. Struct. Geol. 4(4): 443-455.

Garcia Celma,A., 1983. C-axis and shape-fabrics in quartz-mylonites of Cap de Creus (Spain); their properties and development. Thesis State University of Utrecht, 130 pp.

Ghosh,S.K. and Ramberg, H., 1976. Reorientation of inclusions by combination of pure shear and simple shear. Tectonophysics 34(1-2): 1-70.

Greenwood, H.J., 1976. Metamorphism at moderate temperatures and pressures. In: The Evolution of the Crystalline Rocks, eds. D.K. Bailey and R. MacDonald. Acad. Press. New York: 187-259.

Grocott, J., Eeckhout van den, B. and Vissers, R.L.M., 1986 in press. Mantled gneiss antiforms and fold nappes in the Rinkian belt, W.-Greenland: diapiric structures or structures formed in a thrust system? J. Royal Soc. London, 143.

Guitard, G., 1970. Le métamorphisme hercynien mésozonal et les gneis oeilles du massif du Canigou (Pyrénées orièntales). Mem. B.R.G.M. 63: 353 pp.

Hanna, S.S. and Fry, N., 1979. A comparison of methods of strain determination in rocks from southwest Dyfed (Pembrokeshire) and adjacent areas. J. Struct. Geol. 1(2): 155-162.

Hartevelt, J.J.A., 1970. Geology of the Upper Segre and Valira valleys, Central Pyrenees, Andorra/Spain. Leidse Geol. Meded. 45: 167-236.

Hatcher, R.D., 1977. Macroscopic polyphase folding illustrated by the Toxaway dome, eastern Blue Ridge, South Carolina - North Carolina. Geol. Soc. Am. Bull. 88: 1678-1688.

Henderson, G., 1969. The use of structural contour maps in the study of gneiss-metasediment relations in the Umanak area, West Greenland. Geol. Assoc. Can., Spec. Pap. 5: 129-142.

Henderson, J.R., 1981. Structural analysis of sheath folds with horizontal X-axes, northeast Canada. J. Struct. Geol. 3: 203-210.

Henderson, J.R., 1984. Description of a virgation in the Foxe fold belt, Melville Peninsula, Canada. In: Precambrian Tectonics Illustrated, eds. A. Kröner and R. Greiling, p. 251-261.

Hess, P.C., 1969. The metamorphic paragenesis of cordierite in pelitic rocks. Contrib. Mineral. Petrol. 24: 196-207.

Hibbard, M.J., 1965. Origin of some alkali feldspar phenocrysts and their bearing on petrogenesis. Am. J. Sci. 263: 245-261.

Hickman, A.M., 1984. Archean diapirism in the Pilbara Block, Western Australia. In: Precambrian Tectonics Illustrated, eds. A. Kröner and R. Greiling. E. Schweizerbart'sche Verlagsbuchhandlung, Germany, Stuttgart, 113-127.

Hobbs, B.E., 1968. Recrystallization of single crystals of quartz. Tectonophysics 6(5): 353-401.

Hobbs, B.E., 1971. The analysis of strain in folded layers. Tectonophysics 11: 329-375.

Holdaway, M., 1971. Stability of andalusite and the aluminium silicate phase diagram. Am. J. Sci. 271: 97-131.

Hoschek, G., 1969. The stability of staurolite and chloritoid and their significance in metamorphism of pelitic rocks. Contrib. Mineral. Petrol. 22: 208-232.

Jäger, E. and Zwart, H.J., 1968. Rb-Sr age determinations of some gneisses and granites of the Aston-Hospitalet massif (Pyrenees). Geol. en Mijnbouw 47: 349-357.

Jansen, J.B.H., 1973. Geological map of Naxos, Athens. Inst. for Geol. and Subsurface Research 1973.

Jegouzo, P., 1980. The south Armorican shear zone. J. Struct. Geol. 2: 39-47.

Kerrich, D.M., 1968. Experiments on the upper stability limit of pyrophyllite at 1.8 kb and 3.9 kb water pressure. Am. J. Sci. 266: 204-214.

Konert, G. and Eeckhout van den B., 1983. Data on the tectonic evolution of the Alhamilla unit, Sierra Alhamilla (Betic Cordilleras, SE Spain) with emphasis on tectonics below moving nappes. Geol. Rdsch. 72(2): 619-636.

Kröner, A., 1984. Dome structures and basement reactivation in the Pan-African Damara belt of Namibia. In : Precambrian Tectonics Illustrated, eds. A. Kröner and R. Greiling. E. Schweizerbart'sche Verlagsbuchhandlung, Germany, Stuttgart, 191-206.

Lapré, J.F., 1965. Minor structures in the Upper Vicdessos Valley (Aston massif, France). Leidse Geol. Meded. 33: 255-274.

Law, R.D., Knipe, R.J. and Dayan, H., 1984. Strain path partitioning within thrust sheets: microstructural and petrofabric evidence from the Moine thrust zone at Loch Eriboll, northwest Scotland. J. Struct. Geol. 6(5): 477-499.

Le Pichon, X., Bonnin, J., Francheteau, J. and Sibuet, J.C., 1971. Une hypothèse d'évolution tectonique du Golfe de Gascogne. Editions Techniq. Paris VI.16.1-VI.16.18.

Lisle, R.J., 1985. Cleavage patterns around folds produced by constrictional strain. Int. Conf. on Tectonic and Structural Processes, Utrecht, 93.

Lister, G.S., Paterson, M.S. and Hobbs, B.E., 1978. The simulation of fabric development in plastic deformation and its application to quartzite: the model. Tectonophysics 45: 107-158.

Lister, G.S. and Paterson, M.S., 1979. The simulation of fabric development during plastic deformation and its application to quartzite: fabric transitions. J. Struct. Geol. 1: 99-115.

Lister, G.S. and Williams, P.F., 1979. Fabric development in shear zones: theoretical controls and observed phenomena. J. Struct. Geol. 1: 283-297.

Lister, G.S. and Hobbs, B.E., 1980. The simulation of fabric development during plastic deformation and its application to quartzite: the influence of deformation history. J. Struct. Geol. 2(3): 355-370.

Lister, G.S. and Dornsiepen, U.F., 1982. Fabric transitions in the Saxony granulite terrain. J. Struct. Geol. 4(1): 81-92.

Lister, G.S. and Williams, P.F., 1983. The partitioning of deformation in flowing rock masses. Tectonophysics 92: 1-33.

Lister, G.S. and Snoke, A.W., 1984. S-C mylonites. J. Struct. Geol. 6(6): 617-638.

Luth, W.C., Jahns, R.H. and Tuttle, O.F., 1964. The granite system at pressures of 4 to 10 kilobars. J. Geophys. Res. 69: 759-773.

Maar, P.A. van der, 1980. The geology and petrology of Ios, Cyclades, Greece. Ann. Geol. Pays Helleniques XXX/I: 206-224.

Majoor, F.J.M., De Bresser, J.H.P., 1984. Stauroliet-omzettingen in het Rioumajou - La Pez gebied, Centrale Pyreneeën. Int. Rapp. vakgr. Struct. en Toegep. Geol. unpubl.

Malzac, J. and Rousseau, A., 1982. Gravimétry des Pyrénées ariègeoises: quelques conséquences structurales. Bull. Soc. Géol. Fr. (7) XXIV: 739-753.

Mather, J.D., 1970. The biotite isograd and the lower greenschist facies in the Dalradian rocks of Scotland. J. Petrol. 11: 253-275.

Mattauer, M. and Henry, J., 1974. The Pyrenees. In: Mesozoic-Cenozoic orogenic belts. Data for orogenic studies, ed. A.M. Spencer. Geol. Soc. London, Spec. Publ. 4: 3-23.

Matte, Ph., 1969. Le problème du passage de la schistositée horizontale à la schistositée verticale dans le dôme de la Garonne. C.R. Ac. Sci. 268: 1841-1844.

Matte, Ph., 1986. Tectonics and plate tectonics model for the Variscan belt of Europe. Tectonophysics 126: 329-374.

McCaig, A., 1983. Kinematics, geochemistry and age of shear zones in the Aston-Hospitalet massif, Pyrenees. Unpubl. Ph.D. thesis, Cambridge, 274 pp.

McKenzie, D., 1978. Some remarks on the development of sedimentary basins. Earth Plan. Sci. Lett. 40: 25-32.

Means, W.D., Hobbs, B.E., Lister, G.S. and Williams, P.F., 1980. Vorticity and non-coaxiality in progressive deformations. J. Struct. Geol. 2: 371-378.

Mey, P.H.W., 1967a. The geology of the upper Ribagorzana and Baliera valleys, Central Pyrenees, Spain. Leidse Geol. Meded. 41: 153-220.

Mey, P.H.W., 1967b. Evolution of the Pyrenean basins during the Upper Paleozoic. Int. symp. Devonian system, Calgary 2: 1157-1166.

Mey, P.H.W., 1968. Geology of the upper Ribagorzana and Tor valleys, Central Pyrenees, Spain. Leidse Geol. Meded. 41: 229-292.

Michard-Vitrac, A., Albarède, F., Dupuis, C. and Taylor, H.P., 1980. The genesis of Variscan (Hercynian) plutonic rocks: inferences from Sr.Pb ad o studies on the Maladetta igneous complex, Central Pyrenees (Spain). Contr. Miner. Petrol. 72: 57-72.

Mirouse, R., 1966. Recherches géologiques dans la partie occidentale de la zone primaire axiale des Pyrénées. Mém. expl. carte géol. det. Fr. 451 p.

Muller, P.D. and Chapin, D.A., 1984. Tectonic evolution of the Baltimore gneiss anticlines, Maryland. In: The Grenville event in the Appalachian and Related Topics, ed. M.J. Bartholomew. Geol. Soc. Am., Spec. Pap. 194: 127-148.

Myashiro, A., 1973. Metamorphism and metamorphic belts. London, Allen & Unwin. 492 pp.

Myers, J.S. and Watkins, K.P., 1985. Origin of granite-greenstone patterns, Yilgarn Block, Western Australia. Geology 13: 778-780.

Nagtegaal, P.J.C. and de Weerd, J.T., 1985. Provenance of Cambro-Ordovician to Oligocene sandstones in the Southern Pyrenees. Geol. Mijnbouw 64: 25-40.

Naylor, R.S., 1968. Origin and regional relationships of the core-rocks of the Oliverian Domes. In: Studies of Appalachian Geology: Northern and Maritime, eds. E-An Zen, W.S. White, J.B. Hadley and J.B. Thompson. Wiley-Interscience, New York, 231-240.

Nitsch, K.H., 1970. Experimentelle Bestimmung der oberen Stabilitätsgrenze von Stilpnomelan. Fortschr. Mineral. 47 (Beiheft 1): 48-49.

Oele, J.A., 1966. The structural history of the Vall Ferrera Area, the transition zone between the Aston Massif and the Salat-Pallaresa anticlinorium (Central Pyrenees, France, Spain). Leidse Geol. Meded. 38: 129-164.

Pannekoek, A.J., 1937. Die Jungtertiäre morphologisch-tektonische Entwicklungsgeschichte der ostlichen Pyrenäen. Ass. Et. Géol. Médit. Occ. (Géol. Pays Catal.) III, no. 4, partie I, 25 pp.

Platt, J.P. and Vissers, R.L.M., 1980. Extensional structures in anisotropic rocks. J. Struct. Geol. 2(4): 397-410.

Platt, J.P., 1980. Archean greenstone belts: a structural test of tectonic hypotheses. Tectonophysics 65: 127-150.

Platt, J.P., 1984. Secondary cleavages in ductile shear zones. J. Struct. Geol. 6: 439-442.

Raguin, E., 1977. Le massif de l'Aston dans les Pyrénées de l'Ariège. Bull. B.R.G.M. (2) sect. 1, 2: 89-119.

Ramberg, H., 1967. Gravity, deformation and the earth's crust studies by centrifuged models. Academic Press, London, 214 pp.

Ramberg, H., 1981. Gravity, deformation and the earth's crust: Theory, experiments and geological application, 2nd ed., 452 pp. Academic press, London.

Ramsay, J.G., 1967. Folding and fracturing of rocks. McGraw-Hill, New York, 568 pp.

Ramsay, J.G., 1980. Shear zone geometry; a review. J. Struct. Geol. 2: 83-99.

Ramsay, J.G. and Graham, R.H., 1970. Strain variation in shear belts. Can. J. Earth Sci. 7: 786-813.

Raymond, D. and Weyant, M., 1982. Individualisation de deux séries hétéropiques au sein du Dévonian et du Carbonifère inférieur de la zone axiale pyrénéenne entre les vallées de l'Aude et de l'Ariège (France). Bull. Soc. Géol. France (7), t. XXIV, no. 2: 265-274.

Respaut, J.P. and Lancelot, J.R., 1983. Datation de la mise en place synmétamorphe de la charnokite d'Ansignan (massif de l'Agly) par le méthode U/Pb sur zircons et monazites. Neues Jahrb. Mineral. Abh. 147: 21-34.

Richardson, S.W., 1968. Staurolite stability in a part of the system Fe-Al-Si-O-H. J. Petrol. 9: 448-467.

Roux, L., 1977. L'évolution des roches du faciés granulite et le problème des ultramafites dans le massif de Castillon (Ariège). Thèse, Toulouse, 530 pp.

Royden, L.H., Horvath, F. and Burchfiel, B.C., 1982. Transform faulting, extension and subduction in the Carpathian Pannonian region. Geol. Soc. Am. Bull. 93: 717-725.

Sawyer, E.W., 1981. Damaran structural and metamorphic geology of an area southeast of Walvis Bay, South West Africa/Namibia. Geol. Survey SW Africa, mémoir 7: 94 pp.

Schuiling, R.D., 1960. Le dôme gneissique de l'Agout (Tarn et Herault). Mém. Soc. Géol. Fr. 91(1): 59 pp.

Schuiling, R.D. and Kreulen, R., 1979. Are thermal domes heated by CO_2-rich fluids from the mantle? Earth Planet. Sci. Lett. 43: 298-302.

Schwerdtner, W.M., 1981. Identification of gneiss diapirs. In: Diapirism and gravity: report of a Tectonic Studies Group conference at Leeds University, 25-26.3.1980, ed. M.P. Coward. J. Struct. Geol. 3: 90-91.

Schwerdtner, W.M., Sutcliffe, R.H. and Troeng, B., 1978. Patterns of total strain within the crestal region of immature diapirs. Can. J. Earth Sci. 15: 1437-1447.

Schwerdtner, W.M., Stone, D., Osadetz, K., Morgan, J. and Scott, G.M., 1979. Granitoid complexes and the Archean tectonic record in the southern part of nothwestern Ontario. Can. J. Earth Sci. 16: 1965-1977.

Schwerdtner, W.M., 1984. Archean gneiss domes in the Wabigoon Subprovince of the Canadian Shield, northwestern Ontario. In: Precambrian Tectnics Illustrated, eds. A. Kröner and R. Greiling. E. Schweizerbart'sche Verlagsbuchhandlung, Germany, Stuttgart, 129-134.

Sclater, J.G., Royden, L., Horvath, F., Burchfiel, B.C., Semken, S., Stegena, L., 1980. The formation of the intra-Carpathian basins as determined from subsidence data. Earth Planet. Sci. Lett. 51: 139-162.

Séguret, M., 1972. Etude tectonique des nappes et séries décollées de la partie centrale du versant sud des Pyrénées. Série. Géol. Struct. 2, Montpellier.

Séguret, M. and Daignières, M., et al., 1985. Coupes balancées d'échèlle crustale des Pyrénées. C.R. Acad. Sci. Paris 30: 341-346.

Seifert, F., 1970. Low temperature compatability relations of cordierite in haplopelites of the system K_2O-MgO-Al_2O_3-SiO_2-H_2O. J. Petrol. 11: 73-99.

Seifert, F. and Schreyer, W., 1970. Lower temperature stability limit of Mg-cordierite in the range 1-7 kb water pressure: a redetermination. Contrib. Mineral Petrol. 27: 225-238.

Simpson, C. and Schmid, S.M., 1983. An evaluation of criteria to deduce the sense of movement in sheared rocks. Geol. Soc. Am. Bull. 94: 1281-1288.

Snowden, P.A., 1984. Non-diapiric batholiths in the Zimbabwe Shield. In: Precambrian Tectonics Illustrated, eds. A. Kröner and R. Greiling.E. Schweizerbart'sche Verlagsbuchhandlung, Germany, Stuttgart, 135-145.

Soula, J.C., 1982. Characteristics and mode of emplacement of gneiss domes and plutonic domes in central-eastern Pyrenees. J. Struct. Geol. 4(3): 313-342.

Soula, J., Lucas, C. and Bessière, G., 1979. Genesis and evolution of Permian and Triassic basins in the Pyrenees by regional simple shear acting on older Variscan structures: field evidence and experimental models. Tectonophysics 58: t1-t9.

Soula, J.C., Debat, P., Déramond, J., Guchereau, J-Y., Lamouroux, C., Pouget, P. and Roux, L., 1986. Evolution structurale des ensembles métamorphique des gneiss et des granitoides dan les Pyrénées centrales. Bull. Soc. Géol. France (8) II 1: 79-93.

Souquet, P., Peybernes, B., Bilotte, M. and Debroas, E.J., 1977. La chaine Alpine des Pyrénées. Géol. Alp. 53: 193-216.

Souquet, P., Debroas, E.J., Boiric, J.M., Pons, P., Fixari, G., Roux, J.C., Dol, J., Thieuloy, J.P., Bonnemaison, M., Manivit, H. and Peybernes, B., 1985. The black flysch (Albian - Early Cenomanian) from the Pyrenees. Bull. Centres Réch. Explor. - Prod. Elf-Aquitaine 9(1): 183-252.

Speksnijder, A., 1985. Anatomy of a strike-slip fault controlled sedimentary basin, Permian of the Southern Pyrenees, Spain. Sediment. Geol. 44: 179-223.

Speksnijder, A., 1986. Geological analysis of Paleozoic large-scale faulting in the south-central Pyrenees. Thesis State University of Utrecht. Geol. Ultraiectina 43: 211 pp.

Staal, C.R. van, and Williams, P.F., 1983. Evolution of a Svecofennian-mantled gneiss dome in SW Finland, with evidence for thrusting. Precambrian Res. 21: 101-128.

Stephansson, O. and Johnson, K., 1976. Granite diapirism in the Rum Jungle area, Northern Australia. Precambrian Res. 3: 159-185.

Sylvester, A.G. and Christie, J.M., 1968. The origin of crossed-girdle orientations of optic axes in deformed quartzites. J. Geol. 76: 571-580.

Talbot, C.J., 1971. Thermal convection below the solidus in a mantled gneiss dome, Fungwi Reserve, Rhodesia. J. Geol. Soc. Lond. 127: 377-410.

Talbot, C.J., 1974. Fold nappes as asymmetric mantled gneiss domes and ensialic orogeny. Tectonophysics 24: 259-276.

Talbot, C.J., 1979. Infrastructural migmatitic upwelling in East Greenland interpreted as thermal convective structures. Precambrian Res.: 77-93.

Tex den, E., 1975. Thermally mantled gneiss domes: the case of convective heat flow in more or less solid orogenic basement. In: Progress in Geodynamics, eds. C.J. Borradaile, A.R. Ritsema, H.E. Rondeel, O.J. Simon, K.N.A.W., Amsterdam.

Thompson, J.B.Jr., Robinson, P., Clifford, T.N. and Trask, N.J.Jr., 1968. Nappes and gneiss domes in West-Central New England. In: Studies of Appalachian Geology: Northern and Maritime, eds. E-An Zen, W.S. White, J.B. Hadley and J.B. Thompson. Wiley-Interscience, New York, 203-218.

Vail, J.R., 1963. Monte Senga-Senga, a domal structure in central Moçambique. Geol. Rdsch. 53: 679-686.

Verhoef, P.N.W., Vissers, R.L.M. and Zwart, H.J., 1984. A new interpretation of the structural and metamorphic history of the Western Aston Massif (Central Pyrenees, France). Geol. Mijnbouw 63(4): 337-416.

Verspyck, G.W., 1965. The geology and petrology of the Artiès-Siguer-Valira del Norte Valleys, Aston-Hospitalet massif (France, Andorra). Leidse Geol. Meded. 33: 275-318.

Vielzeuf, D. and Kornprobst, J., 1984. Crustal splitting and the emplacement of Pyrenean lherzolites and granulites. Earth Planet. Sci. Lett. 67: 87-96.

Vielzeuf, D., 1984. Rélations de phases dans le faciès granulite et implications géodynamiques. l'Example des granulites des Pyrénées. Thèse, Clermont II, 358 pp.

Vitrac, A. and Allègre, C.J., 1971. Datation ^{87}Rb-^{87}Sr des gneiss du Canigou et de l'Agly (Pyrénées orièntales, France). C.R. Ac. Sci. 273: 2411-2413.

Wegmann, C.E., 1935. Zur Deutung der Migmatite. Geol. Rdsch. 26: 305-350.

Weijermars, R., 1982. Definition of vergence. J. Struct. Geol. 4: 505.

Wickham, S.M. and Oxburgh, E.R., 1985. Continental rifts as a setting for regional metamorphism. Nature 318: 330-333.

Williams, G.D., 1985. Thrust tectonics in the south central Pyrenees. J. Struct. Geol. 7(1): 11-17.

Williams, G.D. and Fischer, M.W., 1984. A balanced section across the Pyrenean orogenic belt. Tectonics 3(7): 773-780.

Williams, G.D. and Fischer, M.W., 1984. In: The tectonic evolution of the Pyrenees: a workshop. J. Geol. Soc. London 141: 379-381.

Williams, P.F., 1963. Geology of the Rum Jungle District (Northern Territory) with paricular reference to the origin of the uranium ore bodies. Territ. Enterp. Pty. Ltd. Rep. (unpubl.).

Williams, P.F., 1985. Multiple deformed terrains-problems of correlation. J. Struct. Geol. 7 3/4: 269-280.

Winkler, H.G.F., 1976. Petrogenesis of metamorphic rocks. Fourth Ed., Springer-Verlag, 334 pp.

Zandvliet, J., 1960. The geology of the Upper Salat and Pallaresa valleys, Central Pyrenees, France/Spain. Leidse Geol. Meded. 25: 1-127.

Ziegler, P.A., 1984. Caledonian and Hercynian crustal consolidation of Western and Central Europe - a working hypothesis. Geol. Mijnbouw 63: 93-108.

Zwart, H.J., 1962. On the determination of polymetamorphic mineral associations, and its application to the Bosost area (Central Pyrenees). Geol. Rundschau 52: 38-65.

Zwart, H.J., 1963a. The structural evolution of the Paleozoic of the Pyrenees. Geol. Rundschau 53: 170-205.

Zwart, H.J., 1963b, Metamorphic history of the Central Pyrenees, Part II. Valle de Aran, sheet 4. Leidse Geol. Meded. 28: 321-376.

Zwart, H.J., 1965. Geological map of the Paleozoic of the Central Pyrenees, sheet 6, Aston, France, Andorra, Spain, 1:50.000. Leidse Geol. Meded. 33: 191-254.

Zwart, H.J., 1967. The duality of orogenic belts. Geol. Mijnbouw 46: 283-309.

Zwart, H.J., 1968. The Paleozoic crystalline rocks of the Pyrenees in their structural setting. Krystalinikum 6: 125-140.

Zwart, H.J., 1969. Metamorphic facies series in the European orogenic belts and their bearing on the causes of orogeny. Geol. Ass. Canada, Special Paper 5.

Zwart, H.J., 1979. The geology of the Central Pyrenees. Leidse Geol. Meded. 50: 1-74.

Zwart, H.J., 1981. Tree profiles through the Central Pyrenees. In: the Variscan orogen in Europe. Eds. H.J. Zwart and U.F. Dornsiepen. Geol. Mijnbouw 60(1) special issue: 97-107.

CURRICULUM VITAE

Bas van den Eeckhout werd geboren op 26 september 1956 te Amsterdam. Vanaf 1968 werd een Atheneum-B opleiding genoten te Purmerend. Na het eindexamen in 1974 werd aan de studie Geologie begonnen aan het Geologisch Instituut van de Universiteit van Amsterdam. Daar werd in december 1977 het kandidaatsexamen G3 behaald. In september 1981 werd het doctoraalexamen afgelegd met als hoofdvak Geologie, hoofdrichting Structurele Geologie, en als bijvak Geochemie.
In april 1982 werd aan de promotiestudie begonnen aan het Instituut voor Aardwetenschappen der Rijksuniversiteit Utrecht bij de vakgroep Structurele en Toegepaste Geologie, als wetenschappelijk assistent met 1/4 onderwijstaak. Van april 1986 tot september 1986 was hij werkzaam als toegevoegd docent bij de genoemde Vakgroep.

GEOLOGICAL MAP OF THE WESTERN HOSPITALET MASSIF
(PYRENEES)

by Bas van den Eeckhout 1986

scale 1 : 25.000

Topography : 1 : 50.000 map sheet Andorra ; 1 : 25.000 maps Fontargente (XXI-49 nº 1 - 2,3 - 4 , Carte de France)
Geology : B van den Eeckhout (1982/85) except , north west part (Pic de Besali/northern Riu de Rialb) after McCaig(1983);
trace of Mérens fault east of long 543 after Zwart (1965)

QUATERNARY
- alluvium
- major screes

Hercynian intrusives
A = aplite D = diabase
Q = quartz-(feldspar)-porphyry

hydrothermal rocks
brown weathered phyllites

DEVONIAN
limestones and phyllites

SILURIAN
black slates

CAMBRO-ORDOVICIAN
Massana fm. : mainly quartzites
c = conglomerate

Seo fm. : slate/phyllite/schist
Cap d'Entor mb. : white quartzite
grey quartzite

Ransol mb. : white quartzite
black shale and quartzite
marble

Pic du Sal mb. : pale grey quartzite
marble

K-feldspar augengneisses

planar features
- bedding (arrow denotes younging direction)
- bedding horizontal/ vertical
- S_2 foliation
- S_3 foliation
- mylonitic foliation
- bedding/most prominent foliation traces (other foliations omitted)

linear features
- L_2^0 showing vergence
- L_3^0 / L_3^2
- mineral lineation b=biotite q=quartz f=feldspar

boundaries
- lithological boundary (inferred/observed)
- fault /shear zone (barb to upthrown side)
- anticlinal / synclinal } axial trace of deformation phase x (upright/overturned)
- A : late folds ; presumably alpine
- landslide

topography
- 2000 — 100m contour
- village
- 1500 peak
- frontier Andorra/France
- stream
- lake

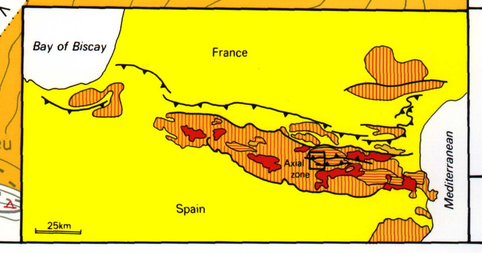

METAMORPHIC MAP OF THE WESTERN HOSPITALET MASSIF (PYRENEES)

by Bas van den Eeckhout 1986

scale 1 : 25.000

Topography: 1:50.000 map sheet Andorra; 1:25.000 maps Fontargente (XXI-49 n° 1-2, 3-4, carte de France)
Geology: B van den Eeckhout (1982/85) except, north west part (Pic de Besali/northern Riu de Rialb) after McCaig (1983); trace of Mérens fault east of long. 543 after Zwart (1965)

CAMBRO - ORDOVICIAN

QUATERNARY
- VV alluvium / major screes

Hercynian intrusives
A = aplite D = diabase
Q = quartz-(feldspar)-porphyry

brown weathered phyllites

DEVONIAN
limestones and phyllites

SILURIAN
black slates

Massana fm.: mainly quartzites
c = conglomerate

Seo fm.: slate/phyllite/schist
Cap d' Entor mb.: white quartzite
grey quartzite

Ransol mb.: white quartzite
black shale and quartzite
marble

Pic du Sal mb.: pale grey quartzite
marble

K-feldspar augengneisses

chlorite zone
biotite zone
andalusite-cordierite zone
staurolite zone
staurolite-out zone

primary chlorite
biotite
andalusite
cordierite
staurolite
staurolite - andalusite transformation
staurolite - mica transformation
sillimanite
garnet
+ biotite

planar features
- bedding (arrow denotes younging direction)
- bedding horizontal/vertical
- S_2 foliation
- S_3 foliation
- mylonitic foliation
- bedding/most prominent foliation traces (other foliations omitted)

linear features
- L^0_2 showing vergence
- L^0_3 / L^2_3
- mineral lineation
  b = biotite q = quartz f = feldspar

boundaries
- lithological boundary (inferred/observed)
- fault/shear zone (barb to upthrown side)
- anticlinal / synclinal } axial trace of deformation phase x (upright/overturned)
- A: late folds; presumably alpine
- landslide

topography
- 2000 100 m contour
- village
- 1500 peak
- frontier Andorra/France
- stream
- lake

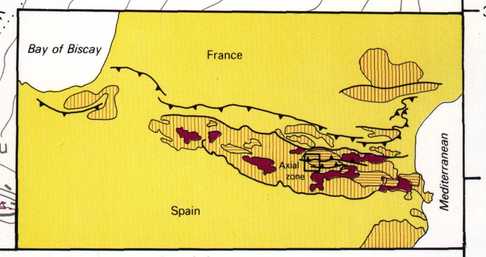

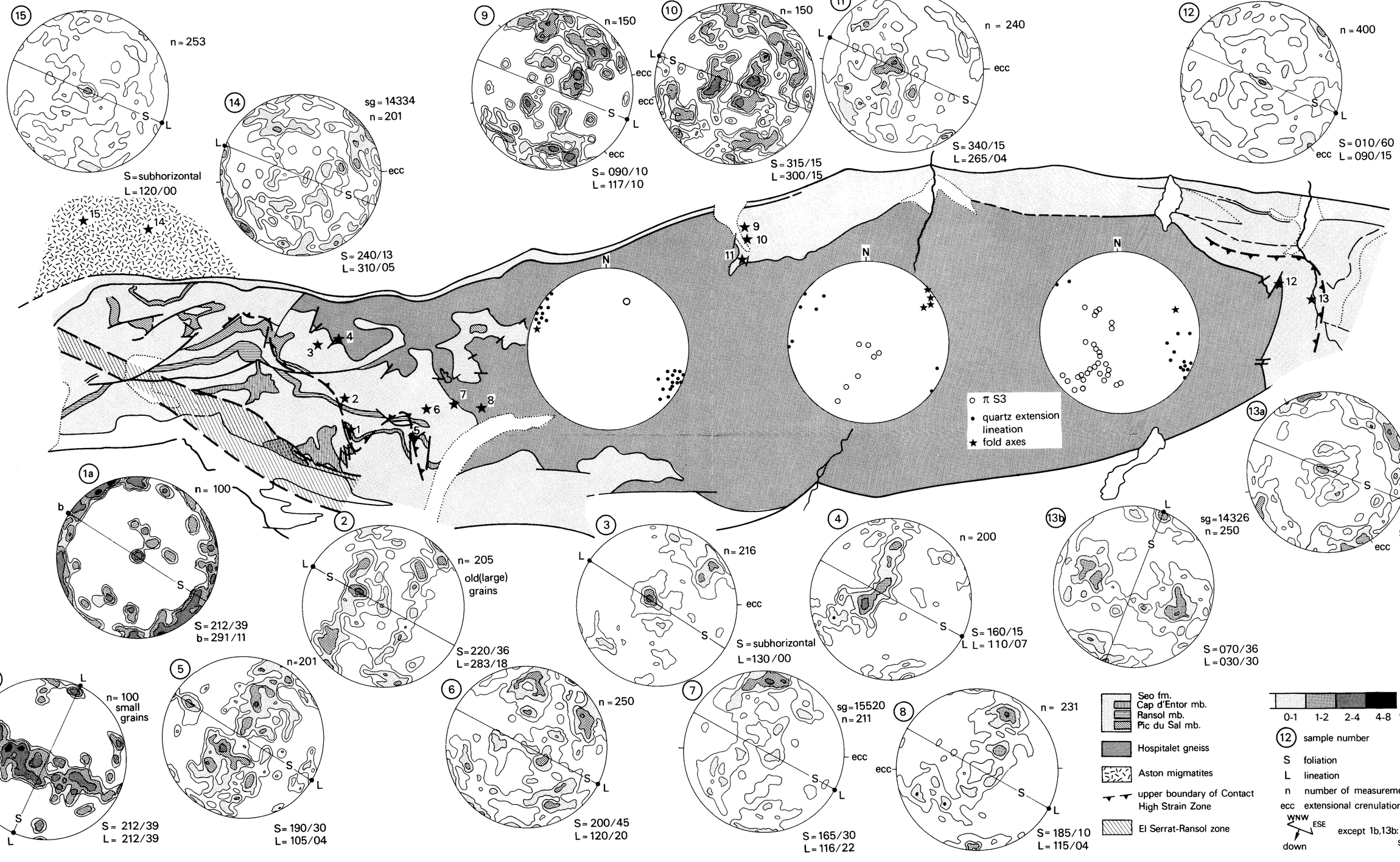
15
n = 253
S
L
S = subhorizontal
L = 120/00
14
sg = 14334
n = 201
ecc
S = 240/13
L = 310/05
9
n = 150
ecc
S = 090/10
L = 117/10
10
n = 150
S = 315/15
L = 300/15
11
n = 240
S = 340/15
L = 265/04
12
n = 400
S = 010/60
L = 090/15
N
π S3
quartz extension lineation
fold axes
1a
n = 100
b
S = 212/39
b = 291/11
2
n = 205
old(large) grains
S = 220/36
L = 283/18
3
n = 216
S = subhorizontal
L = 130/00
4
n = 200
S = 160/15
L = 110/07
13a
n = 250
S = 070/36
L = 120/25
13b
sg = 14326
n = 250
S = 070/36
L = 030/30
1b
n = 100
small grains
S = 212/39
L = 212/39
5
n = 201
S = 190/30
L = 105/04
6
n = 250
S = 200/45
L = 120/20
7
sg = 15520
n = 211
S = 165/30
L = 116/22
8
n = 231
S = 185/10
L = 115/04
Seo fm.
Cap d'Entor mb.
Ransol mb.
Pic du Sal mb.
Hospitalet gneiss
Aston migmatites
upper boundary of Contact High Strain Zone
El Serrat-Ransol zone
0-1 1-2 2-4 4-8 % percent area
12 sample number
S foliation
L lineation
n number of measurements
ecc extensional crenulation cleavage
WNW ESE down
except 1b,13b:
NNE SSW down